Naval Research Laboratory

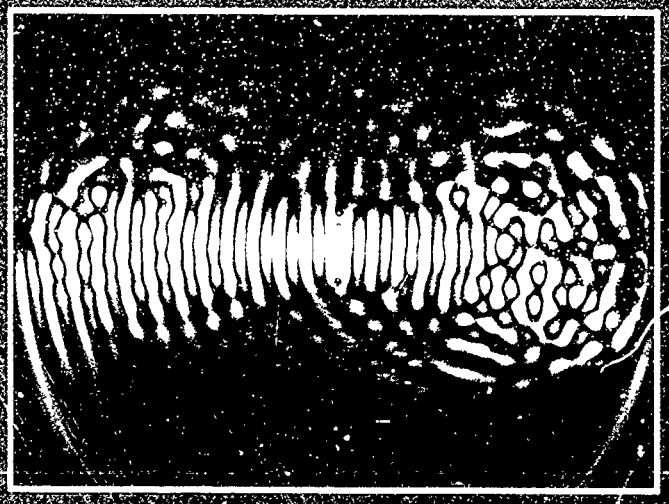

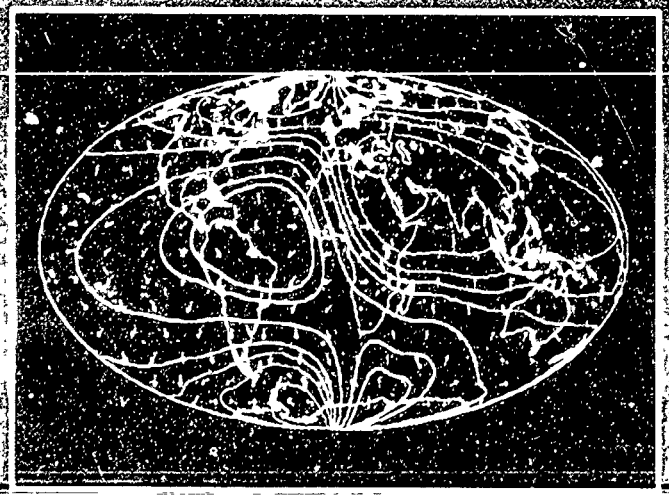

1991 NRL Review

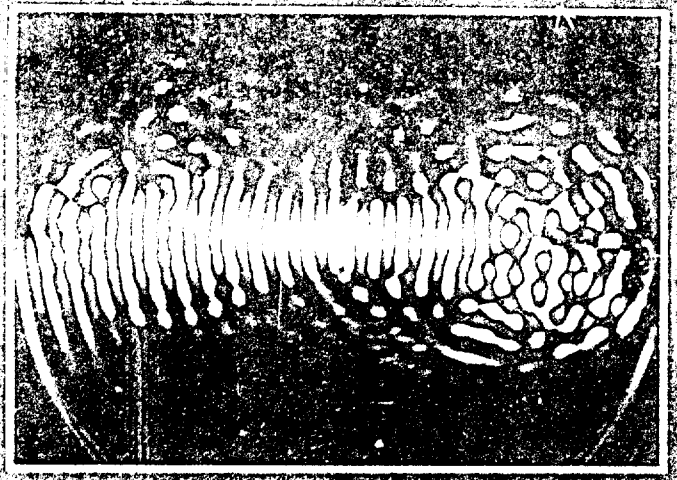

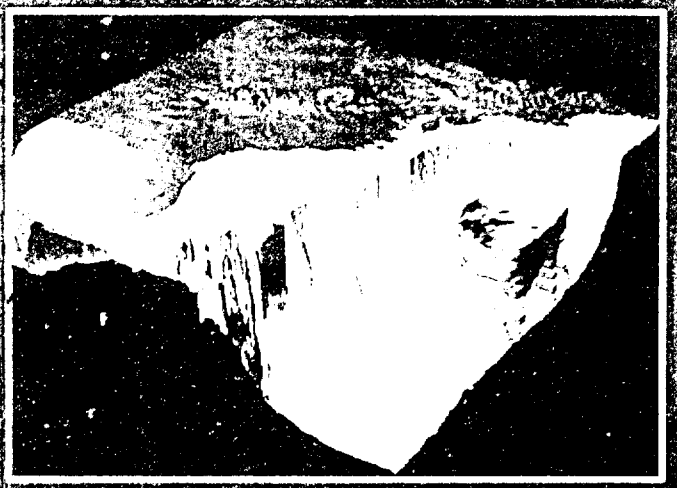

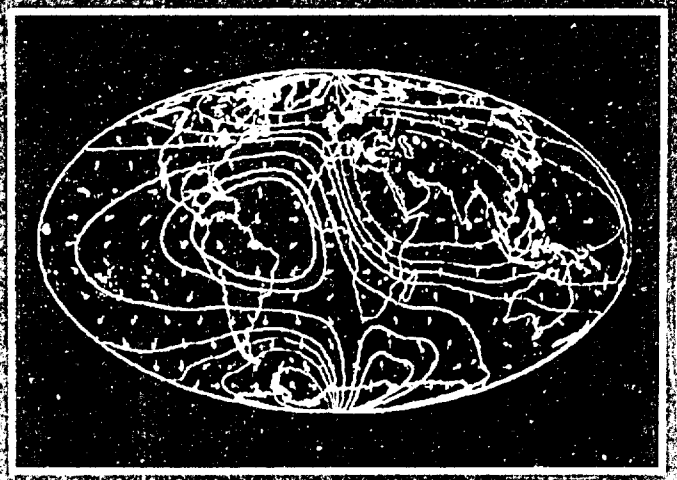

1991 NRL Review

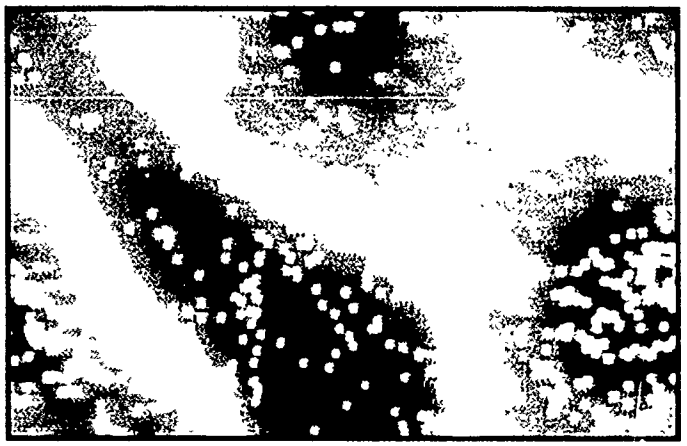

Electrostatic particle simulation of a two-dimensional cross section of plasma: The particles are a randomly chosen set of ions, and the background field represents the potential. As the simulation enters a feedback loop, the positive ions cluster in the negative regions, and negative ions collect in the positive regions. The colors of the field are blue for negative, green for neutral, and red for positive. (John Reynders (ONR Doctoral Fellow))

On the cover, top to bottom:

Lattice gas simulation of sound waves. The six sources in the center have varying outputs to generate a single beam on either side. The simulation models a beam interacting with a school of fish (green dots). The peaks of the sound waves are green with different phases shown in yellow and purple (Rudolph Krutar, Susan Numrich, and George Schmitt)

WRAP simulation WRAP is an acoustic propagation model The model takes pressure, salinity, and temperature factors and computes decibel loss from a single sound source The image depicts a surface contour at a constant decibel loss (green) through the three-dimensional data. The data are displayed with bathymetric data for geographic reference (Edward Jennings, Paul Anderson, and Eric Hoffman)

Weather environment This simulation computes wind velocity, direction, and pressure for a given area The scene represents the weather data with isobaric contours, yellow being high pressure, magenta being low pressure, and a mesh of vectors showing wind direction The weather data are combined with shoreline reference data and are displayed by using a mollewide projection (James Tuccillo, Paul Anderson, Henry Dardy, Glenn Heinle, Eric Hoffman, George Lamb, and John Shirron)

These computer graphics were produced by the Acoustic Division's Connection Machine Facility through the efforts of Glenn Heinle and Eric Hoffman

Seven of the articles in this publication are featured in a companion video. Page x gives the video contents and additional information.

DISCLAIMER NOTICE

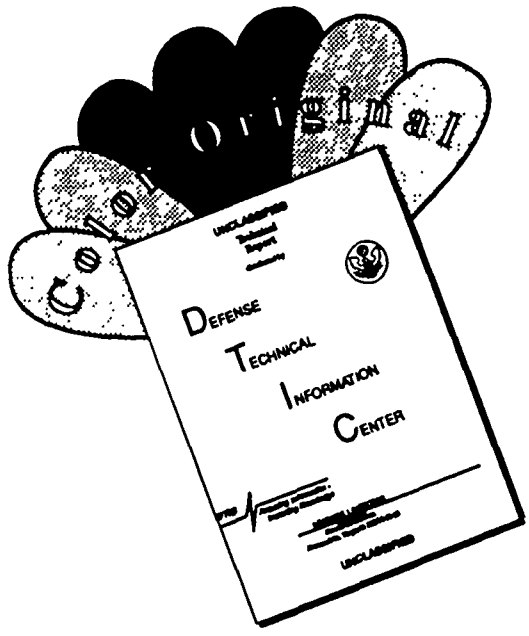

THIS DOCUMENT IS BEST QUALITY AVAILABLE. THE COPY FURNISHED TO DTIC CONTAINED A SIGNIFICANT NUMBER OF COLOR PAGES WHICH DO NOT REPRODUCE LEGIBLY ON BLACK AND WHITE MICROFICHE.

REPORT DOCUMENTATION PAGE

Form Approved
OMB No 0704-0188

1. AGENCY USE ONLY (Leave blank)	2. REPORT DATE	3. REPORT TYPE AND DATES COVERED
	May 1991	Annual, Fiscal year 1990

4. TITLE AND SUBTITLE

1991 NRL Review

5. FUNDING NUMBERS

N/A

6. AUTHOR(S)

See "Contents" of publication

7. PERFORMING ORGANIZATION NAME(S) AND ADDRESS(ES)

Naval Research Laboratory
Washington, DC 20375-5000

8. PERFORMING ORGANIZATION REPORT NUMBER

NRL Publication 181-4830

9. SPONSORING/MONITORING AGENCY NAME(S) AND ADDRESS(ES)

N/A

10. SPONSORING/MONITORING AGENCY REPORT NUMBER

N/A

11. SUPPLEMENTARY NOTES

A companion video is available from DTIC or on loan from the Naval Research Laboratory, Ruth H. Hooker Technical Library and Technical Information Center, Code 4820, Washington, DC 20375-5000

12a. DISTRIBUTION/AVAILABILITY STATEMENT

Approved for public release; distribution is unlimited.

12b. DISTRIBUTION CODE

13. ABSTRACT *(Maximum 200 words)*

Presents highlights of several unclassified research and development programs performed at the Naval Research Laboratory (NRL) during fiscal year 1990. Also presents history of NRL, highlights of NRL research in 1990, and general information.

14. SUBJECT TERMS

See individual papers in publication

15. NUMBER OF PAGES

260 + cover

16 PRICE CODE

17 SECURITY CLASSIFICATION OF REPORT	18 SECURITY CLASSIFICATION OF THIS PAGE	19. SECURITY CLASSIFICATION OF ABSTRACT	20 LIMITATION OF ABSTRACT
Unclassified	Unclassified	Unclassified	SAR

Naval Research Laboratory

NRL REVIEW

In this NRL Review, *we present highlights of the unclassified research and development programs for fiscal year 1990. This book fulfills a dual purpose: it provides an exchange of information among scientists, engineers, scholars, and managers; and it is used in recruiting science and engineering professionals. As you read this* NRL Review, *you will become even more aware that the Laboratory is a dynamic team working together to promote the programs, progress, and innovations that will continue to foster discoveries, inventiveness, and scientific advances for the Navy of the future.*

REFLECTIONS FROM THE COMMANDING OFFICER

In last year's Preface, I discussed what it might be like to transition to a peacetime Navy. This year, Iraq and the Persian Gulf War have taught us that peace is indeed a fragile thing. Through advances in the electronic media, we see the conflict virtually in real time. We see the performance of technology that has been engineered into systems. When a TV commentator talks about high-tech weapons, it is easy to perform a mental leap about technology and to disregard the necessity for good engineering and manufacturing to produce these systems. Most of us at the Naval Research Laboratory know that the concepts and early development for these systems were completed here and at other laboratories many years ago. We also know that the scientific and engineering talent that produced those concepts is a resource that must be constantly renewed.

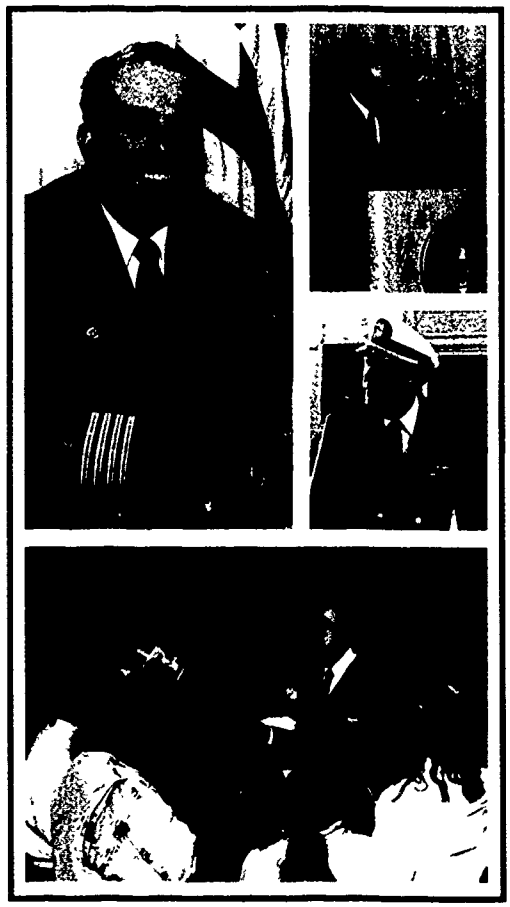

We will continue to maintain our excellence in research in these areas; there are, however, three items that I believe will become important in the next few years. First, the Navy shore establishment will draw down as the Fleet is drawn down. Now that we have won the Cold War and there is no predominant enemy such as the Soviet Union, we can expect defense budgets to shrink. I think this shrinkage will affect the shore side as well as the operating forces. The country will likely turn its attention to solving serious fiscal problems. In the 1992 budget, the President has asked for substantial increases in both civilian and military R&D accounts. We need to be ready to do this research wisely in spite of reductions.

Second, the electronic media will become an increasingly powerful method to convey science. At NRL, we have the beginning capabilities to exploit this new area. RCD's Scientific Visualization Lab, the Library's Microcomputer Software Support Center, and TID's Video Services Section have the tools to transition into modern areas of communication. They have the task to be innovative and to present scientific and technical information in increasingly graphic formats. I believe they deserve your support.

And third, a renewal of science and engineering educations among our young people is a paramount objective. Nowhere is this more important than at NRL. The greatest joy of my assignment here has been the opportunity to show off the NRL family to young people—to expose them to the wonders that are part of your everyday world.

As I move to my new assignment, I am optimistic that NRL will remain a vital and prolific institution. It has been a distinct privilege to have been associated with you.

RADM (Sel) John J. Donegan, Jr., USN

AND THE DIRECTOR OF RESEARCH

I began last year's Preface with the statement, "It is of course not possible to predict with any certainty what the world situation will be by the year 2000—in science and technology, or politics, or economics." I am preparing this year's statement while sitting in front of the television watching the CNN reports on the war in the Middle East. The television reports present a panorama of interwoven issues involving science and technology, politics, and economics. It brings home very vividly the complex interaction among these factors and the overall unpredictability of it all. There are, however, some very serious truths of which this episode reminds us. We marvel at the high technology resources that the allies have brought to bear. The scene is almost surrealistic: precision guided munitions, ballistic missile intercepts. It almost makes one too comfortable by obscuring what it took to produce these levels of sophistication. These magnificent weapons systems did not emerge instantly, as from a cartoonist's imagination. The systems, in fact, have their roots in many years of basic research studies in laser physics, materials science, solid state electronics, signal processing mathematics, and many other scientific disciplines. This research was followed by reduction to practice by scientists and engineers and finally was brought to completion through the complex process of weapons systems development. The real message from these current events to organizations like NRL is the profound responsibility that we bear. We live in a very complex world, where at any instant of time, the nation may be called upon to exercise its military capabilities. The adversaries we face are likely to be quite sophisticated. The ground work that must be laid to effectively compete in modern combat is very extensive, and the lead times are very long. The technology development requires a steadfast commitment, a perseverance through the ups and downs of funding for defense research. It is only by this steadfast commitment of those employed at NRL and elsewhere that the nation can maintain the eternal vigilance to which we were exhorted by our founding fathers. The true mission of NRL is to ensure, in concert with many other organizations, that this nation is never surprised nor defeated by a technologically superior foe. That is the business of defense research and engineering.

Dr. Timothy Coffey

NEW COMMANDING OFFICER

On February 22, 1991, CAPT Paul G. Gaffney II replaced RADM (Sel.) John J. Donegan, Jr. as the Naval Research Laboratory's Commanding Officer.

MISSION

To conduct a broadly based multidisciplinary program of scientific research and advanced technological development directed toward new and improved materials, equipment, techniques, systems, and related operational procedures for the Navy.

RESPONSIBLE FOR NAVY-WIDE LEADERSHIP IN:

- The performance of primary in-house research for the physical and engineering sciences.
- The conduct of a broadly based exploratory and advanced development program in response to identified and anticipated Navy needs;
- The development of space systems for the Navy.

CONTENTS

VIDEO CONTENTS

This video is available for loan from the Naval Research Laboratory, Ruth H. Hooker Research Library and Technical Information Center, Code 4820, Washington, DC 20375-5000.

The Naval Research Laboratory

THE NAVAL RESEARCH LABORATORY

"I believe [that] the Government should maintain a great research laboratory, jointly under military and naval and civilian control. In this could be developed the continually increasing possibilities of . . . all the technique of naval progression ....

"When the time came, if it ever did, we could take advantage of the knowledge gained through this research work and quickly produce the very latest and most efficient instruments ...."

Thomas A. Edison
The New York Times Magazine
May 30, 1915

THE NAVAL RESEARCH LABORATORY

Our Heritage

Today, when government and science seem inextricably linked, when virtually no one questions the dependence of national defense on the excellence of national technical capabilities, it is noteworthy that in-house defense research is relatively new in our Nation's history. The Naval Research Laboratory (NRL), the first modern research institution created within the United States Navy, began operations in 1923.

Thomas Edison's Vision—The first step came in May 1915, a time when Americans were deeply worried about the great European war. Thomas Edison, asked by a *New York Times* correspondent to comment on the conflict, argued that the Nation should look to science. "The Government," he proposed in a published interview, "should maintain a great research laboratory.... In this could be developed...all the technique of military and naval progression without any vast expense." Secretary of the Navy Josephus Daniels seized the opportunity created by Edison's public comments to enlist Edison's support. He agreed to serve as the head of a new body of civilian experts—the Naval Consulting Board—to advise the Navy on science and technology. The Board s most ambitious plan was the creation of a modern research facility for the Navy. Congress allocated $1.5 million for the institution in 1916, but wartime delays and disagreements within the Naval Consulting Board postponed construction until 1920.

The Laboratory's two original divisions, Radio and Sound, pioneered in the fields of high-frequency radio and underwater sound propagation. They produced communications equipment, direction-finding devices, sonar sets, and, perhaps most significant of all, the first practical radar equipment built in this country. They also performed basic research, participating, for example, in the discovery and early exploration of the ionosphere. Moreover, the Laboratory was able to work gradually toward its goal of becoming a broadly based research facility. By the beginning of World War II, five new divisions had been added: Physical Optics, Chemistry, Metallurgy, Mechanics and Electricity, and Internal Communications.

The War Years and Growth—Total employment at the Laboratory jumped from 396 in 1941 to 4400 in 1946, expenditures from $1.7 million to $13.7 million, the number of buildings from 23 to 67, and the number of projects from 200 to about 900. During WWII, scientific activities necessarily were concentrated almost entirely on applied research. New electronics equipment—radio, radar, sonar—was developed. Countermeasures were devised. New lubricants were produced, as were antifouling paints, luminous identification tapes, and a sea marker to help save survivors of disasters at sea. A thermal diffusion process was conceived and used to supply some of the ^{235}U isotope needed for one of the first atomic bombs. Also, many new devices that developed

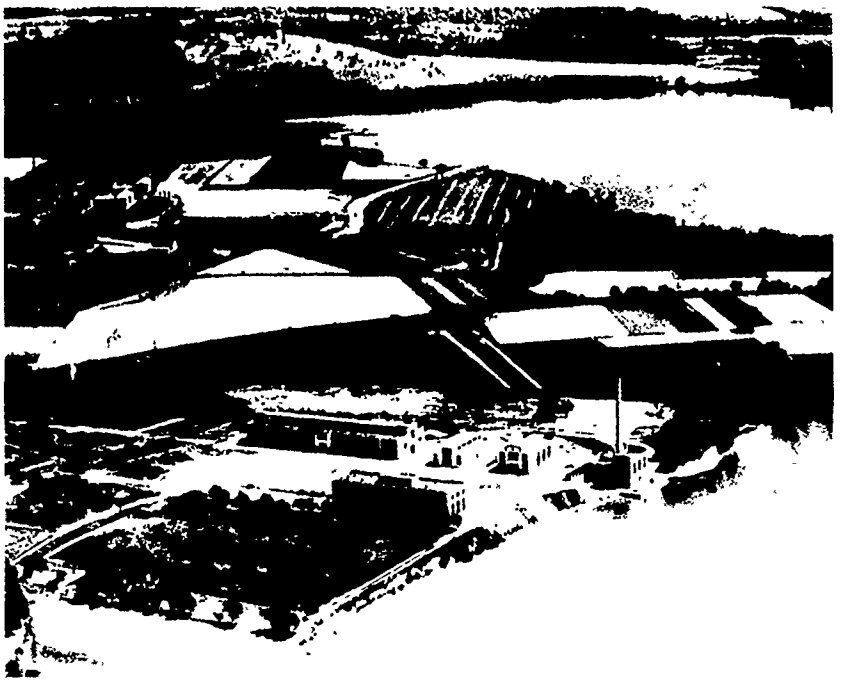

The original Naval Research Laboratory in 1923 among the farmlands of Blue Plains as viewed from the Potomac River

from booming wartime industry were type tested and then certified as reliable for the Fleet.

NRL Reorganizes for Peace—Because of the major scientific accomplishments of the war years, the United States emerged into the postwar era determined to consolidate its wartime gains in science and technology and to preserve the working relationship between its armed forces and the scientific community. While the Navy was establishing its Office of Naval Research (ONR) as a liaison with and supporter of basic and applied scientific research, it was also encouraging NRL to broaden its scope and become, in effect, its corporate research laboratory. There was a transfer of NRL to the administrative oversight of ONR and a parallel shift of the Laboratory's research emphasis to one of long-range basic and applied investigation in a broad range of the physical sciences.

However, rapid expansion during the war had left NRL improperly structured to address long-term Navy requirements. One major task—neither easily nor rapidly accomplished—was that of reshaping and coordinating research. This was achieved by transforming a group of largely autonomous scientific divisions into a unified institution with a clear mission and a fully coordinated research program. The first attempt at reorganization vested power in an executive committee composed of all the division superintendents. This committee was impracticably large, so in 1949 a civilian director of research was named and given full authority over the program. Positions for associate directors were added in 1954.

The Breadth of NRL—During the years since the war, the areas of study at the Laboratory have included basic research concerning the Navy's environments of Earth, sea, sky, and space. Investigations have ranged widely from monitoring the sun's behavior, to analyzing marine atmospheric conditions, to measuring parameters of the deep oceans. Detection and communication capabilities have benefited by research that has exploited new portions of the electromagnetic spectrum, extended ranges to outer space, and

provided means of transferring information reliably and securely, even through massive jamming. Submarine habitability, lubricants, shipbuilding materials, fire fighting, and the study of sound in the sea, have also been steadfast concerns.

The Laboratory has pioneered naval research into space, from atmospheric probes with captured V-2 rockets, through direction of the Vanguard project—America's first satellite program—to involvement in such projects as the Navy's Global Positioning System. As part of the SDI Program, the Low-Power Atmospheric Compensation Experiment (LACE) satellite was designed and built by NRL. Today, NRL is the Navy's lead laboratory in space systems research, fire research, tactical electronic warfare, microelectronic devices, and artificial intelligence. NRL has also evaluated new issues, such as the effects of intense radiation and various forms of shock and vibration on aircraft, ships, and satellites.

NRL scientists and engineers produced a number of important scientific and technical innovations within the last year. One team of Laboratory scientists developed a technique for study of the detection of light by thin films of high-T_c metal oxide superconductors. Other researchers have produced a process for development of 20-kg heavy-metal fluoride glass windows, the largest fluoride glass windows yet made. Scientists at the Underwater Sound Reference Detachment have developed a reliable underwater electrical cable connector that increases the life of sonar devices; they have also produced an inexpensive closed-chamber test facility for shock testing naval sonar transducers. A compact, lightweight, high-current modified betatron accelerator that may have important shipboard, commercial, and environmental applications, was developed at the Laboratory. This work demonstrates for the first time that cyclic accelerators can confine injected electron beams with currents in excess of 1000 amperes for a period of several thousand revolutions. NRL scientists worked on developing means of verifying undersea volcanic eruptions that accompany underwater earthquakes. A scale model Sea Launch and Recovery (SEALAR) vehicle was successfully tested in a drop test for the first time. Other laboratory researchers developed a highly sensitive and precise instrument to measure the coefficients of thermal expansion in materials. This apparatus will be useful in measuring the stability of space optics. Several NRL-designed experiments went aloft on the Combined Release and Radiation Effects Satellite (CRRES) launched by NASA in July 1990. The CRRES is designed to provide improved

NRL's Heavy Ions in Space (HIIS) Experiment, which was one of 57 experiments aboard NASA's Long Duration Exposure Facility, was retrieved from space by the crew of the Space Shuttle Columbia on January 12, 1990. See article on p. 196.

knowledge of ionospheric and magnetospheric phenomena. A new Low-Altitude/Airspeed Unmanned Research Aircraft (LAURA) was developed to carry electronic warfare payloads for long flight at shiplike speeds. Also new in 1990 was a laboratory Epi-Center established to promote work in the combination of magnetic and semiconducting integrated circuitry. A Human-Computer Interaction Laboratory (HCIL) was founded to investigate improved human-computer interaction in information systems. In related work, NRL scientists investigated methods by which computer users can communicate commands to computers through eye movements.

One goal, however, has guided NRL's diverse activities through the years—to conduct pioneering scientific research and development that will provide improved materials, equipment, techniques, systems, and operations for the Navy, for the Department of Defense (DoD), and for the U.S. Government.

NRL Today

ORGANIZATION AND ADMINISTRATION

The position of NRL within the Navy is that of a field command under the Chief of Naval Research.

Heading the Laboratory with joint responsibilities are the naval commanding officer, Capt. John J. Donegan, Jr., USN, and the civilian director of research, Dr. Timothy Coffey. Line authority passes from the commanding officer and the director of research to five associate directors of research and the director of one technology center. Research is performed in the following areas:

- General Science and Technology
- Warfare Systems and Sensors Research
- Materials Science and Component Technology
- Naval Center for Space Technology.

Further details of the Laboratory's organization are given on the organizational chart appearing in the "General Information" section.

NRL operates as a Navy Industrial Fund (NIF) activity. As a NIF activity, all costs, including overhead, must be charged to various research projects. Funding in 1990 came from the Chief of Naval Research, the Naval Systems Commands, and other government agencies, such as the Defense Advanced Research Projects Agency, the Department of Energy, and the National Aeronautics and Space Administration as well as several nongovernment activities. NRL's relationship with its sponsoring agencies, both inside and outside DoD, is defined by a comprehensive policy on interagency support agreements.

Besides funding for scientific work, NRL receives Navy monies for general construction, maintenance, and operations.

PERSONNEL DEVELOPMENT

At the end of 1990, NRL employed 3680 personnel—47military officers, 67 enlisted men and women, and 3566 civilians. In the research staff, there are 768 employees with doctorate degrees, 392 with masters degrees, and 652 with bachelors degrees. The support staff assists the research staff by providing administrative, computer-aided designing, machining, fabrication, electronic construction, publication, personnel development, information retrieval, large mainframe computer support, and contracting and supply management services.

Opportunities for higher education and other professional training for NRL employees are available through several programs offered by the

NRL today as viewed from the east

Employee Development Branch. These programs provide for graduate work leading to advanced degrees, advanced training, college course work, short courses, continuing education, and career counseling. Graduate students, in certain cases, may use their NRL research for thesis material.

For non-NRL employees, several post-doctoral research programs exist. There are also cooperative education agreements with several universities, summer and part-time employment programs, and various summer and interchange programs for college faculty members, professional consultants, and employees of other government agencies.

NRL has active chapters of Women In Science and Engineering, Sigma Xi, Toastmaster's International, and the Federal Executive and Professional Association. Three personal computer clubs meet regularly—Edison Atari, NRL IBM-PC, and Edison Commodore. An amateur radio club, a drama group—the Showboaters, and several sports clubs are also active. NRL has a recreation club that provides swimming, sauna, whirlpool bath, gymnasium, and weight-room facilities. The recreation club also offers classes in martial arts, aerobics, swimming, and cardio-pulmonary resuscitation.

A community outreach program at NRL provides tutoring for local students, science fair judging, participation in high school and college career day programs, an art and essay contest during Black History Month, student tours of NRL, and a Christmas party for disadvantaged children with gifts donated by Laboratory employees.

NRL has an active, growing Credit Union with assets of $118 million and a membership numbering 15,250. Public transportation to NRL is provided by Metrobus.

For more information, see the *NRL Review* chapter entitled "Programs for Professional Development."

SCIENTIFIC FACILITIES

In addition to its main campus of about 130 acres and 152 buildings, NRL maintains 12 other

research sites including a vessel for fire research and a Flight Support Detachment. The many diverse scientific and technological research and support facilities are described in the following paragraphs.

Research Facilities

• Space Science

NRL is the Navy's main laboratory for conducting basic research and development in the space sciences. The Space Science Division has a number of commitments for space experiments in the areas of upper atmospheric, solar, and astronomical research aboard NASA, DoD, and other space projects. Division scientists are involved in major research thrusts that include remote sensing of the upper atmosphere by using ultraviolet sensing, studies of the solar atmosphere by using spectrographic techniques, and studies of astronomical radiation ranging from the ultraviolet through the cosmic rays. The division maintains facilities to design, construct, assemble, and calibrate space experiments. A network of VAX computers, super minicomputers, image processing hardware, a PDS microdensitometer, and Cray and Connection Machine access are used to analyze and interpret space data.

• Center for Advanced Space Sensing

The Center for Advanced Space Sensing conducts a program of basic research, science, and applications to develop new concepts for sensors and imaging systems for objects and targets on the Earth and in the near-Earth environment, as well as in deep space. The research, both theoretical and experimental, leads to discovering and understanding the basic physical principles and mechanisms that give rise to the background environmental emissions and targets of interest and to absorption and emission mechanisms of the intervening medium. Accomplishing this research requires the development of sensor systems technology. The development effort includes active and passive sensor systems used for the study and analysis of the physical characteristics of phenomena that evolve from naturally occurring background radiation, such as that caused by the Earth's atmosphere and oceans and man-made or induced phenomena, such as ship/submarine hydrodynamic effects. The research includes theory, laboratory, and field experiments leading to ground-based, airborne, or space systems for use in remote sensing, astrometry, astrophysics, surveillance, nonacoustic ASW, and improved meteorological/oceanographic support systems for the operational Navy. Special emphasis is given to developing space-based platforms and exploiting existing space systems.

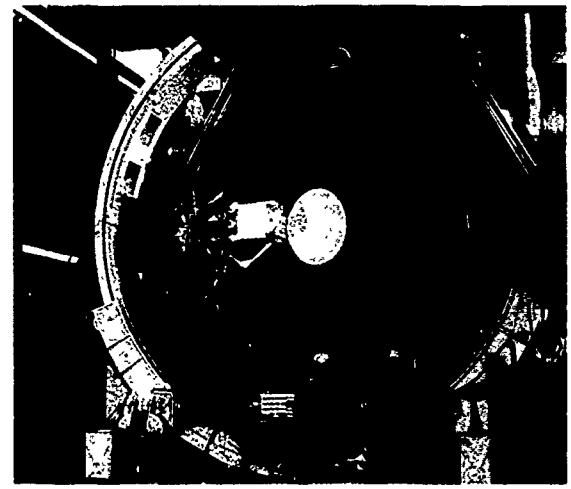

The MAS flight instrument is shown here entering a large thermal vacuum chamber and being readied for a space flight in June 1991. The instrument spectrometer was designed and fabricated in NRL's newly established Center for Advanced Space Sensing.

• Computational Physics and Fluid Dynamics

The Laboratory for Computational Physics and Fluid Dynamics (LCP&FD) has developed a Graphical and Array Processing System (GAPS). The system provides communications and common memory for large simulations on parallel array processors and immediate displays of results from other sources on high-resolution, high-speed graphics monitors. The system is front ended by two VAX 11/780s that provide control and

communication to other sites at NRL and outside laboratories. A 1.4-gigabyte high-speed disk is incorporated for simulations storage and replay. The computational engines are six 30-megaflop array processors supported by a vectorizing FORTRAN compiler. The current graphics devices are a Tektronix and a Metheus with 1024 × 1280 color raster resolution and high-speed block data transfer capability, and an IRIS 4D vector display. A 64-million word Convex C210 has recently been installed and incorporated into the NRL network.

The LCP&FD also maintains fluid dynamic laboratory facilities that include a 30-m wind/wave tank to study nonlinear ocean wave processes and fluid/structure interactions; a 20-m stratified tow channel to study geophysical flows, jets, and wakes; and blow-down water tunnels to study hydroacoustics, turbulent boundary layers, and non-Newtonion flows. Experimental efforts using these facilities are supported by flow measurement systems including multicomponent laser velocimeters and anemometers; digital image processing of flow visualization; hydrophones; imaging infrared radiometers; and a variety of microwave radar measurement systems for remote sensing studies of hydrodynamic processes. On-line experiment control, data acquisition, and processing are achieved with a central HP1000 system or one of a number of smaller, portable units.

• Condensed Matter and Radiation Sciences

Ion Implantation Facility—The facility consists of a 200-keV ion implanter with specialized ultrahigh vacuum chambers and associated in situ specimen analysis instrumentation. The facility is used to develop advanced surface treatments of materials to modify their properties and improve corrosion and wear resistance.

3-MeV Tandem Van de Graaff—This facility is used to study charged particle radiation damage effects such as occur in space, to perform Rutherford backscattering spectroscopy and nuclear reaction analysis to provide high-sensitivity composition depth profiles, and to perform MeV energy implants in materials.

60-MeV Electron Linear Accelerator (LINAC)—The LINAC produces intense electron beams with 10 to 65 MeV energies. Pulse rates from 1 to 360 s and widths from 50 ns to 1.4 ms are selectable. This facility is widely used to study radiation effects on microelectronics and materials for both NRL and other important DoD satellite and missile programs. It is also used to study radiation effects on the new, high-critical-temperature superconductors. Single beam pulses can be analyzed and stored in a fast multichannel digitizer system.

Hypervelocity Impact Facilities—Three facilities are used for ballistics research at speeds exceeding 6 km/s with toxic or explosive targets. The projectile velocity, orientation, and dynamic projectile-target interaction can be measured.

Synchrotron Radiation Facility—An intense monochromatic X-ray photon source, tunable from 10 eV to 12 keV, is available on the NRL-developed beam lines at the National Synchrotron Light Source at Brookhaven National Laboratory. Environmental target chambers can span a pressure range from ambient to several hundred kbar and temperatures from 10 to 1500 K. A six-circle computer controlled goniometer is used to control and position targets.

• Plasma Physics

The Plasma Physics Division is the major center for in-house Navy and DoD plasma physics research. The division conducts a broad experimental and theoretical program in basic and applied research in plasma physics, which includes laboratory and space plasmas, pulsed-power sources, intense electron and ion beams, atomic physics, laser physics, and numerical simulations. The facilities include an extremely high-power laser, PHAROS III, for the laboratory simulation of space plasmas and high-latitude nuclear

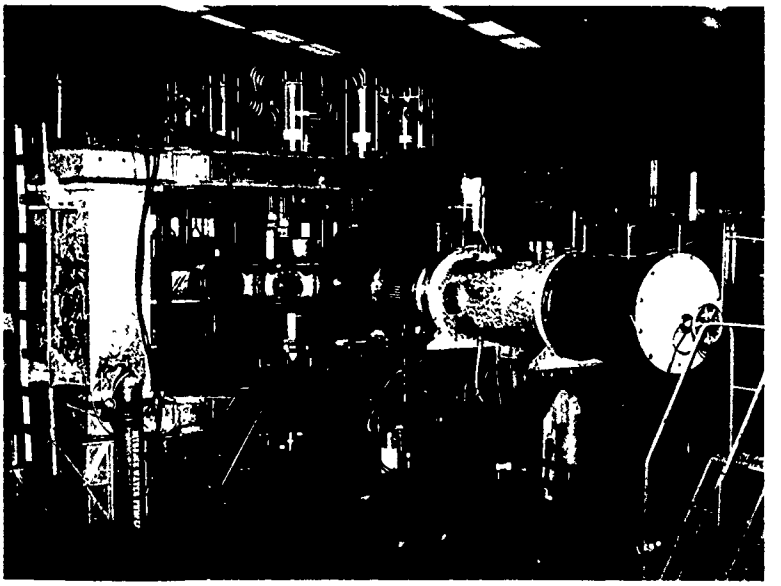

This compact, lightweight, high-current torodial accelerator was recently developed by scientists of the Plasma Physics Division It has potential commercial and environmental applications, such as generation of high-power microwaves, sterilization of pharmaceuticals and potable water, sludge disinfection, vulcanization of rubber, crosslinkage of polymers, and cracking of crude oil

explosion effects studies. The division has developed a variety of pulsed power sources to generate electron and ion beams. powerful discharges, and various types of radiation. The largest of these pulsers, GAMBLE II, is used to study the production of megampere electron beams and for producing very hot, high-density plasmas. Other generators are used to produce particle beams that are injected into magnetic fields and/or cavities to generate intense microwave pulses. A charged-particle-beam (CPB) propagation facility exists for testing advanced CPB propagation (both endo- and exoatmospheric) concepts. A 5-MW generator injects pulses of electron current into preheated ionization channels to study the effectiveness of propagation under various conditions. This division also operates a modified betatron facility for studying methods to accelerate high-current electron beams to energies in the 25- to 50-MeV range.

• Acoustics

NRL's facilities in support of acoustical investigations are located at the main Laboratory site and in Orlando, Florida, at the Underwater Sound Reference Detachment (USRD). At the main Laboratory site, there are three research tanks instrumented to study echo characteristics of targets and to develop devices. There is also an underwater acoustic holography facility for research in acoustic fields and a water tunnel having a large blow-down channel with a 15-m test section used for acoustic and flow-induced vibration studies of towed line arrays and flexible cables. NRL is investigating dynamic GPS interferometric navigation to extend the capabilities of their fixed-wing airborne gravity measurement system, which is accurate to better than 3 mGal (3×10^{-5} m/s^2), to operation over land. In addition to providing the accurate positioning necessary for airborne gravimetry, GPS interferometric altimetry, in conjunction with radar altimeters, may be used in the future to study oceanographic phenomena and to obtain accurate ice profiles in glaciated parts of the world. The Connection Machine, an experimental facility that exploits the natural computational parallelism inherent in data-intensive research problems, has

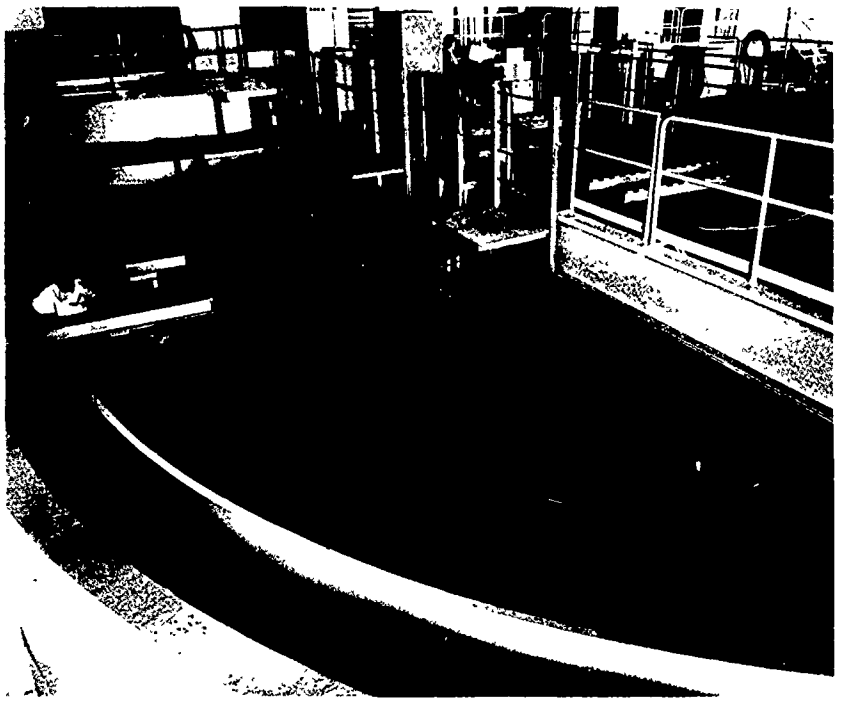

NRL's facilities in support of acoustic investigations are located at the main Laboratory site in the Acoustic Division and in Orlando, Florida, at the Underwater Sound Reference Detachment (USRD). At the main Laboratory site, there are three research tank facilities—one instrumented for near-field acoustical holography, one for acoustic scattering measurements, and a third recently completed facility for the study of underwater structural acoustics The latter is instrumented with state-of-the-art robotic controllers for acoustical scanning of large, irregularly shaped bodies

been established for use by researchers both within and outside the Laboratory. The USRD facilities are described with NRL's field stations.

• Radar

NRL has gained worldwide renown as the "birthplace of radar" and has maintained its reputation as a leading center for radar-related research and development for a half century. An impressive array of facilities managed by NRL's Radar Division continues to contribute to this reputation. These include airborne and laboratory radar cross section measurement systems, an airborne APS-137 radar with ISAR image processing, and an airborne adaptive array laboratory. Also, the division manages and maintains a radar display test bed, an IFF ground station, a digital signal processing facility, and a radar cross section prediction facility. A radar research and development activity is located at the Chesapeake Bay Detachment (CBD), Randle Cliffs, Maryland. It has separate facilities for specific types of systems that range from high-frequency, over-the-horizon systems to millimeter wave radars. The SENRAD radar test bed, a flexible and versatile system for demonstrating new developments in radar, and a point defense radar test bed are also located at CBD.

• Information Technology

The Information Technology Division, which includes the Navy Center for Applied Research in Artificial Intelligence, is at the forefront of DoD research and development in telecommunication, computer science, and artificial intelligence. The division maintains a local area computer network to support its research.

The network comprises a Gould 9005 UNIX machine, Symbolics, LISP machines, SUN and

NRL scientists in the Human Computer Interaction Laboratory are investigating methods by which computer users can communicate commands to computers through eye movement, as demonstrated here

Apollo workstations, laser printers, network gateways, and terminal servers. A Butterfly 128-node parallel processor is also part of the division's computer resources. The network is connected to NRL's Central Computing Facility and to the MILNET, ARPANET, and other university networks. The network will become part of the Strategic Defense Initiative (SDI) Battle Management Technology validation facility.

• Electronic Warfare

The scope of research and development at NRL in the field of electronic warfare covers the entire electromagnetic spectrum, from basic technology research, component and subsystem development, to system design and effectiveness evaluation. Major emphasis is placed on providing the methods and means to counter enemy hostile actions in all battle phases, from the beginning—when enemy forces are mobilized for an attack—through the final engagement stages. For this purpose, NRL has constructed special research and development laboratories, anechoic chambers, and facilities for modeling and simulation. NRL has also added extensive new facilities where scientists can focus on the coordinated use of all organic defensive and offensive resources now present in the Fleet.

• Laboratory for the Structure of Matter

The Laboratory investigates the atomic arrangement of matter to improve old materials or to invent new materials. Various diffraction methodologies are used to make these investigations. Subjects of interest include the structural and functional aspects of energy conversion, ion transport, device materials, and physiologically active substances such as drugs, antibiotics, and antiviral agents. Theoretical chemistry calculations are used to complement the structural research. A real-time graphics system aids in modeling and molecular dynamics studies.

• Center for Bio/Molecular Science and Engineering

The Center for Bio/Molecular Science and Engineering conducts research in biotechnology aimed at solutions of Navy and Department of Defense problems. Long-term research directions focus on complex biomolecular systems and are aimed at gaining a fundamental understanding of the structures and functions of biologically derived systems. The staff of the Center is an interdisciplinary team performing basic and applied research in a number of diverse areas including biochemistry, biophysics, synthesis, and thin-film fabrication. Because of the interdisciplinary nature of this work, most of the research being performed in the Center is of a collaborative nature. The Center's associate concept is a key way of establishing this collaboration. Center associates come from other research areas within NRL as well as universities, industry, and other Government laboratories.

• Chemistry

NRL has been a major center for chemical research in support of Navy operational requirements since the late 1920s. The Chemistry Division continues its tradition with a broad spectrum of basic and applied research programs concerned with fuels and combustion, corrosion, advanced polymeric materials, ultrasensitive detection methods for chemical agents, and special

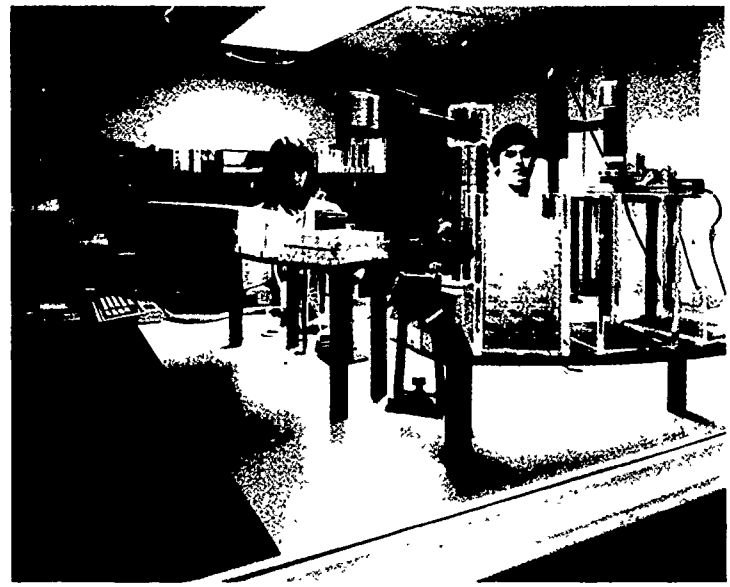

Shown is the automated protein crystal growth system developed by the Laboratory for the Structure of Matter to prepare large, single crystals of proteins for X-ray diffraction studies

Lipsome-encapsulated hemoglobin (LEH) is made for in vitro and in vivo studies in small animal models by NRL's Center for Bio/Molecular Science and Engineering

materials for electronic warfare applications. Modern facilities for research include a wide range of the most modern optical, magnetic, and ion-based spectroscopic devices, a 325-m^3 (11,400 ft^3) fire research chamber (Fire I), multiple facilities for materials synthesis and physical/chemical characterization, high- and low-temperature equipment, and extensive surface-analytical instrumentation. The division has recently developed the 475-ft ex-USS *Shadwell* (LSD-15) into an advanced fire research ship.

• Materials

NRL has capabilities for X-ray and electron diffraction analyses and for electron and Auger

spectroscopy. It has a secondary ion mass spectrometer for surface analysis that significantly extends the diagnostic capability of the technique. A high-resolution, reverse-geometry mass spectrometer is used to probe reactions between ions and molecules. The Laboratory has a fully equipped fatigue and fracture laboratory, a modern vacuum arc melting furnace for reactive metals, an ultrasonic gas atomization system for making metal powders, and hot isostatic press facilities. The Laboratory's cryogenic facilities include dilution refrigerators and superconducting magnetic sensors for measuring ultrasmall magnetic fields. Also available are two molecular beam epitaxy devices for growing thin films.

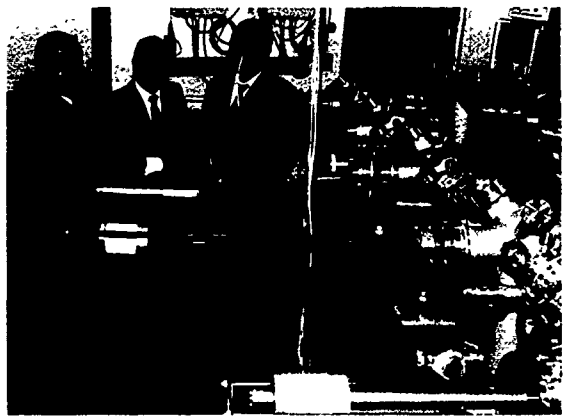

A new Epi-Center was recently dedicated at NRL for the epitaxial growth of magnetic and electronic materials. This is the first multichambered growth system devoted to combining magnetic and semiconducting integrated circuitry at NRL and the first at a DoD laboratory. The $1.4M facility is sponsored and funded jointly by the Materials Science and Technology Division and the Electronics Science and Technology Division.

• Optics

Ultralow-Loss, Fiber-Optic Waveguides—NRL has developed record-setting ultrahigh transparency infrared waveguides. These fluoride glass materials offer the promise of long-distance communications without the need of signal amplification or repeaters.

Focal Plane Evaluation Facility—This facility has extensive capabilities to measure the optical and electrical characteristics of infrared focal plane arrays being developed for advanced Navy sensors.

IR Missile-Seeker Evaluation Facility—This facility performs open-loop measurements of the susceptibilities of infrared tracking sensors to optical countermeasures.

Large Optic, High-Precision Tracker—NRL has developed a tracker system with an 80-cm primary mirror for atmospheric transmission and target signature measurements. By using a quadrant detector, the servo system has demonstrated a 12-mrad tracking accuracy. An optical correlation tracker system tracks objects without a beacon.

High-Energy Pulsed Hydrogen Fluoride, Deuterium Fluoride Laser—NRL has constructed a pair of pulsed chemical lasers each capable of producing up to 30 J of laser energy at 2.7 to 3.2 mm and 3.8 to 4.5 mm in a 2-ms pulse. This facility is used to investigate a variety of research areas including stimulated Brillouin scattering, optical phase conjugation, pulsed laser amplification, propagation, and beam combining.

Fiber-Optics Sensors—The development and fabrication of fiber-optic sensor concepts, including acoustic, magnetic, and rate-of-rotation sensors, are conducted in several facilities within the Laboratory's Optical Sciences and Acoustics Divisions. Equipment includes facilities for evaluating optical fiber coatings, fiber splicers, an acoustic test cell, a three-axis magnetic sensor test cell, a rate table, and various computers for concept analysis.

Digital Processing Facility—This facility is used to collect, process, analyze, and manipulate infrared data and imagery from several sources.

Emittance Measurements Facility—NRL routinely performs measurements of directional hemispherical reflectance from 2 to 16 mm in the infrared by using a diffuse gold integrating sphere and a Fourier Transform Spectrophotometer

(FTS). Sample temperatures can be varied from room temperature to 250°C and incidence angles from 0° to 60°.

• Electronics Science

In addition to specific equipment and facilities to support individual scientific and technology programs in electronics and electronic-materials growth and analysis, NRL operates the Nanoelectronics Processing Facility that provides services to electronics programs throughout the Laboratory and to external organizations. This facility provides support for NRL programs that require microelectronics processing skills and equipment. The facility includes a nanowriter that can be used to fabricate nanoscale (80 Å) structures and, in general, supplies NRL programs with a range of items from discrete structures and devices to complete integrated circuits with very large scale integration (VLSI) complexity based on silicon metal oxide semiconductors (MOS) submicrometer technology.

• Naval Center for Space Technology

In its role as a center of excellence for space systems research, the Naval Center for Space Technology (NCST) designs, builds, analyzes, tests, and operates spacecraft, as well as identifies and conducts promising research to improve spacecraft and their support systems. NCST facilities that support this work include large and small anechoic radio frequency chambers, clean rooms, shock and vibration facilities, an acoustic reverberation chamber, large and small thermal/vacuum test chambers, and modal analysis test facilities. NCST has a facility for long-term testing of satellite clock time/frequency standards under thermal/vacuum conditions linked to the Naval Observatory; a 5-m optical bench laser laboratory; and a hologram research laboratory to conduct research in support of the development of space systems.

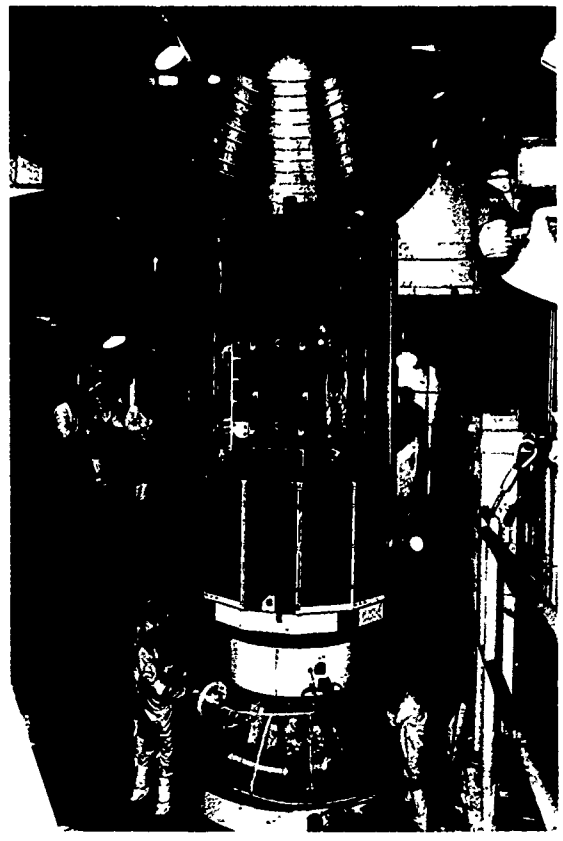

A satellite system designed and built by NRL to carry Strategic Defense Initiative Organization (SDIO)-sponsored experiments was launched on February 14, 1990. Shown here is the half-nose fairing being installed on the Delta II rocket that launched the Low-power Atmospheric Compensation Experiment (LACE) satellite.

• Center for Advanced Space Sensing

The Center for Advanced Space Sensing conducts a broad program in sensing applications at wavelengths from radio to optical. This program includes space experiments, radio, IR, and optical astronomy by using ground-based facilities operated by the Center of national facilities (such as the Very Large Array of the National Radio Astronomy Observatory), and relevant technology applications to remote sensing, precise tracking, navigation, and imaging. To accomplish these programs, the Center operates Maryland Point Observatory, which consists of 84- and 85-ft radio antennas, which are used primarily for Very Long Baseline Interferometry (VLBI) and background

A new technique has been developed to make holograms with diode lasers. Here a researcher places a holographic slide in a holder while another researcher observes the laser diode beam through an infrared viewer.

environmental emissions at radio wavelengths. For the processing of VLBI data, the Center is a partner in the Washington, DC, Correlator Facility. For actively illuminated objects at radio wavelengths, the Center has a SAR image processing facility consisting of high-density digital recorders, super minicomputers, and software to process images. The Center is also developing space-based sensor technology. The middle-atmosphere sounder is a limb-scanning microwave spectrometer designed to fly on the Space Shuttle. At optical wavelengths, an interferometer capable of precision measurements of the size and positions of celestial objects is operated on Mount Wilson, California. To satisfy the computing needs generated for image processing and other data processing needs, the Center has an Alliant VFX-40 visualization graphics supercomputer.

Research Support Facilities

• Technical Information Services

The Ruth H. Hooker Research Library and Technical Information Center contains more than one million items including current journals. Its collections can be searched by computer-based catalogs. The Library also provides interlibrary loans, on-line literature searches, access to CD ROM databases, loans of microcomputer software, and a full range of reference services, including assistance in selecting and using microcomputer software.

Publication services include writing, editing, composition, phototypesetting, and publications consultation. The primary focus is on using computer-assisted publication techniques to produce scientific and technical information containing complex artwork and equations.

The diversity of the research conducted at NRL requires a corresponding diversity of graphic support, such as technical and scientific illustrations, computer graphics, design services, photographic montages/composites, airbrushing/ photographic retouching, calligraphy, display panels, and framing.

Photography services include motion picture, video, and still-camera coverage for data documentation both at NRL and in the field. A photographic laboratory offers custom processing and printing of black and white and color films. Video services include producing video reports of scientific and technical programs. A new video studio and editing facility with 3/4 in. and VHS editing equipment were recently dedicated.

Information specialists prepare written and visual materials for dissemination to the public for use at exhibitions, professional meetings and seminars, and for internal information.

The DICOMED computer graphics system produces high-resolution, high-quality color images on 35-mm slides, 8 in. × 10 in. viewgraphs, 16-mm movies, or microfiche. It is driven by tapes generated on many different computer systems. It also accepts MacIntosh files in PICT or Scrapbook format.

• Central Computing Facility

The Central Computing Facility (CCF) consists of a Cray X-MP/216 Class 6.5 supercomputer supported by five DEC/VAX 700/8000 front-end systems. The peak processing speed of the two-processor Cray supercomputer is 470 million-floating-point-operations-per-second (MFLOPS). It has 16 million (64-bit) words of static MOS memory in 32 interleaved

banks and three interconnected I/O processors with four million words of shared buffer memory.

The system is accessed by VAX minicomputers at the central computing site by local area networks at NRL, by the Internet (MILnet/DDN), and by SURAnet/NSFnet at remote sites. The CCF front-end system provides terminal access by direct line, dial-up, local area networks, or the Internet. It also provides database management, document processing, and graphics support. FORTRAN, PASCAL, and C are the primary programming languages for the Cray system. A wide range of scientific, statistical, and mathematical software is also available. MSC NASTRAN, NAG, IMSL, and ABAQUS are available on the Cray

A complete range of graphics output devices is available including graphics terminals, laser printers, and plotters. Graphics software can also generate tapes for the DICOMED film-processing system located in TID. An IRIS 4D/GT graphics workstation with Matrix camera, color printer, and NTSC video output is available in the VISc lab at the Research Computation Division.

FIELD STATIONS

NRL has acquired or made arrangements over the years to use a number of field sites or auxiliary facilities for research that cannot be conducted in Washington, DC. They are located in Maryland, Virginia, California, Colorado, Alabama, and Florida. The two largest facilities are the Chesapeake Bay Detachment (CBD) and the Underwater Sound Reference Detachment (USRD).

- Chesapeake Bay Detachment (CBD)

CBD occupies a 168-acre site near Chesapeake Beach, Maryland, and provides facilities and support services for research in radar, electronic warfare, optical devices, materials, communications, and other subjects. Because of its location high above the Chesapeake Bay on the western shore, unique experiments can be performed in conjuntion with the Tilghman Island site 16 km across the bay from CBD. Some of these experiments include low clutter and generally low background radar measurements. By using CBD's support vessels, experiments are performed involving dispensing chaff over water and radar target characterizations of aircraft and ships. Basic research is also conducted in radar antenna properties, testing of radar remote sensing concepts, use of radar to sensor ocean waves, and laser propagation. CBD also hosts facilities of the Navy Technology Center for Safety and Survivability, which conducts fire research on simulated carrier, surface, and submarine platforms.

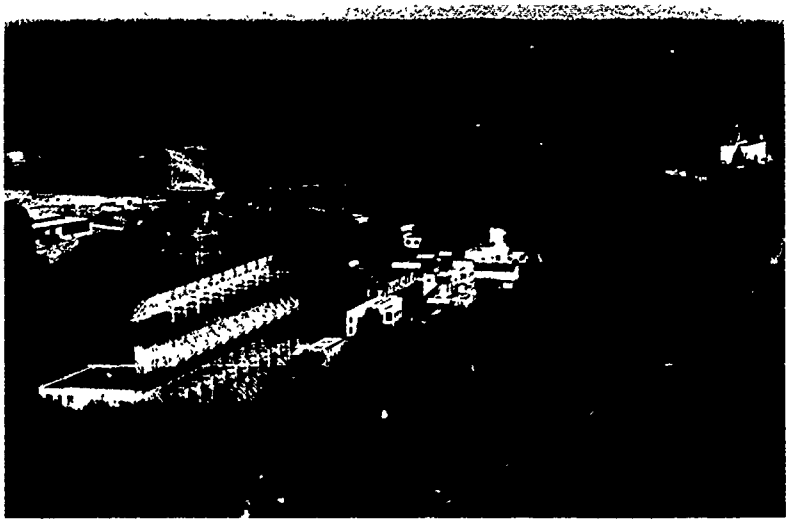

The Chesapeake Bay Detachment, located at Chesapeake Beach, Maryland

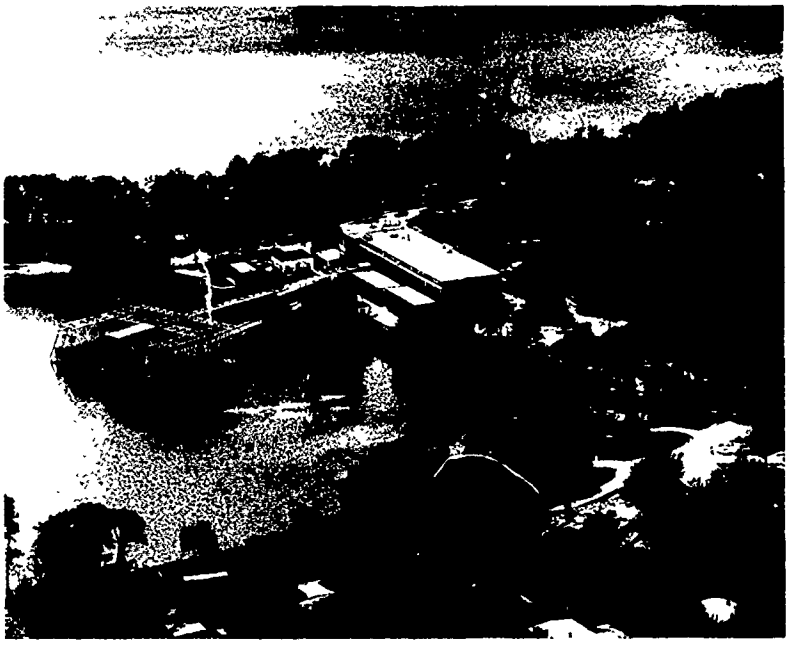

The Underwater Sound Reference Detachment, Orlando, Florida

• Underwater Sound Reference Detachment (USRD)

Located at Orlando, Florida, USRD functions as a link in the traceability of underwater sound measurements to the National Institute of Standards and Technology and also performs R&D for sonar transducers and related acoustic materials. Its semitropical climate and two clear, quiet lakes (the larger 11-m deep and nearly circular) are distinct assets to its research and development on sonar transducers and underwater reference standards and to its improvement of techniques to calibrate, test, and evaluate underwater acoustic devices. USRD has two large, high-pressure tanks for simulating ocean depths to approximately 700 m and 2100 m. Smaller pressure tanks simulate depths to approximately 7000 m. A spring-fed lake, located in a remote area about 40 miles north of USRD (the Leesburg Facility), provides a natural tank for water depths to 52 m with an ambient noise level 10 dB below that for sea state zero; larger objects can be calibrated here. A 15-cm shock tube simulates 60 pounds of high explosive at a range of 20 ft for shock testing small sonar transducers. The detachment provides acoustic equipment and calibration services not only to hundreds of Navy activities and their contractors but also to private firms and universities not engaged in DoD contracts.

• Marine Corrosion Test Facility

Located on Fleming Key at Key West, Florida, this facility offers an ocean-air environment and clear, unpolluted, flowing seawater for studies of environmental effects on materials. Equipment is available for experiments involving weathering, general corrosion, fouling, and electrochemical phenomena, as well as coatings, cathodic protection devices, and other means to combat environmental degradation.

• Flight Support Detachment (NRL FSD)

Located on the Patuxent River Naval Air Station at Lexington Park, Maryland, NRL's FSD provides facilities and service for airborne research. Four P-3 variant aircraft are maintained and operated by NRL and Detachment personnel.

The Marine Corrosion Facility, located at the Naval Air Station in Key West, Florida, has 1000 feet of seawall, 8000 square feet of laboratory and test areas, and an endless supply of natural seawater for evaluating ship systems and components

These airplanes annually log over 2000 hours of flying time on a wide variety of projects ranging from bathymetry and electronic countermeasure research to studies of radar signal reflections.

• Other Sites

Some field sites have been chosen primarily because they provide favorable conditions to operate specific antennas and electronic subsystems and are close to NRL's main site. Maryland Point, south of NRL, operates two radio telescopes (25.6 and 26 m in diameter) for radio astronomy research. NRL's Waldorf Facility, south of NRL, operates 18.3-m, X-band and S-band antennas for space and communications research. Pomonkey, a field site south of NRL, has a free-space antenna range to develop and test a variety of antennas. The antenna model measurement range in Brandywine, Maryland, has a 4.6-m diameter turntable in the center of a 305-m diameter ground plane for conducting measurements on scale-model shipboard and other antenna designs.

• Research Platforms

NRL uses ships and aircraft to conduct some of its research. Ocean-going research ships are obtained from a pool of vessels maintained by the Naval Oceanographic Office Bay St. Louis, Mississippi.

Scientists from NRL's Space Science Division and Woods Hole Oceanographic Institution (WHOI) are working together to conduct a series of air-sea interaction experiments by using airships In these experiments, the scientists will make microwave scatterometer and oceanic surface-flux measurements from a manned airship to develop an improved, satellite-based, remote wind-sensing system

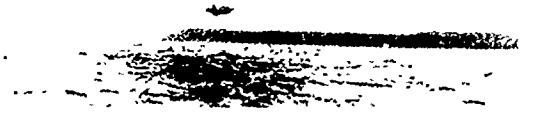

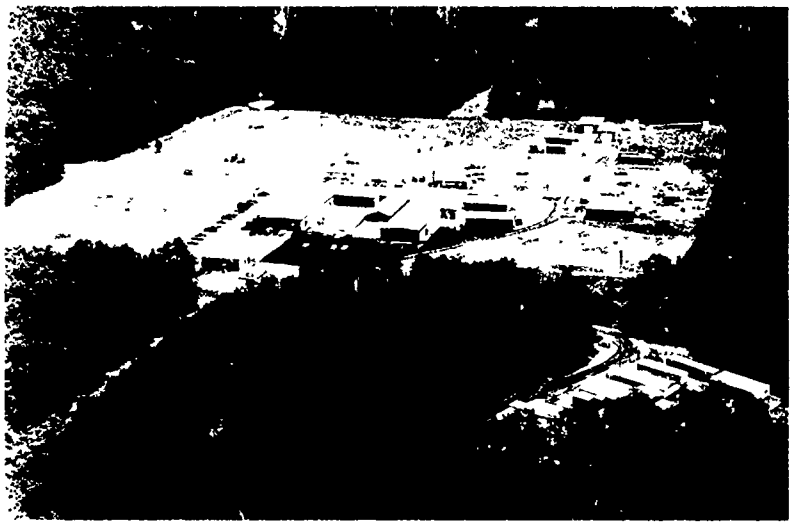

The Blossom Point Satellite Tracking and Command Facility

The ex-USS *Shadwell* (LSD-15), now anchored in Mobile Bay, Alabama, serves as a fire test platform for the Navy's Systems Commands, under the control of NRL's Navy Technology Center for Safety and Survivability

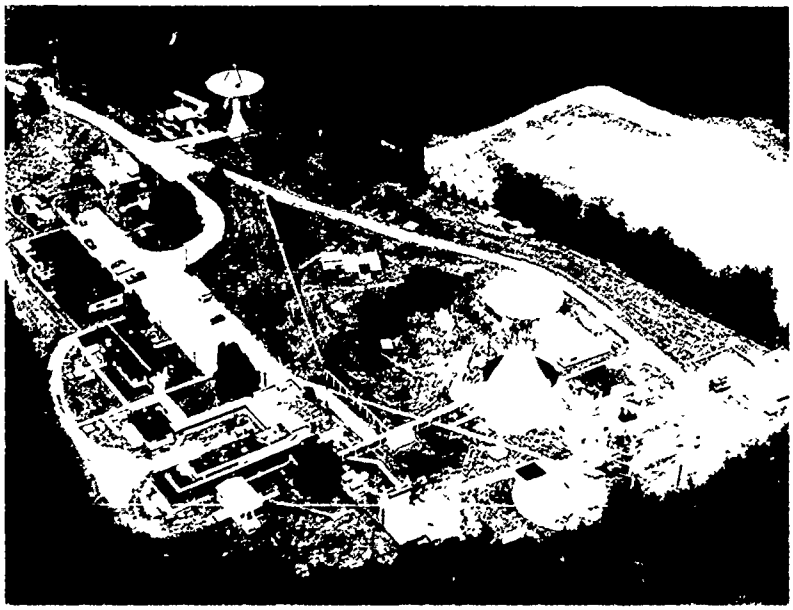

The Microwave Space Research Facility

NRL in the Future

To continue its growth and provide preeminent research for tomorrow's Navy, NRL must maintain and upgrade its scientific and technological facilities at the forefront. Its physical plant to house these facilities must also be adequate. NRL recently embarked on a Corporate Facilities Investment Plan (CFIP) to renew its physical plant. This plan and future facility plans are described below.

THE CORPORATE FACILITIES INVESTMENT PLAN (CFIP)

The CFIP is a financial spending plan to provide modern research facilities at NRL by the year 2000. The plan calls for both Congressional and Laboratory investment and is updated and altered as changes occur in scientific emphasis and Congressional attitude. Over the past several years, Congressionally approved military construction (MILCON) funds were used to construct the new Electro-Optics laboratory and to complete the final phase of the Tactical Electronic Warfare facility. At this time, funds are being requested to build a second wing to the Electro-Optics Building and a facility to house the Naval Center for Space Technology.

In the past years, NRL general and administrative (G&A) funds were used to renovate Buildings 16, 32, 34, 35, 46, 47, 56, 58, and major portions of several other buildings. Approximately $4 million of Laboratory funding is budgeted for modernization each year.

- Center for Bio/Molecular Science and Engineering

The Center for Bio/Molecular Science & Engineering (BMSE) was established in October 1989 to conduct research on biomaterials and biotechnology of interest to the Navy. Work is now under way on the renovation of Building 12 to house this research effort. In Phase I, 5000 ft^2 in the basement of Building 12 are being renovated to contain a complete electron microscopy facility, including three electron microscopes and preparative work areas. Additional facilities will include a darkroom and laser laboratories. This work is scheduled for completion in FY 91. Major renovations on the remainder of the 35,000 ft^2 projected for FYs 93 and 94 will provide modern facilities for biotechnology research, such as sterile hoods, controlled temperature rooms, biochemistry and genetic engineering wet labs, and stringent clean rooms.

- Vacuum Ultraviolet Space Instrument Test Facility

The Space Science Division will soon install a new vacuum ultraviolet space instrument test facility. This facility will be capable of housing space instrumentation up to 2 m in diameter and 5 m in length. While exposed to high vacuum (10^{-7} torr), instruments can be illuminated by a simulated solar spectrum for alignment and verification tests. The facility will also include a 13-m evacuated extension containing sources to simulate the solar corona. An externally mounted 1-m diameter heliostat will be employed to project a beam from the sun directly into the vacuum chamber. In the near future, the facility will be used to test space instruments that are presently under development for flight on NASA's Orbiting Solar Laboratory spacecraft and European Space Agency's Solar and Heliospheric Observatory spacecraft. The facility will be fully operational in 1991.

- Optical Sciences

In FY 91, NRL will begin construction of the second phase of the Electro-Optics Research Laboratory (MILCON Project P-115). This will be a 50,000 ft^2 addition to the existing Bldg. 215 and will accommodate approximately 120 scientists and engineers and their research facilities. Completion and occupancy should occur in the last quarter of FY 93 or the first quarter of

FY 94. This facility will allow consolidation of the fiber optics and glass materials activities into one location and will replace obsolete and inadequate silica glass facilities in Bldg. 12 with new, state-of-the-art facilities. It will allow closer coordination between the infrared detector development activity and sensor system activities. Many computational sensor testing and modeling facilities will be contained in the new structure.

• Plasma Physics Facilities

A major, 2-kJ KrF-laser facility will be established in the Plasma Physics Division by the end of FY 93. This facility is being initiated to provide intense radiation for studying inertial confinement fusion target heating at short wavelengths. A new 3-MJ, 10-MA pulsed-power facility, ROOK, is being constructed for inductive energy storage research and should be ready in the FY 90-91 timeframe.

• Center for Materials Research

The Department of the Navy is in the process of programming construction of a special-purpose laboratory. This special facility will provide stringently clean laboratories with carefully controllable temperature, humidity, vibration isolation, ambient dust, and power for investigations in the rapidly evolving fields of electronic technology and nanometrics.

• Midway Research Center

NRL's newest field site, the Midway Research Center (MRC), is located on a 158-acre site in Stafford County, Virginia. Located adjacent to the Quantico Marine Corps Base, the MRC consists of a 5000 ft^2 operations/administration building and two of three programmed 60-ft diameter parabolic antennas housed in 100-ft radomes. When completed, the MRC, under the Navy Center for Space Technology, will provide NRL with a state-of-the-art facility dedicated solely to space communications and research.

• Electronics Science and Technology

In collaboration with the Materials Science and Technology Division, a new epitaxial materials center, the "Epi-Center," has been established. At the heart of the Epi-Center is an MBE system that consists of two linked chambers, one dedicated to narrow energy gap semiconductors and the other dedicated to large energy-gap semiconductors. Work on mixed narrow energy-gap, large energy-gap semiconductor systems can be carried out by transferring samples from the respective chambers.

Other important division emphases are the continual upgrading of the Nanoelectronics Processing Facility and expanding activities in the nanoelectronics physics program. A key feature of the latter is the comparison of lithography by means of a state-of-the-art E-beam machine with high electron energies and a scanning tunneling microscope (STM) with low electron energies.

• Fire Research Facility

Construction is under way at the Fire Research Facility at CBD to expand the current facilities. Once completed the facility will have a 50 × 50 × 50-ft burn building with an attached control center, three lab/office complexes of about 2500 ft^2 each, and a new, large, concrete minideck (to simulate air-capable ship decks) for expanded large-scale fire-fighting studies. FIRE-I, NRL's 325-m^3 (11,400-ft^3) pressurizable fire research chamber, has been relocated to this site.

• Radar Mode Test System

The Radar Division has acquired the Radar Mode Test System to evaluate the performance of NATO compliant Mark XV IFF radar mode (RM) equipment. It has been used to test equipment from the United Kingdom and will have application to the evaluation of NRL- and contractor-developed RM equipment

REHABILITATION OF SCIENTIFIC FACILITIES

Specialized facilities are being installed or upgraded in several of the research and support divisions.

• Chesapeake Bay Detachment

Three laboratory buildings at the Chesapeake Bay Detachment are scheduled to be renovated in FYs 91 and 92. The two-story buildings, which overlook the Chesapeake Bay, are between 8000 and 8600 ft^2. Plans call for an open lab/office design that can be readily adapted to suit the needs of the tenants. One building is currently unoccupied and will be available for use by any NRL division or other tenant when renovation is completed.

• Information Technology

An expanded computer/communication network is being implemented that will provide each researcher in the division with an office workstation (SUN, Apollo, or equivalent) connected to all the major scientific networks. Special test facilities are also being planned in support of specific R&D tasks. Facilities to support human-computer interaction research include an eye-monitoring system, touch screens and tablets, speech I/O hardware, high-resolution graphic displays, a 6-D tracker, a wall-sized display, and time-stamped video and audio recording equipment for monitoring experiments. An information security testbed is being planned to enable the interconnection of communication security and computer security devices to address network and system security problems.

• Plasma Physics

An inductive energy storage facility, PAWN, is being upgraded to increase the output power from 0.1 up to as much as 1.0 terawatt. This facility will be more than an order of magnitude more compact than similar generators when final development stages are completed. PAWN will be used for intense electron and ion beam generation research and in X-ray laser development. A low-frequency (300 MHz to 10 GHz), high-power microwave facility, which uses a relativistic klystron concept, is being upgraded to produce multigigawatt coherent radiation pulses. A new laser facility is also planned. It will use a powerful KrF laser and a target chamber to conduct inertial confinement fusion research.

• Radar

The Radar Division has installed a computer-aided engineering (CAE) facility to aid in digital system design. The system has seven full-color graphics workstations to provide capabilities for circuit design and simulation and printed circuit board layout. The facility has been used to design systems based on commercially available components as well as advanced systems incorporating VHSIC and gate array technologies. It has proven to be a valuable tool in evaluating new technologies for radar signal-processing requirements. The facility is currently being expanded to include three SUN workstations and ADAS software, which will allow designs to be modeled and simulated at the system level. Future plans call for acquiring VHDL (VHSIC Hardware Description Language) software for the workstations, which is supported by ADAS. This would provide designers with an integrated toolset to model and simulate their designs from the system level down to the device level.

• Acoustics-Target Research Tank

Tank facilities for acoustic target research in the Acoustics Division will be significantly expanded to extend the range of target sizes. The expanded model tank is planned to contain a water volume of approximately 30,000 m^3.

• Underwater Sound Reference

A new, precision measurement system (PMS) is being installed in each of four facilities—at the Lake Facility, the Leesburg Facility, and the two

large high-pressure tank facilities. PMS is a sophisticated, computer-controlled, signal-generation and data-acquisition system that provides significantly increased accuracy, dynamic range, and signal to noise than was previously available. It allows the use of new, sophisticated signal-processing techniques being developed for making lower frequency measurements on sonar transducers and related acoustical coating materials under reverberation-limited conditions, such as in the large, high-pressure tank facilities. PMS will also process acquired data very rapidly so that most results can be presented to customers at the time of the measurements.

• Materials Science and Technology

Renovation is proposed for Building 3, which is now made up of two of the original five buildings at NRL, to contain modern laboratories for studies of thin-film deposition and characterization, superconducting materials, magnetic materials, and other materials science projects. The new space will feature the most modern molecular beam epitaxy and other materials synthesis and processing equipment, an up-to-date fatigue and fracture laboratory and state-of-the-art diagnostic equipment, including electron microscopes, spectrometers, and electron and X-ray diffraction equipment. The renovated building will also contain office and laboratory space for approximately 70 technical personnel.

Further Information: The NRL *Fact Book* gives more details about the Laboratory and its operations. It lists major equipment, current fields of research, field sites, and outlying facilities. It also presents information about the responsibilities, organization, key personnel, and funding of the divisions, detachments, and other major organizational units.

Information on the research described in this *NRL Review* may be obtained by contacting Dr. Richard Rein, Head, Technology Transfer and Special Programs, Code 1003.1, (202) 767-3744. General information about NRL may be obtained from Information Services, Code 4810, (202) 767-2541. The sources of information on the various nonresearch programs at NRL are listed in the *NRL Review* chapter entitled "Programs for Professional Development."

HIGHLIGHTS OF NRL RESEARCH IN 1990

Retrieval of the LDEF/HIIS Experiment

NASA's Long Duration Exposure Facility (LDEF) was retrieved by the Space Shuttle in January 1990 after this nominal one-year mission spent almost six years in space. Aboard LDEF was NRL's Space Science Division's Heavy Ions in Space (HIIS) experiment, a cosmic ray detector designed to address questions important both to astrophysics and to understanding the radiation environment encountered by humans and hardware in space. HIIS has also returned new information on other hazards in the space environment. The multilayer insulation blankets and track detector stacks in HIIS are nearly ideal capture cells for micrometeoroids and space debris. LDEF's largest micrometeoroid impact was found in HIIS. It and numerous other impacts are now being studied by micrometeoroid and space debris experts at the Johnson Space Center. The thermal blankets on the HIIS experiment, well beyond their one year design lifetime, were damaged by UV radiation and atomic oxygen and were partially detached from the spacecraft. These blankets will be studied by spacecraft engineers to investigate the effects of the space environment on them.

***

Development of New Sensors and Techniques for Remote Sensing of Space Weather from Operational Satellites

A Space Science Division's basic research program of upper-atmospheric physics and ultraviolet remote sensing has led to the development of new techniques for optical remote sensing of neutral atmospheric and ionospheric densities from space. New ultraviolet sensors have been developed to measure limb profiles of atmospheric airglow, and new algorithms have been generated to convert these measurements into neutral and electron density profiles. The Defense Meteorological Satellite Program has adopted these new techniques in the form of an operational sensor system called the Special Sensor Ultraviolet Limb Imager (SSULI) for inclusion on its Block 5D3 operational weather satellites. The sensors are derived from ultraviolet instruments developed for the Remote Atmospheric and Ionospheric Detection System (RAIDS) and an NRL proof-concept satellite experiment.

***

Progress in the Development of the NRL Modified Betatron Accelerator

The trapped current and the beam energy in the Plasma Physics Division's modified betatron accelerator have substantially increased during FY 90. Specifically, the trapped current increased from 0.5 kA to 1.5 kA and the beam energy from 12 MeV to 18 MeV. The 1.5 kA current exceeds by 50% the design specification of the device, while the energy is only 10% below the initial specification. The modified betatron accelerator has the potential to lead to a compact, lightweight, high-current device that is suitable for shipboard installation. Net technical assessment studies show that the modified betatron is the lightest and most compact among all the high-current accelerators considered. The modified betatron has

been under development at NRL since 1980. After the successful completion of its construction and testing of the various power subsystems, the device entered its initial phase of operation that includes beam injection and capture and electron ring recirculation. These experiments have provided valuable information on several critical physics issues associated with the high current, toroidal accelerators.

***

Stable Propagation of a High-Current Charged-Particle Beam

A national program studying the feasibility of using a charged-particle beam (CPB) as a directed-energy weapon (DEW) has been in progress for nearly 20 years. This program has been funded by the Defense Advanced Research Projects Agency, the Office of Naval Research, and carried out by NRL's Plasma Physics Division. The research program has three primary goals that would demonstrate feasibility and provide the necessary building blocks for producing a CPB DEW sometime early in the next century. The goals are to prove that a beam can propagate stably in the atmosphere over a significant range, to demonstrate that it is possible to extend the range of such a beam to significant distance, and to develop the technology necessary for a compact, high-energy accelerator. NRL performs experimental and theoretical research in all three areas. A new propagation laboratory, constructed with NRL capital equipment funds, was completed in 1988. Since then this laboratory has been bringing the accelerators and numerous diagnostics on line and performing preliminary experiments aimed at both propagation stability and range extension.

***

Real-Time Adaptive Monopulse Countermeasures (CM)

The Advanced Technology Demonstration (ATD) Program in the Tactical Electronic Warfare Division involves the application of two electronic warfare (EW) technologies designed to counter modern monopulse type, RF-guided antiship missile. The concept involves the use of an on board angle-deception ECM combined with real-time adaptive control and monitoring of the jammer's effectiveness to optimize the ECM's performance against the monopulse threat. The ATD consists of the marriage of two advanced technologies to improve softkill self-defense of a surface ship. The first technology provides an advanced, high-power angle deception capability against monopulse missile seekers. The second technology provides a real-time softkill effectiveness monitoring capability for assessing the effectiveness of ECM. The combination of these two technologies provides greatly improved ship survivability while optimizing the use of shipboard ECM against missile attacks.

***

Biosensor for Cocaine Detection

An antibody-based sensor has been constructed by the Center for Bio/Molecular Science and Engineering for detecting drugs of abuse. The sensor is configured to analyze hundreds of discrete samples rapidly or to be integrated with a continuously operating sample. Antibodies can recognize a drug molecule among millions of other molecules. We have chemically attached these naturally selective antibodies to a solid support, bound-fluorescent cocaine to the active site and introduce a fluid stream. When samples that contain cocaine are introduced into the stream, the free cocaine displaces the fluorescent cocaine that is measured further downstream. This biosensor is faster, less expensive, and as sensitive as any method currently available for cocaine detection. It can be operated by personnel who lack scientific training and can be used outside a laboratory environment.

***

Turbine Blade Rejuvenation

A significant factor in the cost of operating and maintaining aircraft gas turbine engines is the frequent replacement of high-temperature turbine blades that have failed or reached some design limit or life. The Materials Science and Technology Division developed suitable rejuvenation and repair procedures for these blades to save the Navy and the other services several millions of dollars per year. Based on detailed understanding of the failure processes in these blade alloys, interrelation among the microstructure, load, temperature, and environment, NRL has developed methods to rejuvenate or repair these blades so that they can be made to last longer.

***

First Test of Fiber-Optic Hydrophones in the Arctic

In April 1990, two fiber-optic hydrophones measured the ambient acoustic noise under shore-fast ice at the mouth of Independence Fjord, in the vicinity of Kap Eiler Rasmussen, Greenland. Measurements were made by the Optical Sciences Division over a 12-day period and contained data ranging from more than 20 dB below sea-state zero (between 200 and 1000 Hz) to high noise levels caused by the presence of machinery. Noise measurements were made over a 0.03 Hz to 3 kHz frequency range. Several mechanical and operational requirements necessary for future Arctic use of fiber-optic hydrophones were demonstrated. First, the fiber-optic hydrophones and single-mode, fiber-optic cable showed that they are deployable and operational at temperatures between —20° and —40°C. Second, the lasers and electronic systems used to interrogate the fiber-optic hydrophones demonstrated that they could operate at the low noise levels required for high sensitivity in the fluctuating thermal environment of the shelters (tents). Finally, the hydrophone sensitivity and dynamic range were demonstrated to be adequate for future Arctic applications.

***

Launch and Operation of the Low-Power Atmospheric Compensation Experiment (LACE) Satellite

NRL's Naval Center for Space Technology (Space Systems Development Department) was tasked in 1985 to design, integrate, test, launch, and operate a satellite to serve as an instrumented target for low power, ground-based lasers to conduct atmospheric compensation tests. In 1987, tasking was expanded to include acquisition, testing, integration, and operation of an instrument that obtains images of the ultraviolet emission from rocket plumes. Launch of the LACE satellite occurred on 14 February 1990. Data from the LACE satellite's sensor array subsystem will be used in support of atmospheric compensation programs of the Strategic Defense Initiative Organization.

***

Large-Scale, High-Energy Laser Windows from Heavy-Metal-Fluoride Glass

Significant progress has been made by the Optical Sciences Division in the development of large windows from heavy-metal-fluoride (HMF) glasses for high-energy laser (HEL) transmission. These glasses have a theoretical absorption loss minimum of less than 2×10^{-7} cm^{-1} at 2.5 μm and practical losses of less than 5×10^{-4} cm^{-1} between 1 and 5 μm. In addition, HMF glasses exhibit near zero optical-path

distortion when heated by laser fluences. Until 1988, problems associated with the crystallization of these glasses limited the size of windows made from HMF glasses to disks less than 1 cm in thickness and 4 cm in diameter. However, new glass compositions and innovate processing have made the production of much larger windows possible. In FY 90, a 45-kg window, 4 cm in thickness and 60 cm in diameter, was produced. The ability to cast windows of this size makes HMF glasses the best material for high-energy, mid-IR optical components.

***

Effects of Gravity on Flames in Premixed Gases

Differences in the shape and dynamics of flames propagating upward and downward in tubes have been experimentally observed for many decades. Flames propagating in many premixed fuel-air mixtures are prone to various kinds of instabilities. In general, these instabilities result in the flame having a complex, multidimensional structure that also varies in time. Now these flames have been numerically simulated by the Laboratory for Computational Physics and Fluid Dynamics. The simulations provide a better understanding of the interplay among various mechanisms that are responsible for the observed behavior of these flames. Understanding the behavior of flames under reduced and varying gravity situations is crucial for the safe and efficient operation of space systems such as the Space Shuttle and the proposed Space Station.

***

Magnetohydrodynamic Computational Models

Numerical modeling has played an important role in gaining a greater understanding of the phenomena occurring in the solar chromosphere. An important but not yet fully understood problem is the mechanism that heats the solar chromosphere and the effects of the solar magnetic field on this heating. A new, three-dimensional magnetohydrodynamic code has been developed that for the first time permits accurate modeling of the dynamics of solar arcades. Scientists in the Laboratory for Computational Physics and Fluid Dynamics have developed a new three-dimensional, semi-implicit, Fourier pseudospectral-Chebyshev collocation magnetohydrodynamics code for use in numerical studies of coronal heating. A code of this type will allow a greater understanding of the mechanisms that produce heating in the solar coronal that can lead to such phenomena as solar flares.

***

Defect Studies in Semi- and Superconductors

The effect of radiation on the electrical properties of semiconductors (such as silicon, germanium, and gallium arsenide, and the recently discovered high-temperature superconductors) have been found to be directly proportional to the displacement energy (nonionizing energy loss) deposited by the incident particle. This means that once an effect has been measured for one kind of incident particle, a prediction can be made for any other particle of any energy. The scientists in the Condensed Matter and Radiation Sciences Division report that this predictive power is useful in applications including SDI and the NRL/High Temperature Superconducting Space Experiment.

***

Theory of Intermetallic Alloys

The density functional theory (DFT) within the local density approximation points the way toward first principles evaluations of a variety of electronic and mechanical properties in solids. The DFT has been

implemented by using the tools of band-structure methods to determine the equation of state for many materials. Researchers in the Condensed Matter and Radiation Sciences Division have applied the linearized, augmented plane-wave method to calculate the zero-temperature equation of state and the elastic moduli for the following intermetallic compounds: SbY, CoAl, RuZr, NbIr, RuAl, NiAl, and Ni_3Al. The calculated lattice constants and bulk moduli are within 2% and 7% of the experimental values, respectively. In addition, all the elastic constants were calculated and compared with the experiment, where available, with similar 5% to 10% agreement. The predictive capability of these calculations can show experimentalists which intermetallic alloys are the best candidates for exploration as light-weight, high-strength, and high-melting-temperature materials.

***

Digital Sidelobe Canceler Technology Transfer

Shipboard radars are vulnerable to electromagnetic interference (jamming) that enters system receivers through antenna sidelobes. The Radar Division's efforts in exploratory development have developed the technology to provide a considerable increase in sidelobe-canceler performance. Having developed the technology for an improved shipboard sidelobe canceler, consideration was given to adapting this technology to active Fleet systems. The results of this program will significantly improve the performance of this radar in a jamming environment.

***

Unified Network Technology/Advanced Technology Demonstration (UNT/ATD)

Under UNT/ATD, a distributed control, self-organizing, adaptive networking architectural concept called the linked cluster architecture (LCA), has been developed for application to tactical-warfare-stressed scenarios. Accomplishments by the Information Technology Division during FY 90 include both software and hardware development of network and link controllers, performance simulations of the network, system integration and testing, and a seven-node hardware demonstration (involving a ship, an aircraft, and five land-based nodes) of the networking architecture. UNT/ATD's primary objective is to demonstrate the operational benefits of new network technology and its impact on naval communication services. The Linked Cluster Architecture (LCA) network design was developed and applied to a Naval Intrabattle Group (IBG) communication system. The LCA network allows for reconfiguration of communication links under dynamic conditions, improved timeliness and information throughput, and enhanced survivability (since it is not dependent on centralized control).

***

Eye Movement-based Interaction Techniques for Human-Computer Communication

In seeking previously unused methods by which users and computers can communicate in time-critical situations, the Information Technology Division has investigated the usefulness of eye movements as a fast and convenient auxiliary user-to-computer communication mode. The barrier to exploiting this medium has not been eye-tracking technology but the study of interaction techniques that incorporate eye movements into the user-computer dialogue in a natural and unobtrusive way. A set of generic user-computer interaction techniques for the use of eye movements in a real-time, user-computer dialogue has been developed. The eye-movement-based-interaction techniques will provide a rapid, user-to-computer communication channel for time-critical applications such as command and control. A faster, more natural interface incorporating eye movements can make computer use faster and more

convenient for many types of users and can enable a commander to speed up information-gathering and decision-making processes during a crisis.

***

Full-Engagement Decoy Simulator (FEDS) Visualization

Within the last two years, the Effectiveness of Navy Electronic Warfare Systems (ENEWS) Program of the Tactical Electronic Warfare Division has enhanced the visualization capability of the FEDS through the development of a highly flexible display presentation package of the simulation results. The features are selectable by the user to emphasize the particular characters of the engagement that the simulation highlighted. The entire set of missiles or an individual missile can be displayed; the gates for individual missiles or the scanning characteristics of individual emitters can be selected to show detailed results of the simulation. This program can be used both to verify results from other evaluation techniques (such as laboratory and field simulators) and to show the correspondence of FEDS results with those techniques. The relative cheapness of digital simulation, when coupled with a clean presentation of understandable results, makes FEDS simulation an even more valuable asset.

***

Low-Altitude/Airspeed Unmanned Research Aircraft (LAURA)

The Tactical Electronic Warfare Division's LAURA Program has demonstrated the capability of small, remotely piloted air vehicles to fly efficiently at the shiplike speeds needed for electronic warfare (EW) missions. Three of the four aircraft developed in the LAURA Program were successfully flight tested. Test results show that the majority of the design goals were met and that long endurance flight at low airspeeds can be achieved for tactical, autonomous, and remotely piloted unmanned air vehicles (UAVs). The LAURA Program uses research results to demonstrate the practical application of those technologies and proves the feasibility of developing long-endurance, low-speed, tactical-electronic decoy vehicles.

***

MMIC/EW Receiver

With the general development of MMIC RF circuits, it became increasingly apparent that an assembly of these circuits could become the basis of an EW receiver. Thus, MMIC circuits (such as RF broadband low-noise amplifiers (LNAs), mixers, switches, and filters) became the basis from which the Tactical Electronic Warfare Division completed the design and fabrication of an MMIC/EW receiver. This receiver represents a significant improvement in the performance, weight, size, power, and cost of EW receivers through the use of MMIC technology. The availability of the MMIC/EW receiver will revolutionize the application of EW against modern threat emitters by permitting the use of many low-cost, high-performance EW receivers in a single, low-cost EW system.

***

Materials for Towed-Array Hose Walls

Polymeric materials currently considered for use in the TB-23, small-diameter, towed-array hose either do not possess the necessary aging and weathering resistance or satisfactory self-noise performance as a function of temperature. Changes in self-noise performance as a result of fill-fluid permeation and subsequent chemical reaction also often occur. The objective of this work performed by the Underwater

Sound Reference Detachment was to develop an elastomeric material that would exhibit the proper combination of extensional stiffness (Young's modulus) and internal loss, tensile properties, ozone and weather resistance, resistance to swelling and permeation by seawater and fill fluids, adhesion to reinforcing members, and ease of manufacture, for fabrication and evaluation as a reinforced, small-diameter hose wall for Navy use. This accomplishment may allow the Navy to use one type of material for several different types of arrays.

***

Chemical Indicator for Hydrazine Detection: Active and Passive Dosimeter Systems

Hydrazine, monomethylhydrazine (MMH), and unsymmetrical dimethlydrazine (UDMH) are currently being used by DoD and NASA as hypergolic fuels. These hydrazines impose health hazards to personnel who come in contact with them; they are considered potential carcinogens. The threshold limit values (TLV) for exposure to these vapors are established at 100, 200, and 500 ppb respectively, and the exposure limits may be lowered to 10 ppb for all three hydrazines. To minimize the risk to employees, routine monitoring of personnel and their work environments is mandated. While instruments are commercially available to monitor the current TLV, none exists that is capable of monitoring the proposed TLV concentrations. The Chemistry Division has developed a colorimetric dosimeter system that can be used actively or passively to sample ambient air to detect hydrazine and monomethylhydrazine (MMH) at subpart-per-billion (ppb) levels. Acidified vanillin provides a real-time, low-cost indication of the proposed TLV levels of hydrazine and MMH in air. A patent was issued for the colorimetric indicator in February 1990. This technology provides rapid spot checks of the environment or can be adapted into a paper-tape instrument for continuous real-time detection.

***

Halon 1301 Test Gas Simulant

Halon 1301 is used by the Navy as a total-flooding, fire-suppression agent for protecting shipboard machinery spaces. However, Halon 1301 has been identified as contributing to the depletion of the Earth's stratospheric ozone; therefore production has been limited to 1986 levels by the Montreal Protocol. At present, all new and retrofit installations of Halon 1301 total-flooding fire protection systems in U.S. Navy shipboard machinery spaces require an acceptance discharge test. The primary reason for this testing is to verify the system design and performance. Discharge testing accounts for 60% to 70% of the Navy's total usage of Halon 1301. In view of the potential contribution of Halon 1301 to the stratospheric ozone depletion problem, the Navy has an urgent need to develop a simulant for Halon 1301 that would permit discharge testing to be conducted without polluting the atmosphere. After evaluating over 50 possibilities, sulphur hexafluoride SF_6 was found to be an ideal simulant for Halon 1301 for discharge testing. Not only does SF_6 have chemical and physical properties similar to Halon 1301, it is a nontoxic, inert, stable, nonflammable, odorless, and colorless gas. Extensive laboratory tests by the Chemistry Division and full-scale tests on the USS *Chancellorsville* (CG-62) verified the performance of SF_6. The simulant will be used in place of Halon 1301 for all new and retrofit installations of Halon 1301 total-flooding fire-protection systems in Navy shipboard machinery spaces during acceptance discharge tests.

***

Sludge-Preventing Additives for Navy Diesel Fuel

Antioxidant additives to prevent sludge formation of diesel fuels used by the Navy for shipboard mobility are currently not allowed or approved for use. To rectify this situation and to prepare for the

possible use of such additives, NRL served as the lead laboratory in evaluating nine additives from commercial sources. Two of the nine additives evaluated by the Chemistry Division have been shown to possess superior sludge preventing properties. The use of these additives could reduce problems associated with sludge formation in fuels by one half. This will greatly impact the logistics of interrupted fuel movements, which can negatively impact combat readiness. Additionally, the consequences of sludge formation can critically impact ship mobility during combat operations. The cost-per-year to empty, clean, and inspect a one-million-barrel storate depot is about $3 million. The use of these additives will thus save the Navy about $1.5 million per depot per year in 1990 dollars.

***

Deposition of Aligned, High-Quality, Potassium Tantalum Niobate (KTN) Films

KTN has very high electro-optic as well as pyroelectric coefficients. Its Curie temperature can be changed easily, and interesting devices have been made out of KTN bulk single crystals. This makes it attractive to attempt film deposition. Sol gel techniques were used to deposit very-large-area, flaw-free films having a range of tantalum-niobium ratios. A very high degree of crystallographic orientation was observed by scientists from the Materials Science and Technology Division on 111 Silicon and on SiO_2 substrates after 550° heat treatments. The attainment of flaw-free, large-area films is a significant accomplishment and the attainment of crystallographic alignment of these (in particular on silicon and SiO_2) is a major breakthrough. The deposition of electro-optic or pyroelectric films on single-crystal silicon allows the direct integration of electro-optic light modulators on a silicon chip. This increases as speed, reduces size, and provides related device advantages. Pyroelectric arrays integrated on a chip can lead to very small pyroelectric image analyzers.

***

Using Chaos to Drive Stable Systems

Over the last 15 years, the entire scientific community has become aware that another kind of motion exists beyond the usual equilibrium, steady-state, or cyclic (periodic) states known for centuries. That motion has come to be called chaos and appears in many guises in almost every scientific field. Although apparently random in nature, chaotic signals have been shown to be useful and more controllable than thought. Two independent applications that use chaotic signals as inputs were recently found by researchers in the Materials Science and Technology Division. One is the development of techniques to create synchronized but simultaneously chaotic systems. The other is the use of certain chaotic systems as replacements for periodic (cyclic) signals to prevent phase drift yet retain much of the desired behavior of the driven system. The synchronization allows systems to behave in ways that are difficult to predict (as is the nature of chaos) yet to remain acutely coordinated with each other. The chaotic "periodic" driving makes it possible to design complex, nonlinear systems and have behavior similar to simple periodic driving, yet no subelements of the system will get out of phase with any others. It also offers a plausible explanation of why so many chaotic signals are found in physiological systems, like the human body.

***

A New Technique for Controlling the Characteristics of Thin Magnetic Films

Magnetic materials in thin-film form have very important technological applications in magnetic recording, both as media materials and magnetoresistive read heads, as well as potential integrated microwave circuit elements. In almost all of these uses, it is very important to be able to control the

magnetization, anisotropy, and domain structure of the films. Scientists in the Materials Science and Technology Division demonstrated that the dipolar forces tending to keep the moment of magnetic thin films in the plane of the film can be dramatically enhanced by using multilayer films where adjacent layers are strongly coupled antiferromagnetically. By using materials in which materials in each of the layers is completely isotropic, an enhancement of dipolar anisotropy of more than a factor of four has been observed. Also observed is a unique "spin flop" transition, where as a function of applied magnetic field, the spins in each of the layers make a sudden transition from directions parallel and antiparallel to the applied field to directions almost perpendicular to the field. These effects have been explained theoretically and can be used as a unique and valuable tool for basic studies of fundamental interactions in magnetic materials and their interfaces. They have potential application in various kinds of thin-film magnetic devices, such as in magnetic-recording and random-access magnetic memory elements and in fundamental studies of such characteristics as interface exchange interactions and novel magnetotransport phenomena.

***

Flashlamp-Pumped, Solid-State Laser for Medical Applications

Researchers in the Optical Sciences Division have developed a novel, high-efficiency, flashlamp-pumped, room-temperature, solid-state laser that produces optical pulses at a wavelength of 2.014 μm. The laser material is yttrium aluminum garnet (YAG) doped with small concentrations of CR^{3+} (0.6%) and Tm^{3+} (6%). The output wavelength corresponds to a transition of the Tm^{3+} ion, and the Cr^{3+} acts as a sensitizer to permit efficient pumping by an ordinary flashlamp. Output pulse energies ranging from a few millijoules up to several joules have been produced with efficiencies on the order of 4%. The significance of this new laser wavelength for medical applications derives from two factors: infrared radiation at 2.014 μm is readily transmitted by silica-cased optical fibers, and it is in a region of high absorption (water band) in biological tissue. In the near infrared wavelength region, laser ablation is most effective at wavelengths around 2 and 3 μm, which correspond to tissue absorption peaks. With regard to transmission, flexibility, durability, and nontoxicity, silica-based optical fibers have been demonstrated to be the delivery system of choice; their transmission window covers the spectral region between 0.3 and 2.3 μm. The new 2.01 μm laser is ideally suited for such procedures as laser angioplasty, arthroscopic surgery, and repair of herniated lumbar discs. Effectiveness of this laser for ablation of various types of tissue is currently being investigated.

***

Fabrication of Bond and Etch-Back Silicon on Insulator (SOI) by Using a Strained $Si_{0.7}Ge_{0.3}$ Layer as an Etch Stop

Bond and etch-back SOI that uses a strained $Si_{0.7}Ge_{0.3}$ layer has been produced with a silicon thickness of 200 nm by molecular-beam epitaxy (MBE) by the Electronics Science and Technology Division. The material was measured to have a doping level of less than 10^{15} cm^{-3}, which is the residual dopant level of the MBE system. The utility of this material is that it enables good control of the fabrication process resulting in undoped, defect-free SOI. The etch-stop layer is epitaxially grown by using an electrically active element. The resulting material can be used to fabricate fully depleted (0.25-μm channel length) and complementary devices without needing compensation for residual dopant. This material is highly relevant to DoD applications and can be used in satellites or other high-speed equipment that is sensitive to radiation environments. The production of fully depleted devices enables ultrahigh speeds to be obtained. The use of bonded wafers gives the capability of radiation hardening the back channel of the devices, an important

criterion in fully depleted structures. The use of germanium over boron as the etch stop improves the performance of the material because of fewer defects and lower residual doping following fabrication.

***

Linear Theory of Field-Emitter-Array (FEA) Distributed Amplifier

A small signal theory of a continuously distributed FEA amplifier has been developed by the Electronics Science and Technology Division to calculate the gain and bandwidth of the amplifier. The dependence of the linear gain on beam energy, beam current, transmission line parameters, and the emitter performance characteristics is derived to determine the conditions for large amplification. Calculations show that a high gain of 3 dB/cm to 7 dB/cm in the frequency range 20 to 100 GHz with bandwidth in excess of 60% is feasible in this device. The theoretical work has led to a better understanding of the physical processes of the interaction in FEA-distributed amplifiers.

***

High-Resolution Lithography in a Polydiacetylene Negative Resist with a 50 kV E-Beam and a Vacuum Scanning Tunneling Microscope (STM)

A polydiacetylene negative resist developed by the Electronics Science and Technology Division demonstrates very high lithographic resolution when exposed with a 50 kV E-beam or a 5- to 10-V probe in a vacuum STM. A study combining the two lithographic tools addresses the fundamental limitations on the resolution of the resist. The low-voltage probe can both modify the resist topographically and image the resist films in situ. Examination of the latent image in the underdeveloped resist enables the exposure step to be studied independently of postexposure processing. The combined use of the 50 kV E-beam and the STM in a complementary set of experiments is a powerful approach to lithographic research. The STM has been demonstrated as a potentially viable lithographic tool. The results indicate that chemical modifications can improve the ultimate resolution of the resist.

***

MMW Radiometric Background Measurements

Thirty-seven GHz passive microwave measurements of terrain backgrounds were made by the Space Systems Technology Department of winter scenes near Grayling, Michigan, and of desert scenes near Yuma, Arizona. Infrared and 35 GHz radar measurements were made during the same period of time and from the same observation platform, providing simultaneous characterization of the test areas at both IR and microwave. Extensive meteorological measurements were made that supplied excellent ground truth for the experiments. Raster scans of the scenes were performed by using a dual, linearly polarized, Dicke-switched 37 GHz radiometer with a 1° beamwidth. The data were sampled every 0.5° in both elevation and azimuth. Measurements were made from an observation tower looking down on the background scene. Elevation depression angles varied from 10° to 60°, as measured with respect to the horizontal. Measurements of the downwelling sky radiation were also made so that emissivities of the background scene can be calculated. The ability of a sensor to detect and acquire a target depends, among other things, on the presence of clutter or "targetlike" objects in the scene. This study provides a terrain database that may be used to assist in evaluating the clutter level of test sites that are thought to be similar to areas of importance for military operations.

MEET THE SCIENTISTS

Dr. Herbert Gursky, superintendent of the Space Science Division, heads a highly successful effort of astronomy and atmospheric science. Division scientists have responsibility for major NASA- and DoD-sponsored experiments in the areas of solar physics, gamma ray astronomy and the higher portions of the atmosphere, including the analysis of space data and the modeling of the observed phenomena. Dr. Gursky is a pioneer in the observation of X rays from astronomical objects in space.

Dr. Frances S. Ligler, deputy head of the Center for Bio/Molecular Science and Engineering, leads NRL's interdisciplinary programs in biosensor technology. These programs are targeted toward the ultrasensitive detection of chemicals and pathogens in applications such as drug interdiction, aircraft safety, and defense against biological warfare agents. She and her group have initiated industrial negotiations for pertinent technology transfer to an industrial effort that plans clinical trials by 1994. This is patterned on their successful transfer of the NRL research on an artificial red blood cell, liposome encapsulated hemoglobin. "I am most proud of those aspects of our research that have direct application to the health and safety of Naval personnel and the general public."

Dr. Robert W. Timme is the associate superintendent and civilian executive officer of the Underwater Sound Reference Detachment in Orlando, Florida. Prior to this assignment, he was head of the Transducer Branch and manager of the Navy's Sonar Transducer Reliability Improvement Program. Dr. Timme is involved with solving the problems of today's Fleet sonar and with developing new concepts to meet future Fleet requirements. He finds his job most satisfying because "it provides me the opportunity to make clear and tangible contributions toward solving the Navy's present and future problems. These contributions had their beginnings in NRL's research programs." Dr. Timme is a Fellow in the Acoustical Society of America, a three-time winner of the Alan Berman Research Publication Award, and has been presented the Superior Civilian Service Award.

COLOR PRESENTATION

For visual interest, we present here some of NRL's latest scientific achievements and state-of-the-art equipment.

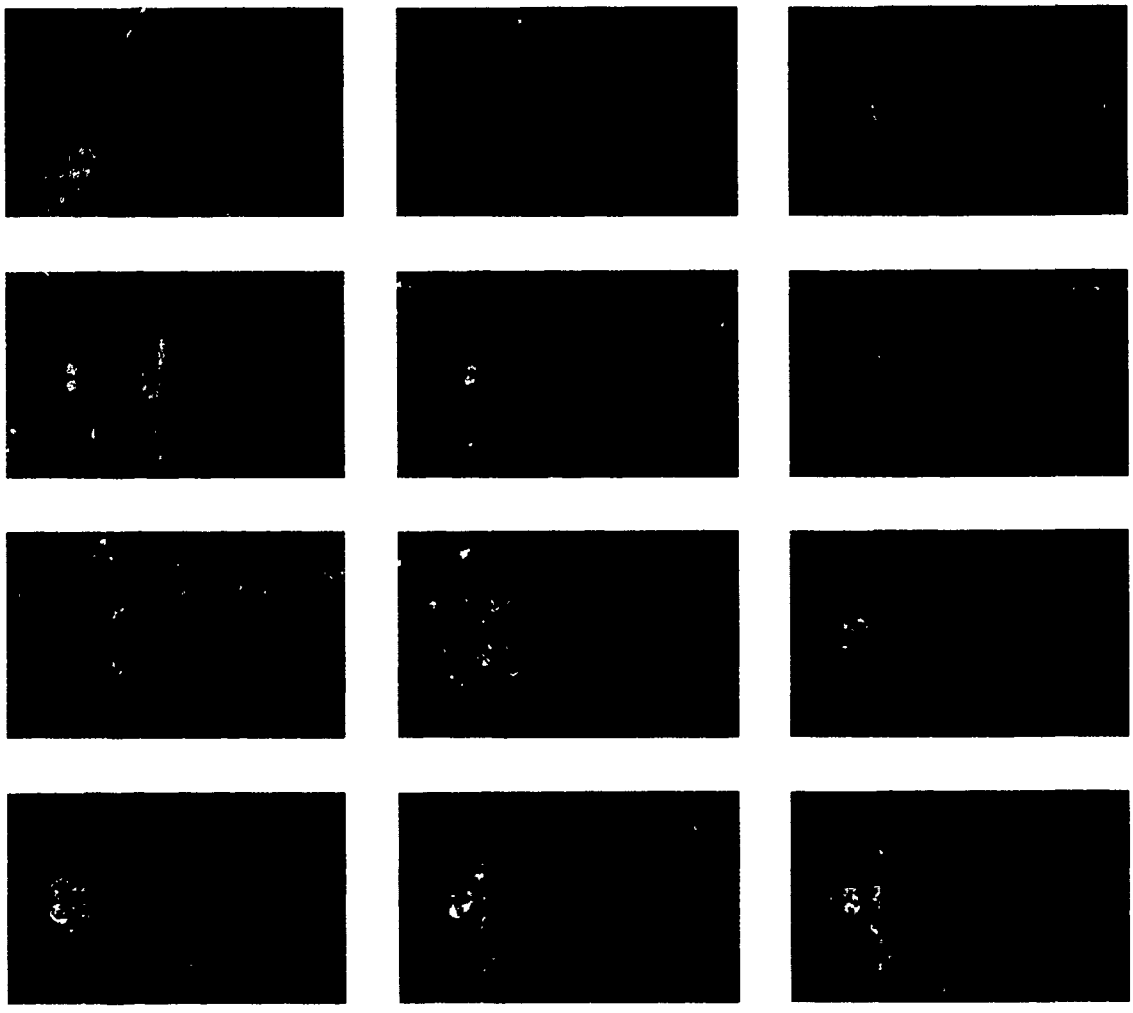

The hydrogen mass-fraction from numerical simulations of the evolution of interface structures between hydrogen and air generated by the Rayleigh-Taylor instability caused by the expansion waves is shown. Interface instabilities between fuel and air flows could be used to enhance the mixing and, therefore, increase the combustion efficiency in air-breathing engines. (C. Li, Code 4410)

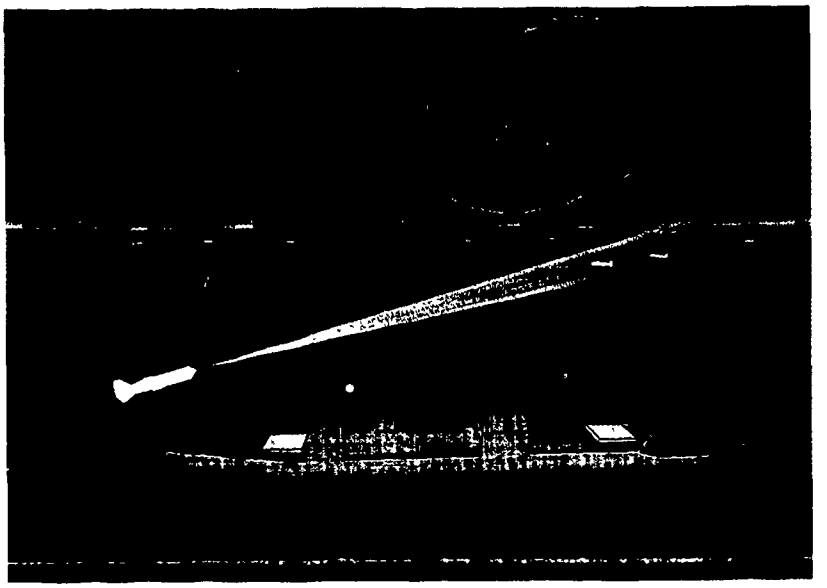

An Effectiveness of Navy Electronic Warfare Systems (ENEWS) simulation of an AEGIS cruiser ("Ticonderoga Class," CG-47 ship) is shown with deployed chaff clouds and an electronic decoy arranged to defend the ship from a wave of antiship cruise missiles. (W McIntyre, Code 5707)

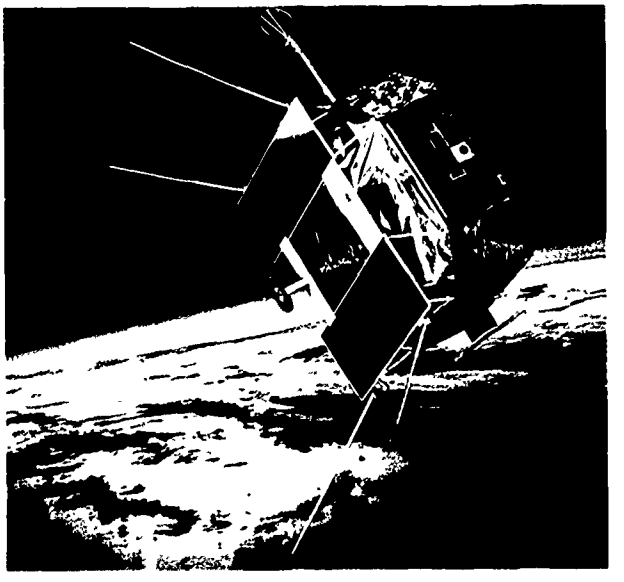

The Combined Release and Radiation Effects Satellite (CRRES) is designed to get a deeper understanding of several ionospheric and magnetospheric phenomena. Here is the CRRES spacecraft as it appears in orbit. The solar panels support four LASSII antenna booms, which are used to measure electron densities and electric fields. The LASSII loop antenna for measuring magnetic field fluctuations is mounted on the spacecraft side Chemical canisters for the release experiments are stored in the spacecraft side panels (P Rodriguez, Code 4785)

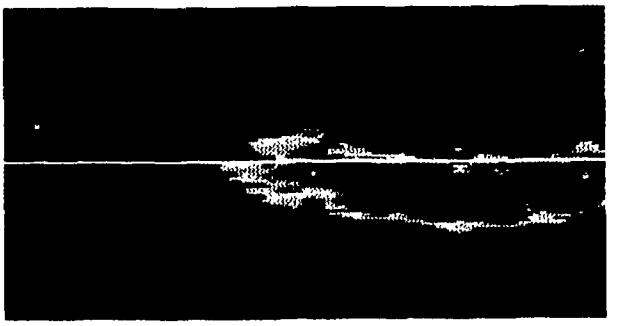

Beam density contours from a particle simulation of a high current, relativistic electron beam propagating in air at atmospheric pressure The beam is moving from right to left and shows the effects of erosion, instability, and tracking in a channel of reduced air density The model represents a beam generated by the NRL Super-IBEX experiment (G Joyce, Code 4790)

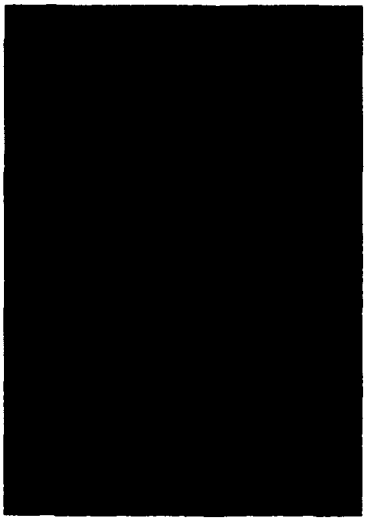

Helical peptides associated in a paired coupling by interdigitating long side chains in a zipper motif. (I. Karle, Code 6030)

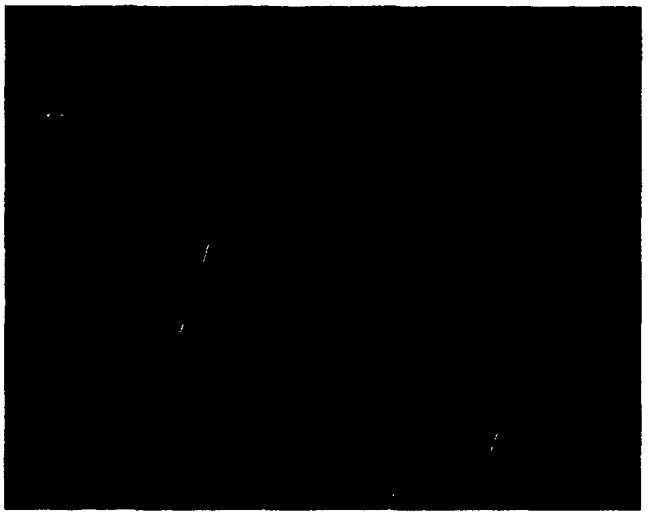

An instantaneous flow visualization from a typical, simulated plane wake by using the NRL finite-difference bluff-body code is shown. One can see streamwise vortices distinctly superimposed to a vortex street in the saddle regions between distorted spanwise rollers. The streamwise vortices appear as legs of horseshoe vortices in response to cross-stream spanwise excitation of the inflowing streams. Vortex reconnection phenomena lead to the formation of unconnected closed vortex loops. This research allows an improved characterization of the underlying fluid-dynamical processes in 3-D bluff-body near-wakes, with important applications for external flows over bodies, such as ships, submarines, torpedoes, and planes. (F.F. Grinstein, Code 4410)

Here the vorticity in a two-dimensional shear layer during the evolution of a strong instability is shown. The shear layer, a region of high velocity gradient, has been subjected to disturbances whose wavelengths are 1/2 and 1/3 of the computational domain. At this stage of the computation, the original shear layer has evolved into two distinct vortices as a result of the dominant 1/2 mode. At later stages of the calculation, the vortices will merge into one as a result of the modulation of the 1/2 mode by the 1/3 mode. (R. Handler, Code 4220)

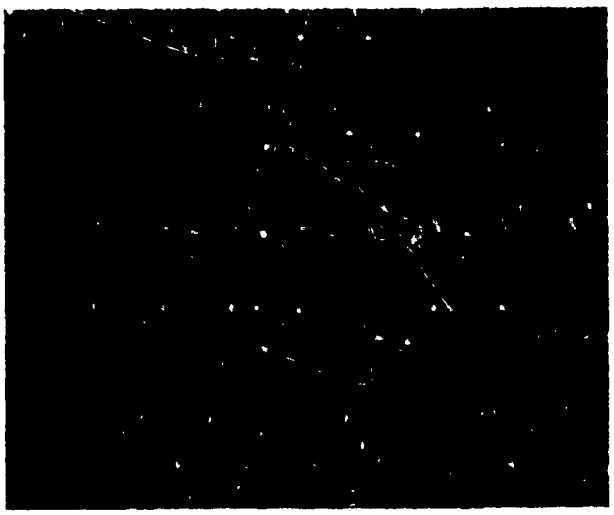

Scanning tunneling microscopy image of the surface order of a nematic liquid crystal, 4-cyano-4'-hexylbiphenyl, on graphite. The image is a 11.7 nm × 11.7 nm false color plot of raw data taken at room temperature. The high resolution image gives details about the long-range order and the packing of the cyanobiphenyl (head) and the alkyl (tail) groups. The head groups organize in rows containing alternating 'X' and 'I' patterns colored pink in the image. The 'X' represents one cyanobiphenyl group lying flat on the surface, and the 'I' represents another head group lying on its side. The alkyl tail, from a molecule lying on its side, extends down across the blue-colored band and aligns with a tail extending upward from a molecule lying flat in the next row below. The bluish holes in the ordered structure show the graphite substrate. (S. Brandow, D. DiLella, R. Colton, Code 6177, and R. Shashidhar, Code 6090)

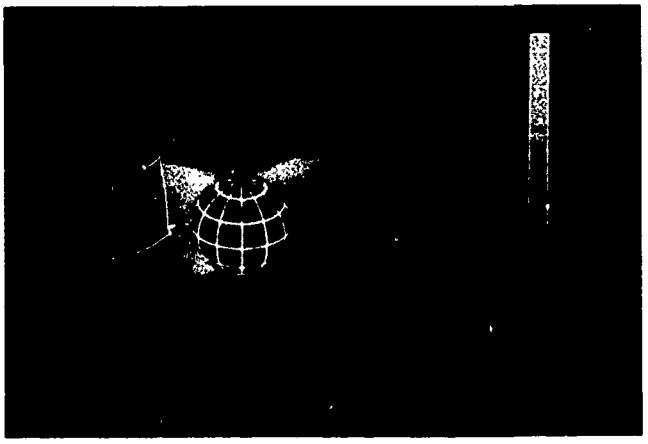

False color extreme ultraviolet image of a model of the Earth's plasmaspheric helium ion emission produced by scattering of sunlight at 304 Å. Helium ions are trapped within the plasmasphere or region of closed magnetic field lines, which extend in this model to 4.25 Earth radii at the magnetic equator or about 60° latitude at the Earth. The Sun is to the left; the Earth's shadow can be seen on the right, passing through the plasmasphere. (R. Meier and S. Thonnard, Code 4140)

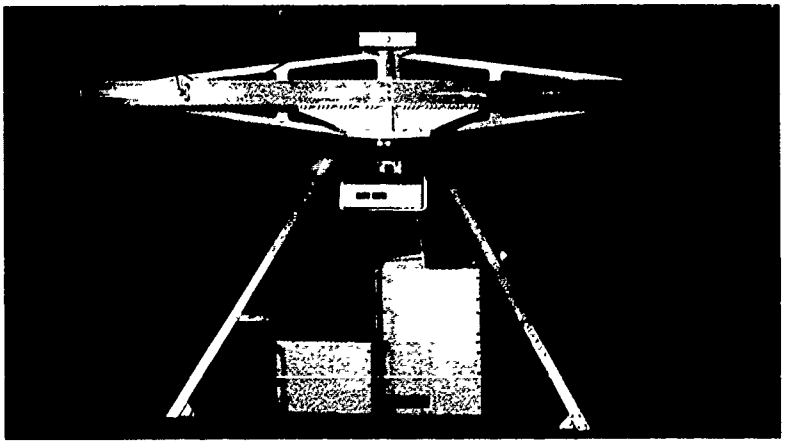

The precision direction-finding system measures the direction-of-arrival of received RF signals with extreme accuracy, extending the technology in direction-finding accuracy by more than two orders of magnitude, from typically 1 to 5 spatial degrees to 0.01 spatial degrees. (R. Oxley, Code 5724)

In cooperation, the Space Systems Technology Department and the Laboratory for Computational Physics and Fluid Dynamics developed a towable device, STEMS (Surface TEnsion Measuring System), to spatially measure in situ surface tension with high resolution. STEMS is shown being towed across a ship wake in that experiment. The smoke flare marks the wake edge. Four humpback whales show their interest in the project. (See paper entitled "Development of a Mobile Oceanographic Platform," in this *NRL Review*. (J. Kaiser, Code 8310) 8310)

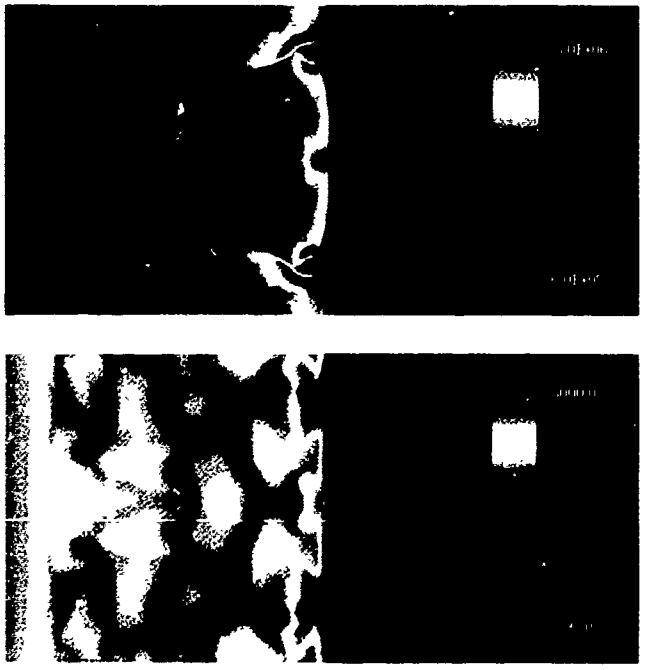

The structure of a propagating detonation: The figure shows that the instantaneous structure of a detonation propagating in a channel is complex and consists of multiple shock waves interacting at the detonation front. The pressure field (top photo) clearly shows the high pressure region (red) where the multiple shock waves interact. The transverse waves (propagating transverse to the direction of propagation of the detonation) are brought out distinctly in the pressure field. The temperature field (bottom photo) indicates that the energy release reactions take place at different distances behind the different shock waves This is an important factor crucial for sustaining a propagating detonation (K Kailasanath, Code 4410)

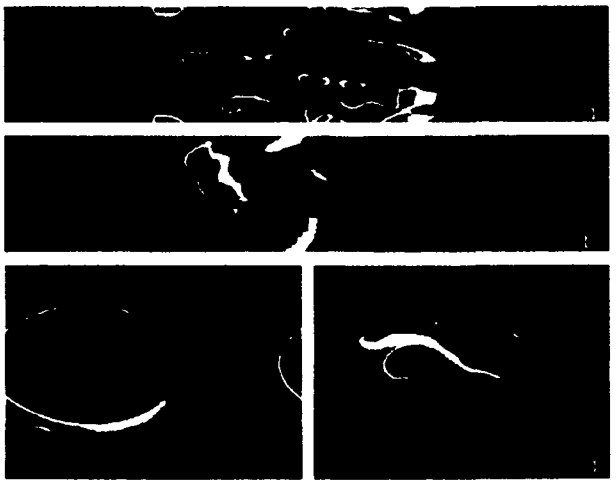

The development of ionosphere-magnetosphere coupling models: Panels (a) and (b) show the nonlinear evolution of density-gradient-driven plasma interchange instabilities generated in the high latitude ionosphere (a) without and (b) with magnetospheric coupling. Panels (c) and (d) display the evolution of the velocity-shear-driven Kelvin-Helmholtz instability in the high latitude magnetosphere (c) without and (d) with ionospheric coupling. (M. Keskinen, Code 4780)

Molecular graphic representation of two orientations of a DMBC lipid bilayer. (B. Gaber, Code 6090)

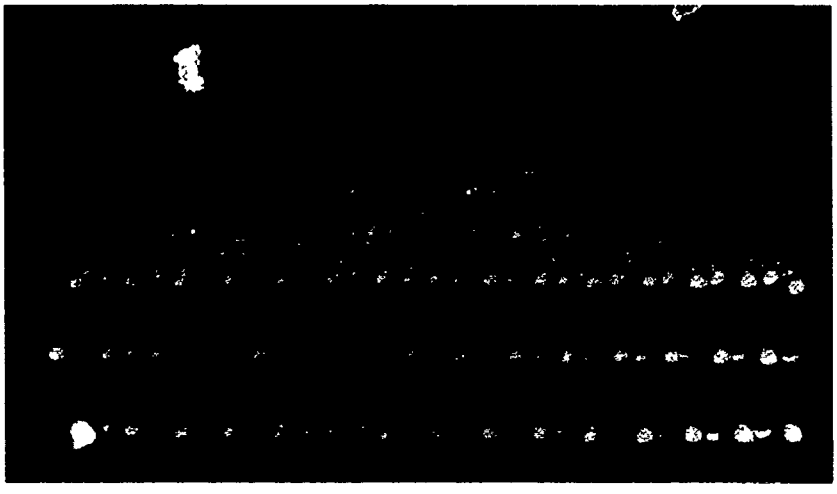

Studying the atomic mechanisms of adhesion, nanoindentation, and fracture mechanics. As the nickel tip (red spheres) pulls away from the gold surface, it takes a layer of gold atoms (yellow spheres) with it and pulls a thin neck of gold atoms from the second layer (green spheres). The photo visualizes a molecular dynamics simulation that predicts what will happen when a nickel tip makes contact with a gold surface and is removed again. The simulations were obtained on a Cray supercomputer by Uzi Landman and David Luedtke of Georgia Institute of Technology in collaboration with Nancy Burnham and Richard Colton of the Chemistry Division, who are using an atomic force microscope to measure the tip-surface interactions and to test the theoretical model. (R. Colton, Code 6177)

Featured Research at NRL

FEATURED RESEARCH AT NRL

Since its inception, NRL has grown in stature, has become the Navy's Corporate Research Laboratory, and has become a national and international leader in research and development in areas of naval interest. Multifaceted research programs embrace acoustics, artificial intelligence, biomolecular engineering, ceramics and composites, chemistry, electronics, ocean technologies, optics, plasmas, materials and their properties, radiation, sonar, space (near and far), and tactical electronic warfare, to name a few. This chapter is devoted to an in-depth look at the latest developments in adaptive radar, new energetic materials, and synchrotron X-ray radiation research.

Adaptive Radar

Frederick W. Lee and Mark E. Burroughs
Radar Division

Introduction

Future radars must operate in a world of ever increasing electromagnetic interference resulting in a degradation in system performance because of the presence of these undesired noise signals. The interfering signals may consist of intentional electronic countermeasures (ECM), unintentional radio frequency interference (RFI), or clutter returns. To combat the effects of ECM or RFI signals, several radar systems employ auxiliary receiving channels, known as sidelobe cancelers, to reject signals entering the radar receiver through the antenna sidelobes. To handle strong clutter returns, airborne surveillance radars use moving target indication (MTI) to make use of differences in Doppler shifts to distinguish between moving targets and "stationary" clutter. Although effective, both sidelobe cancelers and MTI systems suffer from critical performance limitations. Specifically, sidelobe cancelers are ineffective when ECM or RFI signals enter the radar receiver through the main beam of the antenna. In the case of MTI, clutter returns entering through the sidelobes of the antenna are shifted in Doppler, thereby becoming indistinguishable from Doppler shifts induced by target motion. To solve these problems, engineers at the Naval Research Laboratory (NRL) investigated a linear array system for airborne surveillance radars that detects the presence of interference sources and automatically adjusts to suppress these sources while simultaneously enhancing the reception of the desired radar returns. This type of system is known as an adaptive array radar.

Adaptive Array Radars

The use of an array of sensors for transmitting and receiving signals is becoming more common in modern radar systems. The Navy's E2-C Airborne Early Warning (AEW) radar system currently uses a linear array of sensors that allow for an increase in directivity and power capacity over a single sensor system. An adaptive array radar differs from this conventional array system by allowing dynamic control of the antenna beam pattern. This dynamic control is achieved by replacing the fixed beamforming network of the conventional system with a beamforming network that allows individual control of the antenna element weights. To control the weights, a real-time adaptive processor is needed. The purpose of the adaptive processor is to determine the optimum element weights that maximize the probability of detection for a fixed false alarm rate. This maximization of the probability of detection is equivalent to a maximization of the signal-to-noise ratio (SNR), where the signal is the desired radar return and the noise is the undesired interference.

The ability to maximize the SNR suggests that differences exist between the desired signals and the undesired noise that can be exploited. In the case of a radar system where the direction of arrival of the desired signals is known, spatial differences can be exploited by introducing beam pattern nulls in the directions of the undesired signals. Similarly, clutter returns are rejected by introducing nulls in the Doppler frequency domain. Research at NRL has demonstrated that

adaptive nulling of spatially distributed sources and Doppler frequency shifted clutter returns can be accomplished simultaneously by using space-time adaptive processing.

Proof of Concept

NRL's initial investigations of space-time adaptive processing involved an extensive computer simulation of a fully adaptive array radar. The model was of an active-pulse Doppler radar that simulated clutter returns and a selective number of spatially distributed interference sources. This computer model was used to investigate both transient and steady-state properties of a variety of adaptive algorithms.

Figure 1 shows that the nature of the adaptive space-time processor used in the computer simulation is best illustrated by examining its functional block diagram. Each antenna element in the system has a similar set of adaptive correction computers, multipliers, and a delay line that delays the element signal by one interpulse period. The two adders accumulate the outputs of the multipliers for each antenna element thereby forming the antenna beams. The front beam is formed from the summation of the weighted signals received during the current interpulse period. The back beam is formed from the summation of the weighted signals received during the previous interpulse period. Each beam has the ability to adaptively null spatially distributed interference sources and, by combining the two beams, nulls are formed in the Doppler frequency domain to simultaneously reject Doppler shifted clutter returns.

Figures 2 and 3 show typical outputs of the simulation in the unadapted and adapted response curves, respectively. The unadapted response is calculated by setting the output of the adaptive correction computers that drive the element weights to their quiescent or initial settings. The system then adapts to the particular scenario—in this case, stationary clutter—forming multiple nulls to attenuate signals that arrive from any angle with an apparent normalized target Doppler frequency of 0 Hz. Notice that this was accomplished without adversely affecting the main beam response at 90° for all other target Doppler frequencies.

Flight Test

After proving that space-time adaptive processing would work in a simulated environment, the next logical step was to test the feasibility of this processing against actual radar data. To accomplish this next critical step, NRL undertook an ambitious hardware development project to build a multichannel, real-time data recording system and then integrate this system with a specially modified airborne surveillance radar.

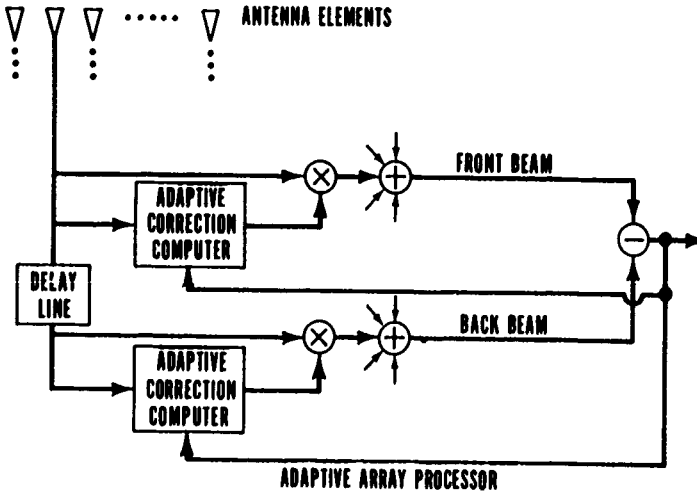

Fig. 1 — The adaptive space-time processor

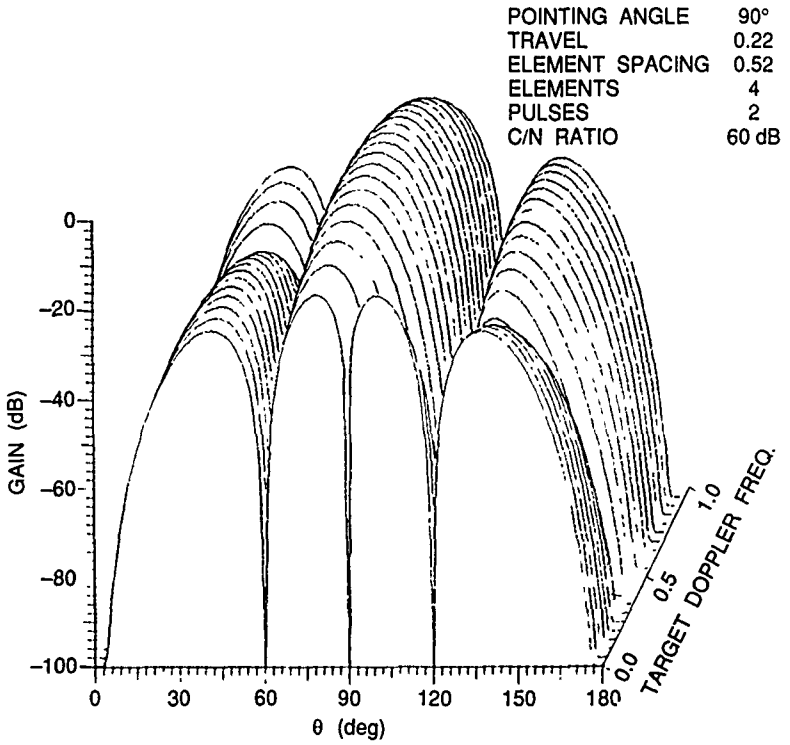

Fig. 2 — Unadapted response of adaptive space-time processor

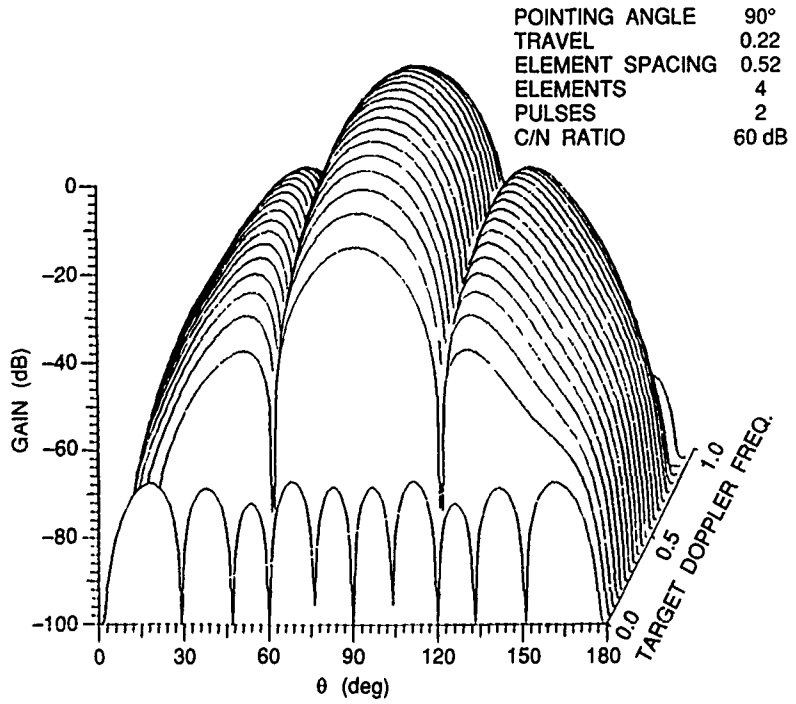

Fig. 3 — Adapted response of adaptive space-time processor

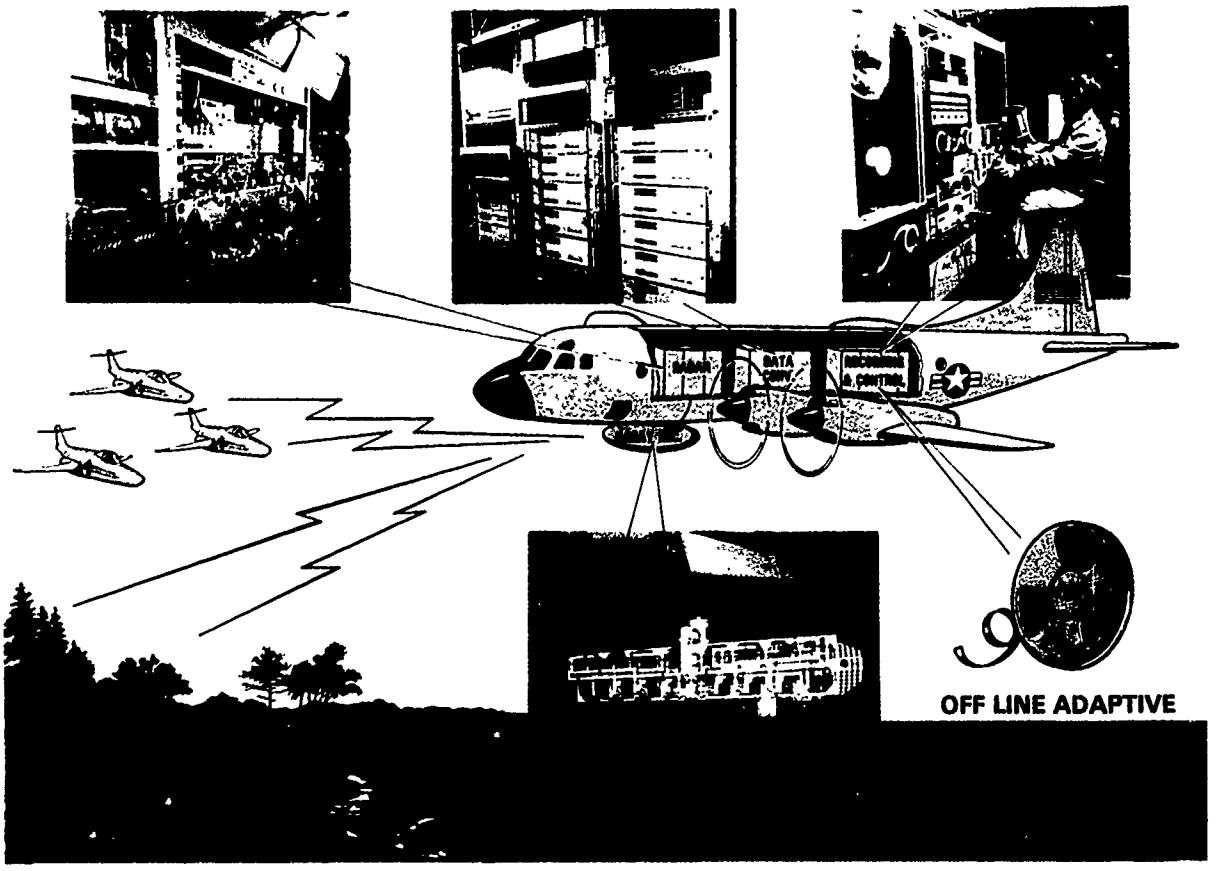

Fig 4 — Space-time adaptive radar system layout

The modifications to the radar, performed under contract by the General Electric Company, were quite extensive. The original antenna system was replaced by a ten-element linear array of dipoles mounted in a 90° corner reflector. The end two dipoles were terminated leaving eight active elements with essentially identical element patterns. Each active element of the antenna was connected to a separate matched receiver that down-converted the received RF signals to the radar's intermediate frequency (IF). The eight IF channels were filtered to remove out-of-band signals, and then each channel was synchronously demodulated, yielding eight complex pairs consisting of inphase (I) and quadrature (Q) baseband video signals.

The result of such an elaborate receiving system is to preserve both the amplitude and phase of a channel's received RF signal in the channel's corresponding I and Q baseband video signals. Because video frequencies are lower than RF frequencies, the I and Q video could be more readily converted to digital data and stored for off-line processing. NRL designed and constructed a multichannel, real-time recording system to perform this function. The system consisted of a bank of 16 high-speed, analog-to-digital converters, one for each of the I and Q signals. The digital data were then synchronously buffered in a high-speed bulk memory array that was then spooled out to a magnetic tape recorder. The data on the magnetic tape could then be stored for off-line processing in a general purpose computer.

This system was flown aboard NRL's research aircraft (Fig. 4) and recorded a wide variety of live signal environments. Several of the flights used the radar strictly in a passive mode,

recording interference received from ground-based or airborne noise sources. On other flights, the radar actively captured returns from targets of opportunity while simultaneously being jammed by the noise sources. Because the data is in a recorded digital format, other jamming scenarios have been derived by superimposing one data set onto another, allowing for an even greater variety.

This database, which NRL maintains, also has one of the most complete sets of multichannel UHF land clutter data available to the research community. As an example, land clutter was obtained from such diverse regions as the Appalachian Mountains (near the border of Virginia and West Virginia) to the midwestern farmland of Indiana (Fig. 5). By examining the three-dimensional clutter spectra from these vastly different regions (Fig. 6), the difficulties in overland radar performance become evident. The differences in the dynamic structure of the clutter for the different regions, as well as the clutter variations of the same region for different antenna pointing angles, illustrate that the radar's ability to adapt to these changes is the key to successful radar performance in land clutter.

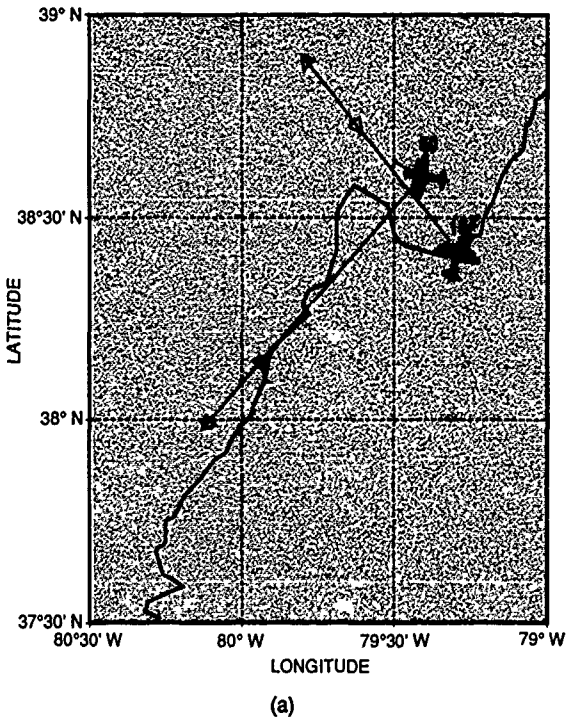

Fig. 5 — (a) Test area flight paths 15 and 50, (b) test area flight paths 65 and 66

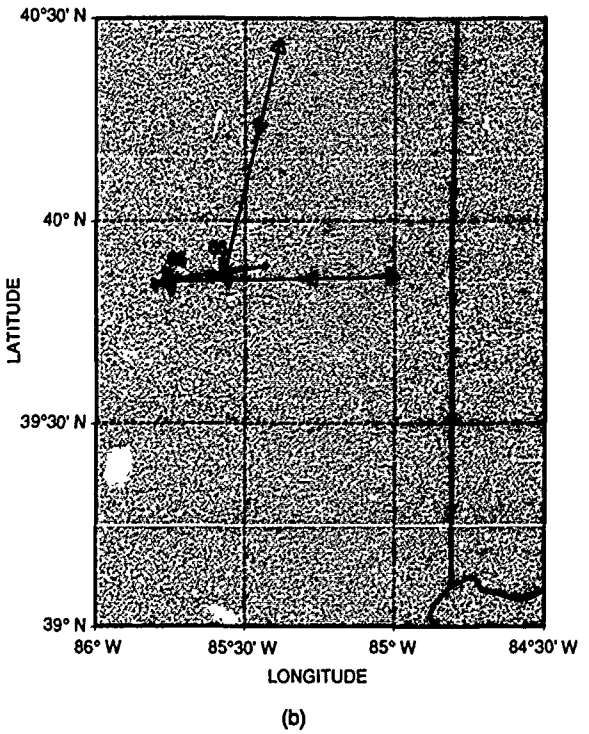

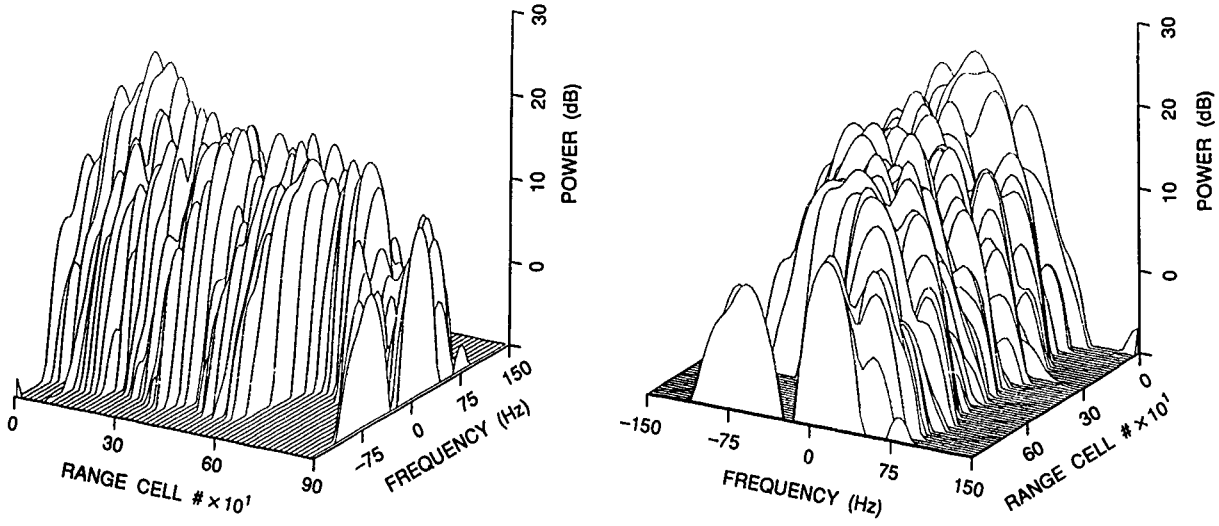

(a)

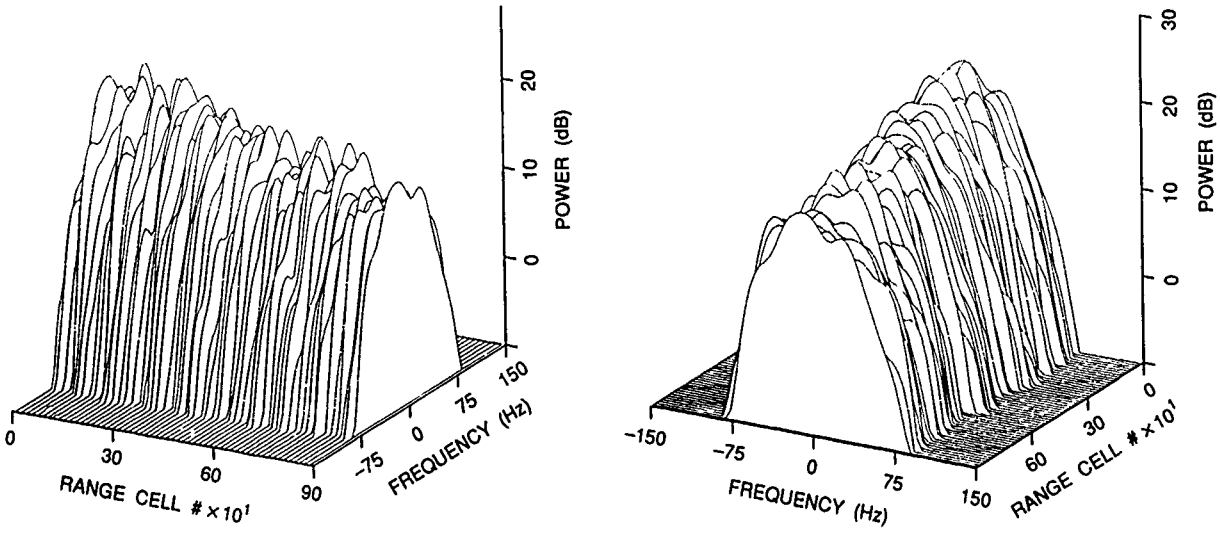

(b)

Fig. 6 — Land clutter spectra for: (a) flight path 15, 276 knots groundspeed, —67.7° antenna angle; (b) flight path 50, 224 knots groundspeed, —78.2° antenna angle; (c) flight path 65, 312 knots groundspeed, 8.7° antenna angle; and (d) flight path 66, 311 knots groundspeed, —65.8° antenna angle

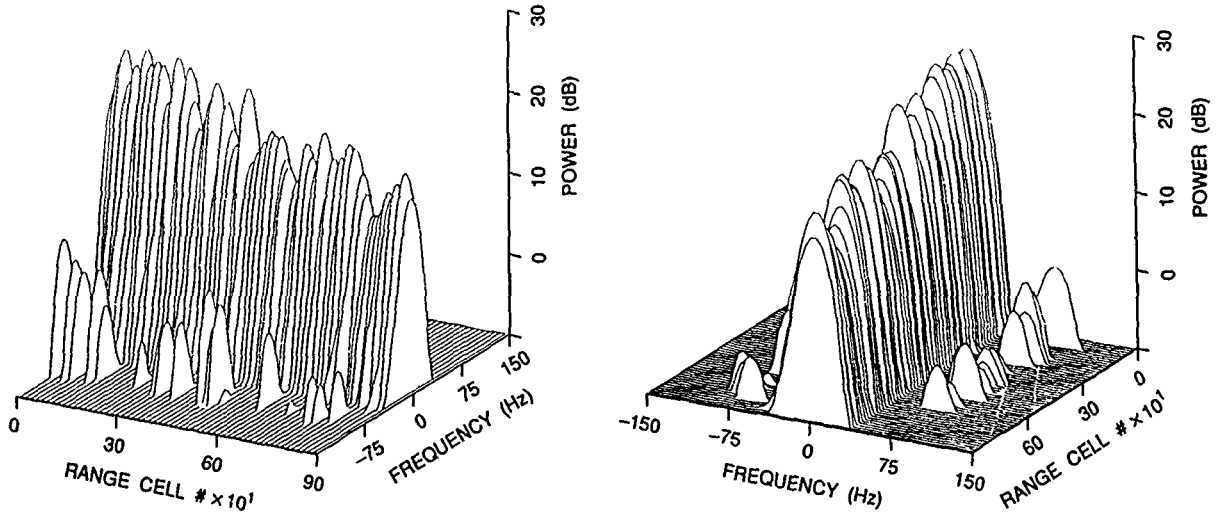

(c)

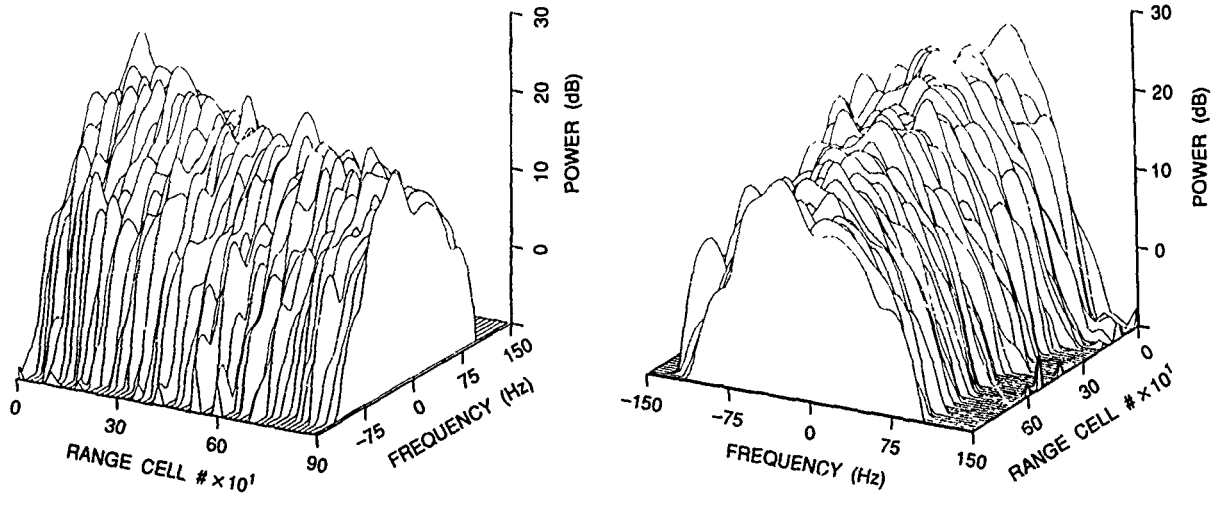

(d)

Fig. 6 (Continued) — Land clutter spectra for: (a) flight path 15, 276 knots groundspeed, —67.7° antenna angle; (b) flight path 50, 224 knots groundspeed, —78.2° antenna angle; (c) flight path 65, 312 knots groundspeed, 8.7° antenna angle; and (d) flight path 66, 311 knots groundspeed, —65.8° antenna angle

Adaptive Processing Laboratory

On completion of the flight tests, the system was relocated into the Adaptive Processing Laboratory for advance hardware and algorithm development. A signal injection unit was constructed to emulate the live signal environment. The signal injection unit combines generated test targets with up to three spatially correlated RF noise sources to simulate the signal environment. The spatial correlation of the noise sources was accomplished by splitting (eight-to-one) the amplified output of each noise diode, yielding eight coherent channels for each of the three noise sources. A separate programmable phase shifter is then inserted into each of the paths followed by a three-to-one adder that combines an output for each of the three sources into a single output for each of the eight radar channels. By progressively varying the phase shifters, the signal injection unit generates noise signals that appear to come from three different angles of arrival with the test targets arriving from a fixed angle. The output of the signal injection unit is connected directly to the eight receivers with the rest of the laboratory system unchanged from that of the flight test system (Fig. 7).

The first advancement made in the laboratory was the development of a real-time adaptive digital beamformer. With recent progress made in the field of digital signal processing, it is possible to construct a system that applies the element weights in a digital format to the synchronous data stream coming out of the analog-to-digital converters. Also in the laboratory, a digital beamformer allows for an instantaneous analysis of the effectiveness of adaptive algorithms against contrived signal scenarios. In an operational system, the beamformer is one of the critical elements necessary for an adaptive radar. By demonstrating its capabilities in the laboratory, it is hoped that the inherent risk of implementing digital beamforming and thus, adaptive processing, is reduced to an acceptable level.

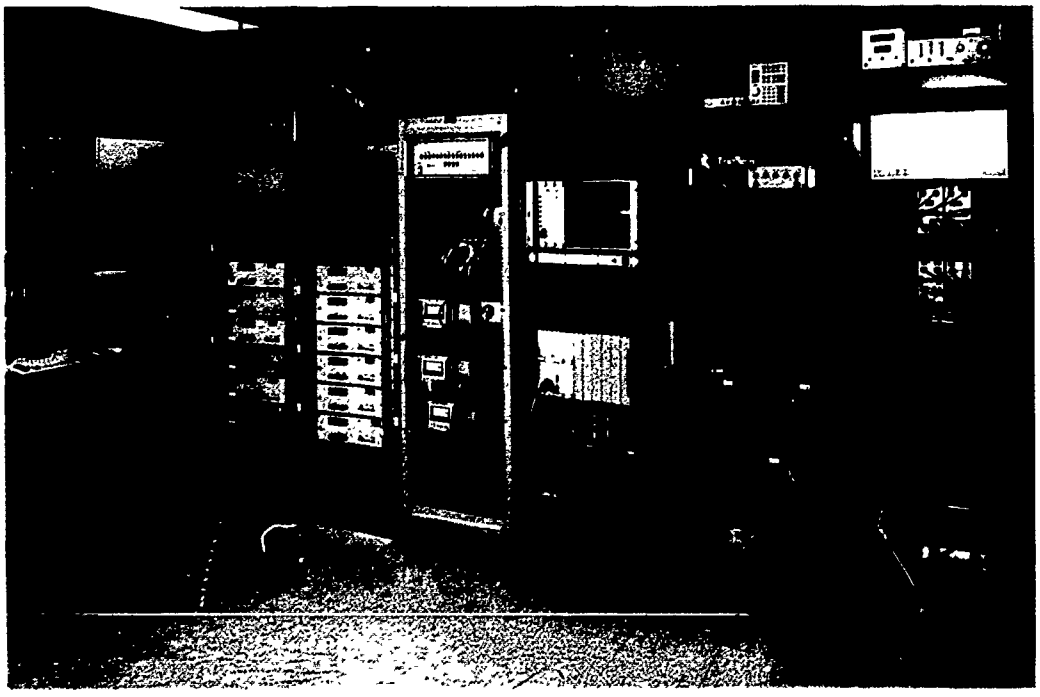

Fig. 7 — Adaptive Processing Laboratory

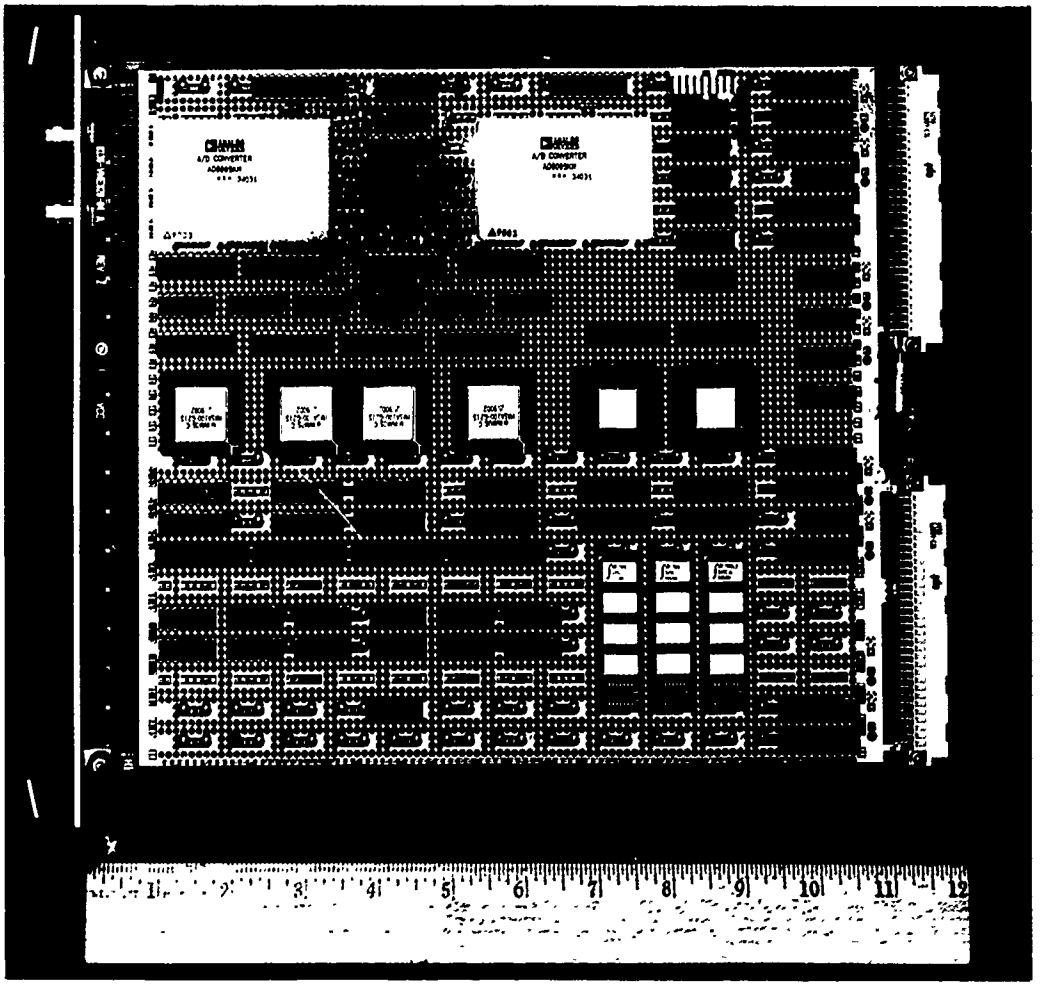

Fig. 8 — Digital equalization filter (prototype)

Currently, work is underway to develop an adaptive equalization filter bank to dynamically calibrate the radar channels to increase the overall cancellation ratio of the system. The prototype circuit (Fig.8) makes use of very large-scale integrated (VLSI) circuit technology yielding a computational performance of approximately 200 million operations-per-second. By operating these signal processing elements in parallel with each other, the overall system will exceed a billion operations-per-second. Along with the hardware developments, the Adaptive Processing Laboratory is being used to develop and refine adaptive algorithms, superresolution algorithms, and radar waveforms.

Conclusion

The use of adaptive radars has been demonstrated by NRL to be the key to successful operation of future Navy AEW radar systems. By using the NRL database, researchers continue to develop new and more effective adaptive algorithms that can be used in future radar systems. The development at NRL of real-time digital signal processors has demonstrated that the critical technologies necessary to field an operational adaptive radar system exist. The next crucial step is to fly an adaptive radar system in an operational environment to demonstratethe expected increases that adaptive processing adds to the detection

performance in dense clutter and jamming environments.

Acknowledgments

We thank Fred Staudaher for supplying the clutter spectra presented as well as for his support and guidance on this project. Thanks also to Herb Meadows for his outstanding technical support on the development of the digital signal processors used in the Adaptive Processing Laboratory.

This work was supported under the Airborne Surveillance Block by the Office of Naval Technology through the Naval Air Development Center.

THE AUTHORS

FREDERICK W. LEE received his B.S.E.E. degree from the University of Maryland, College Park, Maryland in 1986. He is currently working on his M.S.E.E. degree in communications at The George Washington University. Mr. Lee joined NRL's Radar Division in 1986, working for the Airborne Radar Branch on digitally controlled analog signal processors. Present research activities focus on real-time control system and digital signal processing. He is a member of the IEEE Acoustics, Speech, and Signal Processing Society.

MARK E. BURROUGHS received his A.A.E. degree (with high honors) from Prince George's Community College, Largo, Maryland, in 1982, and his B.S.E.E. degree (with honors) from the University of Maryland, College Park, Maryland, in 1984. In 1985, he joined NRL's Radar Division as an Electronics Engineer. Until 1988, his research centered on use of computer graphics to enhance radar imaging. Since then, his research has focused on real-time digital signal processing of radar data. Current work involves adaptive array beamforming.

Synthesis and Structures of New Energetic Materials

Richard D. Gilardi and Clifford F. George
Laboratory for the Structure of Matter

At the beginning of the 1980s, the Office of Naval Research (ONR) identified a strong need for the production of new, high-energy-density materials, an emerging area of research named by the Department of Defense as one of the 20 technologies "most critical to our long-term defense" [1]. Better materials in this area will enable improvements in performance coupled with increased safety in the next generation of naval ordnance. To meet these requirements, a number of research initiatives were spawned that focus on the synthetic chemists who synthesize new energetic materials and engage the expertise of researchers from many other scientific disciplines, from rocket engineering to quantum chemistry.

The sudden production of hundreds of new energetic compounds and precursors to energetic compounds by this ONR program provided an opportunity for NRL's Laboratory for the Structure of Matter (LSM) to demonstrate the utility of rapid structural analysis to a synthesis program. Each new material in the program was submitted to NRL. LSM's X-ray analyses quickly corroborated the expected structural formula for most syntheses but sometimes revealed completely unexpected products. The analyses also indicated the nature and quantity of solvent incorporation (if any) in solid samples and provided accurate densities of these new materials. In the longer run, the details of the molecular structures furnished by these analyses have provided a firm basis for mathematical relations between structure and properties in this class of compounds. Such correlations may be used to predict the properties of as yet unsynthesized "target compounds" and can aid in deciding whether an all-out effort to synthesize them would be worthwhile.

Energetic Materials

What exactly do we mean by an energetic material? Most organic compounds provide energy (heat) when burned. Many common substances will even explode when finely dispersed in air or oxygen. But the special focus here is on high-density organic solids used as major components of explosives and propellants. These compounds are generally useful only if they contain within themselves a balance of elements such that no solids remain after burning or explosion, even in the absence of air. It is this conversion from dense solid to a large volume of hot gases that produces the desired effect. In a propellant, conversion by burning at a rapid but controlled rate and expulsion of the hot gases through a nozzle produces the momentum transfer that propels a missile or spacecraft. In an explosive, the components are chosen to favor maximum reaction velocity. The large, almost instantaneous volume change produces a loud noise and pressures that may be high enough to pierce steel armor. Despite the differences in rate and effect, the compounds and techniques used in formulating solid propellants and explosives are very similar.

Structure Analysis

In this article, structure analysis means the determination of the atomic arrangements in a material in its crystalline state. This is usually done at NRL by observing in great detail what happens

to a beam of X rays as it passes through a tiny (dimensions from 0.02 to 0.5 mm), single crystal of the pure material. There are a number of aspects to X-ray structural analyses. These aspects are often used to identify unknown substances since they can be performed without prior knowledge of molecular structure or chemical composition. In addition, it is possible to determine the connectivity of a molecule, its absolute configuration, the magnitude of its thermal (vibrational) motion, and how the molecule packs regularly to form a crystal. With careful experimentation in properly chosen cases, accurate electron density distributions (and thus the electrostatic interactions of the molecules) can also be evaluated.

Applications of this type of information are evident in various areas of science, such as synthetic organic chemistry, natural products chemistry, pharmaceutical chemistry, reaction mechanism studies, biomolecular engineering, and in understanding a host of biochemical interactions. In addition to understanding the relationship of structure to function, structural information plays a valuable role in the development of new and improved energetic materials.

Structural Databases

One consequence of the general availability of rapid methods of X-ray structural analysis has been a flood of published crystal structure analyses. As of January 1991, a major computerized database of crystal-structure analyses—the Cambridge Structural Database [2]—contained results on over 82,000 chemical structures. This database is restricted to organic chemical compounds; it can be searched by computer to find any desired formula, element, or molecular fragment and thus is helpful in the design of substances with desired properties, such as drug design. The investigation of the structures of over 300 energetic materials (and related precursors) at NRL provides the basis for an energetic materials database that is maintained by LSM; it serves as a useful source of information for making predictions concerning the possible success in the synthesis of new materials.

Energetic Materials—Density, Pressure, and Impulse

Density plays an important role in the behavior of energetic materials. The pressure in explosions and the impulse produced by the same compound when burned as a propellant are related. The detonation pressure (the pressure of the shock wave behind a detonation front) is proportional to the square of the density times the specific impulse. So, if we are considering molecules of the same general chemical type, and we increase the density by some factor—say 1.2, the detonation pressure is expected to increase by at least 1.2 squared, or 1.44. The other factor affecting the pressure is the specific impulse I_{sp}, which is the maximum momentum imparted by burning a gram of the substance. I_{sp} depends on the volume of gas produced and the quantity of heat released. Since each of these quantities tends to increase slightly as the density goes up, the overall dependency of the detonation pressure on the density may be even greater than the square of its increase. Figure 1 shows two examples of dense energetic materials widely used for military purposes, RDX and β-HMX.

After making and studying a large number of dense energetic molecules, one may ask, "Can we extrapolate these results to compounds not yet made and assess hypothetical target molecules?" Algorithms have been developed that statistically relate the density of all the known energetic compounds to their structural formula, and they seem to predict densities of the known compounds to within ~3%. It is possible to conceive of many target molecules that are completely or almost completely substituted with nitro groups. Figure 2 shows two hypothetical target molecules. These two have densities that are predicted to be higher than any known nitro compounds.

Both of these molecules are called cage compounds, because the center of the molecule is surrounded by a linked network of rings, like a spherical cage. The molecule on the left-hand side

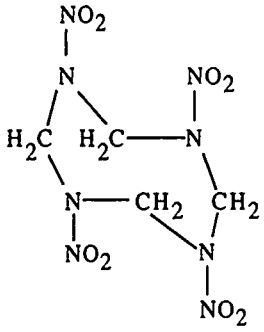

ß-HMX

Density 1.90 Mg m^{-3}

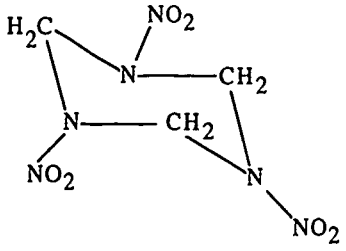

RDX

Density 1.81 Mg m^{-3}

Fig. 1 — HMX and RDX, two well-studied dense energetic compounds widely used as explosives and as components of solid rocket fuels

Hexanitrohexa-aza-adamantane

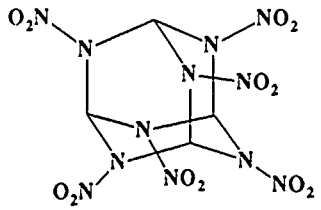

Predicted Density = 2.0–2.2 Mg m^{-3}

Octanitrocubane

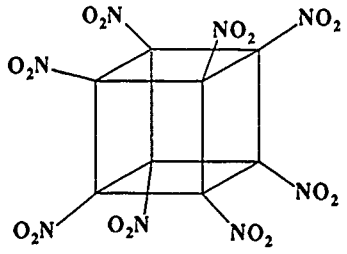

Predicted Density = 2.0–2.1 Mg m^{-3}

Fig. 2 — Two major high-energy targets for synthetic chemists

is called an adamantane and the one on the right-hand side, a cubane, after the names of the unsubstituted parent compounds. The nitro-substituted adamantane is made up of modules that resemble the successful explosive, RDX (Fig. 1). The cubane nucleus has, in addition to high energy through density and massive nitro substitution, a large inherent strain energy.

Energetic Materials—Strain Energy

What is strain energy? Molecules generally behave as if their atoms are connected by a flexible set of connections, which we call bonds. These bonds can be extended or compressed by external forces but tend to assume certain values for their distances and for their interbond angles. However, it is impossible to connect some of the more complex ring systems found in molecules except by forcing some of the bond angles (or, more rarely, distances) to remain at values far from their ideal. Cubanes are close to the top of the list in overall strain energy, for all the carbon bond angles are forced to remain near 90° to maintain closure of its rings; the preferred bond angle values in this type of compound are 109.5°.

Though octanitrocubane (ONCU) (Fig. 2) is still a dream compound, three nitro-substituted cubanes, a di-, a tri-, and a tetranitrocubane, have been synthesized by DoD-assisted synthetic chemists at the University of Chicago. All are quite stable. Their crystals were studied at NRL, and their densities were found to be proportional to the number of nitro substituents, namely, 1.66, 1.74, and 1.814 Mg/m^{-3}, respectively. Figure 3 shows the densest one, known as 1,3,5,7-tetranitrocubane, along with several other new cage compounds analyzed at NRL as part of this program.

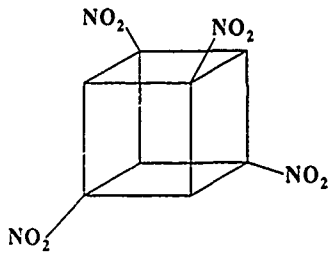

1,3,5,7-Tetranitrocubane

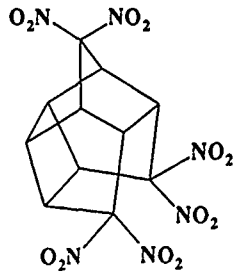

A Hexanitropentacycloundecane

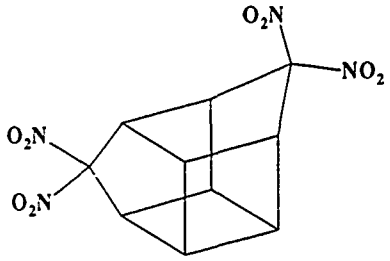

A Tetranitrobishomocubane

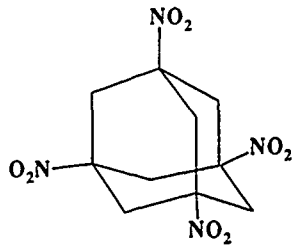

1,3,5,7 Tetranitroadamantane

Fig. 3 — Structures of four recently synthesized energetic cage compounds

Energetic Cubane Compounds

ONCU was identified early in the ONR synthesis program to be a highly desirable energetic material because of the dual predictions of high density and high energy of combustion. However, there are still other favorable indicators. ONCU contains enough oxygen to completely oxidize all of the carbon atoms in the compound to gaseous CO or CO_2, leaving no unburned residue, such as soot. In addition, it contains no hydrogen atoms and thus produces no water when burned. Oxygen-balanced, zero-hydrogen propellants tend to leave little or no visible smoke behind the rocket and therefore are called *low-signature* propellants. A dense rocket plume allows enemies to more easily track such a rocket, and the smoke produced obscures sensors of friendly forces attempting to monitor a battle scene.

If ONCU is promising in so many ways, why don't we just make some and test it? This brings up a major problem in computer-aided molecular design. We often can predict (roughly) the properties of a hypothetical compound and can calculate that the compound will (probably) be stable when made, but then we find that no known reactions will produce the compound from available precursors. This is particularly the case in the area of energetic materials—especially strained ones such as cubanes.

The discovery of cubane was first reported and its structure confirmed in 1964 [3]. Though it attracted immediate and lasting attention in the world of organic chemistry, only a few new cubane compounds were made in the next 20 years. Once a cubane compound was made, it was difficult to transform it without "zipping open" the strained cage. In the 1980s, with the support of Army and Navy research programs, new reactions were found that could be used to add new substituents to the cubane cage without destroying it, and a large number of new compounds have since been reported. Figure 4 shows a sample of energetic cubane compounds whose structures were analyzed at NRL. Figure 5 portrays some novel polycubane compounds analyzed at NRL that may be precursors of future energetic materials.

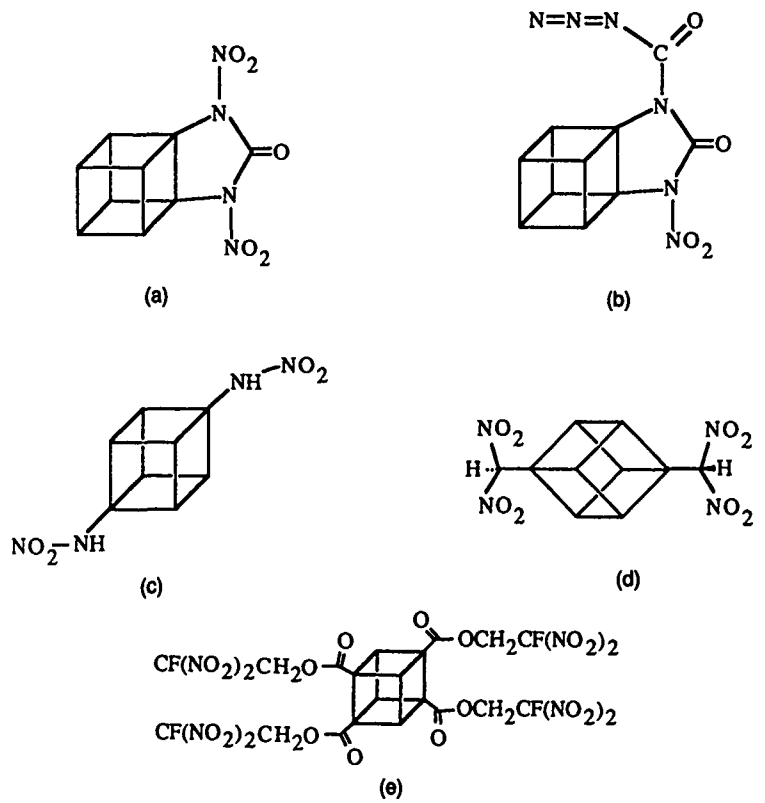

Fig. 4 — High-density cubanes with energetic substituents: (a) N,N'-dinitrocubanourea; (b) N-azidocarbonyl-N'-nitro-cubanourea; (c) N,N'-dinitro-1,4-cubanediamine; (d) 1,4-bis(dinitromethyl)cubane; and (e) an energetic ester of 1,2,4,7-cubanetetracarboxylic acid. The densities of these new energetic materials are: (a) = 1.69, (b) = 1.73, (c) = 1.70, (d) = 1.64, and (e) = 1.77 Mg/m^{-3}. These are almost as dense as HMX or RDX, and compounds (a)-(d) have ample room for additional substitution. Denser variants will be made and tested as chemical techniques for making these compounds and their cubane precursors improve.

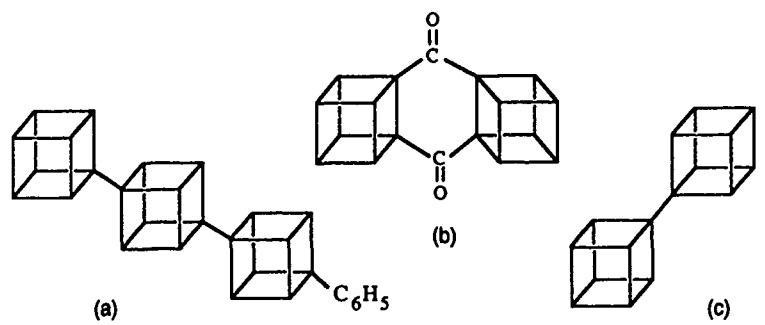

Fig. 5 — New polycubyl compounds: (a) a phenyltercubane: (b) a cubane/cyclohexadione fusion, and (c) cubylcubane

There is still a major problem looming ahead for ONCU as an energetic material: no compound has yet been made that puts two nitro groups on *adjacent* corners of a cube. [Note that the tetranitrocubane shown in Fig. 3 is the one possible tetra-isomer that avoids adjacent-atom substitution.] Calculations indicate that this is not due to any inherent instability in a cubane with adjacent nitro groups but is due to an instability in the usual precursor compounds in which an amino group is adjacent to a nitro group. No one has thus far found a way around this problem, though in principle another route may exist. In the meantime, a number of approaches that avoid putting nitro groups directly on the cube have been proposed (Fig. 4) that may lead to equal or even superior materials. Figure 6 shows one of the first cubane salts where the cube is cationic because it is substituted with four ammonium substituents.

An eventual problem for any cubane fuel, propellant, or explosive is cost. At present, all syntheses of cubane compounds from low-priced industrial chemicals require a dozen or more steps, which lead to low yields and high costs (estimated at over $10K/lb at present). But there is no intrinsic reason requiring that this remain so; tomorrow some chemist may discover a catalyst that will make a cubane in one step from a low-cost starting material. For example, chemists have often pointed out that acetylene and cubane are related in principle by the reaction:

$$4\ C_2H_2\ (\text{acetylene}) \rightarrow C_8H_8\ (\text{cubane}),$$

and that this reaction is exothermic (energetically favoring the right-hand side) despite the high strain energy in the cubane cage.

RDX & HMX—Background

Two of the most important military explosives are RDX and HMX (Fig. 1), which combine high densities and extremely high detonation velocities (>9 km/s) with thermal stability and moderate sensitivity to shock. RDX was first reported in 1899 but apparently not recognized as an explosive

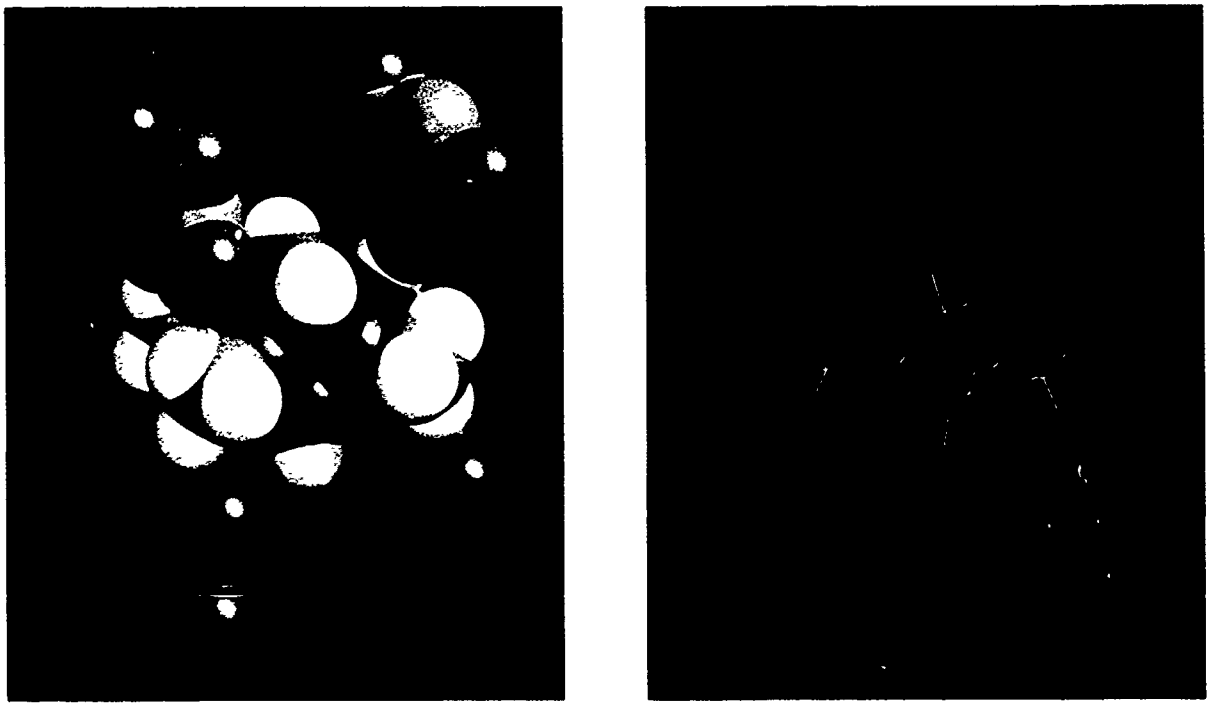

Fig. 6 — Computer representations of an energetic cubane salt. The view on the left-hand side uses a ray-tracing algorithm to generate a picture of a solid (space-filling) model, while the one on the right-hand side shows a "stick-model" of the molecule imbedded in a matrix of dots located on the surface of the molecule.

until 1920. From then until 1938 or so, it was quietly investigated in several countries as a possible military explosive. With the coming of WWII, many chemists became involved in RDX research, and several new syntheses were found that could be practical on an industrial scale. These were rapidly developed, and by the end of the war, some 300 tons a day were being produced in the United States [4]. HMX was discovered to be a higher-melting impurity present at a level of 5% to 10% by weight in the RDX produced in one of these plants. Fortunately, HMX was found to be superior to RDX in its explosive properties. Both compounds are said to be excellent in thermal stability, which means that they are not subject to deterioration by exposure to normal ranges of temperature and humidity. One of the most common failings of new energetic materials is the tendency to react with the water in the atmosphere.

Energetic Nitramines

RDX and HMX are called monocyclic nitramines. A nitramine is a compound in which nitro groups ($-NO_2$) are bonded directly to amine nitrogen atoms (i.e., those in -NH2 or -NH- groupings). Each nitro group replaces one of the hydrogen atoms normally found on amines. Because of the excellent stability of RDX and HMX, a large portion of the recent ONR effort has concentrated on discovering new classes of nitramines and measuring their properties. As mentioned above, densities tend to be strongly correlated with good explosive and propellant properties and are also predictable with reasonable accuracy (±3%). Thus the search was often directed by the question: What kinds of nitramines will have higher densities than RDX and HMX?

Certain structural arrangements are known to maximize density. The first consideration is the atomic composition, or empirical formula. Replacement of light atoms (such as hydrogen) by nitrogen or oxygen atoms invariably increases the density. However, the structural topology also plays a role; for a given C:N:O ratio, density generally increases as one proceeds structurally from acyclic → monocyclic → bicyclic → polycyclic → caged polycyclic types of molecules. Over 80 of the new materials submitted to NRL/LSM for analysis and subsequent archiving in the LSM energetic database are nitramines, representing all of the above classes. Figure 7 shows some of the new polycyclic nitramines.

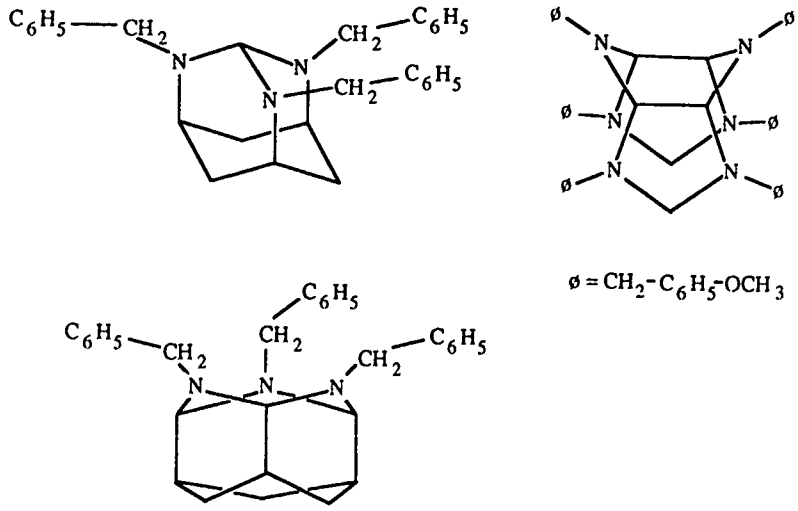

Fig. 7 — Three polycyclic cage compounds with aza (i.e., nitrogen atom) substitution at several sites in the cage systems. The three types of cage compounds shown here are known as adamantane, wurtzitane, and isowurtzitane (according to the name of the parent hydrocarbon).

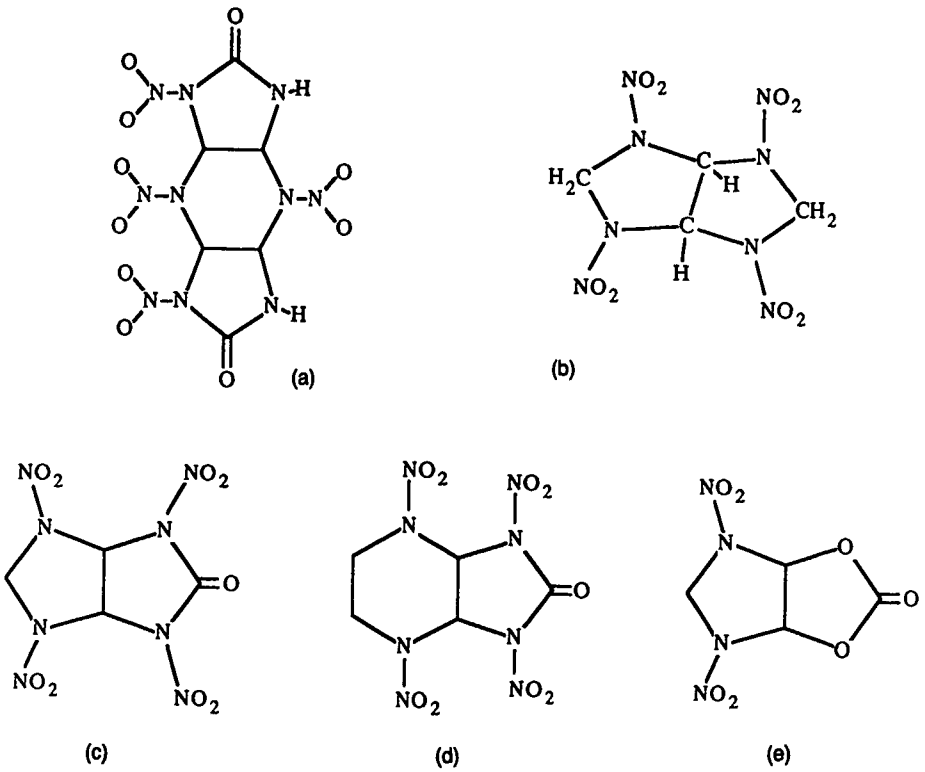

Fig. 8 — Structural formulae of several dense polycyclic nitramines made at the Naval Surface Warfare Center and at the Livermore National Laboratory. The structural subcomponents of these compounds resemble those in proven monocyclic materials such as RDX and HMX. The densities of these compounds range from 1.868 Mg/m^{-3} (for (b)) to 1.969 Mg/m^{-3} (for (d)).

In many cases, target nitramines are produced in the final stage by the nitration of polycyclic amines. (Nitration, as used here, simply means the replacement of hydrogen atoms by NO_2 groups.) However, polyamino compounds are uncommon, so the first subproblem to be resolved is the synthesis of new cages with many of the carbon atoms replaced by amine nitrogen atoms. Figure 8 shows three of the N-substituted cages that have been made in this program; in each of these cases, the structures made and corroborated by X-ray analyses were N-benzyl derivatives of the parent cage compounds, where the amino hydrogens were replaced with benzyl ($C_6H_5CH_2$-) or p-methoxybenzyl ($CH_3OC_6H_5CH_2$-) groups.

Nitramine Structure Analysis

When a number of related structures are studied, basic structural parameters such as preferred bond distances and angles for chemical groupings can be derived through statistical analysis. In addition, subtler structural features may be ascertained. For example, examination of the structures of the nitramine groups in the Cambridge and NRL/LSM databases shows that the amino nitrogen atoms in nitramines are rather flexible; i. e., in some molecules, the three bonds to the amino nitrogen atom are coplanar, while in others they are decidedly nonplanar, and the N atom is described as "pyramidal." Figure 9 illustrates the distribution of the out-of-plane bending angles for the amino group. The histogram for the amino bend ranges from 0° to 60°; though dominated by small (0° to 20°) angles of bending, they range up to 59° as observed in one example. Figure 9 also shows that the nitrogen atom in the nitro group of the nitramine is much less flexible and seldom departs from a planar conformation by more than a few degrees. In the flexible amino portion of the nitramine, it is also of interest to note that a correlation exists between the C-N-C angle and the amino bend (Fig. 10). This

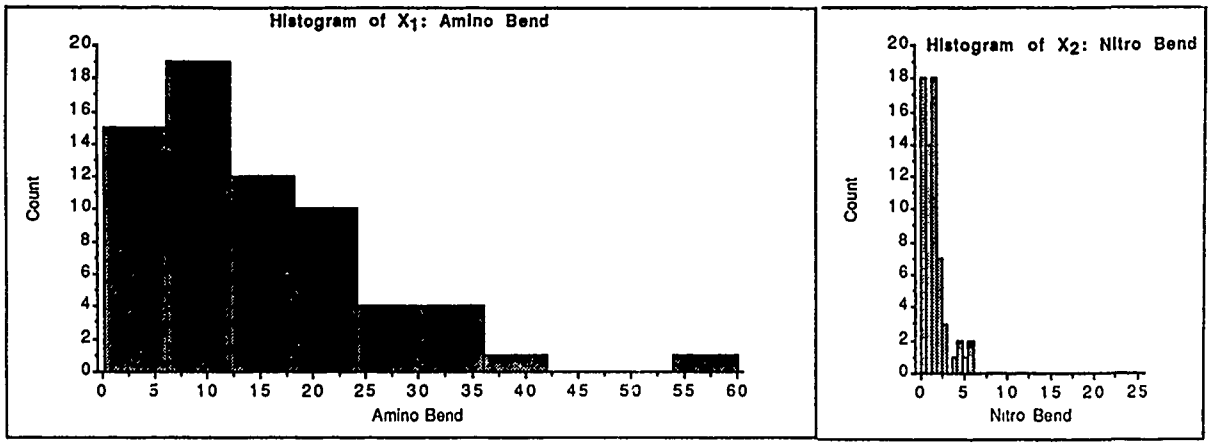

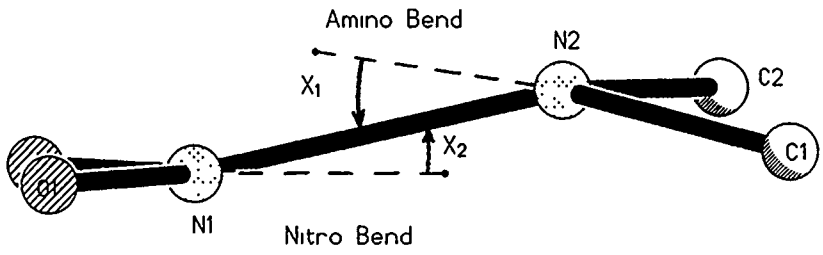

Fig. 9 — Frequency distributions for two out-of-plane deformations of the nitramino group

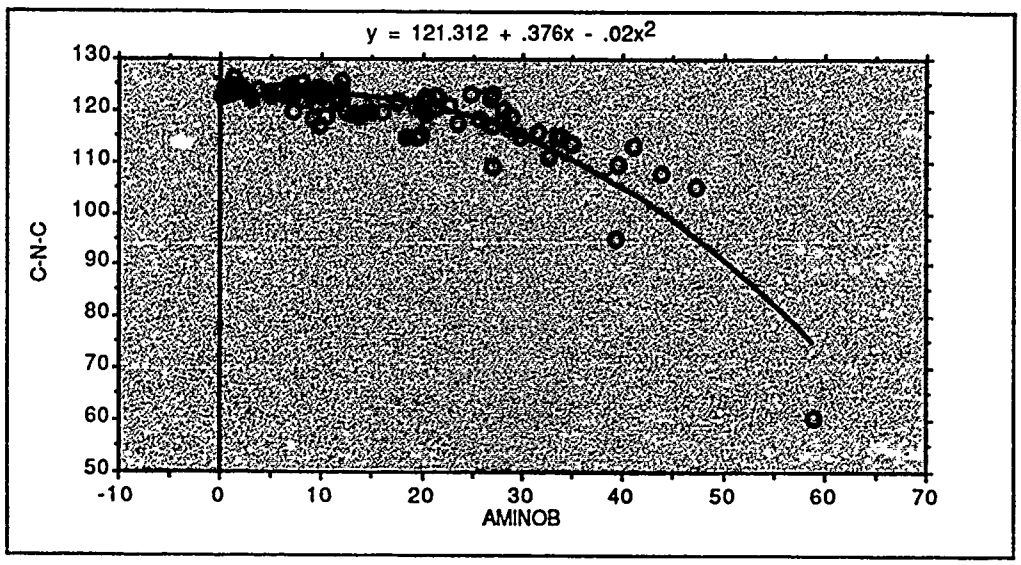

Fig. 10 — The amino C-N-C bond angle and the amino bend (in degrees, see Fig. 9 for definition) of the nitramino group, as observed in more than 60 X-ray structural determinations. The curved line represents the best fit to the data by a second-degree polynomial function.

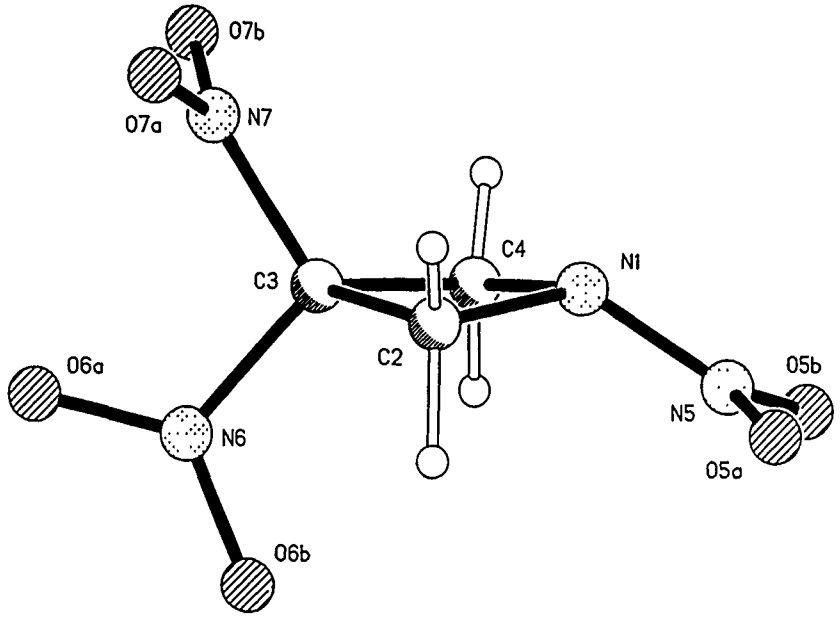

Fig. 11 — 1,3,3-trinitroazetidine as observed in the crystal

means that nitramines, which are part of small rings and thus adopt a small C–N–C bond angle, will have a tendency to be pyramidal at the amino nitrogen atom. An example of such a structure is 1,3,3-trinitroazetidine (Fig. 11), a dense strained nitramine wherein the N1 to N5 bond makes a 39.7° angle with the C2–N1–C4 plane.

After (and partly as a result of) this study of nitramine structures, an extensive quantum-mechanical analysis of a simple nitramine, dimethylnitramine, was carried out at the University of Texas [6]. This calculation indicated that a dimethylnitramine model containing a planar amino nitrogen has the lowest energy, but only 400 cal/mol were needed to bend the amino–nitro bond 40° out of the plane. This is a small amount similar in magnitude to the thermal energy of a molecule at room temperature. Thus, the X-ray structural analyses and the quantum chemical analysis both indicate that weak forces can produce large changes in the amino bend since the energies are not much different for the in-plane and the out-of-plane configurations. This type of structural information is of great interest to the theoretical chemists in the program who are studying the electronic properties of energetic groups and is also helpful in the computer modeling of hypothetical energetic materials.

Summary

What payoffs might come from this research, and what is the prognosis for the future? Hundreds of new materials were synthesized in this program, and more than 300 of these were analyzed at NRL. Some are possible precursors, not meant to be energetic themselves. Others are low-energy model compounds made to demonstrate the usefulness of a new reaction or reagent. Still others were submitted for analysis because they were unknown products or impurities produced in an energetic synthesis. Yet many are energetic compounds that match or even exceed in some useful property the energetic materials now being used (such as RDX and HMX). For security and/or proprietary reasons, the structures of the best materials are not mentioned in this article. However, we can say that one of the new materials known as CL20 exceeds HMX in energy content and is being extensively investigated and tested. LSM/NRL is participating extensively in this effort and has examined over 20 variants of CL20 to monitor the effect of changes in reaction conditions

and crystallization procedures on the properties and purity of the final product. The discovery of this particular compound may lead to economically viable, safer, and/or more powerful propellants and explosives; but its greater significance is as a signal that Navy chemists have advanced the chemistry of energetic materials to the point that members of new classes of highly energy-dense materials are now being made and tested. This new chemistry will eventually lead to a variety of new materials with improved properties.

References

1. R. Seltzer, "Plan for Vital Defense Technologies Issued," *Chemical and Engineering News*, p. 5, Mar. 26, 1990.
2. F.H. Allen, S. Bellard, M.D. Brice, B.A. Cartwright, A. Doubleday, H. Higgs, T. Hummelink, B.G. Hummelink-Peters, O. Kennard, W.D.S. Motherwell, J.R. Rodgers and D.G. Watson, "The Cambridge Crystallographic Data Centre: Computer-Based Search, Retrieval, Analysis and Display of Information," *Acta Cryst.* **B35**, 2331-2339 (1979).
3. P.E. Eaton and T.W. Cole Jr., "The Cubane System," *J. Am. Chem. Soc.* 86, 962 (1964) and E.B. Fleischer, "X-Ray Structure Determination of Cubane," *J. Am. Chem. Soc.* **86**, 3889 (1964).
4. J.T. Edward, "Wartime Research on RDX," *J. Chem. Educ.* **64**, 599 (1987).
5. F.R. Cordell, "Ab initio Study of Dimethylnitramine," 1987 Report, University of Texas, Austin; Government Report Announcement Index (U.S.) 87, Abstr. No. 750,665, NTIS order No. AD-A183414.

THE AUTHORS

RICHARD D. GILARDI graduated from MIT in Cambridge, Massachusetts, in 1961 with a B.S. degree in Chemistry. He received a Ph.D. degree in physical chemistry from the University of Maryland in 1966; his thesis concerned the theoretical analysis of the vibrational behavior and far-infrared spectra of clusters of polar gas molecules. Dr. Gilardi joined the NRL Diffraction Group (now known as the Laboratory for the Structure of Matter) in 1966 as a National Research Council postdoctoral associate to participate in developing and applying new X-ray diffraction techniques to single-crystal analysis. He is an author on over 80 articles in structural chemistry, and he has received six NRL Research Publication Awards. In 1986, Dr. Gilardi received the U.S. Navy Meritorious Civilian Service Award. He is an active member of the American Crystallographic Association, where he has served on several elected committees and organized scientific sessions at several annual national meetings. Over the years, his structural research has involved many types of organic compounds, such as antimalarial drugs from the Walter Reed Army Institute of Research, insect pheromones from the U. S. Department of Agriculture, and various bioactive compounds from the National Institutes of Health. In recent years, Dr. Gilardi's research has concentrated on the structural analysis of real or hypothetical energetic materials (explosives, propellants, and extremely strained organic molecules).

CLIFFORD F. GEORGE graduated from Washington and Jefferson College in Washington, Pennsylvania, with a B.A. degree in physics in 1963 and joined the Diffraction Branch of the Optics Division that same year. He received an M.S. degree in physics in 1971 and a Ph.D. degree in physics in 1978 from Catholic University, where his thesis concerned the structural analysis of thin solid films of amorphous silicon oxides by electron diffraction. Over the years, he has coauthored over 100 publications and professional society presentations in areas of electron and X-ray diffraction. His current areas of interest include energetic materials, neuroactive and therapeutic compounds, and organometallic precursors for ceramics, superconductors and semiconductor device materials.

Synchrotron X-Radiation Research

Milton N. Kabler, David J. Nagel, and Earl F. Skelton
Condensed Matter and Radiation Sciences Division

Early History

Much of science and technology is based squarely upon knowledge gained from the use of X rays over the past 75 years. The Naval Research Laboratory (NRL) has been involved in the exploitation of X rays since the 1920s. In the 1930s, Drs. Robert Mehl and Charles Barrett performed seminal X-ray diffraction measurements on complex metallurgical samples. In the 1940s, Dr. Herbert Friedman and his colleagues began rocket X-ray astronomy, which opened a new field of high-energy astrophysics leading to many notable achievements in the 1950s and beyond. Also in the 1940s, Drs. Jerome Karle and Herbert Hauptman began the work on X-ray diffraction that would produce remarkable results in the 1950s and a Nobel Prize for them in 1985. From that same era, Dr. Isabella Karle pioneered practical methods for X-ray structural analysis.

In the 1950s, LaVerne Birks demonstrated the practical utility of X-ray spectrochemical analysis by using both X-ray fluorescence and electron impact excitation. That work led to a major effort starting in the 1960s on X-ray spectroscopy of plasmas, including measurements on nuclear weapons at a Nevada test site as well as numerous multimillion-degree laboratory plasmas. This plasma research led to the development of sources for X-ray lithography in the 1970s. The 1980s saw NRL scientists exploit the remarkable capabilities of synchrotron radiation to determine the structure and properties of a wide range of materials.

The NRL synchrotron radiation story begins with three sabbaticals. In 1974, the first author spent a year at Oxford University during which time he participated in experiments on both the old Daresbury synchrotron in the United Kingdom and on the ACO storage ring in Paris, France. The second author was at the National Bureau of Standards (NBS) (presently National Institute of Standards and Technology) in 1978 and worked on the Synchrotron Ultraviolet Radiation Facility. And in 1980, the third author pioneered high-pressure diamond anvil experiments at the Stanford Synchrotron Radiation Laboratory. These sabbaticals laid the groundwork for later synchrotron radiation projects involving numerous NRL scientists. Here we give a brief description of the generation and characteristics of synchrotron radiation and review highlights of current research.

Synchrotron Radiation

When electrons or positrons orbiting within an evacuated torus interact with and are accelerated by the strong magnetic fields that steer them around a curved path, they emit synchrotron radiation [1]. The name resulted from the initial observation of "light" in synchrotron particle accelerators built for high-energy physics experiments. Such radiation was a waste of energy from the particle—quite literally, "scrap photons."

Energy is supplied to orbiting particles by synchronous radio frequency fields (synchrotron action) or by linear or other means of particle acceleration followed by injection into a storage ring. The spectrum, intensity, and direction of synchrotron radiation depend on the particle energy and the strength and configuration of the magnetic fields. Figure 1 indicates this schematically. The particles orbit the storage ring in discrete groups or bunches with an energy

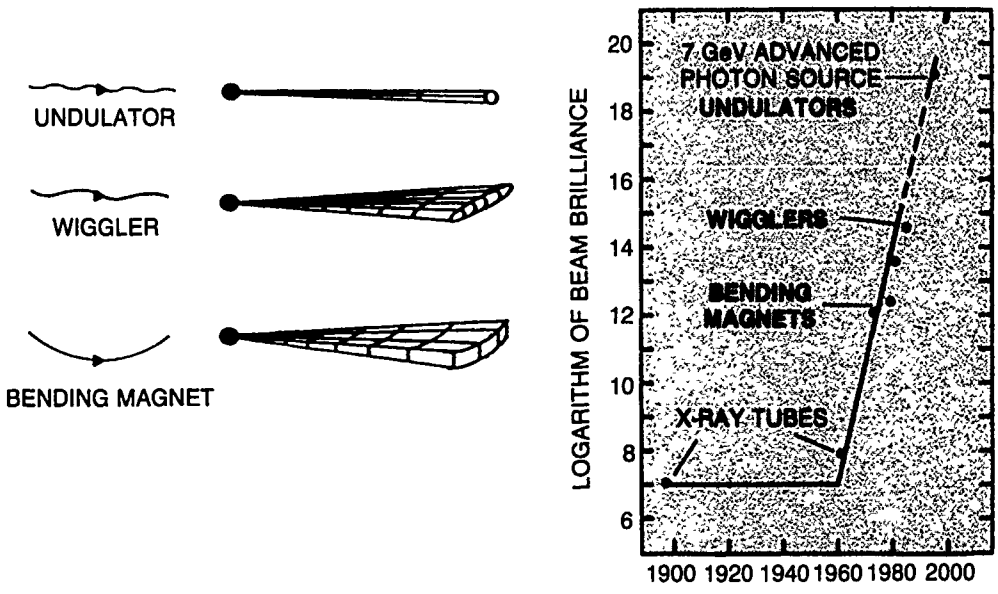

Fig. 1 — At the left-hand side are top views of the paths of electrons through bending magnets, strong alternating-field wigglers, and weaker alternating-field undulators. The X-ray patterns for each case are sketched in perspective. The graph on the right-hand side shows the relative intensities from X-ray tubes and the three types of synchrotron sources. Note that undulators will produce radiation one hundred billion times as brilliant as X-ray tubes.

typically in the range 0.5- to 10-billion electron volts (GeV). The steering (bending) magnets, with fields of about 1 T (10,000 G), cause the particles to emit into a horizontal fan a smooth, continuous spectrum that ranges from the infrared to the hard-X-ray region. The brilliance of bending magnet sources is typically 100,000 times that of the best laboratory X-ray sources. Brilliance is a standard synchrotron radiation unit that takes into account both source size and the angular spread of the beam. It measures the maximum amount of radiation that can be delivered to a small sample.

If a strong, spatially alternating magnetic field produced by a device called a wiggler is employed, the radiation is enhanced by another factor of 10 to 100. If a magnet with more numerous but weaker field oscillations called an undulator is employed, then the X-radiation brilliance can be increased by a factor of as much as 10,000 when compared to a wiggler. Undulator radiation is strongly peaked at certain wavelengths and resembles radiation from free electron lasers.

Most of the early synchrotron radiation experiments in the 1960s and 1970s were done parasitically by using bending magnets on high-energy machines. They proved so promising for physics, chemistry, biology, and material science that in the 1980s, numerous dedicated synchrotron facilities were constructed at costs of tens of millions of dollars. A number of facilities throughout the world will be completed this decade to satisfy this increasing demand. The three largest ever built—one each in Europe, Japan and the United States—will begin operation around 1995. These facilities will have energies in the 6- to 8-GeV range and consist primarily of undulators and wigglers. Undulators on these storage rings will put up to 100 W/mm^2 of radiation on a sample. This extraordinary advance in brilliance, illustrated in Fig. 1, goes far to explain the large investments that the U.S. and many other countries have made.

The ten orders of magnitude increase in brilliance from X-ray tubes to synchrotron X-ray sources is reminiscent of the immense difference between lasers and ordinary light sources. Synchrotron radiation is neither stimulated nor strongly coherent. However, the high intensity, small source size, directionality, and short-pulsed character are laserlike. Will synchrotron radiation

have the broad and commercial impact of lasers? The facility size will preclude this. However, the importance of synchrotron radiation for research in a number of fields already rivals that of lasers.

NRL at the National Synchrotron Light Source (NSLS)

Prime among the dedicated synchrotron radiation facilities in the U.S. is the NSLS at Brookhaven National Laboratory on Long Island, New York, shown in Fig. 2. Construction on this $100M facility began in the late 1970s, and it is currently the world's largest and most productive synchrotron radiation facility with nearly 100 experimental stations in use or under construction.

In the early 1980s, with the support of Dr. Alan Berman, then NRL's Director of Research, NRL and NBS formed one of the first participating research teams (PRTs) at NSLS. Other PRTs at NSLS include organizations such as IBM, AT&T, Bell Labs, Exxon, several DoE laboratories, and numerous universities. NRL is the only DoD laboratory that formed a PRT. The function of each PRT was to design, construct, and operate one or more beam lines linking the storage ring to experiments.

Beam lines are complex vacuum systems that collect radiation from the storage ring, manipulate it, and focus it onto samples in the experimental stations. They comprise various combinations of valves, apertures, and shutters with precision focusing mirrors, diffracting crystals, gratings or multilayers, and associated safety instrumentation. The experiments are conducted inside bathroom-sized enclosures (called hutches) or within elaborate surface science chambers with many additional sample preparation and diagnostics capabilities. In 1980, NRL began building two beam lines and NBS two more on ports X23 and X24 of the NSLS. Figure 3 shows the end stations of the NRL beam lines.

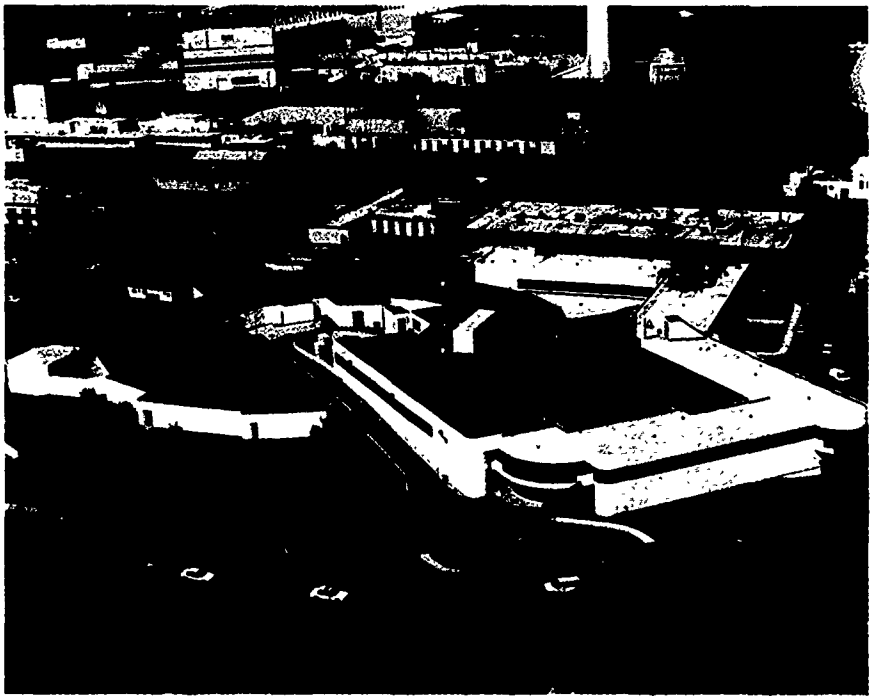

Fig. 2 — The National Synchrotron Light Source. The annular section of the building houses a 2.5 GeV electron storage ring 170 m in circumference. (Photo courtesy BNL).

Fig 3 — NRL beam lines at NSLS. The ultrahigh vacuum surface science chamber for the soft-X-ray line is in the left foreground, and the experiment hutch for the hard-X-ray line is on the right-hand side. Synchrotron radiation reaches the experiments through the vacuum pipes in the background.

To associate a given structural feature or process with a specific species of atom, one generally tunes the synchrotron radiation to excite a transition characteristic of that particular atom. We designed the soft-X-ray beam line to cover a spectral range where there are strong, distinct, core-level transitions in the atoms that make up many of the most important semiconductors, insulators, and metals. Examples are the K edge of carbon; the L edges of silicon, gallium, and arsenic; the K and L edges of nitrogen, oxygen, and aluminum. We also included the valence region in the ultraviolet where transitions occur from the uppermost, filled bands. These provide information concerning the all-important electronic properties but are generally not atom specific.

The soft-X-ray beam line is based on a unique monochromator that was designed and patented by NRL scientists [2]. It uses diffraction gratings, crystals, or multilayers to select a narrow band of synchrotron radiation at a chosen energy in the range from the ultraviolet to several kilovolts. The beam is focused to a size of 1 mm^2 or less at the sample under investigation.

Either of two interchangeable, ultrahigh vacuum experiment chambers terminates this beam line. One contains a reflectometer, which allows us to measure reflected, scattered, or absorbed X rays. The other chamber, which is evident in the left foreground of Fig. 3, enables us to perform a variety of surface science experiments, particularly photoelectron emission spectroscopy. Ultrahigh vacuum conditions are essential to preserve clean, well characterized surfaces. The beam line and instrumentation were developed to facilitate measurements in three principal areas: X-ray optical properties, surface science, and fast transient phenomena. To initiate the latter, we use a pulsed laser coincident with the synchrotron radiation. This particular array of capabilities is, we believe, unmatched by any other beam line in the world.

The second NRL beam line is for diverse, hard-X-ray experiments in the 4- to 10-keV range [3]. The line is used to measure the absorption, diffraction, and fluorescence of X rays. The main objective of these measurements is to determine atomic structures and environments in complex materials that are important in a wide variety of NRL programs. X-ray spectrochemical analysis of trace elements and calibration of detectors employed in plasma physics have also been performed on this beam line. In contrast to the soft-X-ray line with its two interchangeable end stations, the hard-X-ray line has a fixed hutch. Inside it, various experiments are set up and removed, all controlled remotely from outside the hutch in conformity with radiation safety requirements with hard X rays.

The newest NRL capability at NSLS resides on the superconducting wiggler beam line X17, which provides intensities more than ten times higher than those available from bending magnets. NRL's access to this wiggler line came about through the efforts of the third author, who organized a team for high-pressure research in 1985. This group consists of scientists from 11 institutions, including DoE, private labs, universities, and industry. Use of the wiggler beam line is not limited to solid-state research. It has already been employed to measure the crystal

structure of submicron metallic filaments. Chemical analyses of the metallic elements in wood are planned on the wiggler line.

Research Examples

Here we describe examples of recent research on each of the three beam lines. Much of the work has been carried out in collaboration with other NRL divisions

Soft-X-Ray Optics: Our work has concentrated on multilayer reflectors in various forms and uses the reflectometer designed for this beam line by Hunter and Rife [4]. This reflectometer allows the incidence and scattering angles to be varied with high precision, and the plane of polarization of the synchrotron radiation is varied by rotating the entire ultrahigh vacuum chamber housing the reflectometer. Very few reflectometers exist in the world that have similar capabilities.

The fundamental problem with X-ray optics is that, as the photon energy increases above ~20 eV, mirrors made of homogeneous metals (for example, platinum or gold) cease to reflect efficiently except at extreme grazing angles of incidence. For platinum, the grazing angle must be about 2° or less for appreciable reflectivity at or above 2 keV. But grazing incidence reflecting optics, such as those used in telescopes and in most synchrotron radiation beam lines, are subject to severe aberrations and must be figured to extreme tolerances that are costly to achieve.

An X-ray multilayer increases reflectivity so that near-normal instead of grazing-incidence optics can be used, resulting in substantially improved image definition and larger apertures. It is the X-ray analog of multilayer interference coatings used to increase or decrease the reflectivity of visible optics. Multilayers are designed to give enhanced reflectivity over a specific band of wavelengths.

X-ray multilayers are made by depositing alternating layers of two different materials, repeating the process through 10 to 100 layer pairs. The multilayers reflect because the two constituent materials are chosen to have different scattering coefficients. Note that visible multilayers use refractive index variation rather than scattering, but since the refractive index of all materials is near unity in the soft-X-ray range, index variation will not work here. Typical material combinations include W-C and Mo-Si. Since the thickness of a layer pair has to be roughly a half wavelength, thickness and smoothness must be controlled at a single atom level. Technology to do this has evolved in the last decade. A good multilayer coating can yield a normal-incidence reflectivity of 20% or more, increasing toward lower grazing angles. Uncertainties in materials parameters, thicknesses, and smoothness demand that the properties of a given multilayer be measured as well as calculated, providing an important diagnostic function for synchrotron radiation.

X-ray multilayers can be applied directly to diffraction gratings, allowing them to be used at angles of incidence considerably larger than those possible for the bare grating. This represents one of the most promising applications for multilayers, and NRL has been a leader in this area. Rife and coworkers measured substantial increases in grating reflectivity, although multilayer deposition techniques must improve before the reflectivities become comparable to those predicted by theory [5]. Figure 4 gives an example of a spectrum reflected from a W-C multilayer on a blazed grating, which in this instance was mounted in the beam-line monochromator. The grating was scanned in a high order (8th) to optimize the match between the grating parameters and the multilayer spacing. An Al filter cuts off the light at the high-energy end, and structures arising from absorption in the photodiode detector (Ga) and beam line optics (Ni) are evident. The multilayer results in a smooth spectrum with substantially higher throughput.

Many of the multilayer measurements are done by or in collaboration with scientists in NRL's Space Science Division and at Lawrence

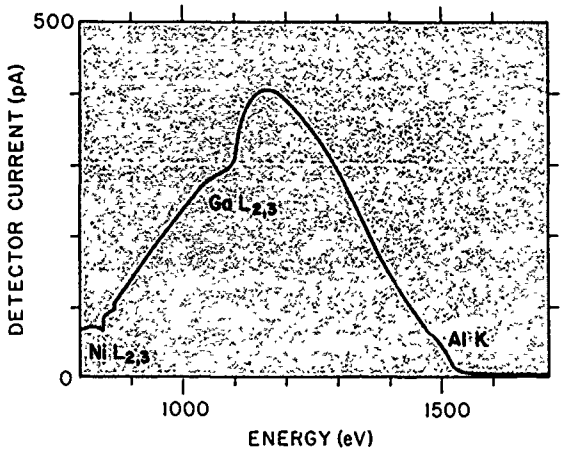

Fig. 4 — Monochromator scan with the W-C multilayer grating and mirror mounted as diffraction elements. The multilayer grating is scanning in 8th order. Measurements made through an Al filter 0.00025-in. thick.

Livermore National Laboratory. Some of this research provided analyses of X-ray optics for an SDI program on nuclear directed energy weapons managed by the Condensed Matter and Radiation Sciences Division.

Semiconductor Surface Passivation: Photoelectron emission spectroscopy (PES) is a major tool of surface science. In combination with a tunable synchrotron radiation source, PES can be sensitive to surface atoms and molecules at coverages much less than a monolayer. PES can differentiate between processes that occur either primarily in the bulk or at the surface, can distinguish the effects of initial and final electron states, and can provide information about electron momentum as well as energy inside a material. These capabilities are one reason why surface science has become a principal product at synchrotron radiation facilities. Surface science has evolved into one of the most complex and demanding disciplines of material science. Nevertheless, it concerns many of the most important modern technologies and is used effectively by many groups at NRL.

A second, ultrahigh vacuum chamber for the soft-X-ray beam line houses our PES experiments at NSLS. This instrumentation is used to attack a formidale problem of semiconductor device technology, the passivation of GaAs surfaces. The research was carried out in collaboration with workers from NRL's Electronics Science and Technology Division and from Wake Forest University.

To passivate a semiconductor surface is to reduce the loss of charge carriers through surface recombination. The usual method is to oxidize the surface simply by passing O_2 over it. Bermudez and collaborators [6] found that by using molecular nitric oxide (NO) rather than O_2, the oxidation could actually be made to proceed faster at 300 K and at relatively high NO exposure. To identify intermediate species in the reaction, they extended their measurements down to temperatures in the 40 to 140-K range and looked carefully at PES in the range that includes the Ga 3d and As 3d core levels and valence excitations of NO. Figure 5 shows spectra for the clean GaAs surface, a thin film of NO on GaAsa, and a thick film of NO. The progressive changes evident in the spectra of (d) and (e) illustrate the oxidation of the surface by a photochemical reaction produced by the synchrotron radiation acting over a time span of minutes. The curves show the relative number of photoelectrons that leave the surface with a given energy; the height of a peak is a measure of the quantity of the species that causes the peak. The features to note in (c), (d), and (e) are the drop in the peaks on the right-hand side due to solid NO and the consequent rise of the oxygen-related satellite near the As 3d peak on another oxygen feature around 82 eV. These and similar data gave strong evidence that, at low temperatures, both thermal and photochemical oxidation occur by a $(NO)_2$ dimer dissociating into an adsorbed oxygen atom and N_2O molecule that leaves the surface. It is possible, in effect, to follow this process from physisorption to reaction to dissociation and desorption. However, there are indications that at temperatures above 100 K, where reactions proceed much faster, a species other than N_2O (perhaps NO^-) is the intermediate in the oxidation.

These experiments illustrate that synchrotron radiation is sufficiently intense to allow us to

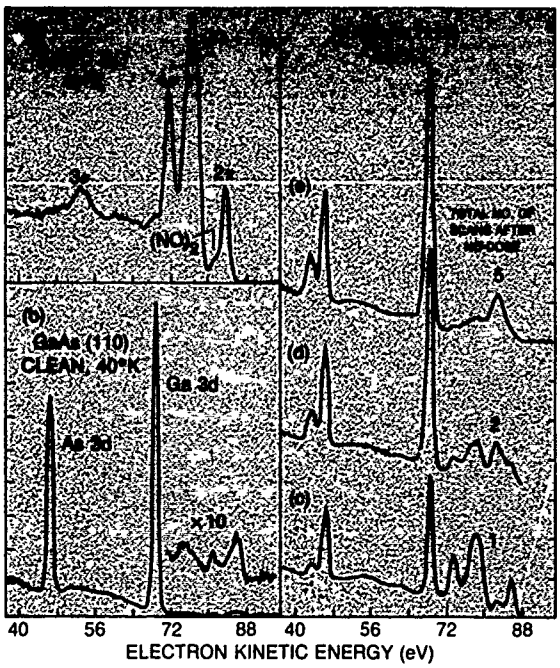

Fig. 5 — Photoemission data at 92 eV photon energy for: (a) solid NO at 40 K; (b) clean GaAs (110); and (c)–(e) a thin NO film after increasing exposure to SR. The labels 3σ,etc., in (a) refer to various molecular orbitals of NO. The inset in (b) shows an expanded valence band spectrum.

observe and identify small quantities of a molecule on a clean surface in times brief enough (depending on temperatures) to allow identification of transient reactions.

Surface Electron Dynamics: The performance of many electronic devices comprising semiconductors and insulators is often affected by surface states whose electron populations can change in times ranging from seconds to nanoseconds or faster. Important processes, including voltage shifts, loss of current carriers through surface recombination, and photochemical reactions that change the surface can occur as a result of these states. Thus we felt that the rewards for developing time-resolved, synchrotron radiation techniques to identify and characterize these states would be substantial.

Our approach was based on the fact that electrons circulating in a storage ring are grouped in well-separated bunches of duration one nanosecond or less. Synchrotron radiation from *one* bunch generally is not intense enough to perturb electronic states measurably. However, a pulsed laser can easily produce measurable perturbations. Thus the two sources were joined to create a repetitive pump-probe experiment, where the pump is a laser pulse and the probe is a burst of synchrotron radiation exciting photoelectrons that can be detected. This required Long and collaborators [7] to develop electronics to synchronize the laser pulse with the synchrotron radiation pulse and to accumulate PES data over nanosecond intervals, not a trivial task. A copper vapor laser has been used so far because its repetition rate is high (6 kHz), its 2.43-eV photon is strongly absorbed in most semiconductors, and its 5-ns pulse is adequately matched to the synchrotron radiation pulse.

To provide background for the experiments, consider how the energy bands of a semiconductor can change as one scans from bulk to surface. If there is no net surface charge, the bands will not change in energy to within an atomic layer or two of the surface. That is, the bands are flat. But if there are surface states in the energy gap between the valence and conduction bands that can trap charge and create a surface potential, the bands will gradually bend, and consequently carrier concentrations will change on approaching the surface. However, if the region near the surface is suddenly flooded with electrons and holes by a laser pulse, the resultant high conductivity will no longer allow the electric field to exist, and the bands will immediately flatten. The excess electrons and holes will begin to decay by several processes, the most interesting being diffusion to and recombination at the surface. The states through which surface recombination occurs can be the same as or different from those that originally trapped the charge that caused band bending. By following the decay of this transient potential or photovoltage in time, one can learn much about transport and recombination processes near the surface. We shall now describe a pioneering combined laser-synchrotron radiation experiment carried out by Long and others that was able to accomplish this [7].

Space-Charge Dynamics on Silicon: The dominance of silicon-based technology dictates that it continue to be one of the most intensely investigated materials, and current research is providing important new information about silicon surfaces. To illustrate results from our laser-synchrotron-radiation research on Si, Fig. 6 shows data for a p-type Si(111) surface saturated with hydrogen. These data were obtained by monitoring the transient shift of the Si 2p core level determined from photoemission. Because of positive charge in surface states, the bands are bent in the dark by about 0.5 eV. During the 5-ns laser pulse, the surface potential changed by an amount ΔV, the photovoltage. Data points in Fig. 6 show the measured decay of ΔV after laser pulses at three different fluences. The fact that reasonable data can be obtained over a range of almost 10^5 in laser fluence indicates the power of the technique.

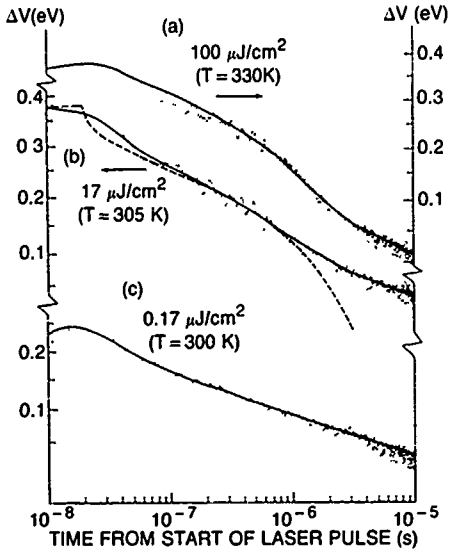

Fig. 6 — Photovoltage (ΔV) decays for a hydrogen saturated, p-type, Si(111) surface for four different laser fluences. Points are experimental data, solid lines are the numerical simulation, and the dashed line is an analytic simulation.

An important parameter characterizing the decay—the so-called surface recombination velocity—was obtained by fitting the experimental data with a numerical transport code, PISCES IIB, which is often used for device modeling. The solid lines are results from this code, and the agreement with the experiment is impressive. The surface recombination velocity for this particular surface turns out to be relatively high. In quantitative terms, the probability is greater than 10% that any hole striking the surface recombines there. Comparison with the numerical model also reveals a previously unappreciated effect of transient space charge separation caused by the trapping of electrons or holes in the surface-potential well arising from the recovered band bending. Note that the dashed line in Fig. 6, which is a good analytic simulation one might use in lieu of the numerical code but which does not include this charge separation effect, fails to match either the experiment or the numerical result.

One of the most significant points of this work and one that purely electrical measurements (e.g. photocapacitance) cannot address is the observation that, even with the high electron and hole concentrations that the laser can produce near these Si surfaces, the photoemission spectra all shift *rigidly* by ΔV and return to their initial energies at some time after the pulse. This shows that the underlying electronic structure remains unaffected. Clearly it would be extremely interesting if this were not the case—that is, if bands actually changed shape or new excited bands appeared. Such changes do occur on GaAs, as we next describe.

Photochemistry on GaAs: Since the surface quality of compound semiconductors is generally poorer than for Si and surfaces are less well understood, they represent an important target for combined laser-synchrotron radiation techniques. Initial measurements on clean GaAs surfaces produced anomalous results, and it soon became apparent that a new photochemical phenomenon was taking place. Goldenberg and Long were using very low laser intensities, being careful to avoid excessive heating of the surface. They were thus surprised when photoelectron emission data

showed that the surface was decomposing under laser irradiation [8]. Stable islands of metallic Ga were forming on the surface at intensities so low that the overall temperature rise was 13°C or less. With such a small temperature rise, there is no doubt that the process is photochemical. While new in itself, this phenomenon is related to several other processes of obvious technological significance. For example, laser irradiation can substantially enhance the etch rate of GaAs exposed to a chlorine atmosphere. Low intensity irradiation can also cause large decreases in the efficiency of photoluminescence. At generally higher intensities, changes in surface lattice structure and emission of constituent species have been observed. For several of these experiments, photochemical mechanisms have been suggested but not proved.

Most of our Ga-island experiments do not directly employ time resolution. A clean GaAs surface is irradiated for a short time, after which any changes are measured by means of PES. Looking first at the photoelectron energy distribution in the valence band region, Long and collaborators saw that as laser irradiation proceeded, electron states were building up in the band gap at and below the Fermi level. This suggests that metal is being produced on the surface. In the surface sensitive Ga-3d core spectra, they also noted the growth of a small shoulder on the main band, a known signature of Ga metal. Aside from this shoulder, the Ga-3d (and the As-3d) spectra changed very little in shape and magnitude indicating that most of the surface remains as it was initially, and the metallic Ga is isolated in islands that cover a small fraction of the surface. There is no evidence that the As released with the Ga remains on the surface, and As leaving the surface has been detected.

One reason this process has not been previously described is its relatively low efficiency. One Ga atom is added to an island for roughly 10^7 photons incident from the copper vapor laser. It appears likely that the laser produces electrons and holes that recombine at the surface, some providing energy to remove a Ga atom that is weakly bound at a surface step or defect and transport it to a Ga island. Needless to say, the individual steps of this photochemical process are of great interest and are being explored, as are broader questions concerning relationships to the performance of various electro-optic devices.

Time-resolved laser-synchrotron radiation experiments contributed to our GaAs work but in a way different from that for the Si research just described. At these GaAs surfaces, the band bending is generally not homogeneous. When photoelectron spectra are measured coincident with the laser pulse, electrons and holes made by the laser effectively smooth out the inhomogeneous potentials, thus sharpening the spectra considerably and making their various components more distinct. In fact, on p-type GaAs, it was necessary to use time resolution to make quantitative measurements of the Ga-island contribution.

The Ga islands are also seen directly by using scanning electron microscopy (Fig. 7). The micrographs show islands that are roughly hemispherical and that have diameters up to several hundred angstroms, depending on exposure. Interestingly, the islands seen in the micrographs are entirely consistent with our more detailed data obtained with synchrotron radiation.

Local Atomic Structure: Extended X-ray absorption fine structure measurements (EXAFS), were virtually unknown before the advent of electron storage rings for synchrotron radiation. However, EXAFS is currently the most frequently used technique on hard-X-ray beam lines. The attenuation of radiation in matter is generally represented by an absorption coefficient $\alpha(E)$, which depends on the photon energy E; this dependence is especially strong in the vicinity of an absorption edge. Typically a beam of radiation emerging from the storage ring is first diffracted by one or more crystals to select a narrow energy

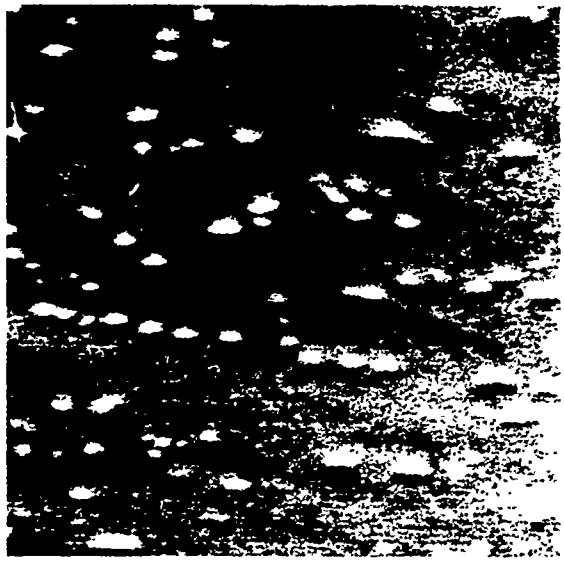

Fig. 7 — Scanning electron micrograph of laser irradiated GaAs(110) surface Electron beam at 20° grazing incidence. The area shown is 400-nm wide.

band of photons. This filtered beam is then directed onto the sample. By varying the angle that the monochromating crystal(s) makes with the beam, the incident photon energy can be tuned. The monochromatic beam is then directed to the sample and $\alpha(E)$ is measured. As the photon energy passes through an absorption edge of any element in the sample, a significant increase in $\alpha(E)$ is observed due to ionization of that element. For energies above the absorption edge, the $\alpha(E)$ curve exhibits a series of complex undulations; the oscillations from about 50 eV to 1 or 2 keV above the edge are the EXAFS. They result from scattering of the primary photoelectrons by the neighboring atoms. The reflected electron waves interfere with the outgoing photoelectron wave, resulting in the observed modulation of $\alpha(E)$.

The great attraction of EXAFS measurements is that they give information about the number, proximity, and thermal vibrational amplitudes of the atoms neighboring the atom in question. That is, EXAFS is element specific. Thus the absorption spectra of a complex chemical mixture can be readily sorted out in terms of the environment of a particular atom. In this manner, EXAFS provides structural data complementary to that obtained by conventional diffraction. Synchrotron radiation is required because the beams that are available from conventional X-ray tubes are too weak to permit acquisition of most EXAFS spectra in reasonable time periods and often have a complex energy structure of their own that precludes interpretation of the data.

Three important materials problems were recently solved by EXAFS experiments on beam line X23B. In one case, we are able to explain the abrupt decrease in the rate of change of the ordinary optical index of refraction with increasing Ti dopant in $LiNbO_3$. In another, we solved the crystallographic structure of a unique metastable cobalt film. And in the third case, we obtained information relating to the aging properties of activated carbon filter materials for gas masks.

The material most widely used for ferroelectric optical waveguide devices is Ti-diffused $LiNbO_3$. Prior to this EXAFS work, there was little understanding of how the Ti is incorporated into the $LiNbO_3$ lattice and, more importantly, why its presence has such a pronounced effect on the optical index of refraction. Based on careful absorption measurements above the Ti edge on a series of samples with varying Ti concentrations, Skeath, Elam, and collaborators were able to demonstrate that the position of the Ti^{4+} ion is concentration-dependent and tends to become disordered for higher concentrations [9]. The dependence of the optical indices on Ti concentration was then calculated based on this positional information, resulting in a much clearer understanding of the relationship between optical properties and impurity site geometry. This work was done in collaboration with NRL's Optical Sciences Division.

Another important materials problem that was solved with EXAFS data is the crystallographic structure of metastable Co films. Based on total energy calculations, it was concluded that a metastable body-centered cubic phase of Co should be possible, but prior to the work mentioned here, no direct confirmation of its

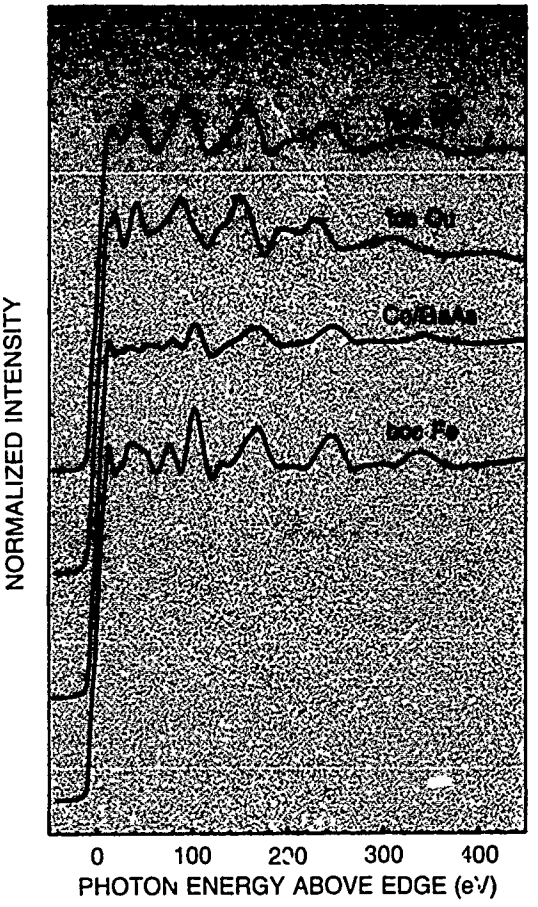

Fig. 8 — EXAFS spectra for HCP-Co, FCC-Cu, Co film deposited on GaAs, and BCC-Fe

existence had been found. One reason was that Co films are grown by molecular-beam-epitaxy techniques on GaAs substrates, and the lattice parameter of the Co very nearly matches half that of the GaAs. Consequently, conventional diffraction studies produce signals from both the Co epilayer and the substrate, and the signal from the Co is lost in that from the GaAs. By carefully measuring the EXAFS above the Co edge, Idzerda, Elam, and collaborators obtained data specifically from the Co film and identified its structure as body-centered cubic with a lattice parameter of 2.88 Å [10]. Figure 8 shows EXAFS spectra obtained from the Co film and three standards for comparison—hexagonal close-packed Co, face-centered cubic Cu, and body-centered cubic Fe. Although detailed information is obtained from Fourier transforms of these spectra, it is clear that the Co spectrum more nearly resembles that of body-centered cubic Fe than of the other structures. This work, done in collaboration with NRL's Materials Science and Technology Division, provides an excellent example of a case where the element-specific nature of EXAFS experiments is vital.

Our third example, impregnated carbon, is used to remove toxic vapors from air streams. Despite years of study, little is known about the structure of the adsorbants or the chemistry occurring on the carbon. This is especially true for the chemical changes on aging. If this chemistry can be understood, new treatments to improve performance, reduce degradation by aging, and provide alternate compositions can be developed. EXAFS studies designed to address this problem were carried out on behalf of the Army Chemical Research and Development Center and the Naval Surface Weapons Center. EXAFS data recorded from appropriate activated carbon samples were used to determined the oxidation states and site geometries of copper and chromium on the carbon surface. The results show that both of these elements are involved in the chemistry of the aging process [11]. More specifically, by comparing data obtained from unaged and 60-day aged carbon samples, the following conclusions are drawn: The Cr is in a mixed oxidation state, containing both Cr^{+6} and Cr^{+3}. The oxidation state decreases on aging, and the local site geometry changes significantly. For the Cu atoms, the oxidation state is initially Cu^{+2} and does not appear to change as the material ages, although there is some indication of movement by the Cu atoms on aging. Thus both the Cr and the Cu are involved in the aging process, and the chemical changes are irreversible for both elements. On the basis of our work, DoD sponsors are presently engaged in further efforts to improve the performance of these carbon filter materials.

Crystal Structures from X-Ray Diffraction: Structural analysis of biological materials is another major field of synchrotron

radiation research. Protein crystallography, from which one can determine the detailed structure of a constituent molecule, is of particular interest. We cite as an example work on the green fluorescent protein aequorea by Perozzo and Ward of NRL's Laboratory for the Structure of Matter [12]. This protein is interesting because of its fluorescence properties. It is often difficult to grow single crystals of proteins large enough for conventional X-ray analysis; in the case of aequorea, Perozzo and coworkers were able to grow crystals of average dimension <0.5 mm. Figure 9 shows a hexagonal speciman. They used 1.63 Å monochromatic radiation from the NRL hard-X-ray beam line to obtain good X-ray diffraction photographs. These data enabled them to determine the structures of both hexagonal and monoclinic crystals while keeping exposures brief enough to avoid damaging the samples—a significant problem with many biological materials.

The highest static pressures that can be generated in a laboratory (in excess of several million atmospheres) are developed by reducing the area over which the force acts to microscopic dimensions and by applying the force through the hardest known substance, diamond. The diamond-anvil pressure cell has evolved to become the single most important research tool in high-pressure science. An important feature offered by the diamond-anvil cell is a relatively low absorption coefficient for a broad spectrum of radiation. This advantage is employed to monitor some of physical properties of the sample by measuring transmitted or reflected radiation from the pressure cavity. If X rays are used, the effect of pressure on the structure of samples can be determined. However, the extreme pressures are achieved at the expense of sample volume; typically, a sample pressurized in a diamond-anvil cell occupies a volume of about 10^{-15} m^3, or about one picoliter. Thus if conventional X-ray sources are employed, extremely long exposure times—tens or even hundreds of hours—are usually needed to obtain useful structural information. Synchrotron radiation reduces the exposure time from days or weeks to minutes or seconds [13].

For high-pressure structural studies of polycrystalline or powder samples, the method of choice is energy-dispersive diffraction, which uses unfiltered synchrotron radiation. The diffracted X rays are analyzed at a fixed angle with an energy-sensitive detector. Diffraction peaks occur at those photon energies that satisfy the Bragg condition for the various crystallographic

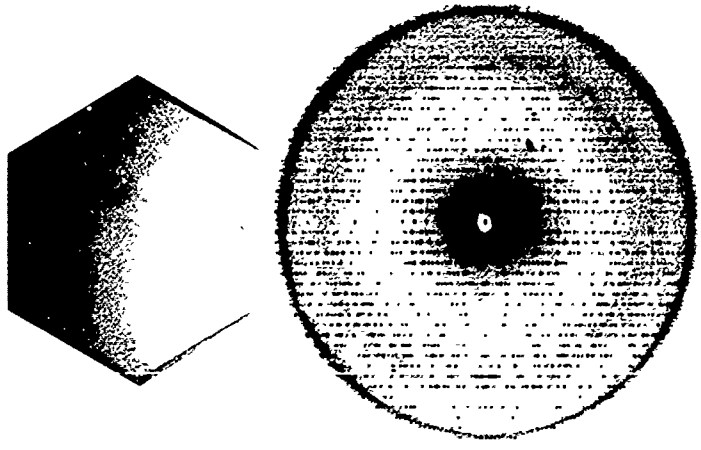

Fig. 9 — Micrograph of half-millimeter crystal of aequorea green fluorescent protein and diffraction of pattern recorded at NSLS by NRL's Ms. Mary Ann Perozzo and Dr. Keith Ward, and Drs. Richard Thompson and William Ward, of the Rutgers University

planes in the sample. From the positions of the peaks, one obtains information about the interatomic spacing and symmetry of the sample. These data are then interpreted in terms of compressibilities and crystal structures, or phases.

A striking example of our data from the diamond-anvil cell is reproduced in Fig. 10, which shows spectra recorded from a mixed sample of KI and NaCl as the pressure is incrementally increased from 0.83 to 3.17 GPa. The lowest energy peak at about 22 keV arises from the (200) planes of KI in the B1, or rocksalt phase; the highest energy peak above 26 keV is the same reflection from the NaCl. The peak at about 25 keV is the (110) peak from KI in the B2, or CsCl phase. At about 1.8 GPa, the KI enters a two-phase region; the (200) peak from its B1 phase and the (110) peak from its B2 phase are simultaneously present. The shift of the NaCl peak is used in combination with the measured temperature and the equation of state of NaCl to calculate the pressure.

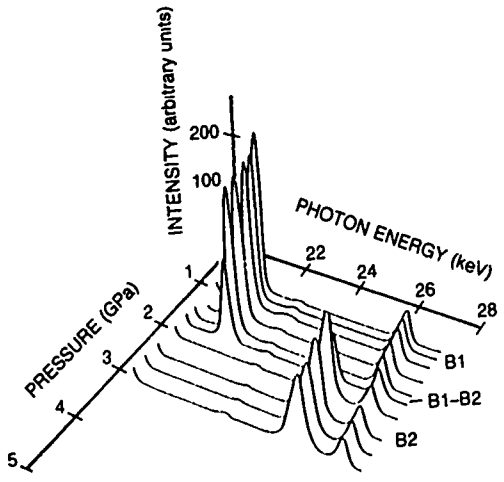

Fig. 10 — Energy dispersive diffraction spectra of the B1-to-B2 phase transition in KI

If a conventional X-ray source were used for this experiment, it would take almost two weeks to collect the data. Instead, each of the 10 spectra shown in Fig. 10 was measured in 2 min. At 1.8 GPa, the KI is in a metastable state, and by monitoring the intensities of the B1 and B2 peaks, it is possible to determine quantitatively the dynamics of the phase transition. This information is then used to test theories describing the transition mechanism.

Small Samples: The high-pressure experiment described is an example of using synchrotron radiation to analyze small quantities of material. We have used the wiggler beam line to investigate the structure of another type of small sample—ultrafine wires. These were made by NRL's Materials Science and Technology Division by drawing fine glass fibers containing single or multiple metallic filaments [14]. Filaments as small as a few μm can be drawn. By cascading this process and by using glasses with properly selected melting temperatures, it is possible to produce a single-filament wire of sub-μm dimension. Because of the minute sample volumes involved, efforts to obtain structural information by using conventional X-ray sources were unsuccessful. Our recent measurements on a Bi filament 0.22 μm in diameter show it to be a single crystal in its normal, tetragonal structure. Even with the incident X-ray beam collimated to a square 10 μm or a side, there is still ample signal from the sample. By adjusting the position of the sample relative to the incident beam, a variety of single-crystal diffraction peaks are measured. Because the diffraction peaks are measured in the energy dispersive mode as in the high-pressure experiments described, an entire family of reflections can be measured simultaneously. The experiment is far from being signal limited; for example, Fig. 11 shows that the (O,h,2h) peaks can be detected in a measurement period as short as 10 ms. The volume of crystal being illuminated for this measurement is 3.8×10^{-19} m^3, or equivalently, 0.38 femtoliters; this corresponds to a mass of 3.7 picograms, which we believe to be a record minimum sample.

These data further show that the Bi crystal is under a negative linear strain of about 1.4% normal to the fiber axis. The implication is that the crystal is under a hoop stress from the surrounding

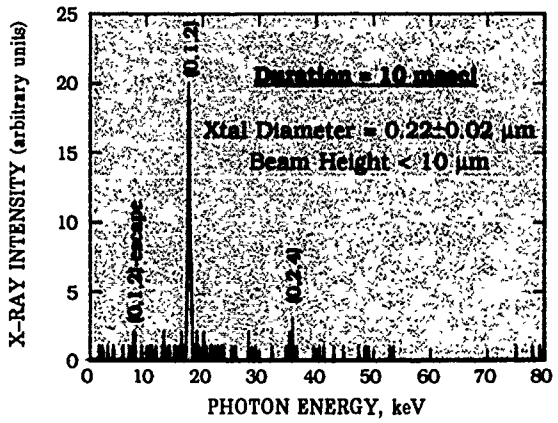

Fig. 11 — Energy dispersive diffraction spectrum of reflections froma 0.22 ± 0.22-μm diameter bismuth filament

glass sheath. This level of strain corresponds to a residual stress of about 1.7 GPa. It is suspected that this stress results from differential thermal contraction upon cooling. Bismuth is known to undergo a first-order phase transformation from Bi-I to Bi-II at 2.25 GPa. Current efforts are directed toward thinner samples where the residual stress may be sufficient to initiate this phase change. Other research with the wiggler beam line involves very thin films, the objective again being to obtain structural information from a sample that would not be "visible" were conventional X-ray sources employed.

Emerging Research Opportunities

Many studies of the structure and dynamics of surfaces and bulk materials along the lines described continue at NSLS. In addition, NRL scientists continue to develop new lines of research in this time frame, two of which we discuss next.

Much of the X-ray work described is performed without attention to the chemical changes that are induced by the absorption of X rays. Such chemical changes are important in fields ranging from X-ray lithography, in which polymeric molecules are either scissioned or cross linked, to radiation biology, specifically the scission of DNA molecules. The extreme intensity available from the wiggler beam line make it possible to perform X-ray photochemistry experiments in reasonable times. For example, Fig. 12 shows a solid plastic that was produced by allowing a beam from the wiggler line to pass through a liquid polymer. The ensuing cross linking increased the molecular weight and produced the solid, which was photographed after decanting the unaffected liquid. Continuing research is expected to be of both scientific and technical relevance. Specifically, X-radiation curing of epoxies may be used for field repair of composities, for example, on aircraft.

Most of the work that uses synchrotron X radiation is aimed at determining the structure of materials, as earlier described. However, X-ray fluorescence induced by synchrotron radiation yields quantitative information on the elemental composition of materials to levels of parts per million. This high chemical sensitivity, combined with the very small, high-intensity beams available from the storage ring, make possible spatially resolved chemical analyses on a wide variety of samples. NRL recently pioneered the application of X-ray fluorescence analysis employing synchrotron radiation to the quantification of metallic elements in wood. For the first time, the fine beam permitted multiple measurements within in a single, annual growth ring of the wood samples [15]. Figure 13 shows the distribution with time of several elements in samples of wood. This work is being extended to the quantitative assessment of lead uptake by trees, which is expected to correlate with the amount of le. l put

Fig. 12 — Clear polymer filament cured by X-ray beam from X17C wiggler be .n line. Filament lays on a scale; dark lines are separated by 1.0 mm.

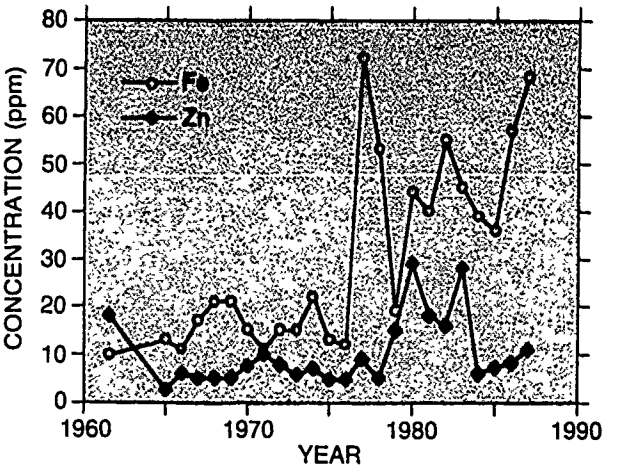

Fig. 13 — Variation of Fe and Zn over the life of a red oak

into the environment from leaded gasoline. Core samples obtained from the bottom of the ocean or from ice fields can be analyzed in much the same way as the tree rings. Numerous environmental studies are planned involving such retrospective monitoring with synchrotron radiation.

Looking Ahead

NRL scientists plan to continue to work at the leading edge of synchrotron X-ray research. Toward this goal, plans are being made to use the $500M Advanced Photon Source X-ray Facility now under construction by the Department of Energy at the Argonne National Laboratory in northern Illinois. Figure 14 shows the storage ring, with a circumference of 1.1 km. The linear accelerator and booster synchrotron are located within the main ring, with laboratory and office spaces around the periphery. Similar facilities are now under construction in France and Japan.

Positrons of 8-GeV energy will orbit in the Advanced Photon Source storage ring, passing through bending magnets, wigglers, and undulators to produce intense, nanosecond bursts of hard X rays with wavelengths suitable for measuring atomic, molecular, and condensed-matter structures. The extreme X-ray intensity, high enough to melt metals in a few seconds, will permit measurements of unprecedented precision. Structural and chemical analyses of materials can be performed down to μm spatial scales. Investigation of phase transformations, chemical changes, and other atomic motions will be possible with a temporal resolution of 100 ps. The high intensity also permits precision monochromators

Fig. 14 — The Advanced Photon Source X-ray Facility under construction by DoE at the Argonne National Laboratory. (Photo courtesy of ANL).

to cut narrow slices out of the synchrotron radiation spectrum to produce energy resolution approaching 10 meV. Similarly, the narrow collimation will permit the measurement of very small angular deflections produced by scattering from samples to resolve very small momentum transfers.

These new capabilities will derive from the unprecedented X-ray brilliance and represent one or more orders of magnitude improvement in the precision of X-ray experiments. The impact of an order of magnitude increase can be appreciated by considering that airplanes fly, on the average, approximately ten times faster than average driving speeds, which are, in turn, approximately ten times higher than walking speeds. For a given travel time, the difference translates into a global reach when compared to a state or country-wide travel or compared to movement around a town or neighborhood. As the NSLS and other synchrotron radiation sources have already done, the Advanced Photon Source will have a strong impact on many areas of science and technology. It will become operational around 1995, the centennial of the discovery of X rays.

References

1. E. E. Kock, ed., *Handbook on Synchrotron Radiation Vol. 1* (North-Holland, Elsevier Science Publishing Company, Inc., New York, 1983).

2. W. R. Hunter, R. T. Williams, J. C. Rife, J. P. Kirkland and M. N. Kabler, "A Grating/Crystal Monochromator for the Spectral Range 5 eV to 5 keV," *Nucl. Instr. and Meth.* **195**, 141 (1982).

3. J. P. Kirkland, D. J. Nagel, and P. L. Cowan, "The Naval Research Laboratory Materials Analysis Beam Line at the National Synchrotron Light Source," *Nucl. Instr. and Meth.* **208**, 49 (1983).

4. W. R. Hunter and J. C. Rife, "An Ultrahigh Vacuum Reflectometer/Goniometer for Use with Synchrotron Radiation," *Nucl. Instr. and Meth.* **A246**, 465 (1986).

5. J. C. Rife, T. W. Barbee, Jr., W. R. Hunter, and R. G. Cruddace, "Performance of a Tungsten/Carbon Multilayer-Coated, Blazed Grating from 150 to 1700 eV," *Physica Scripta* **41**, 418 (1990).

6. V. M. Bermudez, R. T. Williams, G. P. Williams, Jr., M. W. Rowe, H. Liu, A. Wu, H. R. Sadeghi, and J. C. Rife, "Photoemission Study of the Adsorption of Nitric Oxide on Gallium Arsenide (110) at Low Temperature," *J. Vac. Sci. Technol.* **A8**, 1878 (1990).

7. J. P. Long, H. R. Sadeghi, J. C. Rife, and M. N. Kabler, "Surface Space-Charge Dynamics and Surface Recombination on Silicon (111) Surfaces Measured with Combined Laser and Synchrotron Radiation," *Phys. Rev. Lett.* **64**, 1158 (1990).

8. S. S. Goldenberg, J. P. Long, and M. N. Kabler, "Photoemission Study of Low-Fluence, Non-Thermal Laser Damage of UHV-Cleaved Gallium Arsenide (110)," Materials Research Society Symposium Proceedings, to be published.

9. P. Skeath, W. T. Elam, W. K. Burns, F. A. Stevie, and T. H. Briggs, "Concentration Dependence of the Octahedral Ti^{4+} Center in $LiNbO_3$: Its Effect on Refractive Indices," *Phys. Rev. Lett.* **59**, 1950 (1987).

10. Y. U. Idzerda, W. T. Elam, B. T. Jonker, and G. A. Prinz, "Structure Determination of Metastable Cobalt Films," *Phys. Rev. Lett.* **62**, 2480-2483 (1989).

11. W. T. Elam and E. F. Skelton, "Report on the Test Plan for Synchrotron Radiation Study of Activated Carbon Surface Chemistry," NRL Report 9302, Feb. 1991.

12. M. A. Perozzo, K. B. Ward, R. B. Thompson, and W. W. Ward, "X-Ray

Diffraction and Time-Resolved Fluorescence Analyses of Aequorea Green Fluorescent Protein Crystals," *J. Biol. Chem.* **263**, 7713 (1988).

13. E. F. Skelton, "Microdiffraction with Synchrotron Beams," *Adv. in X-Ray Anal.* **31**, 1-7 (1988).

14. J. D. Ayers, "Glass Fibers with Metallic Cores," *1989-1990 NRL Review*, June 1990, pp. 94-97.

15. J. F. Gilfrich, N. L. Gilfrich, E. F. Skelton, J. P. Kirkland, S. B. Qadri, and D. J. Nagel, "X-Ray Fluorescence Analysis of Tree Rings," *X-Ray Spectrometry*, to be published.

THE AUTHORS

MILTON N. KABLER graduated from Virginia Tech with a B.S. degree, and he earned a Ph.D. degree in physics at the University of North Carolina at Chapel Hill. His postdoctoral research was carried out at the University of Illinois at Urbana, where he worked on dislocation dynamics in semiconductors. He came to NRL in 1962. Until the mid-1970s, his personal research concentrated on the optical properties of wide-band-gap solids. Under the Advanced Graduate Research Program, he spent the 1973-1974 academic year at Oxford University, U.K., where his research with synchrotron radiation began. He won the 1973 NRL Sigma Xi Pure Science Award and is a Fellow of the American Physical Society. Dr. Kabler has held administrative positions in several NRL divisions. His research interests range among the electronic properties of semiconductors and insulators and he is currently spokesperson for beam line X24C at the National Synchrotron Light Source, Brookhaven National Laboratory.

DAVID J. NAGEL graduated from the University of Notre Dame (B.S. degree in Engineering Science, 1960) and performed graduate work at the University of Maryland (M.S. degree in Physics, 1969, and Ph.D. degree in Engineering Materials, 1977). During active duty with the Navy, he was Navigator on the USS *Arneb* on OPERATION DEEPFREEZE (1960 to 1962) and then served as a Technical Liaison Officer at the Naval Research Laboratory (1962 to 1964). Since joining the technical staff of NRL in 1964, he held positions as a research physicist, section head, and branch head. Currently, he is superintendent of the Condensed Matter and Radiation Sciences Division and manages a broad experimental and theoretical research and development program. Dr. Nagel's research interests center on X-ray physics, especially spectroscopy, with applications to materials analysis and plasma diagnostics. He served two years on the Program Advisory Committee of the National Synchrotron Light Source. Dr. Nagel has written or co-authored over 100 technical articles, reports, book chapters, and encyclopedia articles. In 1990, he retired as a Captain from the United States Naval Reserve.

EARL F. SKELTON received a B.S degree in physics from Fairleigh Dickinson University in Teaneck, New Jersey, in 1962. He received a Ph D degree in physics from Rensselaer Polytechnic Institute in Troy, New York, in 1967 and came to NRL that year as a National Research Council Post-Doctoral Associate. Dr Skelton has been teaching continuously on a part-time basis since 1968, first at Prince George's Community College, then in the graduate school of the University of Maryland, and at The George Washington University since 1974. He served as a liaison scientist at the Office of Naval Research in Tokyo, Japan, in 1978 and spent a sabbatical year at the Stanford Synchrotron Radiation Laboratory (SSRL), Stanford University in 1980-81. He was elected a Fellow of the American Physical Society in 1980 and served on the Users Organization Executive Committees at both SSRL and the National Synchrotron Light Source (NSLS). He is currently head of the Phase Transformation Section in the Dynamics of Solids Branch and is spokesperson for the Insertion Device Team responsible for Beamline X17C at NSLS. He has authored or co-authored over 200 technical publications, including an encyclopedia article, and has won two NRL publication awards. On a personal note, Dr Skelton has completed over forty 26.2-mile marathons, including every Marine Corps Marathon.

Acoustics

ACOUSTICS

In addition to other oceanographic considerations, the Navy's ability to operate effectively at sea depends upon the continuing development of its capability to detect acoustic signals generated by surface or submerged vessels. Reported in this chapter is work on oceanographic acoustic tomography, underwater imaging, thermoacoustic waves, and edge-diffraction detection.

The Acoustics Division and the Underwater Sound Reference Detachment contributed to the work presented here.

Other current research in acoustics includes:

- Focalization of radiating acoustic sources
- Planar fiber-optic acoustics sensors
- In-water acoustical scattering measurements

A New Approach to Ocean Acoustic Tomography

A. Tolstoy and O. Diachok
Acoustics Division

Introduction: Global change, or warming, can be expected to produce effects throughout the Earth's oceans. Consequently, a major technological challenge has been and continues to be the development of a viable strategy for monitoring the three-dimensional temperature structure of the ocean. Ocean temperature changes on the order of 0.5°C correspond to changes on the order of 2.5 ms in sound speed. The essence of the ocean tomography problem is to determine the sound-speed profiles of an ocean region by computer inversion techniques rather than by extensive invasive measurements. These profiles vary as a function of range, cross-range, depth, and, slowly, as a function of time.

A New Approach: Traditional approaches exploit the time-varying behavior of mid- to high-frequency (above 150 Hz) coded signals transmitted through the region to high-time resolution receivers (the time signature will undergo changes on the order of 10 ms as a result of environmental variability). Such approaches use either ships traversing slowly through the area (requiring weeks of time at sea) or moored source/receivers that can only sparsely sample a large ocean area [1]. Our new approach involves four widely distributed vertical arrays of hydrophones plus simple shot sources detonated at known ranges and depths. The arrays are deployed by ship or air or may be permanently moored; they will be located in the central area of the region of interest. The shots will be distributed around its perimeter and can be dropped from an airplane in only a day or two depending on the size and location of the region (Fig. 1). This process will be fast (a few days duration) and comparatively inexpensive. Then the phases and amplitudes of the narrow-band, low-frequency (10 to 50 Hz)

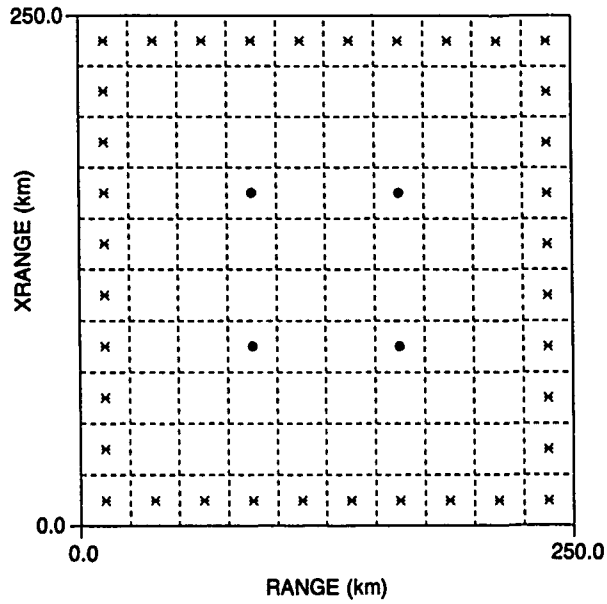

Fig. 1 — Distribution of four arrays (indicated by •) and 36 sources at 100 m depth (indicated by *) for 10 by 10 grid covering 250 km^2

components of these shot-generated acoustic fields (as measured on the arrays) are examined with signal-processing techniques to infer the environmental parameters. Difficulties arise primarily because the description of a family of range-dependent profiles requires that an enormous number of parameters and values be considered. For example, a single acoustic 200-km path through a highly varible region like the Gulf Stream might require 10 or more sound-speed profiles to describe the environmental conditions. If we want to determine the sound-speeds at just one depth and with only two possible values, then the total number of possible conditions is 2^{10}. More generally, we will want to know sound speeds at all depths and over longer ranges. However, highly efficient descriptions of the profiles (in terms of orthonormal basis functions [2]) reduce the solution space considerably. Then careful array placement within the region to allow for many overlapping source-receiver paths can result in extremely successful inversions. The inversion algorithm itself is a new modification of a standard back-propagation algorithm used in medical tomography [3].

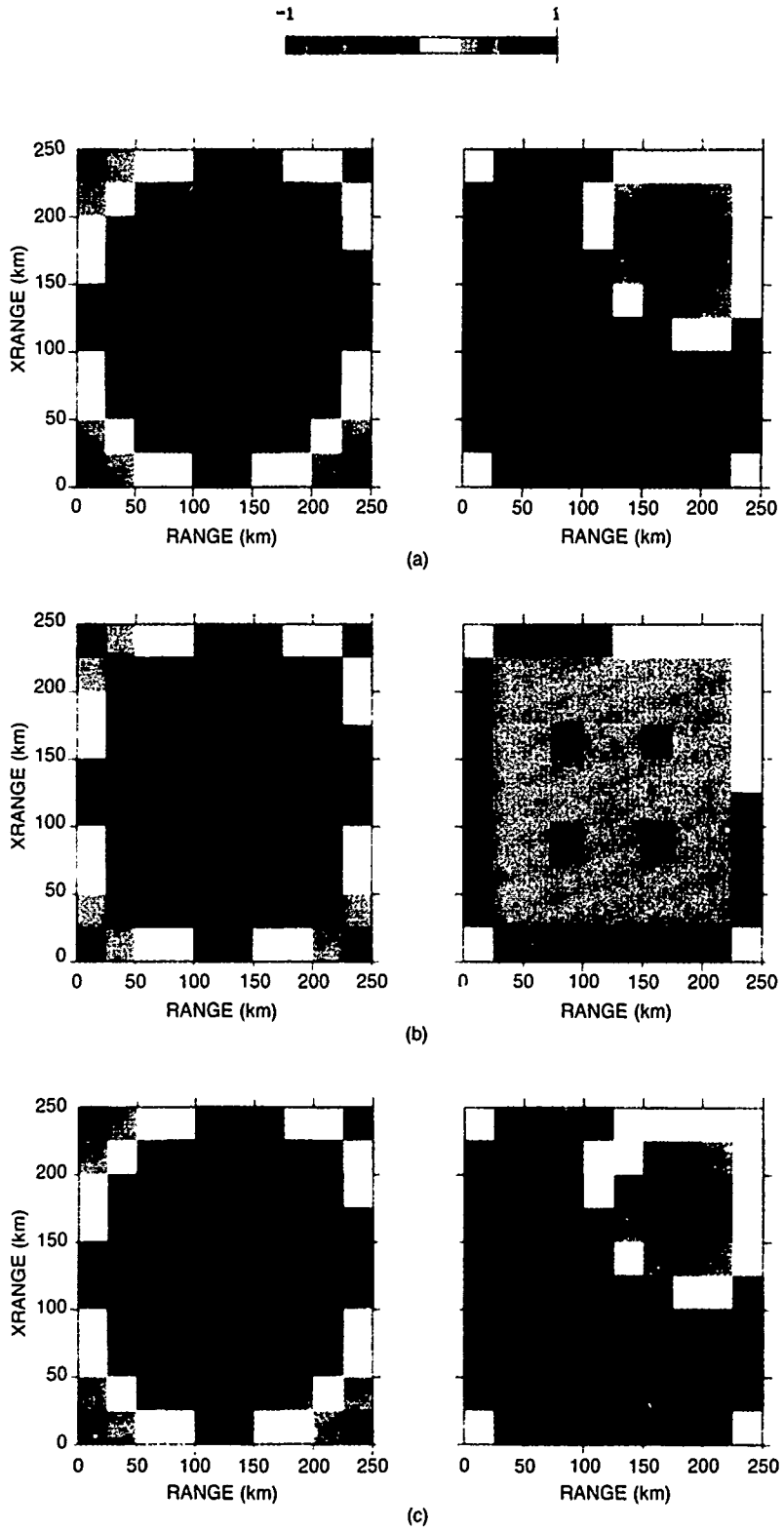

Fig 2 — Sound-speed profile parameters $\beta_1(\chi,\gamma)$ and $\beta(\chi,\gamma)$, the amplitudes of the orthonormal basis function, with scale indicated above pictures. β_1 values shown on left, β_2 values on right. 2(a) shows "true" environmental values; 2(b) shows initial estimates of those values with correct entries at source and array locations; 2(c) shows final estimates after mathematical inversion.

Results: So far, our new technique has examined only simulated data. In particular, by examining Fig. 2, we see a characterization of a sample ocean region where the true environment is represented in Fig. 2(a). We begin our computer inversion by assuming that we have sound-speed measurements where the shots have been dropped and where the arrays are located, but otherwise we have only a crude estimate of the mean environment. Figure 2(b) shows the program initialization. After mathematical inversion, we arrive at a highly accurate estimate of the environment, as shown in Fig. 2(c). We look forward to testing our new approach experimentally in 1992.

[Sponsored by ONR]

References

1. R.C. Spindel and P.F. Worcester, "Ocean Acoustic Tomography," *Sci. Am.*, 94-99, (Oct. 1990).

2. A. Tolstoy and O. Diachok, "Low Frequency Acoustic Tomography using Matched Field Processing," Proceedings of IEEE Oceans 90, Sept. 1990.

3. A. Tolstoy, O. Diachok, and L.N. Frazer, "Acoustic Tomography via Matched Field Processing," accepted for publication by *J. Acoustic. Soc. Am.*, 1991. ■

Underwater Acoustic Imaging

L.J. Rosenblum B. Kamgar-Parsi
Acoustic Division
and
E. Belcher
Applied Physics Laboratory
University of Washington

High-resolution imaging sonars and optical systems are used by the Navy to view underwater shipwrecks and other targets of interest. Optical systems have high resolution but fail in turbid waters, and current sonar systems have limitations for imaging applications. To fill the gap between these systems, a high-performance, forward-looking sonar has been developed that perceives data in a manner similar to the human eye. This acoustic lens system eliminates the need for extensive beamforming electronics. Digital imaging and computer-graphic algorithms produce high-resolution, three-dimensional (3-D) acoustic snapshots of the surrounding environment. The lens is also potentially useful for obstacle avoidance and bottom mapping.

The Acoustic Lens: Traditional sonar systems use mechanical or electrical beamforming techniques to scan a highly directional acoustic beam over a field of view. Acoustic lens technology, on the other hand, places a large number of highly directional acoustic transducers on a grid attached to a hemispherical shell to form a retina. A thin, spherical lens cover is filled with a specially chosen fluid that focuses incoming acoustic waves onto the retina. Transmission time delays determine range, while transducer position yields bearing and elevation coordinates. Lens technology [1] is not new, but recent advances in digital electronics now permit dealing with the large volume of data in real time.

Figure 3 shows the lens within its casing being mounted on the front of a boat for an experiment at Patuxent River, Maryland. The 8.8-in. shell at the front of the lens mounting holds the focusing fluid, with the retina (hidden) behind. The retina is populated with 128 transducers in 8 rows of 16. The transducers in each row are separated by 3°, and the rows are separated by 1.5°. Thus the system has a field of view of 48° in the azimuth and 12° in elevation. The retina mounts on a track that permits shifting the field of view in elevation for performing different missions. Each beam has a conical beam pattern with a —3 dB full beamwidth of 1.5° for transmit and receive. The range bins, defined by the received time delays, are typically about 10 cm. The sensor is designed to go to depths up to 300 m and to focus in an ambient temperature

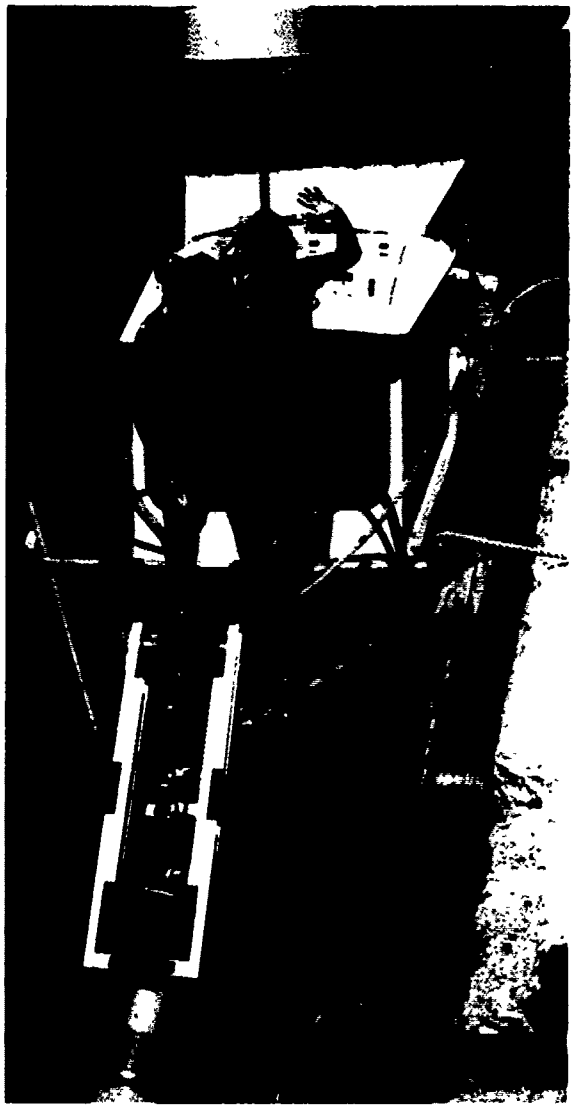

Fig. 3 — The acoustic lens being mounted on a boat as part of a two-day experiment on the Patuxent River

range that spans 10° without having to change the lens fluid. Data is both recorded within the lens unit and sent topside to a PC-based, real-time graphical display.

Acoustic Snapshots: We wish to use the high-resolution (for sonar) acoustic lens data to reconstruct underwater scenes. Our approach is to integrate image processing for data enhancement with computer graphics techniques to obtain a high-resolution, 3-D acoustic snapshot. We begin by dividing space into voxels (volume elements). Subvoxel interpolation algorithms are applied to the conical sections of lens data to estimate the return signal strength within each voxel. Volume visualization algorithms [2] then operate on the voxel data to recreate and display the 3-D scene.

Figure 4 shows an acoustic snapshot of a 1.5-m-long remotely operated vehicle (ROV) on the bottom of a tow tank at the David Taylor Research Center (DTRC). The acoustic lens was placed on a test platform and passed over the ROV. The three small data panels are orthogonal slices of data in which planar volume slices perpendicular to a fixed axis are displayed. We show the along-track, depth, and cross-track slices that contain the largest intersection with the ROV. Since computer memory contains all $60 \times 60 \times 60$ voxels, interactive, real-time orthogonal slicing can be performed without recomputing the

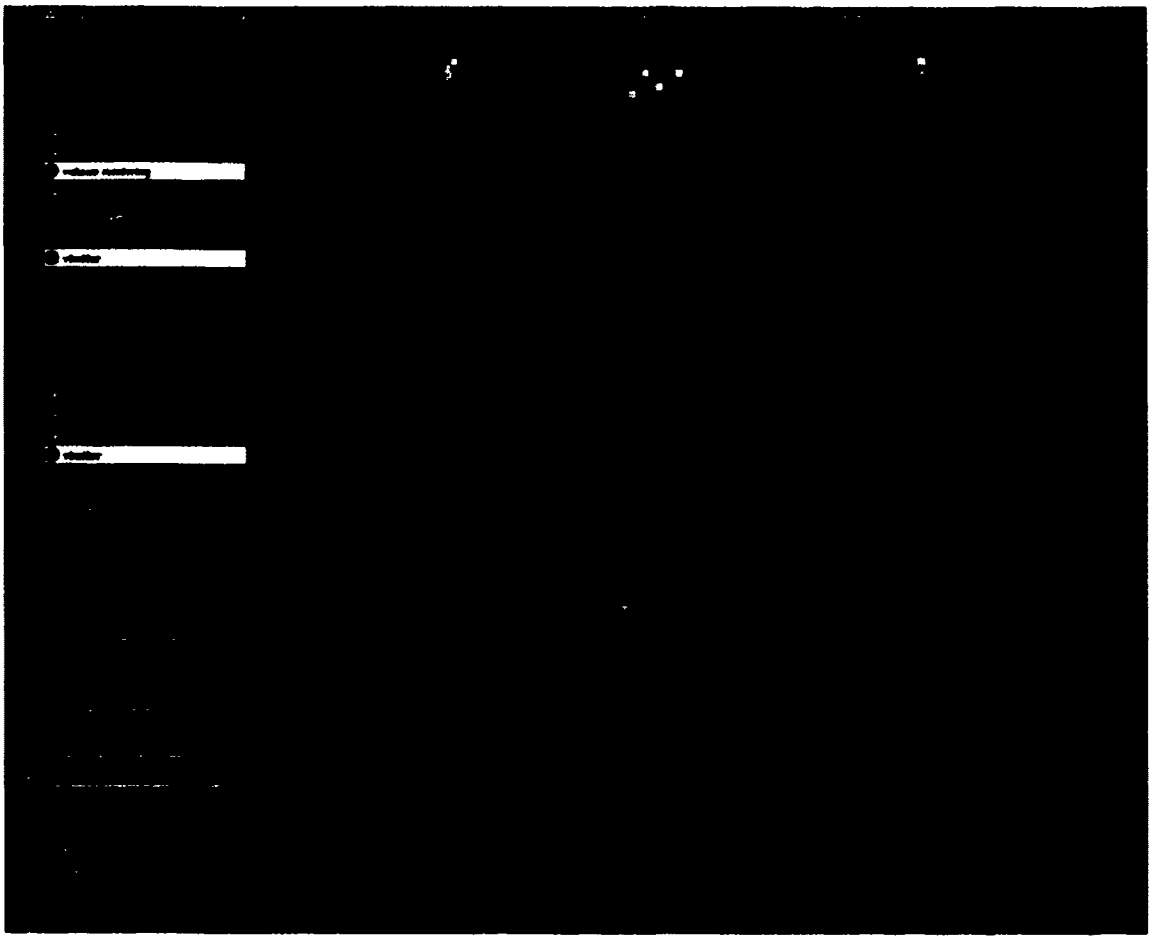

Fig 4 — Image reconstruction of a 1 5-m-long ROV at the bottom of a test tank at DTRC The three top panels show orthogonal slices through the image space, with yellow-to-red representing the largest intensity voxels The solid red line denotes the bottom of the test tank. The bottom panel is a volume rendering of the 3-D scene, with the ROV seen in orange.

volume. This technique is a valuable data-analysis tool. For 3-D object reconstruction, additional 3-D digital filtering operations are applied to the data. The V-buffer volume-rendering algorithm [3] then yields a semitransparent reconstruction of the ROV (the largest panel of Fig. 4).

Acoustic lens data also provides detailed ocean bottom information. Figure 5 shows a small section of bottom from the Patuxent River by using data from the experiment shown in Fig. 3. The use of multiple light sources creates shadows that make visible small features on the river bottom.

Conclusions: The acoustic lens represents an important advance in imaging sonar technology. The lens is a compact, robust sensor that can be used in highly turbid water. As Fig. 4 illustrates, 3-D images can be reconstructed from the volumetric lens data. However, many additional research topics require exploration. These include registering multiple pass data sets, higher resolution imaging through algorithm and hardware improvements, and by using lens data for automated object detection and classification.

Credits: The acoustic lens was designed and constructed at the Applied Physics Laboratory, University of Washington, in cooperation with NRL. The underwater imaging was performed at NRL by using a Stardent 1500 computer and AVS visualization software.

[Sponsored by ONT]

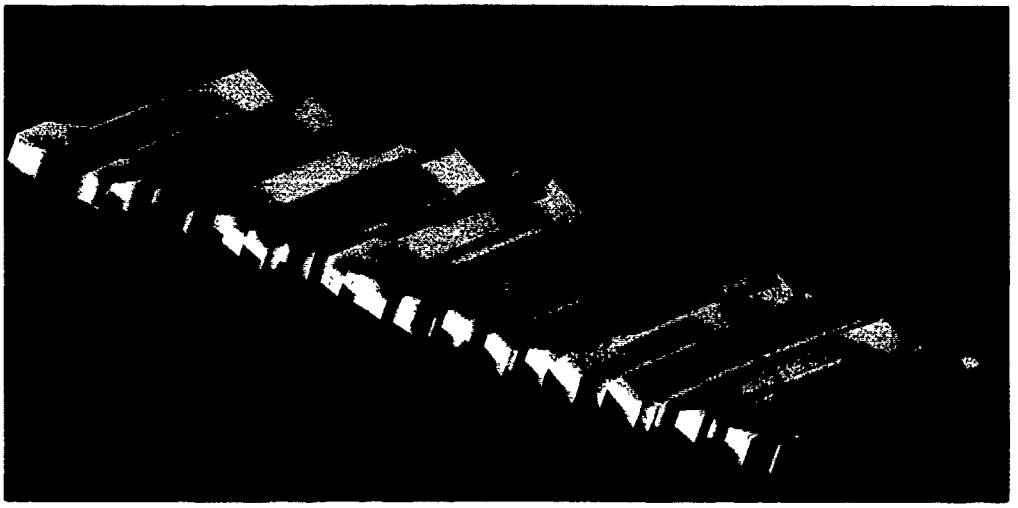

Fig. 5 — Reconstruction of a small section of bottom from the Patuxent River. The largest features are a few feet in height.

References

1. D.L. Folds, "Status of Ultrasonic Lens Development," *Underwater Acoustics and Signal Processing*, Proceedings of the NATO Advanced Study Institute, Copenhagen, Aug. 1980 (D. Reidel Publishing Company, Boston, 1981), pp. 263-279. D.A. Kaufman, *Volume Visualization* (Computer Society Press, Los Alamitos, CA, 1990).

3. C. Upson and M. Keeler, "V-Buffer: Visible Volume Rendering," Proceedings of the SIGGRAPH 88, Aug. 1988, pp. 59-64. ■

Propagation of Thermoacoustic Waves in Elastic Media

A.J. Rudgers

Underwater Sound Reference Detachment

Understanding the processes by which energy is dissipated when sound waves propagate in gasses, liquids, and solids is important to the development of new acoustical materials for use by the Navy. Energy dissipation in a material medium, however, does not arise only from purely mechanical losses, such as losses caused by viscosity. Energy dissipation also results from the thermal processes that accompany the propagation of sound waves in that medium. Consequently, it is necessary to investigate wave-propagation problems in which the thermal as well as the elastic character of the propagation medium is taken into account. For such investigations, one uses the theory of thermoelasticity, which combines the equations of linear elasticity with those of heat conduction [1]. In the present investigation, the equation describing heat conduction has been incorporated into the thermoelastic equations in two different ways—in the classic way, by using the familiar hypothesis of Fourier and in a more modern way, by using a hypothesis originated by Vernotte [2]. This gives rise to a modified equation of heat conduction that does not allow a temperature gradient to be established instantaneously in a heat-conducting medium.

Thermoacoustic Waves: Thermoelastic behavior of a material medium is described by a pair of coupled partial differential equations (PDEs). Upon solving these PDEs, one determines that two kinds of dilatational waves and a shear wave can propagate in an unbounded thermoelastic medium. This is in contrast to the picture that one obtains in ordinary elasticity theory, where one dilatational wave and one shear wave propagate in an unbounded medium.

The waves of interest in the thermomechanical problem are the two-dilatational waves. These are the thermoacoustic waves. (The shear wave is a purely mechanical wave that is uncoupled from the thermal processes.) In each of the two thermoacoustic waves, a particle-velocity disturbance and a temperature disturbance travel together in unison through the propagation medium. Thus each wave comprises both a mechanical and a thermal component. The dispersion relation resulting from the thermoelastic PDEs allows one to calculate the speed and the absorption coefficient associated with each thermoacoustic wave as a function of the frequency w of the wave. The thermoacoustic waves are conveniently designated as Type 1 and Type 2 waves. The Type 1 wave is often called the "acoustic" branch and the Type 2 wave, the "heat-conduction" branch; at very low frequencies, the Type 1 wave mimics many of the features of a purely mechanical wave, and the Type 2 wave mimics pure heat conduction.

Wave-Propagation Phenomena: The dispersion relation shows that when the Fourier hypothesis is used to account for heat conduction in the equations of thermoelasticity, a physically unrealistic picture of thermoacoustic wave propagation results. Figure 6 shows the nondimensional wave speed c of the two thermoacoustic waves plotted as a function of the nondimensional frequency w for two different values of a parameter q (where $0 < q \leq 1$) that characterize the material properties of the propagation medium. In Fig. 6(a), for $q = 3/4$, we see that the speed of the Type 1 wave (acoustic branch) drops from the adibatic sound speed at low frequency to the isothermal sound speed at high frequency, while the speed of the Type 2 wave (heat-conduction branch), which assumes a low value at low frequency, increases without bound as frequency increases. A wave speed that increases without bound as frequency increases indicates that there must be a defect in the theory that describes it, since such wave-propagation behavior is impossible in real physical systems.

Of course, the elementary theory of heat conduction is known to be defective in just this way. One might conjecture, therefore, that the behavior of the Type 2 wave, as observed in Fig. 6(a), simply is a manifestation of this same defect in the thermoelastic theory. The truth of this conjecture, however, is ruled out by the curves shown in Fig. 6(b), which is calculated with $q = 1/4$. In Fig. 6(b), one sees that, as expected, the wave associated with the acoustic branch (Type 1 wave) travels at the adiabatic sound speed at low frequencies and thus behaves like a mechanical disturbance. But as one goes to higher frequencies, the wave speed associated with the acoustic branch increases without bound. Thus the acoustic wave behaves at high frequencies not like a mechanical disturbance but, rather, like classic heat conduction. On the other hand, the wave associated with the heat-conduction branch (Type 2 wave) mimics heat conduction at low frequencies as it should, but mimics an acoustic wave at high frequencies where it travels at the isothermal sound speed. It is clear from these results and from those shown in Fig. 6(a) that when the Fourier hypothesis is used in the thermoelastic PDEs, the theory gives an inconsistent and physically unrealistic picture of thermoacoustic wave propagation.

Realistic Models of Heat Conduction: Figure 6 illlustrates the physically unrealistic picture of wave propagation that can be corrected by incorporating the Vernotte hypothesis into the thermoelastic equations However, to do this requires one to determine the value of the characteristic Vernotte relaxation time for the propagation medium. Since there is as yet no agreed on way to determine this value precisely, the Vernotte relaxation time was estimated in two different ways so that calculations describing thermoelastic dispersion could be carried out. The value was estimated by a lattice model [1], which is based on an idea inherent in the Debye theory of specific heats and by a phonon-gas model, as suggested by Chester [3].

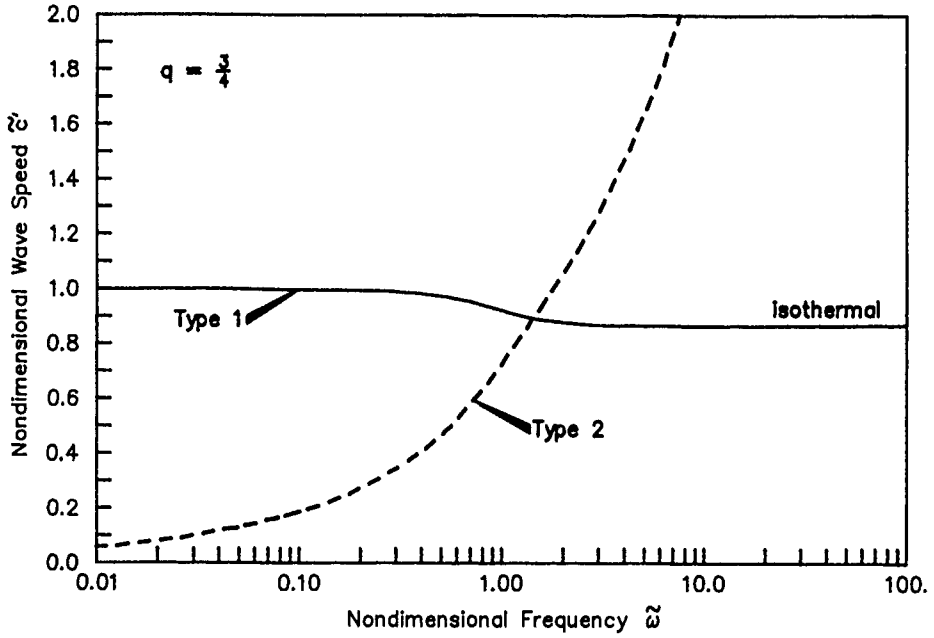

(a)

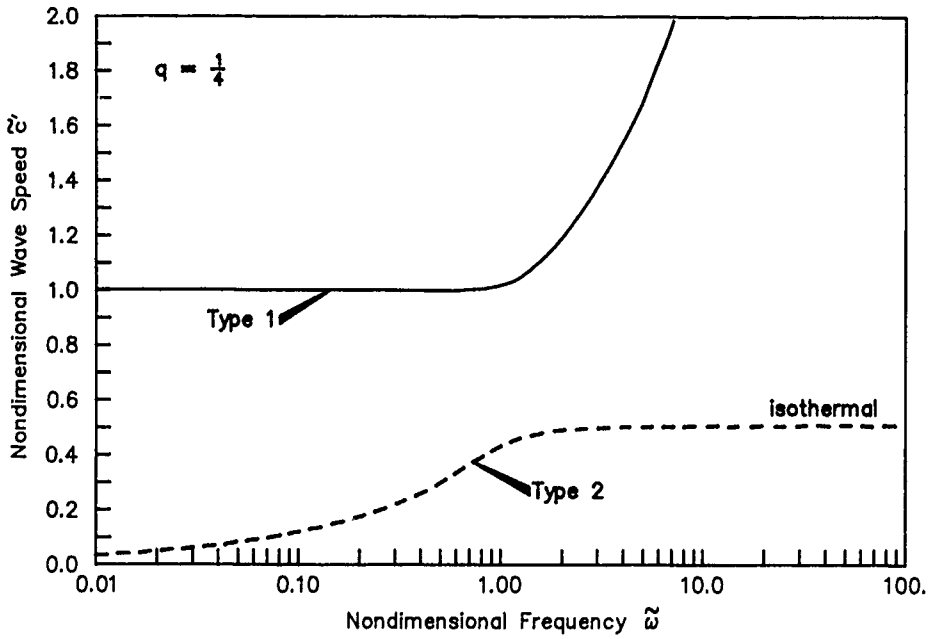

(b)

Fig. 6 — Nondimensional wave speeds of thermoacoustic waves as a function of nondimensional frequency $\tilde{w}$ Computations are made by incorporating the Fourier hypothesis of heat conduction in the thermoelastic equations. Quantity q is a parameter characterizing the propagation medium: (a) q = 3/4; (b) q = 1/4.

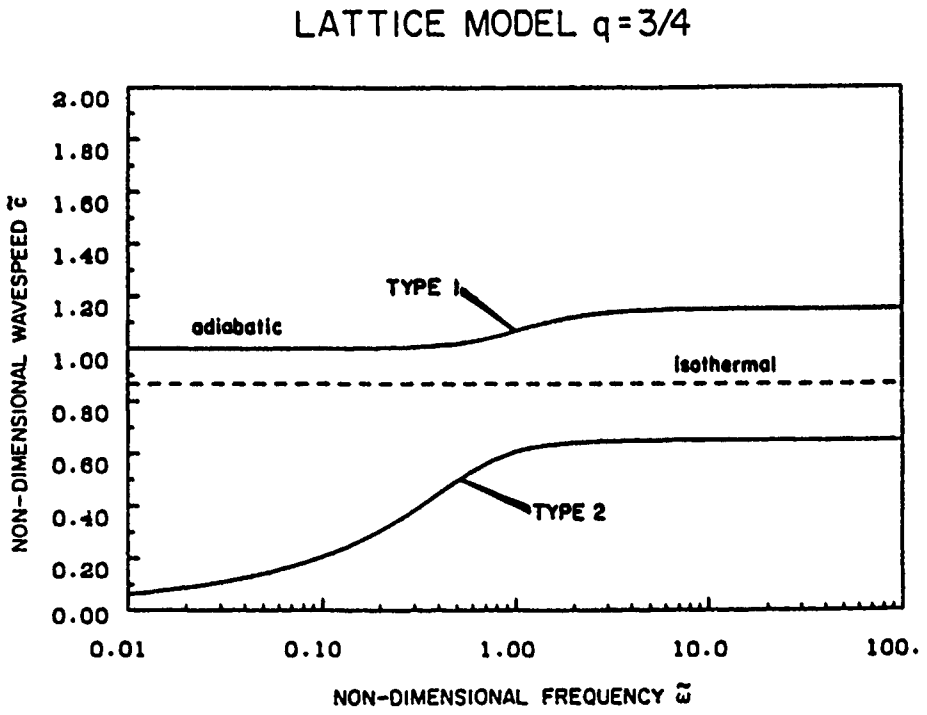

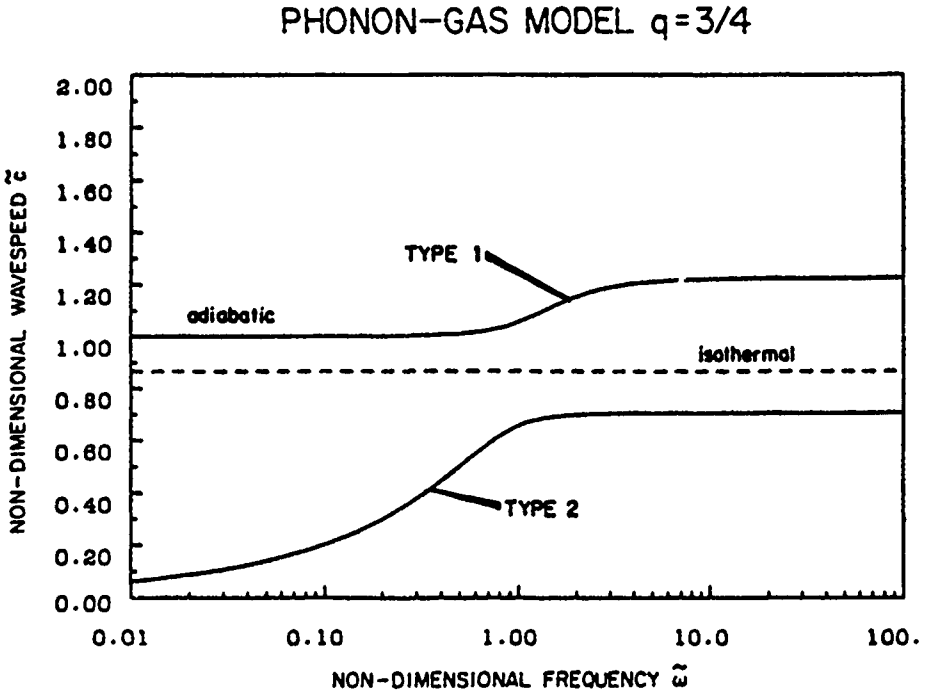

Fig. 7 — Nondimensional wave speeds of thermoacoustic waves as a function of nondimensional frequency $\tilde{w}$. Computations are made by incorporating the Vernotte hypothesis of heat conduction in the thermoelastic equations. Quantity q is a parameter characterizing the propagation medium: (a) lattice model, q = 3/4; (b) phonon-gas model, q = 3/4.

Both the lattice model and the phonon-gas model estimate the Vernotte relaxation time by making use of the concept that at high frequency, heat must propagate in a material by the same physical mechanism by which elastic disturbances are propagated. Consequently, the limiting speed at which the Type 2 wave propagates cannot exceed the speed at which the Type 1 wave travels. Both the lattice model and the phonon-gas model make similar predictions concerning the speeds of the thermoacoustic waves. Figure 7(a) shows predictions for $q = 3/4$, which describes wave propagation according to the lattice model and in Fig. 7(b), which describes wave propagation according to the phonon-gas model. Comparing Figs. 6 and 7, one sees that when the Vernotte hypothesis replaces the hypothesis of Fourier in thermoelastic theory, thermoacoustic wave propagation has a different character. In Fig. 7, one sees that there are no wave speeds that increase without bound. The speed of the Type 1 wave calculated according to either model increases from the adiabatic speed at low frequency to a value greater than this speed in the high-frequency limit. At the same time, the speed of the Type 2 wave increases from the low value associated with heat conduction at low frequency to a value somewhat less than the isothermal sound speed in the high-frequency limit. Figure 7 shows results that incorporate the more realistic model of heat conduction and clearly give a more realistic picture of the dispersion effects (wave speed and absorption coefficient with frequency) that occur in actual substances than do results based upon the Fourier hypothesis.

[Sponsored by ONR]

References:

1. A.J. Rudgers, "Analysis of Thermoacoustic Wave Propagation in Elastic Media," *J. Acoust. Soc. Am.* **88**, 1078-1094 (1990).

2. P. Vernotte, "Théorie Continue et Théorie Moléculaire des Phénomènes Thermo-cinétiques," *C. R. Acad. Sci.* (Paris) **227**, 43-44 (1948).

3. M. Chester, "Second Sound in Solids, "*Phys. Rev.* **131**, 2013-2015 (1963). ■

Edge Diffraction Detection Technique

J.C. Piquette
Underwater Sound Reference Detachment

One purpose for acoustical panel tests is to obtain a comparison between two candidate acoustical materials. For such a comparison to be meaningful, it is important to achieve an experimental configuration that yields measurements approximating those that would be obtained from a sample of infinite lateral extent; in this way, results that are independent of the experimental configuration are obtained. Since an actual test obviously requires the use of a sample of finite size, it is important to determine the extent of the departure of the experimental results obtained from such a sample from those that would be obtained if it were possible to perform a measurement on an infinite sample. Here, we examine an experimental technique that can detect the presence and magnitude of the effects of finite sample size. We also examine a procedure that can significantly suppress these undesirable effects.

The Technique: Figure 8 shows the basic panel measurement configuration consisting of a sound source, two detectors, and a sample panel. One detector senses the reflected wave, the other senses the transmitted wave. The sample panel consists of an acoustical material M that is usually affixed to a support plate typically fabricated from steel. (Although the acoustical material is depicted as a monolayer, samples of interest are most frequently multilayered.)

The experimental technique considered here is based on a theoretical result described previously by Rudgers and Solvold [1]. The results of Ref. 1 imply that if the sample of Fig. 8 were of

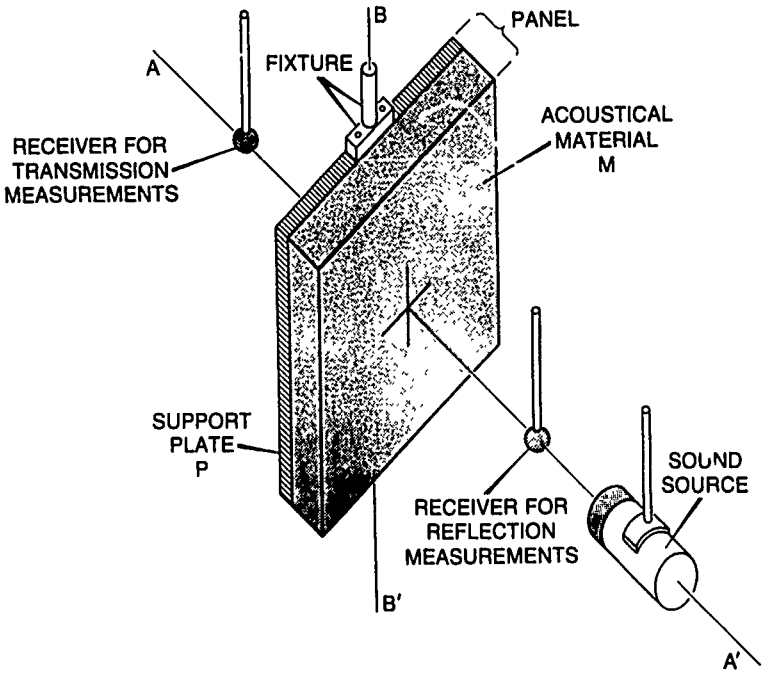

Fig. 8 — The basic panel measurement experimental configuration

infinite lateral extent, the complex transmission coefficient would be the same whether the sample were configured as shown in the figure (i.e., with the support plate positioned opposite the sound source) or whether it were configured so that the support plate faces the sound source. In other words, the signal detected by the receiver for transmission measurements is unaffected if the sample is rotated 180° about the axis BB′, assuming the source and detectors are appropriately repositioned to maintain constant source-to-sample and sample-to-detector spacing. This result applies to measurements obtained from a sample of infinite lateral extent. Differences between waveforms obtained from an actual finite sample are caused by the effects of finite sample size.

Experimental Results: Figure 9 presents digitized waveforms obtained from an actual test sample. The solid-line waveform was obtained with the support plate configured opposite the sound source, and the dashed-line waveform was obtained with the support plate configured to face the sound source. Note from the initial nonzero portions of the waveforms that the received waves are initially identical, as is evidenced by the short region of waveform overlap. This is consistent with what is expected to occur for a sample of infinite lateral extent. Note, however, that shortly after waveform reception, the waveforms diverge. Detailed timing calculations demonstrate that the waveform divergence begins to occur at the moment a signal originating from the sample edges would be expected to arrive at the receiver for transmission measurements. Note that the contaminating contributions of the sample edges are rather significant, causing the received amplitude for one waveform to be more than twice the amplitude of the other. The difference of the two waveforms gives a measure of the amplitude of the contaminating influences of edge effects. In this measurement, the contamination amplitude is more than 100% of that of the transmitted wave, which we are trying to determine.

Edge Effect Suppression: The waveforms presented in Fig. 9 were obtained in measurements performed on a sample material affixed to a standard steel support plate. Since the acoustic

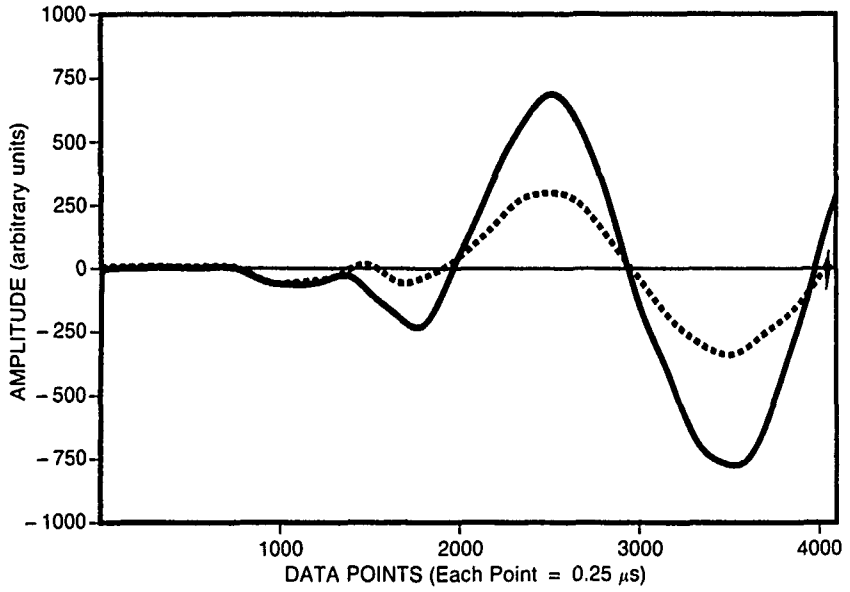

Fig. 9 — Waveforms obtained from a sample acoustical material affixed to a standard steel support plate. Solid line — support plate opposite source; dashed line — support plate facing source

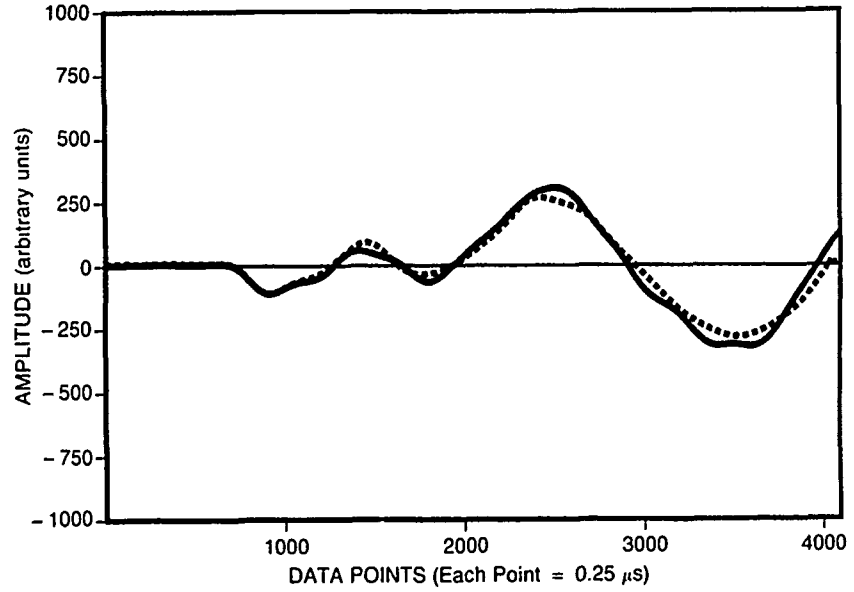

Fig. 10 — Waveforms obtained from a sample acoustical material affixed to a polymethylmethacrylate support plate. Sample acoustical material is the same as that used in the test conducted to obtain the waveforms of Fig. 9. Solid line — support plate opposite source; dashed line — support plate facing source

impedance of steel is more than thirty times greater than that of the surrounding water medium, it is reasonable to suppose that the greatest contribution to the edge effects observed in this measurement arises from the steel plate. Thus, edge effects can be significantly reduced if the steel support plate is replaced by a support plate having an acoustic impedance that matches more closely that of water.

Figure 10 shows waveforms obtained from the same sample that was used to obtain the waveforms of Fig. 9, except that the steel support plate has been replaced with a polymethylmethacrylate support plate. (Polymethylmethacrylate has an acoustic impedance only about two times that of water.) Note also that the waveform differences in Fig. 10 have been significantly reduced from those that were present in the measurements used to obtain the waveforms in Fig. 9. Thus, the contaminating influences of edge effects have been significantly suppressed by the use of the polymethylmethacrylate support material.

Acknowledgment: I am indebted to Dr. Anthony J. Rudgers for permission to use Fig. 8.

[Sponsored by ONR]

Reference

1. A.J. Rudgers and C.A. Solvold, "Apparatus-independent Acoustic-material Characteristics Obtained from Panel-test Measurements," *Acoust. Soc. Am.* **76**, 926-934 (1984). ■

Chemical/Biochemical Research

CHEMICAL/BIOCHEMICAL RESEARCH

Many of the Navy's problems involving polymeric materials, coatings for ship hulls and tank linings, fuels and combustion, materials synthesis, fire fighting, and surface phenomenon call for solutions by chemical means. Application of biomolecular science and engineering has contributed to these solutions. Reported in this chapter is work on the detection of cocaine, studies on polymeric blends, and corrosion and its prevention.

The Center for Bio/Molecular Science and Engineering and the Chemistry Division contributed to the work presented here.

Other current research in chemistry/biochemistry includes:

- Patterned coplanar molecular assemblies
- Lipid microstructures
- Microlithography with polymers
- Nanomechanics of surfaces
- Analytical mass spectrometry

Drug Detection by Using an Antibody-based Sensor: The Flow Immunosensor

G.A. Wemhoff, A.W. Kusterbeck, and F.S. Ligler
Center for Bio/Molecular Science and Engineering

The heightened awareness of illegal drug use in the uniformed services and the civilian community is promoting screening as a standard safety procedure. The potential demand for a fast and simple drug screening protocol is extraordinary. For example, the Navy alone screens over 2 million urine samples a year for drugs, at a cost of nearly $10 million. Available methods are expensive, labor-intensive, and time-consuming. The Center for Bio/Molecular Science and Engineering at NRL is developing a new technology—the flow immunosensor—to decrease the cost and the assay time, enhance the ease of operation, and improve the efficiency of initial drug screening.

Operation of the System: The flow immunosensor relies on the use of antibodies to detect illegal narcotics. The primary advantage to using antibodies is their extreme specificity. Antibodies can discriminate drug molecules among the millions of other molecules present in urine, blood, or saliva samples. While antibodies are a common component in other screens on the market, it is the way in which the antibodies are used in the flow immunosensor that is unique.

In the development of a cocaine-specific system, anticocaine antibody is covalently attached to tiny beads contained within a small column (approximately 1/2-in. long × 1/4-in. wide). A fluorescently labeled signal molecule, similar in structure to the cocaine, is bound to the immobilized antibodies, and a flow stream through the column is established. Because antibody interactions are reversible, cocaine present in test samples introduced into the flowing stream can displace the signal molecule (Fig. 1). Fluorescence in the effluent, caused by the presence of the displaced signal molecules, is measured by using a small fluorimeter. The intensity is directly proportional to the amount of cocaine in the sample (Fig. 2). In addition to immobilized antibody and fluorescent signal molecules, the system consists of a portable, off-the-shelf fluorimeter, a laptop computer, a small peristaltic pump, and the associated plumbing and hardware (Fig. 3).

By using this system, we have addressed such questions as repetitive sampling, detection limits, and sample-analysis time. Since there is a finite amount of antibody and support that can be contained in any single column, each column has a limited amount of signal molecule. To obtain a first estimate of the useful lifetime of a single column, samples of cocaine were repeatedly introduced to

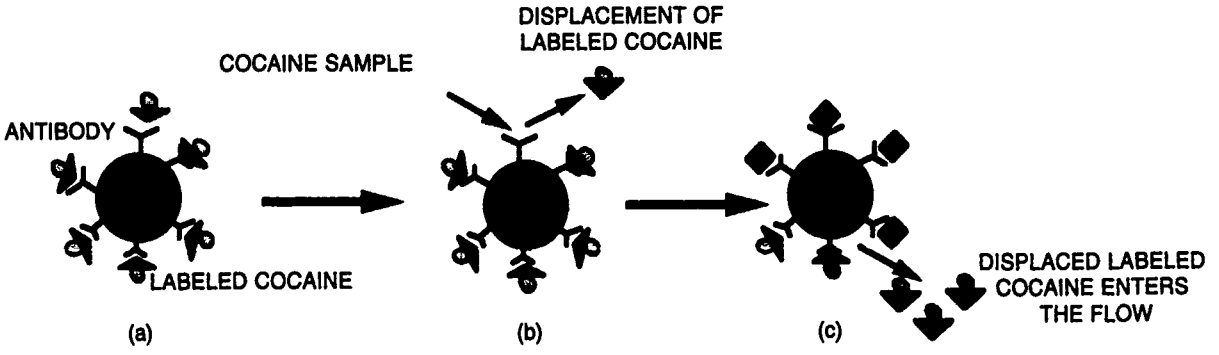

Fig. 1 — Flow immunosensor operation: (a) immobilized anticocaine antibodies are saturated with labeled cocaine molecules; (b) a sample of cocaine is added, and a proportional amount of labeled cocaine is displaced; and (c) the displaced, labeled cocaine is moved by the aqueous flow to the fluorimeter, and a signal is generated.

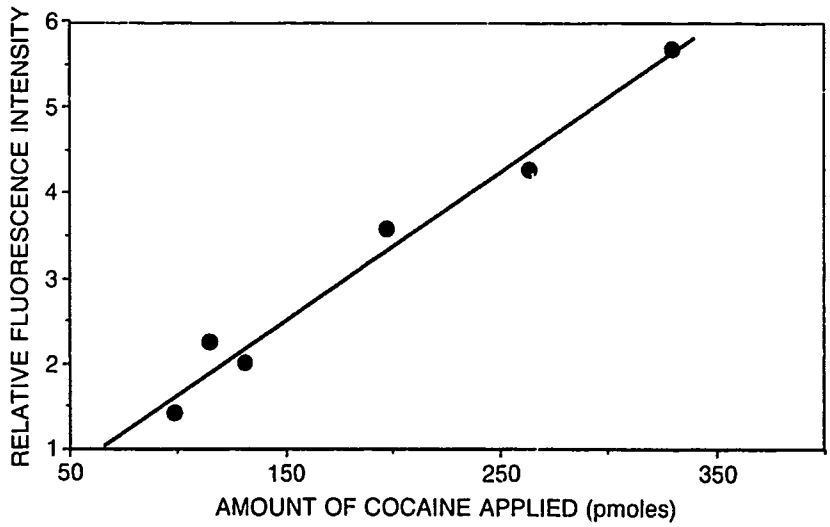

Fig 2 — Standard curve for detecting cocaine–HCl by using the flow immunosensor. Varying amount of cocaine–HCl were applied to a single column at a flow rate of 0.5 ml/min, and the fluorescence signal was collected.

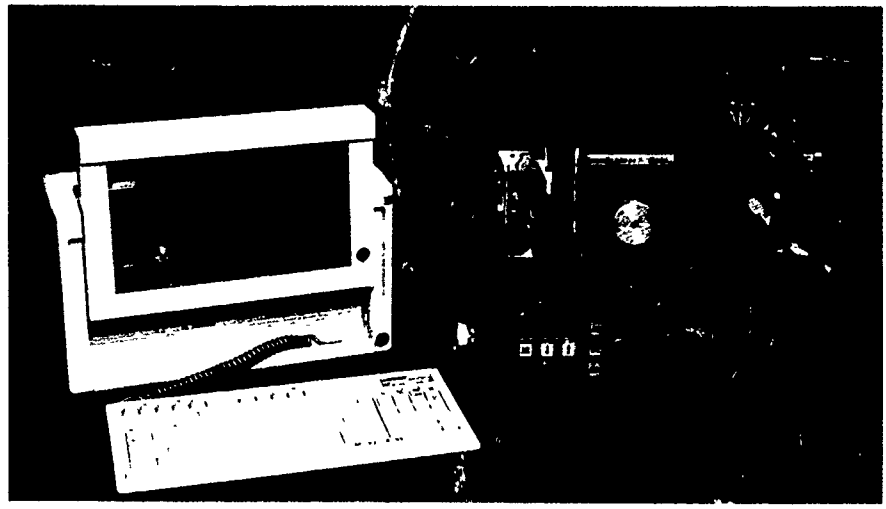

Fig. 3 — The flow immunosensor

the system and the signal recorded. We determined that a significant signal could be obtained for more than 57 consecutive runs (Fig. 4). Typically, randomly screened urine sample processed in the Navy clinics are less than 1% cocaine-positive. In an 8-h day, where 100 sample are processed per hour, less than 8 positives would be expected. This is well below the capacity mentioned above for a single column, thereby requiring that the column be changed no more than once a day.

Finally, the flow immunosensor is sensitive and operates in real time. By using a flow rate of 1 ml/min, we have been able to detect as little as 5 ng of cocaine within 45 s. This rivals the sensitivity of the more widely used but significantly more time-consuming and expensive radioimmunoassay.

Immediate Impact: The flow immunosensor has the potential for reconfiguring the operation procedures for drug abuse screening. Currently, all samples must be collected and shipped to a central facility. Because the flow immunosensor is portable and designed to be operated by using a

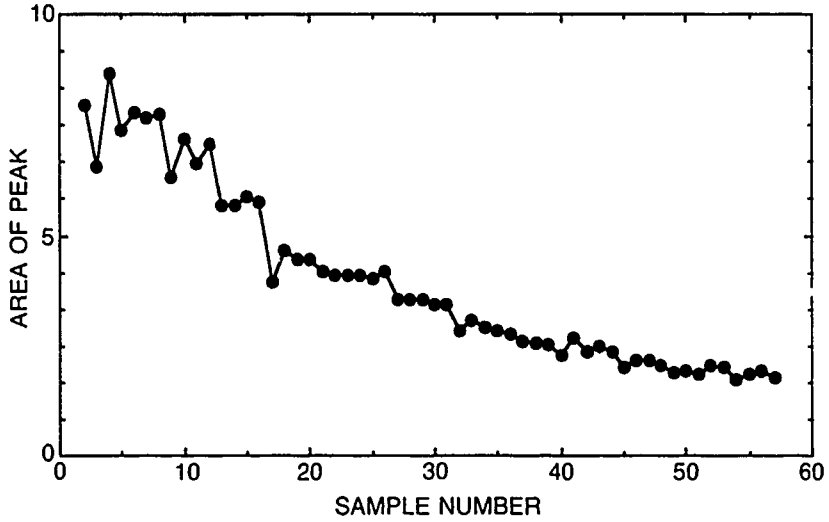

Fig. 4 — Consecutive detection of cocaine samples. Fifty-seven samples of cocaine, 200 μl at 720 ng/ml, were applied to the flow immunosensor. The integrated areas of fluorescence intensity were measured and plotted for each sample.

few key strokes, samples could be run immediately on site by nontechnical personnel.

An additional advantage to the flow immunosensor is the limited amount of reagents required for operation. Since the chemistry of the system is confined to the small in-line column, it is not necessary that numerous reagents be available for operation. Both the fluorophores and the antibody are contained within the column. For continuous 8-h operation, only 500 ml of buffer are required.

Future Directions: The flow immunosensor has been shown to detect cocaine easily in laboratory-prepared samples. Further tests will focus on screening cocaine samples acquired from "real" environments. In the near future, heroin will be included as an analyte for detection by using the flow immunosensor. Also, while screening of urine has been the method of choice for monitoring drug use, we will be investigating the possibility of directly screening saliva. As a noninvasive sample technique, this method should meet with less objection than the collection of urine samples.

A major advantage of the approach used in the design of the flow immunosensor is its ease of adaptability for detecting a wide range of different molecules. Environmental pollutants, therapeutic drug levels in serum, explosives, and numerous other chemicals can be monitored by using this experimental design.

[Sponsored by U.S. Customs Service and FAA] ■

Miscibility Studies of Polymeric Blends

K.J. McGrath, J.B. Miller, C.M. Roland, and A.N. Garroway
Chemistry Division

Introduction: Polymeric blends that are thermodynamically miscible typically exhibit a single glass transition over a narrow temperature range of several degrees. Mixtures that are compatible but not miscible are distinguished by individual glass transitions characteristic of the pure components. Blends of polyisoprene (PIP) and poly(vinylethylene) (PVE) that are very high in 1,2-microstructure exhibit anomalously broad glass transition breadths of approximately 30 K [1]. This unusual behavior is of particular interest because of the potentially broad spectral response that a blend may display in applications such as acoustic damping. Our research efforts therefore focus on the origin of this broad glass transition.

Characterization of glass transitions via calorimetry is typically limited in resolution to structural heterogeneities larger than approximately 10 nm [1]. This suggests that the broad glass transition behavior exhibited by this blend may be due to the presence of a very small-scale phase separation. In this regard, we implement a higher resolution method of probing the scale of polymer blend morphology by characterizing the ^1H nuclear magnetic resonance (NMR) linewidth response in the solid state. In addition, the motional timescales of the individual PVE and PIP chains in the blend are investigated by using high-resolution, solid-state carbon-13 NMR characterization. The results of both techniques lead to an explanation of the origin of the broad calorimetric glass transition behavior observed in this blend [2].

Proton NMR Studies: The magnetic dipole-dipole interaction among hydrogen nuclei (protons) in polymers provides a means of assessing the degree of coupling between nuclear spins in the solid state and, thereby, the degree of intimacy between different components in a polymeric blend. Whenever this interaction is not reduced to its isotropic value (zero) by rapid molecular motion, ^1H NMR spectral linewidths up to many tens of kilohertz may result, depending on the concentration and spatial proximity of the various interacting nuclear dipoles. Thus in the present case, where a blend of two organic homopolymers (PVE and PIP) is of interest, the linewidth of the ^1H resonance will depend primarily upon the degree to which the dipole-dipole interaction is averaged by molecular motion, which in turn will depend upon the degree of motional coupling between the two components.

Figure 5 shows the ^1H NMR spectra for each of the pure components and the blend of interest at 296 K. The spectrum for "pure" PVE (Fig. 5(a)) exhibits a broad linewidth of approximately 20 kHz, which reflects the relative lack of motional averaging of the strong nuclear dipolar interaction in this sample. In contrast, the ^1H spectrum for "pure" PIP (Fig. 5(b) is characterized by a much

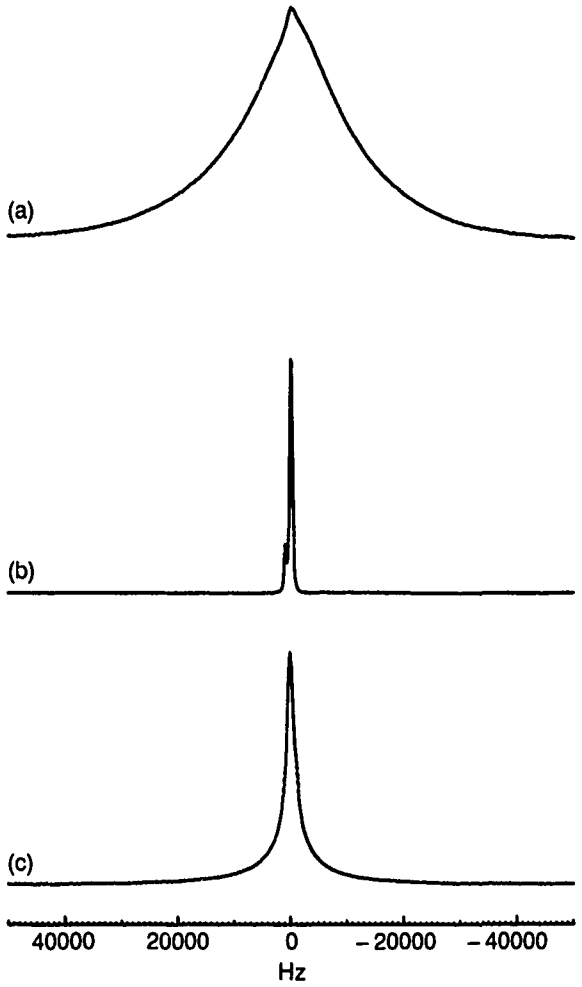

Fig. 5 — ^1H NMR spectra obtained at 296 K: (a) pure PVE; (b) pure PIP; (c) blend. Note that the blend exhibits a linewidth intermediate between the pure components, which confirms miscibility.

narrower linewidth of 600 Hz, a consequence of more complete averaging of the dipolar interaction by molecular motion. This is the expected result since the calorimetric glass transition temperature of PIP is some 70 K below that of PVE. The blend of PVE and PIP, shown in Fig. 5(c), exhibits an intermediate linewidth of approximately 2000 Hz. If the PVE and PIP components were in large segregated domains in the blend ($>>0.5$ nm), a superposition of broad (PVE) and narrow (PIP) lines would result. However, as the size of the individual domains decreases, more contact between the components will result at the interfacial region thereby reducing the intensity of the narrow and broad lines and increasing the intensity of an

intermediate linewidth arising from motional coupling between the two components. Eventually, when the domain sizes decrease to a level where coupling among all segments of each component is possible, a single, intermediate linewidth is obtained. This is the result of Fig. 5(c), which demonstrates that the PVE and PIP components are in contact at the segmental level in this blend.

Carbon-13 NMR Studies: The above ^{1}H NMR linewidth experiments confirm the intimate contact between PVE and PIP components in the blend, and therefore, the broad glass transition behavior exhibited by this blend cannot be attributed to the existence of separate domains. In this regard, we examine the motional timescales of the individual PVE and PIP components in the blend by using carbon-13 NMR spectroscopy. To obtain high resolution ^{13}C spectra in the solid state, high-power proton decoupling is used to eliminate the heteronuclear dipolar interaction between carbons and hydrogen. In addition, the sample is spun rapidly at an angle of 54.7° with respect to the applied static magnetic field (magic-angle spinning (MAS)) to average the orientational variation in chemical shift (chemical-shift) anisotropy (CSA)) to its isotropic value. When the motional timescales of the polymeric components giving rise to the individual resonances in the ^{13}C spectrum are of the same order as the inverse MAS rate or inverse proton decoupling frequency, interference with the modulation of the dipolar and CSA interactions results in an increase in linewidth of the resonance. In the present experiment, a maximum in carbon linewidth would therefore occur when the motional timescale of the carbon of interest is several to tens of kilohertz.

Figure 6 shows plots of the linewidth of the downfield unsaturated carbon as a function of inverse temperature for the respective pure PVE and PIP components (Fig. 6(a)) and the blend (Fig. 6(b)). The maximum linewidth for the pure components occurs at a temperature difference of approximately 52 K, while a difference of only 22 K is observed for the components when

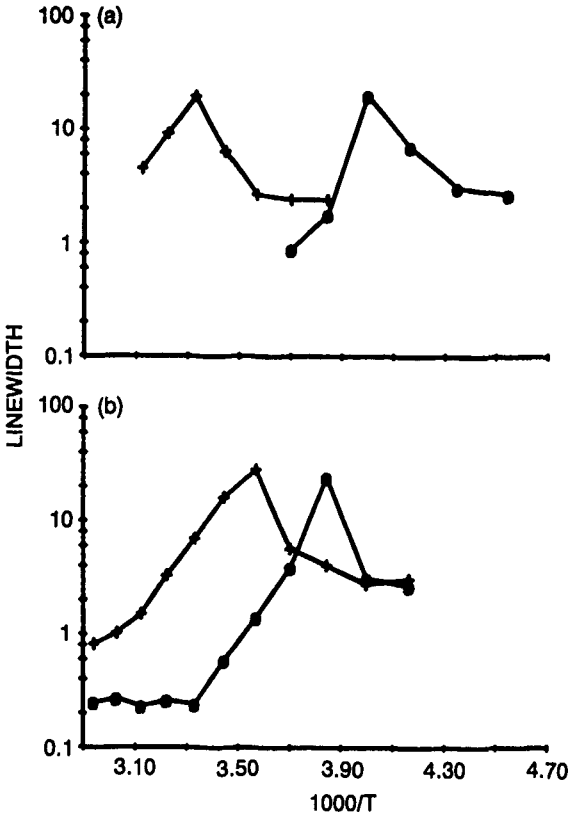

Fig. 6 — Semilogarithmic plots of linewidth as a function of inverse temperature for unsaturated PVE(+) and PIP(0) ^{13}C resonances: (a) pure PVE and PIP; (b) blend. The maximum linewidths (determined by using the first moments of the curves) for PVE and PIP occur at: (a) 302 and 250 K; (b) 288 and 266 K, respectively. From this, we conclude that the individual components in the blend exhibit distinct motional timescales in spite of the confirmed segmental contact between components.

blended. This indicates that a significant level of motional coupling between the PVE and PIP components is realized in the blend, although the two components retain their individual motional timescales to some extent. This broad temperature range at which the individual PVE and PIP components exhibit the same motional timescales, therefore, explains the atypically broad calorimetric glass transition in this polymeric blend.

Conclusions: The thermodynamic miscibility of a PVE/PIP polymeric blend was demonstrated through solid state ^{1}H NMR studies where motional coupling between the intimately mixed components results in a linewidth intermediate between the two pure components. High-resolution carbon-13 NMR studies demonstrate the broad

temperature range at which the motional timescales of the PVE and PIP components are equivalent. The latter observation explains the anomalously broad glass transition observed in calorimetry measurements on this blend.

[Sponsored by ONR]

References

1. C.M. Roland, "Rubber Mixtures," *Rubber Chemistry and Technology* **62**, 456 (1989).

2. J.B. Miller, K.J. McGrath, C.M. Roland, C.A. Trask, and A.N. Garroway, "Nuclear Magnetic Resonance Study of Polyisoprene/Poly(vinylethylene) Miscible Blends," *Macromolecules* **23**, 4543 (1990). ■

Corrosion and Preventing It—the Navy's Water Cooled VLF Transmitters: A Vital Submarine Link

A.M. Ervin, K.A.S. Hardy, and J.C. Cooper
Chemistry Division

Background: The power amplifier (PA) tubes used in most Navy very low frequency (VLF) transmitters dissipate such high power that they must be cooled by water continuously flowing at high velocities through narrow channels located at the outer surface of the anode. Although the cooling water is treated by circulation through a purification system, corrosion of the metallic copper surfaces occurs. This is evidenced by the build-up of black cupric oxide (CuO) in areas of high heat transfer to the coolant. The resulting CuO accumulates in the cooling passages and acts as a thermal insulator, reducing water flow and heat dissipation. The result can compromise the VLF communication system by premature tube failure and system shutdown.

In an effort to control corrosion, we have designed a chemical cleaning method to remove the CuO and developed a corrosion-inhibiting nitrogen purge system at the VLF transmitter site located on Oahu, Hawaii [1,2]. The combination of these two efforts has reduced chemical and electrolytic corrosion to less than one-hundredth of previous levels.

To avoid dismantling plumbing, a cleaning procedure that would not damage the system components was necessary. A solution of 1.5% citric acid, 1.75% dibasic ammonium citrate, and 1% to 2% erythorbic acid was chosen. The mixture is safe to handle and, with neutralization, is easily disposed of and environmentally innocuous. This cleaning method has been tested and validated at four different U.S. Navy VLF transmitter sites [1].

Reaction of oxygen with metal surfaces and electrolysis between dissimilar metals present in a system are the two major sources of corrosion in a closed-water cooling system [2]. Since oxygen participates in both corrosion mechanisms, reducing oxygen concentrations in the water should decrease the amount of corrosion. This may be accomplished by introducing an oxygen-free purge gas stream (such as nitrogen) into the water to displace the dissolved oxygen. The results of an experiment performed on a single VLF cooling system indicated that a continuous nitrogen purge, delivered from a regulated high-pressure tank, was successful in maintaining an oxygen-free atmosphere and reducing corrosion (Fig. 7). Following this demonstrated success, a more permanent system was designed that could deliver nitrogen gas of sufficient purity on a continuous basis economically and with operational simplicity and reliability. Recently, systems based on hollow-fiber membranes, which separate nitrogen from compressed air, have become commercially available. These membrane separators are easy to install, operate, and maintain, and they produce pure nitrogen simply and reliably for one-tenth to one-half the cost of bottled nitrogen. The membranes employ the principle of selective permeation by way of size exclusion to separate gases from a pressurized feed gas (i.e., air).

Results: The first permanent purge system was installed at the Lualualei VLF transmitter site

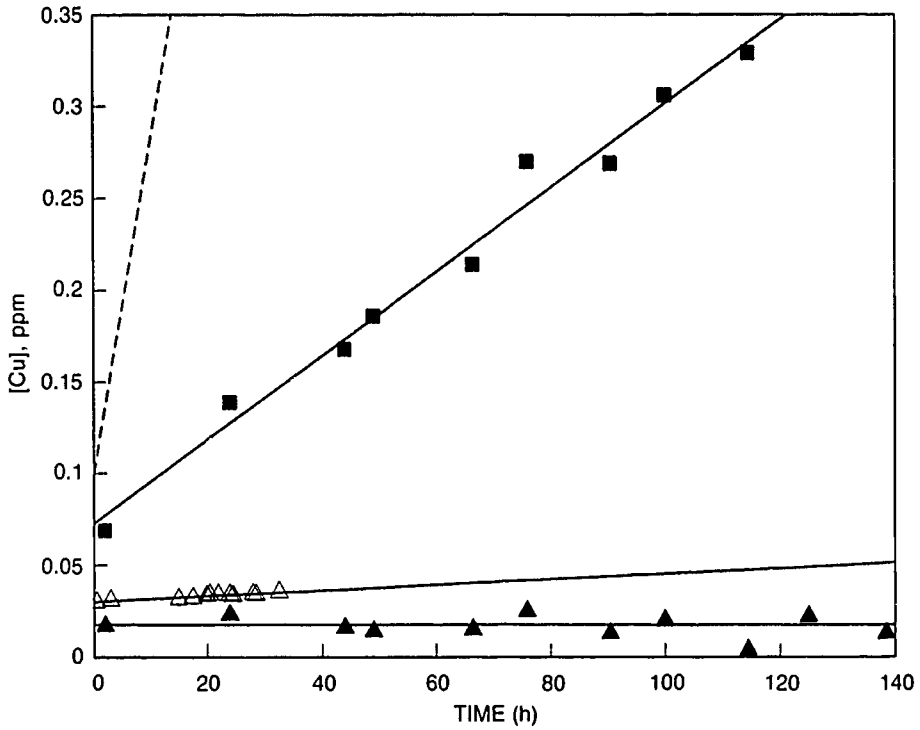

Fig 7— Corrosion in VLF water cooling systems

----- Calculated for unpurged PA, 0 018 ppm Cu/h
—■— Unpurged IPA, 0 0024 ppm Cu/h
—△— Purged PA, 0.000162 ppm Cu/h
—▲— Purged IPA, <0.00001 ppm Cu/h

on Oahu, Hawaii, in April 1989. The four cooling systems were chemically cleaned concurrently with installation and start-up of the nitrogen purge system [1,2]. Approximately one year after installation, inspection of the purge system indicated that there were no major problems and that the system continued to deliver a constant stream of nitrogen, thereby maintaining an essentially oxygen-free atmosphere in the four cooling systems. The purge system is basically maintenance-free and is easily monitored by site personnel. Water-oxygen levels in all four cooling reservoirs are kept well below ambient concentrations of 5 to 7 ppm. The rate of corrosion as determined by the amount of copper formation over time is drastically reduced in the purged systems as compared to the unpurged systems (Fig. 1). Without purging, the calculated corrosion rate in a PA system was 0.018 ppm copper produced per hour. For the smaller intermediate power amplifier (IPA) system, the unpurged corrosion rate was measured to be 0.0024 ppm copper per hour. With nitrogen purging, the corrosion rate drops to less than one-hundredth of the original value. Therefore, the developed chemical cleaning procedure and purge system proved successful in removing and reducing corrosion, and should be applicable in any closed water system under similar conditions.

[Sponsored by Naval Electronics Systems Engineering Command, Portsmouth, and SPAWARS]

References

1. NRL Letter Report 6180-104:KASH, 28 Aug 1990.

2. NRL Letter Report 6180-105:AME, 4 May 1990. ■

Electronics and Electromagnetics

ELECTRONICS AND ELECTROMAGNETICS

Electronic and electromagnetic research involves work ranging from microwave techniques, thin films, semiconductor technology, vacuum electronics, and solid-state circuitry and sensors, to radar (a major Navy sensor and detection capability) and other applications of electromagnetic radiation in the areas of countermeasures, signal simulation, and signal jamming. Reported in this chapter is work on field-effect transistors, infrared countermeasures and the spectral emission of infrared targets, microwave devices from superconducting thin films, and radar cross-section calculations.

The Radar Division, the Tactical Electronic Warfare Division, the Optical Sciences Division, and the Electronics Science and Technology Division contributed to the work presented in this section.

Other current research in electronics and electromagnetics includes:

- Vibration of surfaces
- Epitaxy of InSb
- Preparation and characterization of Mg0 thin films
- Electrical activation of silicon-implanted GaAs
- New shipboard radar display
- Radar electromagnetic interference
- Design of Doppler filters
- Real-time signal processing for radar

Calculating the Radar Cross Section from Multiple-bounce Interactions

D.A. Zolnick
Radar Division

Background: Since the radar cross section (RCS) of a ship directly affects its chance of survival in the modern combat environment, the U.S. Navy is interested in designing and building ships with greatly reduced RCS. As part of this effort, the Radar Analysis Branch in the Radar Division has developed a set of analytical computer programs, collectively called the Radar Target Signature model, or simply RTS, to model complex objects such as low observable targets and to calculate and analyze their RCS.

Computation Methods: The RTS model calculates the RCS of a physical object by using high-frequency, scattering center techniques. The fundamental assumption of these techniques is that the object can be modeled as a collection of basic geometrical shapes. The total RCS of the object is simply the coherent sum of the RCS contributions of each of the individual basic shapes plus the contributions of the interactions among the basic shapes.

The RCS contributions of the basic geometrical shapes are found by RTS by using standard approximations for calculating RCS in the high-frequency region. In particular, RTS uses scattering equations from geometrical optics (GO), physical optics (PO), the geometrical theory of diffraction (GTD), and the physical theory of diffraction (PTD) to make RCS calculations. For example, the RCS of flat polygonal plates is calculated by using PO, and the RCS of straight edges are calculated by using the PTD.

By generalizing the concepts used for calculating the RCS of corner reflectors [1], a robust method of calculating the RCS caused by multiple-bounce interactions among any number of flat polygonal plates has been developed and implemented in the RTS model by using a combination of GO and PO . More specifically, for any given sequence of N polygonal plates, the RCS contribution of the N-bounce interaction (consisting of the sequential scattering from the first plate to the Nth plate) is found by performing a GO or "minor" reflection from the first plate in the sequence; this determines the illuminated portion of the second plate in the sequence. Then performing a GO reflection from the illuminated portion of the second plate finds the illuminated portion of the third plate, and so forth until the illuminated portion of the Nth plate is determined. The illuminated portion of the Nth plate is then treated as a polygonal plate for which the RCS is calculated by using PO. By performing the calculations outlined above on every possible sequence of polygonal plates of length N or less, all the RCS contributions caused by multiple-bounce interactions among the polygonal plates up to N bounces are calculated where, in theory, the number of bounces N can be set arbitrarily large.

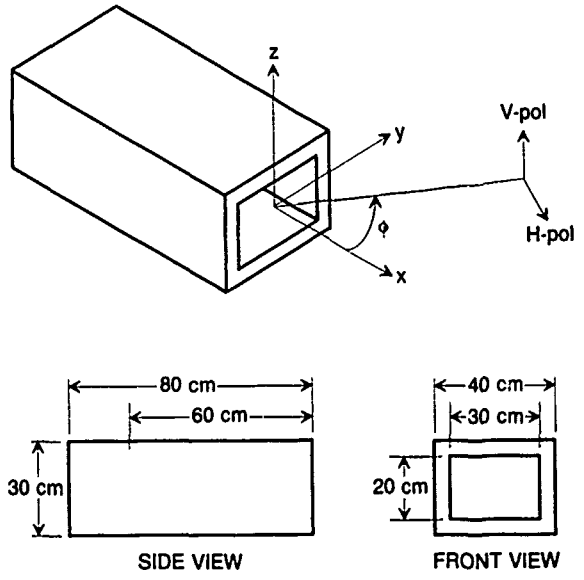

Fig. 1 — Geometry of the cavity

Comparison with Measured Data: To test the accuracy of the RCS calculations with multiple-bounce interactions, the RCS of a box with a rectangular cavity in one end (Fig. 1) was measured by using an X-band radar (wavelength 3 cm) at the indoor RCS test range of the Pacific

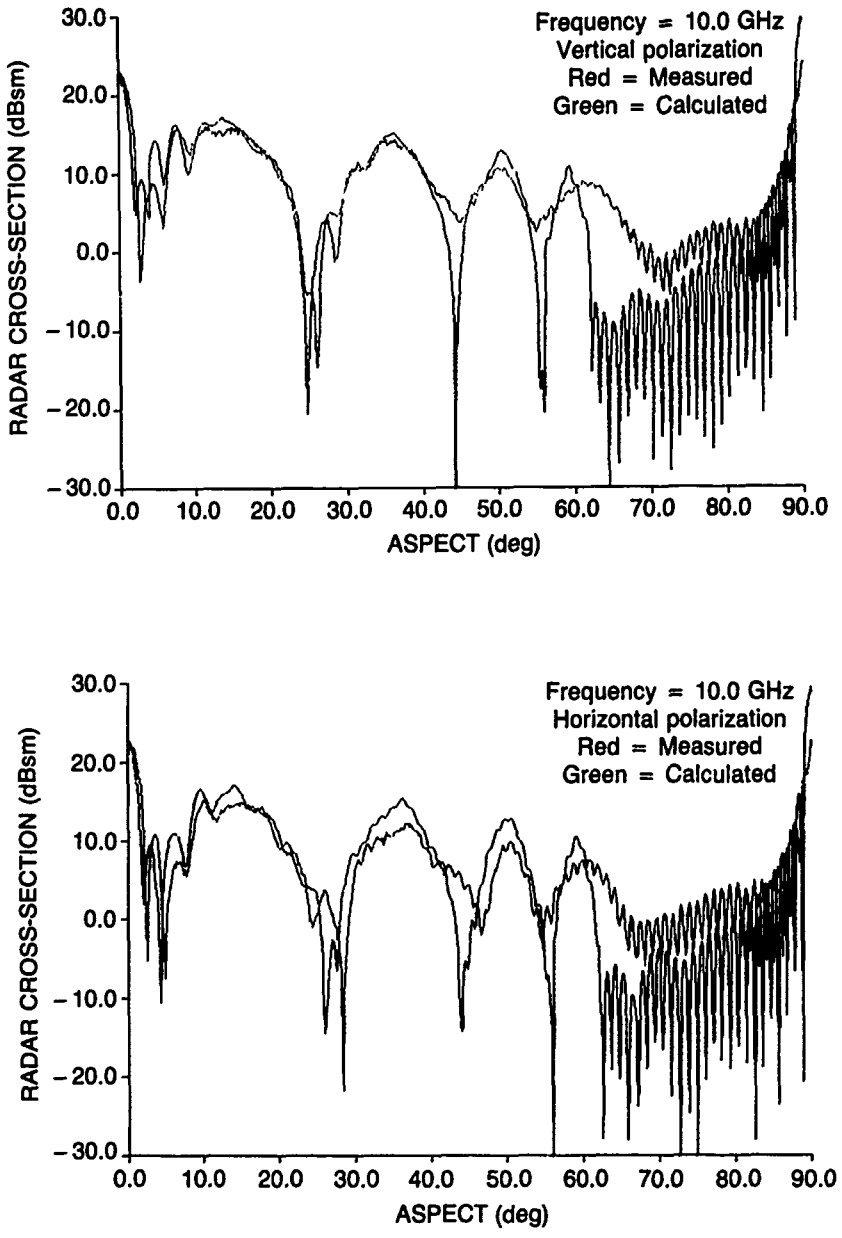

Fig. 3 — Calculated vs measured RCS of cavity at horizontal polarization

Missile Test Center. The dimensions of the cavity were specifically made many wavelengths in extent to satisfy the high-frequency assumptions underlying the RTS calculation methods. Figures 2 and 3 show the measured and calculated RCS for the cavity as a function of the aspect angle ϕ at vertical and horizontal polarization. The calculated RCS includes all the possible multiple-bounce sequences within the cavity up to 8 bounces (the number of bounces is currently limited to 8 by issues unrelated to the multiple-bounce calculation method). In the calculated RCS, the distinct broad lobes centered about $\phi \approx 15°, 37°, 50°$, and $60°$ are due to 2, 4, 6, and 8 multiple-bounce sequences involving the two side walls and the back wall of the cavity. Good overall agreement exists between the measured and calculated RCS everywhere except when ϕ is between roughly $62°$ and $82°$. These differences are due primarily to the 8-bounce limit in the multiple-bounce calculations

and should be greatly reduced when the number of bounces calculated can be increased.

Summary: The method for calculating the RCS produced by the multiple-bounce interactions among flat polygonal plates by using a combination of geometrical and physical optics has greatly improved the usefulness and accuracy of the RTS model in calculating and analyzing the RCS of complex objects of interest to the U. S. Navy.

[Sponsored by NAVSEA]

Reference

1. E.F. Knott, J.F. Shaeffer, and M.T. Tuley, *Radar Cross Section* (Artech House, Inc., Dedham, MA, 1985), Ch. 5. ■

Spectral Emission of Infrared Targets with an FT-IR Interferometer Spectrometer

J.W. Dries
Tactical Electronic Warfare Division
and
A.-T.N. Phan
Mesa, Inc.

Introduction: The Infrared/Electro-Optical (IR/EO) Simulation and Measurement Section, Advanced Techniques Branch, Tactical Electronic Warfare Division, has actively supported research and development in countermeasure programs by obtaining quantified spectral and radiometric data of countermeasure designs in static and dynamic conditions. The staff performed field measurements of many IR emitters having complex, nonblackbody emissions at NRL's Chesapeake Bay Detachment, Blossom Point, and various contractor facilities.

In the last four years, the Bomem DA2 interferometer spectrometer, a system well matched to characterize these targets, has been used extensively in field tests and has proven itself to be a reliable instrument having prompt data-reduction capability. This spectrometer system has been operated in a harsh environment with temperatures ranging from below 0°C to greater than 35°C. (Note: The computer and postsignal processing units are kept in a controlled environment, e.g., an IR van). Figure 4 shows the system, which consists of an optical sensor unit, a control unit, a multitasked host computer, a high-speed vector processor, a system terminal, and a graphics plotter. In addition, different fore-optics, beamsplitters, and detectors are available to provide users with various fields-of-view (3, 12, and 48 mrads), spectral coverage (2 to 14 μm), and spectral resolutions (0.026 to 64 cm^{-1}).

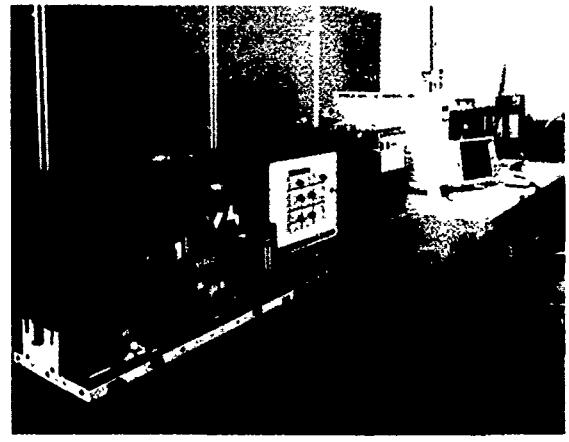

Fig. 4 — The Bomem FTIR Model DA2 interferometer spectrometer system

Calibration: To optimize the spectrometer's response and to account for any variations in the field environment, the system is calibrated daily. Since the data of interest generally consist of the spectral radiant intensity (in units of $W/sr/cm^{-1}$) of the target's emission, the instrumentation is often configured so that the target is completely within the spectrometer's field-of-view. The raw signal, in effect, is a measure of the target's spectral irradiance (in units of $W/cm^2/cm^{-1}$). The spectral irradiance calibration procedure is described as follows.

The calibration is best done by using a collimator to align the spectrometer to a blackbody source. In the field, however, a collimator may not

be available; therefore, the distance between the spectrometer and the blackbody source has to be at least equivalent to the spectrometer's hyperfocal distance so that the target is in focus and the calibration is still valid for a distant target. Two spectra, one of a 1000°C blackbody and the other of ambient temperature, are collected. The difference between these spectra gives the actual irradiance spectrum emitted by the blackbody itself. This resultant spectrum is then divided by its theoretical irradiance spectrum to generate a spectral irradiance instrument response function (IRF). The calibration can be verified in the following manner: (1) obtain another irradiance spectrum of different temperature and aperture; (2) correct this spectrum with the IRF; (3) multiply by square of distance to transform it to its equivalent radiant intensity spectrum; (4) integrate the result in selected bands; and (5) compare the resultant integrated values to the corresponding theoretical integrated values. Generally, the calibration is considered to be acceptable when the measured and theoretical values agree within ±5%. Figure 5 shows a comparison of the measured (after correction) and corresponding theoretical blackbody radiation at 799°C; Fig. 6 shows a sample of a hot mercury lamp radiation. Note that a slight modification of this procedure can be used to generate a spectral radiance calibration (in units of $W/cm^2/sr/cm^{-1}$) for targets with large spatial extent.

Data Measurements: The data reduction procedures for the measurement of targets under investigation are similar to the calibration verification process discussed earlier. The difference is that the radiant intensity measured is further corrected for atmospheric effects by using the atmospheric transmission model LOWTRAN 7, because the measurement is usually taken at a range that introduces some atmospheric loss. Furthermore, because of the experimental nature of the targets, no comparison to the theoretical can be made.

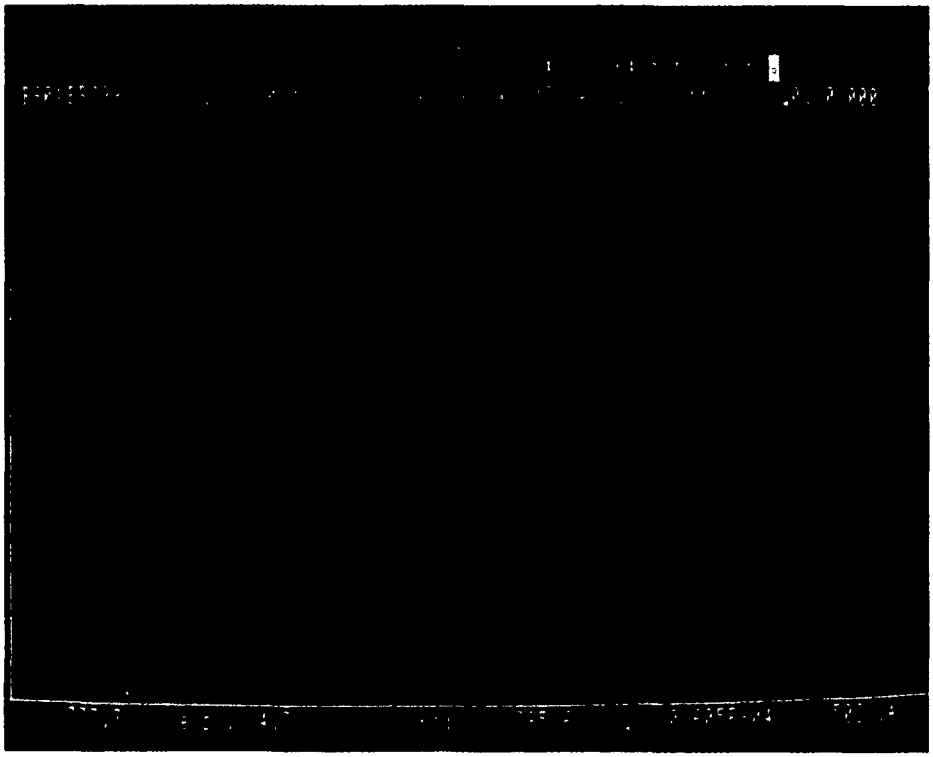

Fig. 5 — Comparison of a measured 799°C blackbody radiation and its corresponding theoretical blackbody

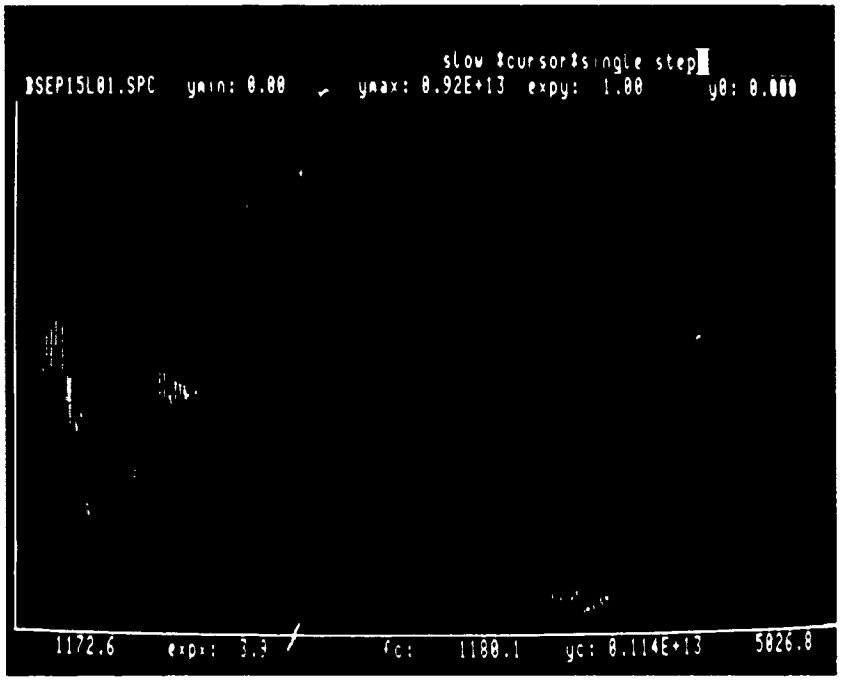

Fig. 6 — Spectrum of a hot mercury lamp's radiation

In a field measurement, the spectrometer's sensor unit is mounted on a tripod or optical tracking mount, together with a circular variable filter radiometer, a TV camera, and thermal imagers. These instruments are carefully boresighted with an IR source at a distance comparable to that expected from the target. This is done to facilitate the tracking task and to optimize the correlation among data collected by each instrument. An eye-safe laser rangefinder is also used to accurately measure the range to the target.

Field measurements by using this instrument have enabled NRL to confidently characterize IR emitters having complex, nonblackbody spectra in realistic operational environments.

[Sponsored by NAVSEA and NAVAIR] ■

Infrared Countermeasures for Naval Aircraft

M.R. Pauli and M.R. Kruer
Optical Sciences Division

Introduction: Over 90% of aircraft losses in hostile action since 1975 have been due to infrared guided missiles. There are over 100,000 of these missiles proliferated throughout the world, varying from small, shoulder-launched, surface-to-air missiles (SAM's) (such as Stinger) to high-performance, air-to-air missiles (such as Sidewinder). The survivability of military aircraft in hostile environments depends critically on the ability to defeat these infrared-guided threats. The Balanced Technology Initiative-Infrared Countermeasure (BTI-IRCM) Program is a broad-based, multiservice program to develop and demonstrate the capability of countering advanced infrared guided-missile threats to both fixed-wing and rotary-wing aircraft. Current IRCM systems rely on the ejection of expendables (cued either by visual observation or by a threat-warning system) or on the use of incoherent, nondirectional lamp jammers. While these systems can protect some aircraft against first generation missiles, they are ineffective against advanced missile threats. Problems with the current IRCM system include the lack of sufficient energy from incoherent lamps, limited stores of expendables, and the inability to handle the recent and projected advanced infrared-guided missiles with the

capability to reject simple IRCM. The BTI-IRCM Program is designed to remedy these shortfalls in the current IRCM approaches. NRL will be the lead agency in this program because of its expertise in infrared physics, lasers, optics, parallel computation, and countermeasure techniques.

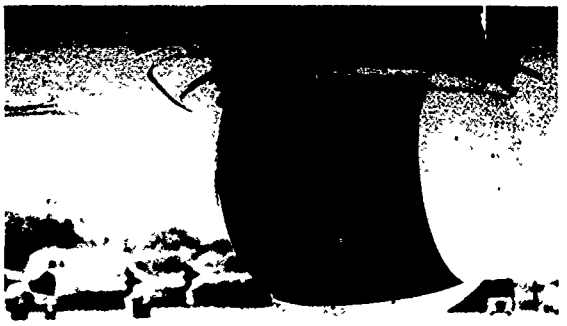

Fig. 7 — Fly's Eye threat-warning system mounted under NRL's P-3 airplane

Program Plans: The BTI-IRCM Program will demonstrate an integrated laser countermeasure system for fixed-wing aircraft in 1993. This demonstration involves the successful integration of a sophisticated threat warning receiver (capable of performing during tactical airplane maneuvers) with a closed-loop, fine tracking and pointing subsystem capable of directing a countermeasure laser beam with small divergence. The threat-warning system consists of an infrared staring sensor built by the Rockwell Missile Systems Division and a compact, flightworthy, real-time image processor. This is an extension of the effort done with the NRL's Fly's Eye threat-warning program (Fig. 7), which successfully measured supersonic missiles on near-intercept trajectories at China Lake, California, in 1989. The threat-warning sensor will cue a pointer-tracker subsystem that uses a modified AN/AAQ-14 LANTIRN targeting pod design (Fig. 8) to be provided by Martin Marietta Electronics Systems in April 1992. The countermeasure laser will be lightweight, will operate in a primary missile-seeker band, and will

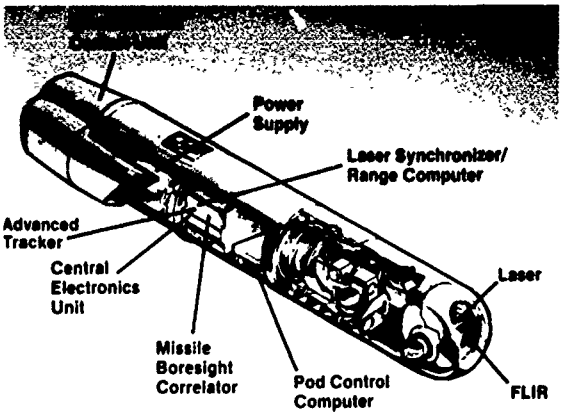

Fig. 8 — LANTIRN AN/AAQ-14 targeting pod

be capable of damaging missile seekers. NRL's Laser Physics Branch is investigating a solid-state laser approach for the countermeasure laser, which is scheduled for delivery in late 1992.

NRL's Patuxent River Flight Support Detachment will support many of the airborne experiments that involve use of the P-3 airplane. After demonstrating the capability of the system against controlled targets from the P-3, the BTI-IRCM equipment is scheduled to be flown on a droned QFR-N against live missile firings at the Naval Weapons Center, China Lake. NRL will direct and analyze these field experiments and system demonstrations.

[Sponsored by ONT] ■

High-Temperature Superconductor Microwave Devices

H.S. Newman and J.M. Pond
Electronics Science and Technology Division

Among the many possible applications of high-temperature superconductors (HTS), those that exploit the greatly reduced microwave losses of superconductors will probably be the first to be transitioned from the laboratory to practical systems. HTS thin-film passive microwave circuits will allow miniaturization of components and will give superior performance to that which can be obtainable by using conventional

conductors. Many electronic components and subsystems (e.g., satellite communication systems) will realize a substantial increase in performance through the integration of HTS thin-film microwave circuits.

Superconducting Thin Films: For microwave applications, a thin-film HTS device must have a very low surface resistance R_s, thus giving rise to the desirable properties of a high quality factor Q and a low insertion loss. In Fig. 9, we plot the measured R_s vs temperature at 36 GHz for a 500 nm-thick film of $Y_1Ba_2Cu_3O_{7-\delta}$ (YBCO) as deposited by NRL's Condensed Matter and Radiation Sciences Division on a magnesium oxide (MgO) substrate and compare it to R_s of copper. The steep transition of R_s near the critical temperature (89 K) and the low R_s below 77 K (the temperature of liquid nitrogen) is typical for high-quality superconductors. The superior performance of this HTS film compared to copper is realized near 83 K, and by 77 K, the loss in the film drops to 1/4 that of copper. Since R_s scales with the square of the frequency for HTS compared to the square root of frequency for normal metals, devices made from these HTS films operating at X band (around 9 GHz) and 77 K can have approximately 32 times less loss than similar copper devices.

Superconducting Devices: YBCO films were deposited by NRL's Condensed Matter and Radiation Sciences and Optical Sciences Divisions on 16 mm × 16 mm × 254 μm MgO substrates and 16 mm × 16 mm × 1.27 mm lanthanum aluminate ($LaAlO_3$) substrates. Microstrip devices were fabricated by using standard, wet-chemistry photolithography, with either HTS or normal metal ground planes. The devices were mounted in space-qualified test fixtures and their microwave performance was measured from 20 to 100 K.

Figure 9 shows the unloaded Q as a function of temperature for several weakly coupled microstrip ring resonators as well as the theoretical Q for an all-copper ring resonator. The Q of a resonator fabricated from a YBCO ring and a copper ground plane on an MgO substrate is about ten times larger than the calculated Q of the

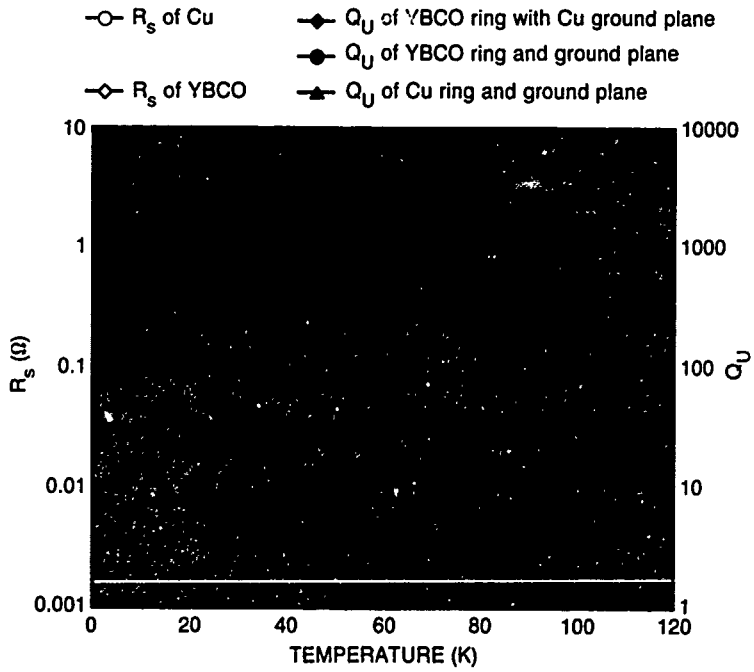

Fig. 9 — The R_s of a YBCO film is compared to the R_s of copper at 36 GHz as a function of temperature. Also shown are the unloaded Qs of several ring resonators demonstrating the performance advantages of HTS films for both the ring pattern and the ground plane.

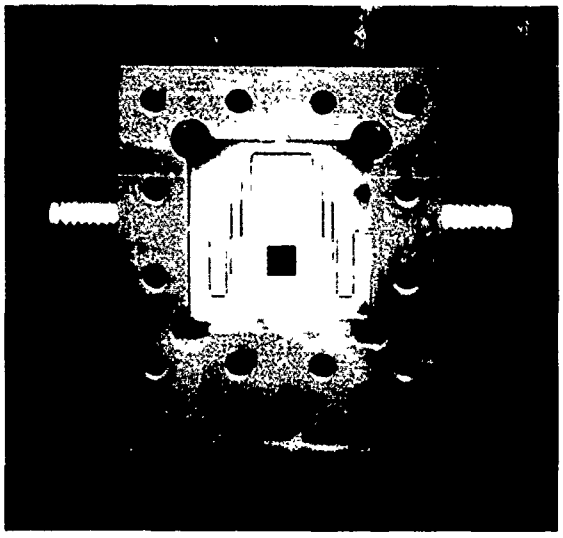

Fig. 10 — Five-pole, parallel-coupled line filter mounted in a space-qualified package

all-copper resonator. At low temperatures, the Q of the HTS device is limited by the losses in the copper ground plane. Also shown is the Q of a resonator consisting of a YBCO ring and a YBCO ground plane on a $LaAlO_3$ substrate. Even though the Q at 77 K is lower than the Q of the YBCO ring on MgO caused by a broader transition of R_s, the higher Q at lower temperatures indicates the desirable properties of an HTS ground plane.

In Fig. 10, we show a five-pole, parallel-coupled line filter implemented in microstrip and mounted in a space-qualified package. The design is based on a classic Chebyschev filter with an additional half-wavelength section inserted in the middle of the circuit to fit the pattern within the MgO substrate. In Fig. 11, the measured transmission coefficient of this HTS filter is plotted vs frequency and compared to the same design made by using gold metallization on an alumina substrate. The greatly improved performance of the HTS filter over the normal metal filter is evidenced by an insertion loss of only 0.8 dB compared to 3 dB for the gold filter. In addition, the narrow skirts and the flat frequency response are indications of good transitions from the HTS circuit to the coaxial cables.

Summary: NRL has demonstrated the ability to fabricate thin-film HTS microwave devices that exhibit performance greatly superior to their normal metal counterparts. The prototype devices are a weakly-coupled ring resonator and a

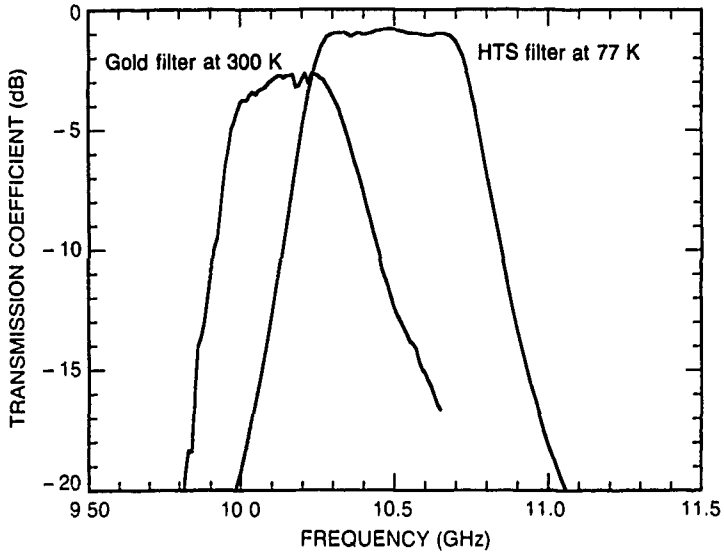

Fig. 11 — The measured transmission coefficient of a YBCO five-pole, parallel-coupled line filter at 77 K is compared to the performance of the same design by using a gold metallization measured at 300 K. The peak insertion loss is only 0.8 dB for the YBCO circuit.

five-pole modified Chebyschev filter. Both of the devices were fabricated from films deposited at NRL on MgO and $LaAlO_3$ substrates. Microwave performance significantly better than that obtained by the use of normal metals is realized above 77 K.

[Sponsored by SPAWARS] ■

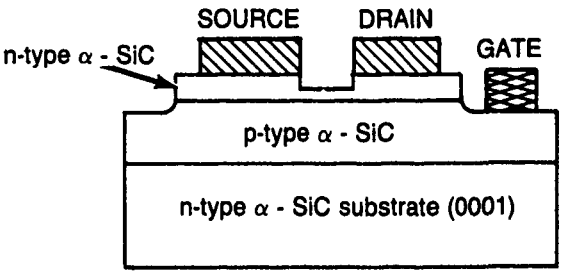

Fig. 12 — Cross-section of the α-Sic buried-gate JFET

α-SiC Buried-Gate Junction Field Effect Transistors

G. Kelner and S. Binari
Electronics Science and Technology Division

The development of SiC semiconducting devices has been a goal of a number of research investigations because of SiC's unique material properties. Also, SiC should prove to be useful in electronic devices operating at high temperature because of its wide bandgap. SiC has a high saturation electron drift velocity of 2×10^7 cm/s, a high breakdown field of 5×10^6 V/cm, and a high thermal conductivity of 3.5 W/cm-°C, which make this material useful for high-power and for high-frequency devices. These properties, combined with thermal stability and chemical inertness, make SiC very promising for electronic device operation in severe environmental conditions. Possible Navy applications areas are the high-temperature or high-radiation environments of aircraft engines, nuclear reactors, and space satellites. Here we report on the fabrication and characterization of an α-SiC buried-gate junction field effect transistor (JFET).

Device Structure and Fabrication: Figure 12 shows the cross-sectional drawing of the α-SiC buried-gate JFET. The current in the channel is modulated by using a p-type α-SiC epitaxial layer as a gate. The SiC material consists of a 1-μm thick N_2-doped n-type α-SiC layer grown on top of an Al-doped p-type α-SiC layer. The α-SiC films were grown on an n-type α-SiC substrate. Devices were fabricated with gate widths of 240 and 185 μm and source-to-drain spacings in the range from 4 to 40 μm. Electrical isolation of the channel was accomplished by using $CF_4 + O_2$ reactive ion etching. The source and drain contacts to the n-type channel were electron-beam-evaporated Ni. A thermally evaporated Al contact was used to contact the p-type gate. The channel between the source and the drain contacts was etched by using $CF_4 + O_2$ reactive ion etching, and the final thickness of the channel was 0.3-μm.

Device Characterization: The measured Hall mobility of the n-type channel was 240 cm^2/V — s, and the carrier concentration of the channel was found to be 5×10^{17} cm^{-3}. The breakdown voltage of the p—n junction is higher than —100 V. Figure 13 shows the current-voltage characteristics of the α-SiC buried-gate JFET with 4-μm gate length at room temperature. The gate voltage varies from 0 to —40 V in 5 V steps. The device displays good saturation and is completely pinched off at the gate voltage of —40 V. The maximum measured transconductance of this device in the saturation region is 17 mS/mm, which is considerably higher than previously reported for devices of similar structure [1]. We also measured the device characteristics over a wide temperature range. The data in Fig. 14 were taken for the device with 39-μm gate length at temperatures of 24°, 270° and 400°C. Device transconductance drops with the temperature increase because of the decrease in the electron mobility. The temperature dependences of the electron mobility deduced from the measured values of the device transconductance and drain conductance are in agreement with temperature-

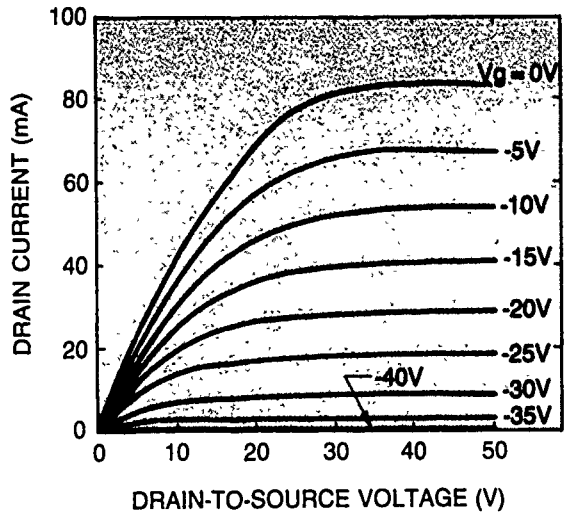

Fig. 13 — Room temperature drain current vs drain voltage (I_d — V_d) characteristics of the burried-gate JFET with 4-μm gate length

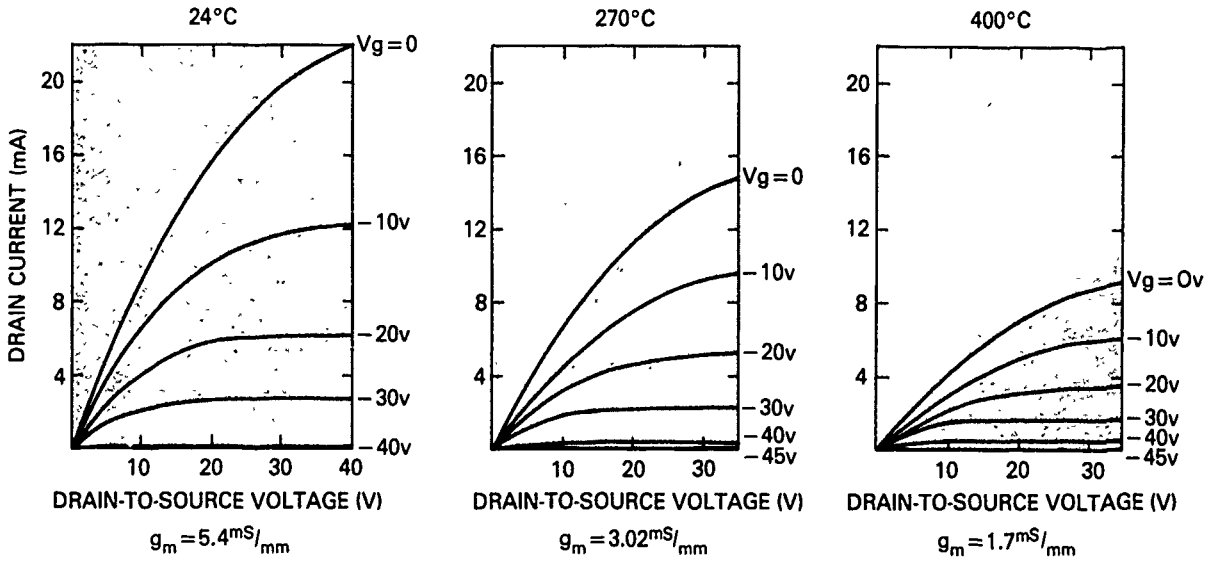

Fig. 14 — Current-voltage characteristics of the burried-gate JFET with 39-μm gate length measured at elevated temperature

dependent Hall mobilities measured in an independent study [2].

Conclusion: Our study demonstrates that α-SiC JFETs can be fabricated with high transconductance, excellent saturation, complete pinch-off, and reverse p—n junction breakdown voltage above 100 V.

[Sponsored by ONR]

References

1. V.A. Dmitriev, P.A. Ivanov, N.D. Ilinskaya, A.L. Sirkin, B.V. Tsarenkov, A.E. Chelnokov, and A.E. Cherenkov, "High Temperature SiC-6H Field-Effect Transistor with p—n Gate," *Sov. Tech. Phys. Lett.* **14** (2) 127-128 (1988).
2. T. Tachibana, H.S. Kong, and R.F. Davis, "Hall Measurements as a Function of Temperature on Monocrystalline SiC Thin Films," *J. Appl. Phys.* **67** (10) 6375-6381 (1990). ■

Energetic Particles, Plasmas, and Beams

ENERGETIC PARTICLES, PLASMAS, AND BEAMS

Development of energetic beam sources with high-energy output continues at NRL. Research is performed in the areas of plasma, lasers, and advanced beam technology and the way such energetic beams interact with matter. Reported in this chapter is work on laser-produced plasmas and NRL's dense Z-pinch program.

The Plasma Physics Division performed the work described here.

Other current research on energetic particles includes:

- Synchrotron radiation excited photoemission spectroscopy
- Few-body atomic and molecular wave functions
- Soft X-ray reflection and transmission spectra of diamond
- Radiation hydrodynamics of puff plasma
- Ionospheric plasma
- Betatron accelator development

Laser-Produced, Strongly Coupled Plasmas

A.N. Mostovych and K.J. Kearney
Plasma Physics Division

The state of matter in stellar interiors and in white dwarfs, in large planets such as Jupiter, in highly shocked or compressed materials, or in the electrons on the surface of liquid helium are examples of strongly coupled plasmas (SCPs). The understanding of SCPs has great promise for astrophysics, inertial fusion, and military applications where ultrahigh density plasmas are produced. The goal of the SCP program at NRL is to produce and study SCPs under controlled laboratory conditions.

SCPs are characterized by ion-ion or electron-electron interaction energies much larger than the thermal energy and occur at very high densities and low temperatures. In contrast, classical or ideal gas plasmas (such as the ones found in our ionosphere, in Tokamak reactors, or in neon sign discharges) occur at low densities and are characterized by interparticle interaction energies much smaller than the average thermal energy. Classical plasma theory is based on the assumption that direct particle interactions or collisions are relatively unimportant. Since in SCPs the opposite is true, it is expected that SCPs will exhibit different behavior in such basic properties as interparticle correlations, absorption and scattering of radiation, transport coefficients, atomic physics, and fusion reaction rates. SCPs have been the subject of many theoretical and numerical investigations; however, the physical conditions under which they occur are difficult to produce and study in the laboratory. As a result, little is known about them experimentally.

Laboratory SCPs: The main challenge in studying SCPs in the laboratory occurs because a plasma that is sufficiently dense and cold for strong coupling is also too transient, opaque, or non-uniform for good diagnositics or measurements of its properties. We have developed new plasma experiments where optically transparent, strongly coupled plasmas are produced under controlled conditions. Our method is based on the idea that since an SCP has very short, mean-free paths for interactions between particles, a very small volume of plasma can be sufficiently thick to have a well-defined bulk equilibrium while thin enough to be optically transparent.

A laser-produced plasma is used as a source for these experiments (Fig. 1). A glass substrate is coated with an aluminum film, and an ultrasmooth [1] laser beam ($I \approx 10^{11}$w/cm^2) vaporizes this film by irradiation through the glass. This produces a highly supersonic metallic vapor with densities up to solid density. As the vapor expands away from the glass, a thin slit shapes the transverse dimension of the vapor into a thin slab, which is optically transparent. After the vapor slab has reached the appropriate expansion length (500 to 100 μm at 50 to 80 ns) and the desired vapor density, a second laser is used to heat and ionize the Al vapor. The heating occurs over a time of 8 to 10 ns and produces a fully ionized, optically transparent, strongly coupled plasma [2].

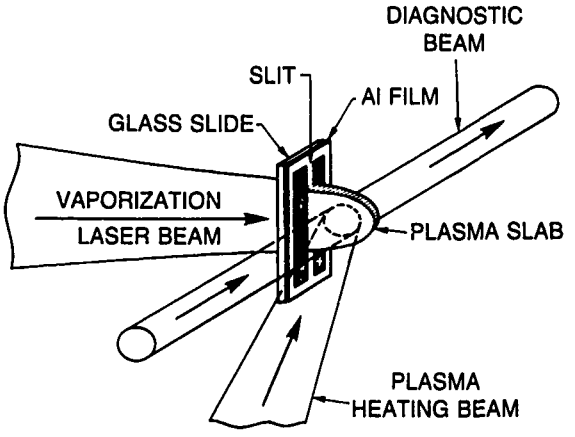

Fig. 1 — Technique used to produce optically transparent SCPs

A third laser beam, as well as various spectroscopic and optical instruments, are used to diagnose our plasmas. Figure 2 shows a sample interferogram of the plasma taken with a mode-locked (300 to 500 ps) glass laser. The plasmas have electron densities and temperatures

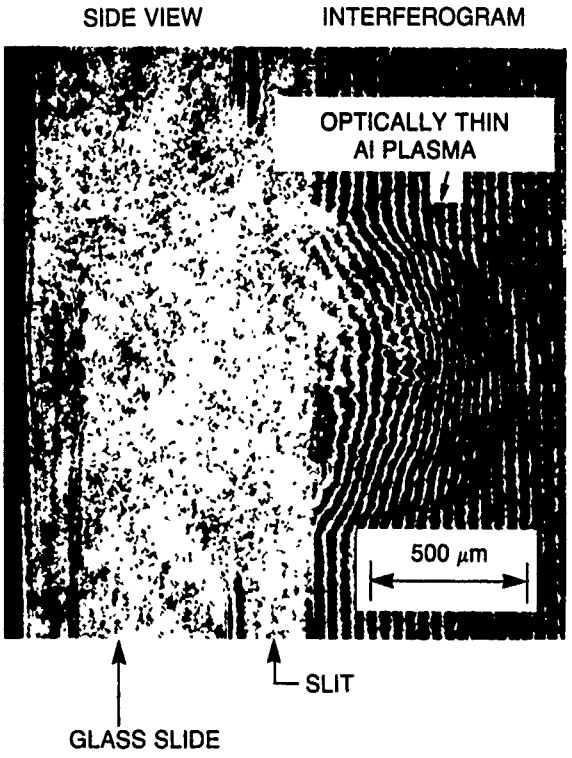

Fig. 2 — Typical plasma after laser heating

of 10^{20} cm^{-3} and 2 to 6 eV. They are strongly coupled because the thermal and interparticle interaction energies are about equal for these temperatures and densities.

Plasma Opacity: The absorption of light by SCPs is an important problem for radiation transport in astrophysical situations and the interaction of moderate-intensity laser beams with solid targets. We have made the first measurement in the visible wavelength range of plasma opacity for an SCP. We find that extrapolations of standard weakly coupled plasma theory underestimate plasma absorption by factors of two or larger, whereas calculations based on strongly coupled theory are found to agree with our measurements.

For our conditions, the plasma absorption at the 0.5 μm wavelength of our laser probe is predominantly because of inverse bremsstrahlung—the absorption of light by free electrons that are accelerated by the light wave and dissipate the wave energy through collisions with ions in the plasma. The details of the momentum transfer in Coulomb collisions between ions and electrons determine the differences in inverse bremsstrahlung absorption between weakly and strongly coupled plasmas. In particular, the electrons see ions that are not independent but are coupled with each other. This difference is contained in the Coulomb logarithm Ln(Λ); the coefficient for inverse bremsstrahlung absorption is directly proportional to this quantity. In Fig. 3, experimental measurements of the Coulomb logarithm are plotted as a function of temperature for constant initial aluminum vapor density. The data are compared to SCP and classical weakly coupled theory. The dashed curve below the data is an extrapolation of the classical (weakly coupled) theory of Dawson and Oberman [3]. This calculation underestimates the absorption by over a factor of two and is undefined for temperatures below 4 eV. On the other hand, for temperatures above 2 eV, SCP calculations of Cauble and Rozmus [4] and Ichimaru and Tanaka [5] (shown

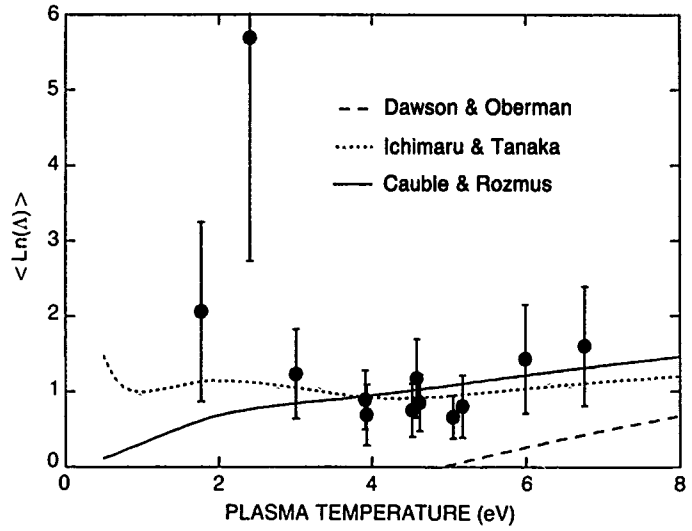

Fig. 3 — Experimental values for average Coulomb logarithm as a function of temperature for a constant initial vapor density. SCP theories agree with the data for temperatures above 2 eV, whereas predictions based on classical (weakly coupled) theory underestimate the absorption by a factor of two or more.

as solid and dotted lines) are in good agreement with the data. The residual disagreement at low temperatures is believed to be due to increased atomic absorption processes at these low temperatures

Summary: We have produced the first optically transparent, strongly coupled plasmas by laser vaporization and heating of aluminum metal-film targets. The data show that the classical Coulomb logarithm that is commonly but incorrectly used for inverse bremsstrahlung calculations is invalid for a strongly coupled plasma.

[Sponsored by ONR]

References

1. Ultrasmooth laser beams are produced by using Induced Spatial Incoherence (ISI), a beam smoothing technique invented in the Laser Plasma Branch at NRL; R.H. Lehmberg and S.P. Obenschain, "Use of Induced Spatial Incoherence for Uniform Illumination of Laser Fusion Targets," *Opt. Commun.* **46**, 27 (1983).

2. A.N. Mostovych, K.J. Kearney, and J.A. Stamper, "Laser Produced Optically Thin Strongly Coupled Plasmas," in *Strongly Coupled Plasma Physics*, S. Ichimaru, ed., (Elsevier Science Publishers, 1990), pp. 589-600; and A.N. Mostovych, J.J. Kearney, J.A. Stamper, and A.J. Schmitt, "Measurement of Plasma Opacity from Laser Produced Optically Thin Strongly Coupled Plasmas," submitted to *Phys. Rev. Lett.*

3. J. Dawson and C. Oberman, "High-Frequency Conductivity and the Emission and Absorption Coefficients of a Fully Ionized Plasma," *Phys. Fluids* **5**, 517 (1962).

4. R. Cauble and W. Rozmus, "The Inverse Bremsstrahlung Absorption Coefficient in Collisional Plasmas," *Phys. Fluids* **28**, 3387 (1985).

5. S. Ichimaru and S. Tanaka, "Theory of Interparticle Correlations in Dense, High-Temperature Plasmas. V. Electric and Thermal Conductivities," *Phys. Rev.* **A32**, 1790 (1985). ■

The Dense Z-Pinch: A Possible Shortcut to Fusion Power

J.D. Sethian, A.E. Robson, and K.A. Gerber
Plasma Physics Division

Introduction: As the Navy and the United States enter the 21st century, the need for a clean and plentiful energy source becomes more acute. One possible source is controlled thermonuclear fusion, a nuclear reaction in which deuterium and tritium nuclei are brought together under conditions of extreme pressure and temperature to produce helium, neutrons, and a large amount of energy. The promise of fusion is tantalizing. The fuel supply would be essentially limitless (deuterium comes from sea water, and tritium can be bred by stopping the fusion neutrons in a blanket of lithium, an abundant element). There would be no chemical pollutants, and the relatively short-lived radioactive wastes could readily be controlled. Despite these promises, the quest for fusion has proven to be difficult, and a system that produces net power has yet to be realized in the laboratory. While the main worldwide fusion research has concentrated on large and complex systems that will require decades to develop, NRL is pursuing an alternative course that could produce a compact and relatively simple fusion power source in a much shorter time.

The Dense Z-Pinch: Figure 4 shows the basis of our approach—the simple, linear z-pinch. An intense current driven through a linear plasma column plays both of the required roles in the fusion process. It heats the plasma through ohmic dissipation, and it confines it by producing an azimuthal magnetic field. The z-pinch is not a new idea; in fact, it was one of the earliest fusion concepts to be tried. However, those early pinches attempted to achieve the high densities required for fusion by imploding low density plasmas with low voltage technology; this led to magnetohydrodynamic (MHD) instabilities that destroyed the pinch. As these results were consistent with the simple MHD theories of the day, the pinch was soon abandoned in favor of more complex schemes.

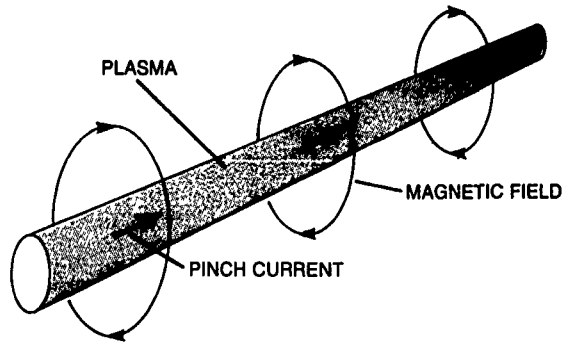

Fig. 4 — The dense z-pinch

Our z-pinch experiment incorporates two significant changes. The pinch is initiated at the required high density by forming it from a thin (0.01-cm diameter) fiber of frozen deuterium (Fig.5), and the current is driven at a rapidly rising rate by using modern, high-voltage (300 to 500 kV) technology. The effect of this rapidly rising current is to quickly ionize the deuterium fiber into a plasma, heat it to over 10^6 K, and confine it to a sub-mm radius. The azimuthal magnetic field can exceed 100 T, which is much greater than can be achieved with external coils. This allows containment of a very high density plasma (typically on the order of 10^{21} cm^3).

Fig. 5 — A 125 μm (.0125 cm) diameter frozen deuterium fiber. The fiber is formed by cooling deuterium to 11 K and extruding it through a small orifice.

We have obtained very encouraging results with z-pinches formed in this manner. The pinch was observed to be stable as long as the current was rising [1], which was over 100 times longer than could be prediced by the simple MHD models. These observations prompted considerable theoretical activity at NRL, Imperial College (UK), and the Los Alamos National Laboratory (LANL), and it has now been shown that stable regimes exist for a z-pinch if the ideal MHD equations are modified to include resistivity and viscosity [2].

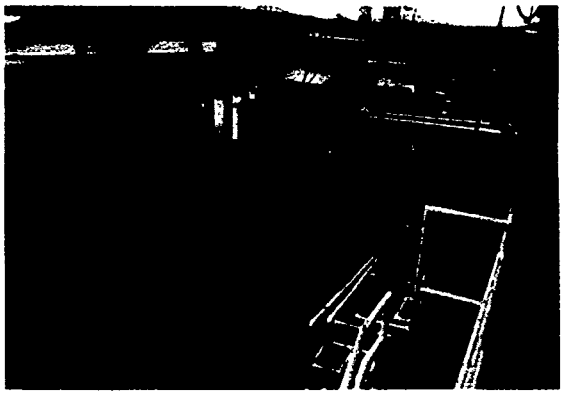

Fig. 6 — The NRL ZFX generator. Each of the large white and black boxes contains a 750 kV, .550 μF water capacitor that is discharged into the pinch. The pinch is located on the platform between the two boxes.

In those first experiments, the pinch was stable as the current rose at a rate of $dI/dt = 4.5 \times 10^{12}$ A/s to a maximum value of 640 kA in 130 ns. We show that if this stability is maintained at currents up to 1.6 Ma, the pinch would produce more energy than it consumed. To reach higher currents, we designed and constructed the ZFX generator shown in Fig. 6. In preliminary experiments with the current and rise time increased to 920 kA and 840 ns, respectively, but the current rate of rise reduced to 1.5×10^{12} A/s, we find the pinch is stable for the first 250 to 400 ns, just as in the previous experiment, but it then shows signs of an instability. This instability is more benign than most in that it does not disrupt the pinch until after peak current. Nevertheless, for a fusion system, it would be more efficient if the pinch were stable for the entire current rise. We believe the reason this is not happening now is because of the lower dI/dt.

Summary: Our goal is to increase dI/dt to the previous levels in an effort to maintain pinch stability all the way to peak current. The longer pulse length of the ZFX generator should then cause the current to exceed the 1.6 MA required for a net energy release. If these experiments are successful, we would envisage that a z-pinch reactor would be based on a repetitively based system not much larger than ZFX capable of providing a compact power source for the Navy as well as for commercial systems.

Acknowledgments: Theoretical support was provided by the NRL Radiation Hydrodynamics Branch and Imperial College, London. Similar experimental studies have been conducted at Imperial College and the Los Alamos National Laboratory.

[Sponsored by ONR and DoE]

References

1. J.D. Sethian, A.E. Robson, K.A. Gerber, and A.W. DeSilva, "Enhanced Stability and Neutron Production in a Dense Z-Pinch Plasma Formed from a Frozen Deuterium Fiber," *Phys. Rev. Lett.* **59**, 892 (1987); ibid 1790.

2. F.L. Cochran and A.E. Robson, "Stability of a Z-Pinch with Rising Current," *Phys. Fluids* **B2**, 123 (1990). ■

Information Technology and Communication

INFORMATION TECHNOLOGY AND COMMUNICATION

Secure communications for use in transmitting critical battle information and its subsequent rapid processing constitutes an important aspect of battle management. Research in this area is conducted on artificial intelligence, information security, and the complex interactions between people and computers. Reported in this chapter is work on neural network research, active learning and bias adjustment, and chaotic systems.

The Radar Division, the Materials Science and Technology Division, and the Information Technology Division contributed to the work presented here.

Other current research on information technology and communications includes:

- Identification friend/foe system
- Network technology
- Decision support methodologies
- Supervised concept learning
- Learning reactive plans

A Neural Net Classified for Similar Objects

A. Schultz
Radar Division

Pattern classification problems that are of practical importance will in many cases deal with objects that are very similar, and it can then be expected that there will be a significant overlap in the associated pattern vectors. For military applications, a typical example might be recognition of a particular ship class from an infrared or radar image. A similar situation will often occur if the objects are tanks or aircraft. For nonmilitary applications in areas of medicine and remote sensing, examples of this type are also typical. What is common to all of these problems is that only a few features in the pattern vector are critical for object recognition. The remaining features not only do not contribute toward recognition, they will in many cases hinder recognition caused by the presence of measurement noise. Effective pattern classification for problems of these types requires a neural net architecture that can focus on the significant differences between pattern classes and tune out the extraneous constant part. From an implementation standpoint, it is more efficient to have these desired features built into the neural net as opposed to a front-end processor.

The Weight Decay Term: The standard learning law for back propagation [1] is modified to include an additional weight decay term that can force certain weights to decay to zero. Assume that there are M objects to be classified and that there is at least one pattern vector from each class. Suppose that N pattern vectors are presented to the neural net in sequence, one from each of the M classes. If the jth component of these vectors is constant over all the pattern vectors except for an additive noise term, then this component contributes nothing to the classification. One would want the weights of all units in the hidden layer connected to the jth input to decay to zero in the learning phase. If the value on the input unit j is observed to change significantly as the pattern vectors are presented, then this component is useful for classification and one would want the normal back-propagation learning algorithm to operate. Reference 2 shows that the behavior can be realized by letting the coefficient of the weight-decay term be a monotone decreasing of the observed variation on each input unit.

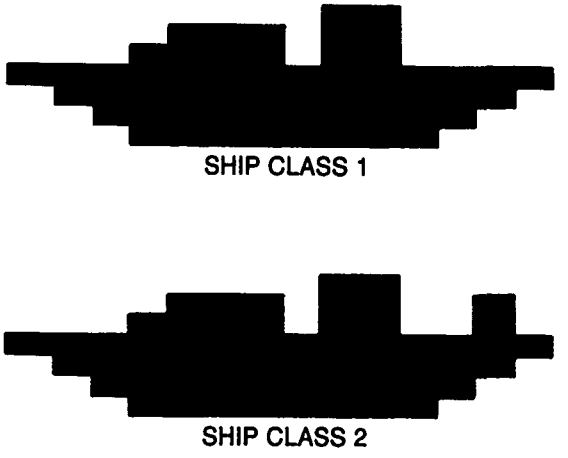

Fig. 1 — Image recognition problem used to test decay law learning

Results by Using Simulated Data: The first example is a simplified ship recognition problem. Figure 1 shows that the two ships are the same except that ship class 2 has an upright structure near the stern. These images differ by two pixels out of the 200 pixels that define the image. In the presence of noise, this is a nontrivial problem. The performance of the two approaches was compared when the training and test data were perturbed by the same type of additive. Gaussian noise with zero mean and the performance of the networks were measured as a function of the standard deviation of the noise. Ten prototypes were used for training the network, and ten protypes were used for testing the network. For a given noise level, each network was trained to the same error value, and then the network's performance was observed for test data that was disjoint from the training data. Figure 2 shows the dependence of the observed square error

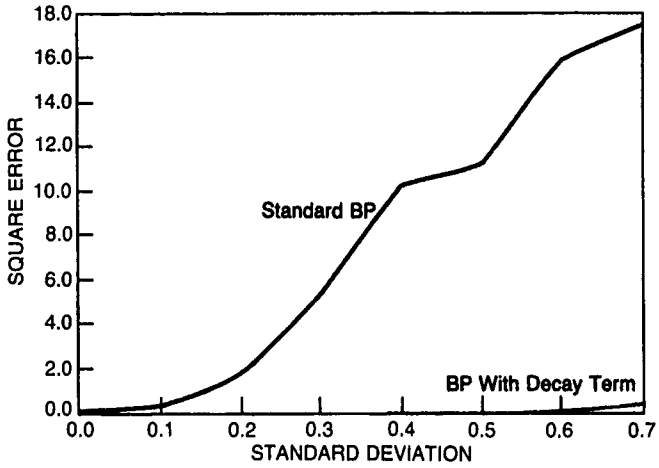

Fig. 2 — Observed error for the two images of Fig. 1 with noisy training data

as a function of the noise standard deviation. It is clear that inclusion of the decay term in the learning law has significantly improved the network's performance. It is also interesting to compare the weights generated by both approaches. Tables 1 and 2 show the weights generated by the two methods, with the weights associated with the pixels that define the upright structure underlined. Table 1 shows that although these are the largest weights in the array, many of the other weights are of comparable size. This is in strong contrast to Table 2, where the underlined elements are a few orders of magnitude larger than the other weights.

Table 1 — Weights Generated by Computer Simulation of Standard Back Propagation for the Two Images of Fig. 1 with Noisy Training Data. Underlined Elements Refer to the Pixels Where Ship Classes 1 and 2 Differ.

0.70	−0.05	−0.38	1.69	−0.02	−0.41	−0.06	0.66	0.28	−0.32
0.86	0.48	−0.42	−0.57	0.91	−1.36	−0.68	−0.00	−0.26	1.30
0.67	0.39	0.31	−0.44	−1.01	−0.57	−0.21	0.28	−0.91	0.20
1.01	0.88	1.20	−1.87	−0.22	0.33	0.80	−0.22	−1.50	−0.26
−0.66	−0.28	1.76	0.22	−1.43	−0.17	0.36	0.28	0.16	1.48
−0.56	−0.00	−1.64	0.96	−0.37	1.13	−1.13	−0.78	1.15	0.07
0.09	−0.25	−0.87	0.39	0.10	0.68	0.69	−1.83	−0.73	0.81
0.81	−0.66	1.18	−0.41	−0.62	0.97	0.58	−0.40	0.01	1.80
−0.08	−0.39	−0.17	0.71	0.21	0.58	−0.77	0.42	0.46	0.29
−0.68	0.40	0.10	−0.25	−1.40	0.07	−0.03	−1.14	−0.37	−0.91
0.07	0.07	−0.94	−0.05	0.20	0.75	−1.36	−0.23	0.63	0.34
−0.34	−1.02	0.19	−0.67	1.45	1.33	−4.11	−0.21	−0.29	0.40
2.23	0.80	−0.84	−0.07	1.29	1.71	0.84	−0.55	0.03	−1.10
−1.10	0.64	−0.13	−0.15	−0.56	0.20	−3.75	0.61	−0.05	−1.71
0.73	0.92	−0.22	−0.37	0.58	−0.73	−0.90	0.55	−0.68	−0.75
0.90	−0.66	1.00	−0.47	−0.64	0.53	−0.34	−1.35	0.75	0.82
1.11	1.29	−0.81	1.49	0.04	−0.74	−0.47	0.30	−0.09	−0.35
−0.90	−0.02	−1.37	0.49	1.65	0.97	0.14	0.16	−0.68	1.63
0.62	0.76	0.23	−0.66	1.26	1.29	0.79	−1.08	−0.12	−0.45
−1.48	0.76	1.01	−1.26	0.60	0.70	0.49	0.41	−0.06	−0.94
−0.37									

Table 2 — Weights Generated by Computer Simulation of Back Propagation with Decay Term for the Two Images of Fig. 1 with Noisy Training Data. Underlined Elements Refer to the Pixels Where Ship Classes 1 and 2 Differ.

−0.03	0.00	0.00	0.02	−0.00	−0.01	0.00	0.00	0.00	−0.02
0.04	0.00	0.00	0.00	0.00	−0.01	0.00	0.02	0.01	0.01
0.00	0.00	0.00	−0.01	−0.01	−0.00	0.01	−0.00	−0.01	−0.01
0.00	0.02	0.04	−0.04	−0.00	−0.00	0.01	0.00	−0.01	0.00
−0.00	−0.02	0.03	0.01	−0.02	−0.00	0.01	−0.00	0.00	0.00
−0.00	0.00	−0.01	0.00	0.00	0.02	−0.02	−0.00	−0.00	0.02
−0.00	0.02	−0.00	−0.00	0.01	0.00	0.01	−0.02	−0.01	0.00
0.00	−0.00	0.01	−0.02	0.00	0.00	0.00	−0.00	0.00	0.02
0.01	−0.00	0.01	−0.00	0.00	0.01	0.01	0.00	−0.00	−0.00
−0.01	0.00	0.01	−0.00	0.00	−0.01	−0.00	−0.01	0.01	−0.05
0.00	−0.01	−0.01	0.00	0.02	0.01	−0.01	−0.00	0.01	−0.01
0.00	−0.00	0.00	−0.00	0.01	0.01	−6.61	0.00	0.00	−0.00
0.01	0.00	−0.00	−0.01	0.01	0.02	−0.00	0.01	−0.00	−0.01
−0.00	−0.00	−0.00	0.01	0.00	−0.01	−6.05	0.00	0.00	−0.03
0.01	0.03	0.01	0.00	−0.00	0.00	−0.00	−0.00	−0.00	−0.00
−0.00	0.00	−0.01	−0.00	0.00	0.00	0.01	0.00	−0.00	0.01
0.01	0.01	−0.00	0.02	−0.00	−0.01	−0.00	0.00	0.00	−0.00
−0.00	−0.01	−0.00	0.00	0.03	0.00	−0.00	0.01	−0.00	0.01
0.01	0.04	0.02	0.00	0.00	0.01	0.00	−0.03	0.00	0.00
−0.00	0.00	0.00	−0.02	0.00	0.01	0.01	−0.00	−0.02	−0.01
0.00									

Summary: The pattern vectors associated with a particular classification problem will contain components that are essential for classification, as well as redundant components. It is intuitively plausible that in the presence of measurement noise, the redundant components of the pattern vectors have the potential to degrade the performance of a pattern recognition system. The primary advantage of the technique described here over many existing neural net classification systems is that it contains a built-in procedure for tuning out the redundant components. Tests done on this network for both simulated data and gray-level radar ship images [2] have shown an incremental performance over the standard back propagation method.

[Sponsored by ONR]

References

1. J. McClelland and D. Rumelhart, *Parallel Distributed Processing* (MIT Press, Cambridge MA, 1986), Vol. 1.

2. A. Schultz, "A Neural Net Learning Paradigms for Pattern Classes Containing a High Degree of Similarity," *J. Neural Network Computing*, Winter, 1991. ■

Active Learning and Bias Adjustment

D. F. Gordon
Information Technology Division

Concept learning is a major subarea of artificial intelligence. Concept learning typically

involves a learner, a concept to be learned, a set of examples, and a teacher or environmental feedback mechanism that can classify each element of this set as a positive or negative example of the concept.

The task in concept learning is to take a subset of the examples (called the training set) and formulate a generalized description that fits all positive examples and no negative examples (i.e., counter examples) in the training set. The generalized description is a hypothesis for estimating the concept. The learner uses this hypothesis to predict the classification of examples not in the training set. After predicting, the learner obtains external feedback regarding the true class of the new examples. This feedback may be used to refine the hypothesis. Finally, the new examples are added to the training set.

Frequently, many hypothesis fit the examples. Bias is any basis for hypothesis preference. Bias is important in concept learning because a strong, correct bias can dramatically reduce the cost of learning. A strong bias limits the number of hypothesis to consider. A correct bias is one that allows a system to learn the concept.

All learners begin with some bias. A number of methods exist for automatically improving the bias. However, our approach is unique because it involves active experimentation for diagnosing and resolving problems with the original bias to sensibly select a new bias.

The PREDICTOR System: We have implemented a concept learning system called PREDICTOR that actively tests and adjusts it bias [1]. The bias that PREDICTOR tests and adjusts is the language for expressing hypotheses. The system uses features (such as the length, beam size, speed, and number of guns and torpedos of a ship) both for describing examples and for the language of hypotheses. PREDICTOR expresses hypotheses by using a Boolean combination of feature values. For instance, a battleship might be described as any ship having at least 13 guns and a beam size greater than 107 ft.

PREDICTOR searches for a strong, correct bias. The system makes its bias stronger by reducing the number of features and their values in its hypothesis language. Furthermore, PREDICTOR both strengthens and corrects its bias by making explicit, tentative assumptions about the nature of the desired bias, actively testing these assumptions, then adjusting the bias based on the test results.

PREDICTOR is an augmented version of a concept learning system called Iba's Algorithm Concept Learner (IACL) [1]. PREDICTOR differs from IACL only by its additional bias testing and adjustment capabilities.

Empirical Results: We have run numerous experiments to characterize the advantages and disadvantages of this method [2]. Comparisons of PREDICTOR and IACL demonstrate that PREDICTOR's bias adjustment method not only restricts the number of hypotheses to consider but can also significantly reduce the number of training examples needed to learn concepts. Figures 3 and 4 show PREDICTOR demonstrating a 3- and 2-fold advantage in convergence rate over IACL, respectively, when learning two different concepts called TC1 an TC2. Each point in the graph represents, for a given training set size, the percentage of correct predictions made over a set of 10 new examples. Once the system maintains 100% correct predictions, it has learned the concept.

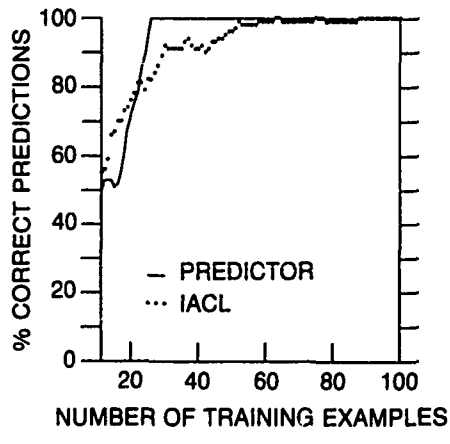

Fig. 3 — TC1: PREDICTOR and IACL

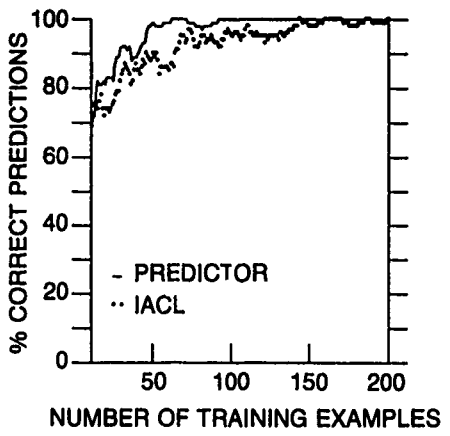

Fig. 4 — TC2: PREDICTOR and IACL

Summary: Active bias testing and adjustment can improve concept learning. Addition of this capability to an existing concept learner reduces the number of potential hypotheses and may also produce a large improvement in the rate of concept acquisition.

[Sponsored by ONR]

References

1. D. Gordon, "Active Assumption Testing and Bias Adjustment for Concept Learning," submitted to *Machine Learning*.

2. D. Gordon and D. Perlis, "Explicitly Biased Generalization," *Computational Intelligence*, 5(10), 67–81 (1989). ■

Synchronization in Chaotic Systems

L. M. Pecora and T. L. Carroll
Materials Science and Technology Division

Introduction: Chaotic systems are dynamical systems that defy synchronization [1]. Two identical autonomous chaotic systems started at nearly the same initial points in phase space have trajectories that quickly become uncorrelated even though each maps out the same attractor (trajectory) in phase space. It is thus a practical impossibility to construct identical, chaotic, synchronized systems in the laboratory.

Here we show how to link two chaotic systems with a common signal or signals so that when the signs of the Lyapunov exponents for the subsystems are all negative, the systems will synchronize. By synchronize we mean that the trajectories of one of the systems will converge to the same values as the other, and they will remain in step with each other. The synchronization appears to be structurally stable.

General Theory of Synchronous Subsystems: Consider an autonomous n–dimensional dynamical system

$$u = f(u). \qquad (1)$$

Divide the system arbitrarily into two subsystems ($u = (v, w)$),

$$v = g(v, w),\ w = h(v, w), \qquad (2)$$

where $v = (u_1, \ldots, u_m)$, $g = (f_1(u), \ldots, f_m(u))$, $w = (u_{m+1}, \ldots, u_n)$, and $h = (f_{m+1}(u), \ldots, f_n(u))$.

Now create a new subsystem w' identical to the w system, substitute the set of variables v for the corresponding v' in the function h, and augment Eqs. (2) with this new system, giving

$$v = g(v, w),\ w = h(v, w),\ w' = h(v, w'). \quad (3)$$

The subsystem components w and w' will synchronize only if $\Delta w \to 0$ as $t \to \infty$. In the infinitesimal limit, this leads to the variational equations for the subsystem. The behavior of the variational equation or its matrix version [2] depends on Lyapunov exponents of the w subsystem. We refer to these as sub–Lyapunov exponents. We now have the theorem: The subsystems w and w' will synchronize only if the sub–Lyapunov exponents are all negative.

The synchronization is not greatly affected by small differences in parameters between the w and w' systems, which would be found in real applications.

Applications to a Model: We found that in the Rössler system, it was possible to use the y

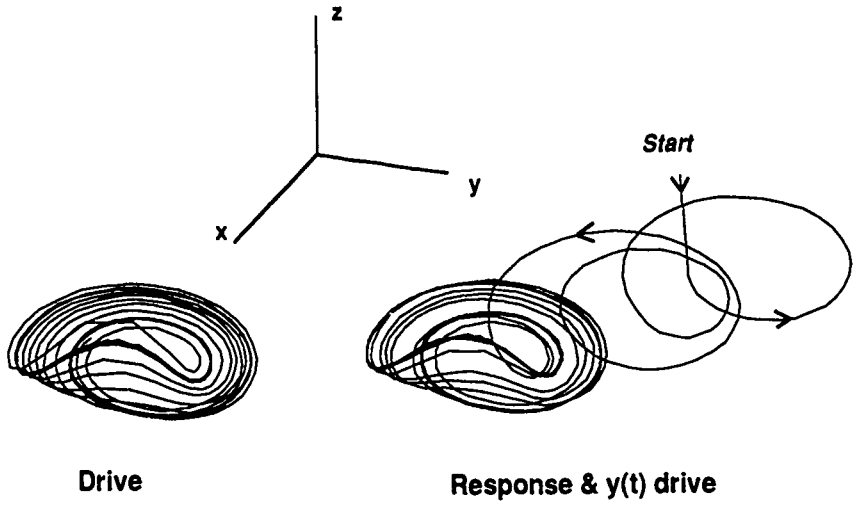

Fig. 5 — The attractors for the Rossler drive system and the (x' – z') response system + $y(t)$ drive variable [1]

component to drive an (x', z') response Rossler system and attain synchronization with the (x, z) components of the driving system. Figure 5 shows the three-dimensional views of the drive and response systems for a particular set of parameters in the chaotic regime. One can see that although the response system starts far away from the drive values, it soon spirals into the same type of attractor where it remains in synchronization with the drive system attractor. The conditional Lyapunov exponents for the Rossler setup are negative, as required.

Application to a Real System: We used a modified version of an electronic chaotic circuit to test these ideas on a real system. The drive circuit consists of an unstable, second-degree oscillator coupled to hysteritic circuit that continually shifts the center of the unstable focus causing the system to be reinjected into the region near one of two unstable foci. This keeps the motion bounded and chaotic.

Figure 6 shows oscilloscope traces of a voltage in the drive circuit vs its response counterpart for the synchronizing circuits for two different parametric values. Even though the sub-Lyapunov exponents in the latter cases both remain negative, synchronization is degraded.

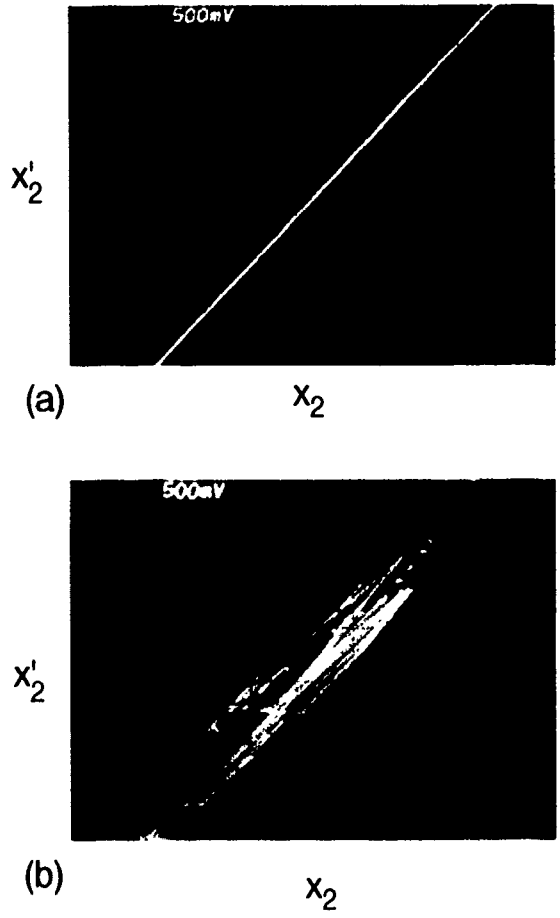

Fig. 6 — Oscilloscope traces of the response voltage x'_2 vs its drive counterpart voltage x_2 for (a) circuit parameters the same and (b) circuit parameter different by 50% [1]

Conclusions and Remarks: The ability to design synchronizing systems in nonlinear and, especially, chaotic systems may open interesting opportunities for applications of chaos to communications thereby exploiting the unique features of chaotic signals. One now has the capability of having two remote systems with many internal signals behaving chaotically yet still synchronized with each other through the one linking drive signal. This may have implications for secure communications.

Recent interesting results [3,4] suggest the possibility of extending the synchronization concept to that of a metaphor for some neural processes. Reference 3 suggests that one should view the brain response as an attractor. The process of synchronization can be viewed as a response system that "knows" what state (attractor) to go to when driven (stimulated) by a particular signal. It would be interesting to see whether this dynamical view could supplant the more "fixed-point" view of neural nets [5,3].

[Sponsored by ONR]

References

1. L.M. Pecora and T.L. Carroll, "Synchronization in Chaotic System," *Phys. Rev. Lett.* **64**, 821 (1990).

2. J. Gukenheimer and P. Holmes, *Nonlinear Oscillations, Dynamical Systems, and Bifurcations of Vector Fields* (Springer, New York, 1983), p. 25.

3. C. Skarda and W.J. Freeman, "How Brains Make Chaos in Order to Make Sense of the World," *Behavioral and Brain Sciences* **10**, 161 (1987) and the commentaries following the article.

4. A. Garfinkel, "A Mathematics for Physiology," *Am. J. Physiol.* **245**, R455 (1983)

5. Proceedings of the IEEE Conference on "Neural Information Processing Systems—Natural and Synthetic," (IEEE, New York, 1987). ■

Marine Technology

MARINE TECHNOLOGY

Besides the capability to detect marine acoustic signals, the Navy's ability to operate effectively in the sea largely depends upon its understanding of the vagaries of this milieu. Understanding is achieved through oceanographic research and the development and maintenance of hardware for marine use. Reported in this chapter is work on upper-ocean water movement, sonar-system maintenance, and the development of specialized oceanographic research platforms.

The Acoustics Division, the Information Technology Division, the Underwater Sound Reference Detachment, and the Space Systems Technology Department contributed to the work presented here.

Other current research in marine technology includes:

- Remote sensing of the Gulf Stream
- Sonar certification
- Elastic-wave propagation

Mushroomlike Currents on the Ocean Surface

R. P. Mied and G. J. Lindemann
Acoustics Division

The surface of the ocean is an indicator of the complicated underlying motion that takes place in the ocean on a wide variety of scales from centimeters to thousands of kilometers. An understanding of these motions is important because they serve to displace and distort surface manifestations of ship wakes. A knowledge of the naturally occurring motions that serve to alter wake signals is therefore important.

The advent of satellite-based remote-sensing instruments has made it possible to image synoptically large portions of the ocean in a fashion not previously feasible. An example of a recent interesting observation is the presence of dipole vortices in many coastal regions—for example, the southern coast of Alaska, the region west of Vancouver Island, and in the California and Norwegian coastal currents. When a surface tracer is present, basic structures of the dipole vortices have a surface signature that is best described as mushroomlike.

A Numerical Simulation: Mushroomlike formations are frequently observed when a large quantity of surface water has been impulsively ejected from a coastal region by an abrupt increase in wind stress or by an offshore jet of upwelled water originally residing at depth. In order to model the near-surface properties of the flow, a two-layer model is chosen, and both the lower layer and the interface between the two layers are initially at rest. The initial velocity in the upper layer is chosen to be the spatially bounded patch of upper ocean momentum shown in Fig. 1. Because we are attempting to model the view that a remote sensor would observe, we include a tracer in the upper layer of the modeled system to simulate gradients in surface temperature, biota, or a thin veneer of floating ice. The initial tracer distribution gradient is chosen as a constant.

Tracer Evolution: With initial conditions specified on the initial tracer distribution, layer velocities, and interface displacement, the fluid dynamical equations of motion are integrated as an initial value problem on a rotating Earth at a typical middle latitude (30°N). The evolution of the tracer distribution reveals the most interesting feature of the simulations. The initial velocity distribution in Fig. 1 evolves into two vortices: a counterclockwise vortex to the north and a clockwise vortex to the south. These two circulations, in turn, advect fluid around their centers, and the resulting form resembles the mushrooms (Fig. 2) observed in so many remote-sensing images. The shape asymmetry has several causes but is due in large measure to the differing ways in which the Coriolis and centripetal accelerations contribute to the pressure balance in clockwise or counterclockwise flows.

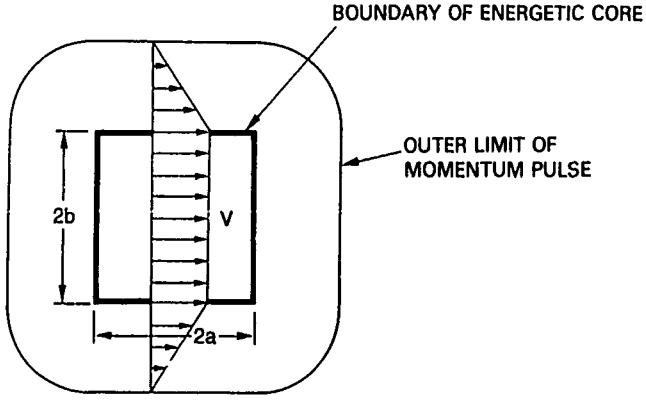

Fig. 1 — The initial velocity distribution $V(x, y, t = 0)$ in the upper ocean. At the beginning of the experiment, the lower layer is at rest and the interface displacement is zero.

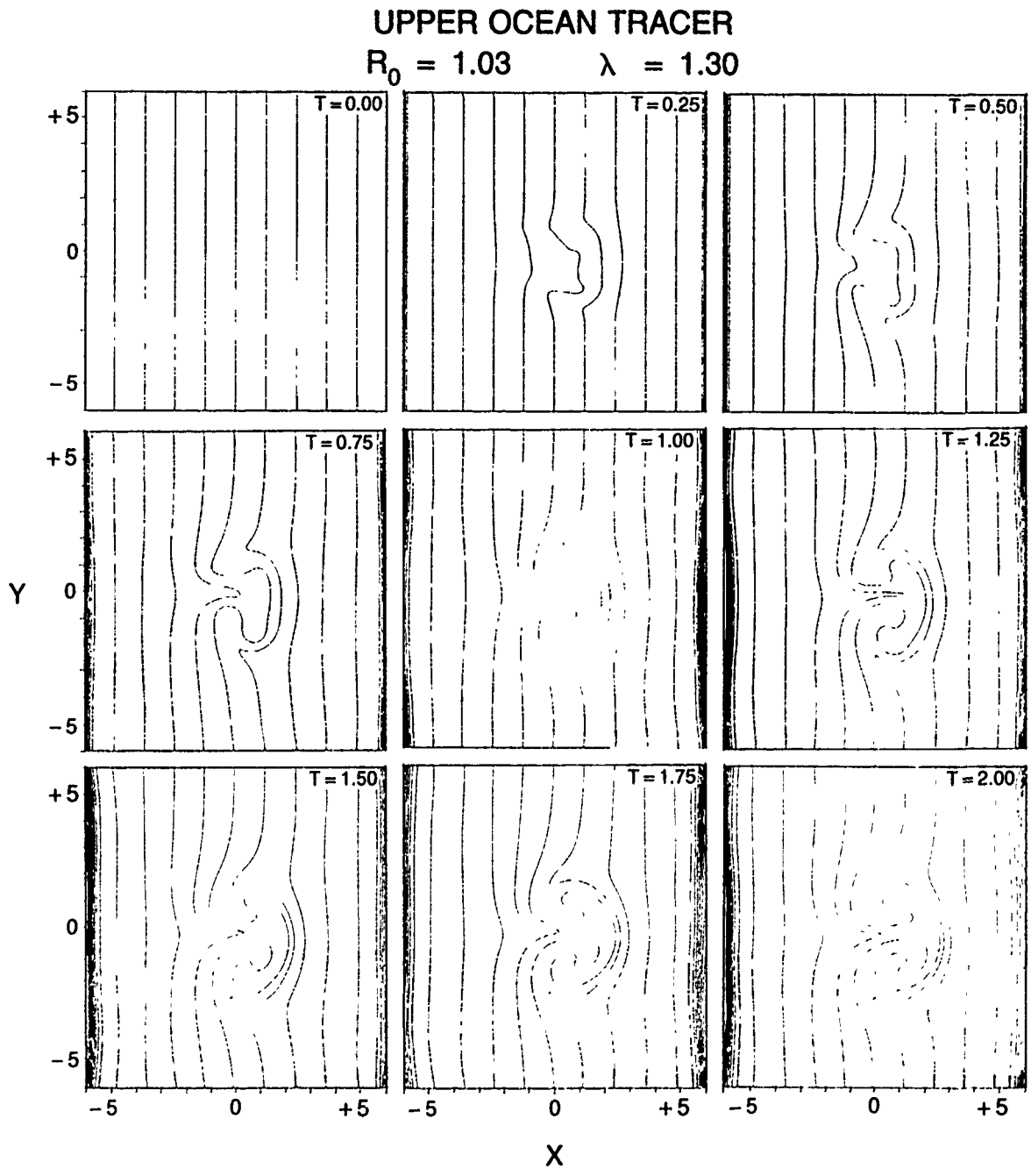

Fig. 2 — The evolution of the tracer for times given in inertial periods. Contour interval = 0.1. The bunched lines at the ends of the computational domain are due to the diffusion of the tracer across the periodic boundaries to the left and right.

Depending upon the width and velocity magnitude of the original momentum pulse (2b and V in Fig. 1, respectively), the form of the resulting mushroomlike shape can vary from one case to another. Figure 3 shows the results of many such experiments by their positions on a strength–length scale plane. Both of these values are in a nondimensional form. Strength is indicated by the Rossby number (V scaled by 2b and the Coriolis parameter). The length scale λis the pulse width 2b divided by an environmental length known as the Rossby deformation radius. We see that when both the length scale and strength are large, the mushroom is asymmetric, like the one shown in

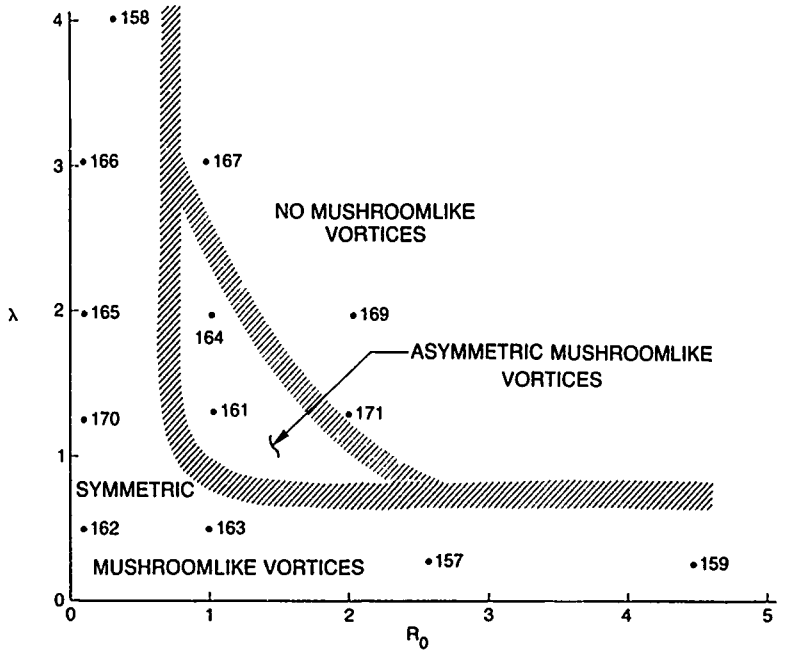

Fig. 3 — The distribution of experiments in the length scale (λ), strength (R_0) plane. The aspect ratio of the initial momentum patch is fixed at 1 ($b = a$ in Fig. 1). Three types of responses are observed, and these regions are indicated.

Fig. 2. Other responses include symmetric mushrooms or an unsteady regime that produces no mushrooms.

This study illuminates the dynamics of near-surface ocean motions that have length scales on the order of 10 km and can significantly distort surface ship wakes by altering their appearance and compromising our ability to sense them remotely.

This work is the result of a collaboration between the authors at NRL and James C. McWilliams at the National Center for Atmospheric Research.

[Sponsored by ONR]

References

1. R.P. Mied, J.C. McWilliams, and G.J. Lindemann, "The Generation and Evolution of Mushroomlike Vortices," *J. Physical Oceanography* **20**(3) (1991).

2. R.P. Mied and J.C. McWilliams, "Properties of Mushroomlike Vortices in the Ocean," *EOS* **71**(2), p. 87. Presented at the AGU/ASLO Ocean Sciences Meeting, New Orleans, LA, Feb. 12–16, 1990. ■

Maintenance Expert for Surface Ship Sonar System

J. A. Molnar
Information Technology Division

Technological developments in electronics have fostered an increase in military system capability. Complexity accompanies the growth in capability. The Navy develops extensive training programs to prepare the personnel who use and repair these systems. Even with intensive training, technicians need the experience of working with a system to understand the intricacies involved in maintaining it. Since personnel are periodically rotated through different duty sites, the expertise of system technicians fluctuates. When system faults and failures occur, the operator must quickly analyze and isolate the defect. Experience is an

important factor in resolving the problem. An expert system can help replace the need for experience.

Expert systems have evolved as specific examples of applied artificial intelligence. An expert system features the artificial intelligence techniques best suited for a particular problem. The developer refines the expert system to make it efficient in solving the problem.

NRL, in a cooperative project with the Naval Oceanographic and Atmospheric Research Laboratory (NOARL), has developed an expert system to help technicians diagnose and repair faults in a sonar system. We have named it the Technician's Assister System (TAS). The purpose of TAS is to provide all technicians with a software program that helps them find faults independent of their experience level. The sonar system is the AN/SQS-53B installed on AEGIS cruisers. The AN/SQS-53B has multiple cabinets of electronics that fill several compartments on the ship. To demonstrate the applicability of an expert system to assist in fault isolation, a prototype was developed for one cabinet of electronics. This cabinet, unit 26, contains 100 replaceable modules, most incorporating analog components. It is one of the system's higher failure units.

Expert System Architecture: The expert system architecture exploited the physical characteristics of the sonar system. A TAS software layer, Local Area Expert (LAE), performs shallow reasoning by using heuristic rules of repair. The rules are based on the monitoring capabilities of the sonar system. Another layer of software, the Fault Isolation Layer (FIL), contains detailed design information on the sonar system. The FIL uses model-based reasoning to determine module faults. The two layers are integrated to improve operating speed while maintaining accuracy. Figure 4 shows the relationship of these two TAS layers to the sonar system.

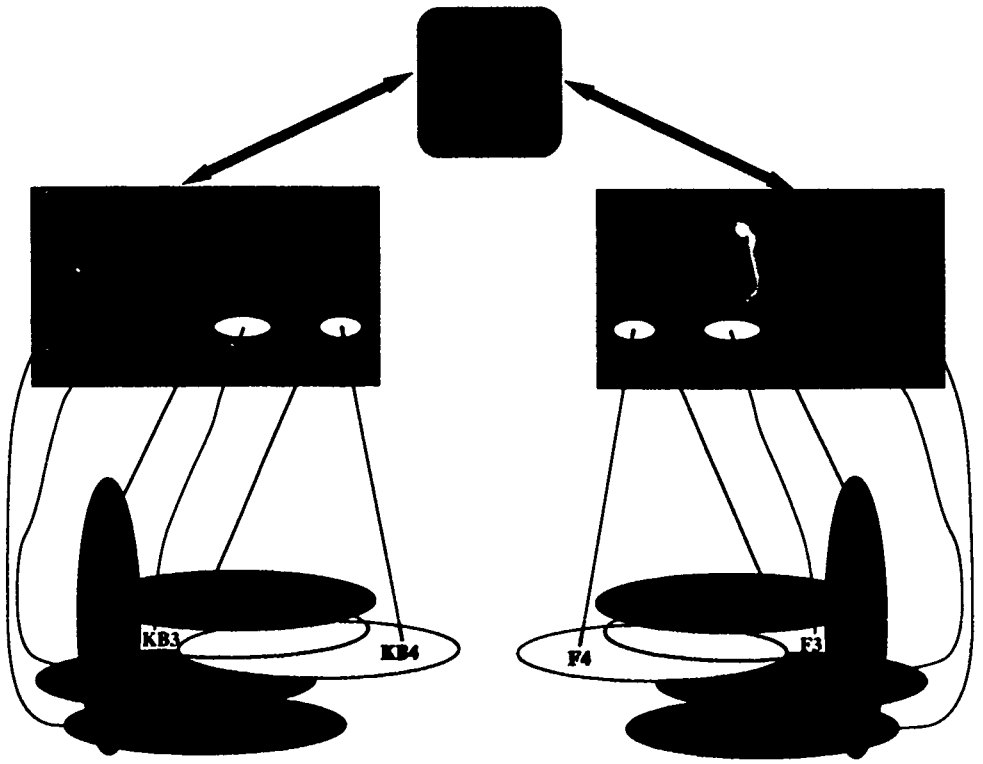

Fig. 4 — Mirror image of the sonar system's functionality in the architecture of the TAS as perceived through the interaction with the technician

NOARL created the LAE based on their experience with the performance-monitoring capabilities of the sonar system. Heuristic rules describe the relationship of sonar fault codes to functional abnormalities. Empirical observations made by a technician provide information that allows TAS to recognize faults. Through information on system status, TAS isolates malfunctions to one of twelve functional areas. TAS discerns both single and multiple malfunctions, but isolation to the module level is accomplished sequentially according to heuristic rules.

According to an order defined in LAE, control passes to the FIL layer. FIL then loads a knowledge database corresponding to the functional area into memory. There is an analogous knowledge database for each functional area of the sonar system. FIL is based on NRL's fault isolation system (FIS) software package [1]; both use the knowledge database as a logical model of electronic interconnections. Causal relationships like the ones shown in Fig. 5 become the rules of knowledge database. Approximately 3600 rules describe the model of unit 26.

The FIL evaluates the data received from the LAE layer and uses the detailed model information to direct the technician in performing specific tests. TAS continues to make test recommendations until it attains a threshold. At the threshold, it provides a decision on the probable faults. TAS continues this procedure until faults in all functional areas are removed. The presence of faults is assessed by TAS through the functional analysis performed in the LAE layer.

Verification: Isolation of faults by TAS depends entirely on the integrity of information contained in the rules. Several software tools were used to assure the integrity of the rules. These tools inspected the knowledge database to present inconsistencies, syntactic abnormalities, or flaws in continuity. Once alerted to a flaw in the knowledge database, the rules were modified by referring to the fundamental information in the unit 26 design.

After verifying the fundamental design of the knowledge database, a simulation was performed to prove the procedural accuracy of the TAS system. Simulations were performed with a simulator built into the FIS software. During the simulation process, the course of testing was assessed to determine that TAS operated fast enough for the intended application.

Validation: TAS has been used to isolate multiple faults within the sonar system during trials to test its effectiveness. NOARL is currently testing TAS with sonar technicians to validate and assess ease of use. Design modifications to TAS will be performed at NRL based on these test results.

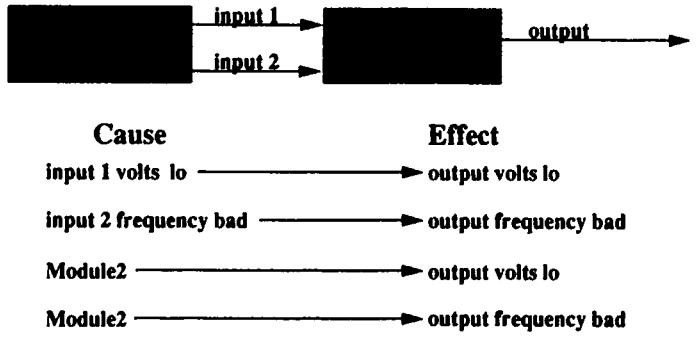

Fig. 5 — Structure of knowledge database causal rules and their relationship to the electronic system

Conclusions: NRL has successfully developed an expert system that diagnoses faults in one unit of a deployed sonar system. The technique used is extensible to the entire sonar system or to other electronic systems. The system is also flexible enough to handle multiple faults. Because it was designed to address the difficulties of isolating faults in analog components, it can diagnose the most difficult faults in many electronic systems.

[Sponsored by NAVSEA]

Reference

1. F.J. Pipitone, K.A. DeJong, and W.M. Spears, "An Artificial Intelligence Approach to Analog Systems Diagnosis," NRL Report 9219, Sept. 1989. ■

Improved Reliability Submarine Sonar Connector

G. D. Hugus
Underwater Sound Reference Detachment

An underwater electrical connector with improved reliability has been developed for the AN/BQR-7 sonar system. This sonar system includes a conformal hull array of up to 147 hydrophones on SSN- and SSBN-class nuclear powered submarines. The three-contact connector used on each of these hydrophones is presently specified by MIL-C-24231 and is also known as the "Portsmouth plug." It provides a watertight outboard connection to a receptacle, called a hull penetrator, which carries electrical signals from the hydrophone through the submarine pressure hull.

Problem: The MIL-C-24231 connector presently in use has an average service life of three years and is very expensive to replace—sometimes requiring drydocking of the submarine. Also, failure of this connector is wrongly identified many times as failure of the sonar transducer to which it is attached, thus causing unnecessary replacement of the transducer. As a result of many years of experience with this connector, it was determined that the failure mode is debonding of the molded elastomeric boot to the metal body, thereby allowing seawater to leak into the connector and causing an electrical short circuit. However, the failure mechanism was never determined.

The Underwater Sound Reference Detachment has gained extensive experience in solving reliability problems with wet-end sonar equipment by identifying failure modes and determining failure mechanisms as part of its Sonar Reliability Improvement Program (STRIP). As a result of research sponsored by the STRIP and performed by the Texas Research Institute, Inc. (TRI) in the rapid degradation of rubber-to-metal adhesive bonds in seawater [1,2], the mechanism identified as causing this connector failure mode is cathodic delamination. This mechanism is an electrochemical process that results from the galvanic coupling of the metal connector body to the zinc anodes protecting the submarine hull from corrosion and occurs with the adhesive primers and elastomers used.

Approach: The approach taken was to develop a replacement for the MIL-C-24231 connector. The objective was to achieve a 15-year average service life and yet connect with existing hull penetrators. To achieve this objective, candidate designs were tested by in-service installations on submarines concurrently with laboratory accelerated life test (ALT).

Modified MIL-C-24231 connector configurations that still had standard Monel metal body material were evaluated to see if they improved in-service reliability. When the modified connectors did not prove to have an adequate increase in reliability, the connector body was redesigned (as shown in Fig. 6) by changing the body material to a nonconductive glass reinforced epoxy (GRE) composite. The GRE material is known to be an excellent substrate for

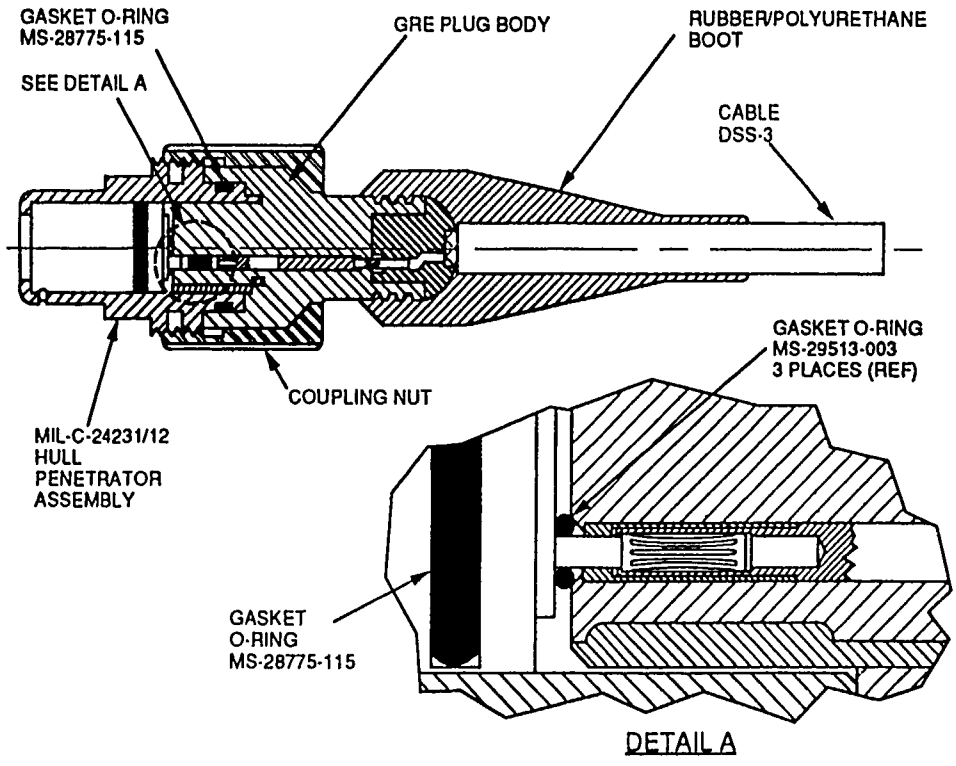

Fig. 6 — The extended-life Portsmouth connector

bonding to polyurethane and polychloroprene, the elastomeric boot materials commonly molded to this connector. Other objectives achieved by the new design, referred to as the extended life Portsmouth connector (EXLPC), are the ability to plug into any existing three-conductor MIL-C-24231 hull penetrator; fabrication can be done in shipyards and repair facilities with existing elastomeric boot-molding equipment; use of nonproprietary design and materials that are documented for competitive procurement in a completely specified drawing package; the Navy-owns the patent; and secondary o-ring seals of each of the three electrical contacts (Fig. 6, Detail A) enables electrical operability if the connector primary o-ring fails and the connector faces floods with seawater.

Results: To adequately evaluate the proposed EXLPC and other candidate designs for Fleet use, additional testing was successfully conducted with the following results: no electrical failures occurred after two underwater explosives shock tests (one required for outboard sonar transducers and the other more severe test for pressure-hull-mounted components); additional Fleet trial installations of EXLPC and competing candidate designs resulted in no EXLPC failures after more than three years of use in submarines; and accelerated life testing in the laboratory by TRI of EXLPC and competing designs resulted in no EXLPC failures after 15 equivalent years [3].

As a result of this research, a replacement for the MIL-C-24231 three-contact connector has been developed, and the design has been documented for Fleet use. The replacement extends the average service life from 3 years to 15 years.

[Sponsored by NAVSEA]

References

1. J. S. Thornton, R. E. Montgomery, and J. F. Cartier, "Failure Rate Model for Cathodic Delamination of Protective Coatings," NRL Memorandum Report 5584, May 1985.

2. J. S. Thornton, R. E. Montgomery, and J. F. Cartier, "Cathodic Delamination of Rubber-to-Metal Bonds—Cause and Control," Polymeric Mater. Sci. and Eng., Proc., ACS Div. of Polymeric Mater., *Sci. and Eng.* **53**, (1985).

3. S. L. Arnett and C. J. Corley, "Accelerated Life Testing of Candidate Designs for the Extended Life Portsmouth Connectors," Texas Research Institute Austin, Inc., Report 86190-504F; SLA, July 1989. ■

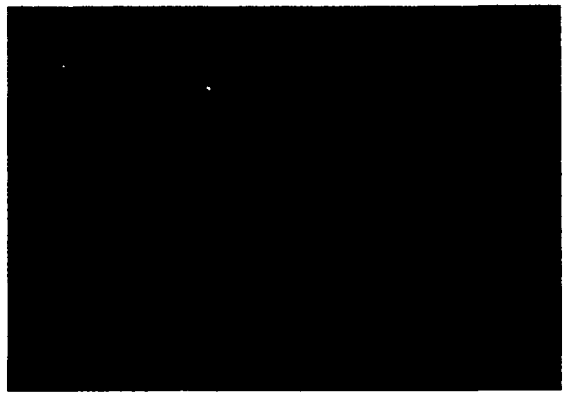

Fig. 7 —The ocean surface showing the drastic change in small-scale roughness at the edge of a slick. This change in roughness drastically modulates active electromagnetic images of the ocean surface.

Development of a Mobile Oceanographic Platform

J. A. C. Kaiser,* F. Fine,
P. W. Richardson,*and N. J. Pollack*
Space Systems Technology Department
and
R. Baldwin
Bendix/Applied Signal Corp.

For many years, radars have been used to survey and study ocean surface features. Variations in ocean surface roughness modulate the radar cross section and produce signatures that delineate features on radar images (and on optical ocean images). Major modulations occur through the interaction of ocean surfactants (surface-active chemicals) and straining (surface current modulation) fields with the shorter surface gravity waves. The careful, coordinated study of these processes, in addition to past field experience with the limitations of a towed, instrumented catamaran [1], motivated the development of the Mobile Autonomous Research Vehicle (MARV). Figure 7 shows the type of surface roughness modulation that MARV is suited to study. The drastic change in surface roughness that is due to one or more processes is very pronounced.

Platform Description: Figure 8 shows the MARV, a 24-ft-long pontoon boat having an 8-ft beam and two 2-ft by 2-1/2-ft foam-filled fiberglass hulls. The 8-ft wide by 10-ft long cabin contains the pilot station, racks for scientific instrumentation, navigation equipment, storage batteries, and a small galley. The boat is powered by a 90-HP, single-screw outboard engine that propels MARV at 20 knots and an electric trolling motor for very slow (< 1 knot), quiet operations. A 6.5 KW marine generator supplies 110V AC and 12V DC. It carries enough fuel for 8 h of operation (typically 40 mi). The 12V DC storage batteries provide 600 amp hours of power that can sustain navigation and other crucial functions of MARV for 3 hours if the 110V AC is lost because of such factors as generator failure.

The forward deck of MARV has two hatches between the hulls to mount instrumentation. The forward hatch is designed to accommodate the Surface TEnsion Measuring System (STEMS) [1], and the rearward hatch can accommodate a small, towed instrument package. A mast with a 3-ft yardarm for meteorological instrumentation is mounted on the forward, starboard side of the cabin. The mast can be extended to 6 ft above the cabin. A collapsible instrument "platform" is mounted on the forward portion of MARV, as shown in the stowed position in Fig. 8. This platform was designed to accommodate such

*Presently with the Center for Advanced Remote Sensing

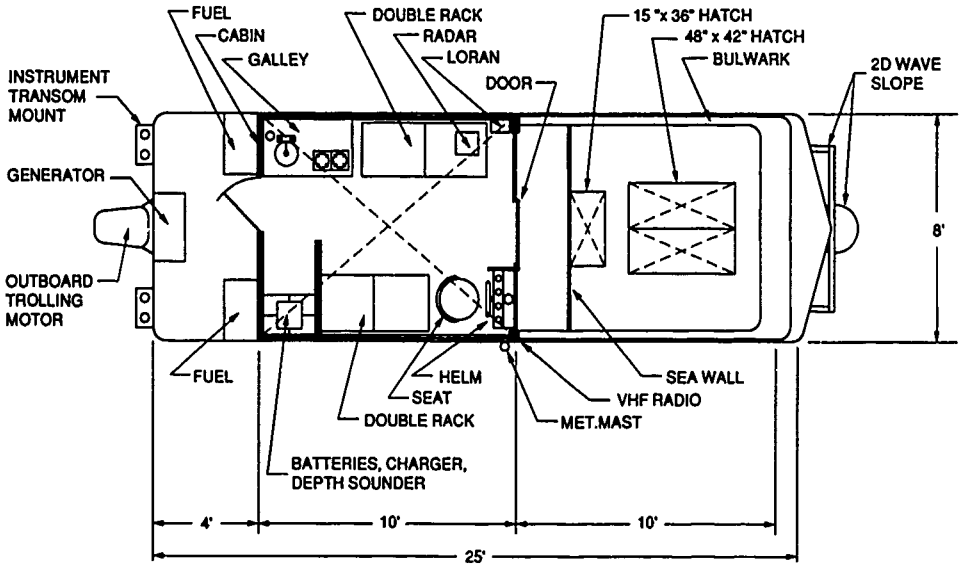

(a)

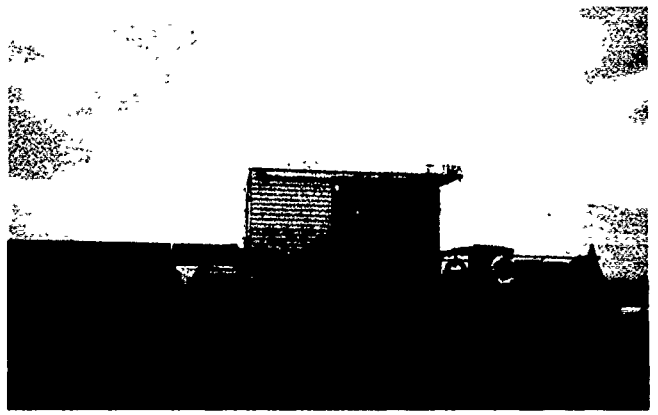

(b)

Fig. 8 — (a) Top and (b) side views of MARV

equipment as video cameras, scatterometers, passive microwave radiometers, and radiation thermometers.

Instrument Configuration: Table 1 gives a summary of the instruments deployed on MARV, and Fig. 9 shows the location of all instrumentation. The major instruments are STEMS, which records on video tape the spreading behavior of a set of 24 calibrated spreading oils that are deposited drop by drop on the water surface [2]; laser wave-slope gauge, which measures the two-dimensional slope spectra of capillary and capillary-gravity waves (0 to 75 Hz) by using the refraction of a laser beam through the water surface; scatterometer, which measures radar cross sections at horizontal and vertical polarizations in the look direction (typically 45°) at a 150 Hz rate on this 15-GHz (Ku-band) CW instrument; video camera, which looks at the same 1-m circular patch as the scatterometer by using a shutter speed of 1/500 s and a red filter to reduce upwelling light; passive microwave radiometer, which measures emitted and reflected electromagnetic radiation both horizontally and vertically polarized at 19 GHz (1.6 cm) from the

Table 1 — Specifications of MARV Instrumentation

Systems	Parameters	Specifications	Processing
STEMS-2	Surface tension	34 to 70 mN/m: Resolution 2 mN/m; 70 to 74.5 mN/m: Resolution .5 mN/m; Temporal resolution .5 s	Sample rate variable 2.0 to 0.1 Hz. Read spread-no-spread from video
Laser wave slope (Castor)	Wave slope	Spectra BW-0 to 75 Hz	Sample rate-150 Hz Slope data corrected for pitch and roll
Water samples	Equation of-state of surfactant		Measure in Langmuir trough
Ku-band scatterometer	Radar cross-section	45° Incidence angle H and V polarization measured at 150 Hz and averaged over 1 s, 1 m^2 spot size	Average over 1 s, time series and correlations
Spot video camera	Optical roughness	1 m^2 spot, 45° incidence angle, 1/500 s shutter with red filter	None
19 GHz passive microwave radiometer	Surface emission temperature (or emissivity)	1 m^2 spot, 1°C sensitivity read at 150 Hz and averaged over 1 s, H and V polarizations	Average over 1 s, time series and correlations
Wide-angle video	Optical appearance of water surface out to horizon	Standard color video	None
Environmental package	Air temperature Humidity Wind speed, direction Solar insolation Water temperature Water conductivity	.3°C accuracy, .1°C resolution 2% accuracy, .1% resolution .1 m/s resolution, .5 m/s accuracy 1° accuracy and resolution 0.1° C resolution and accuracy .01 S resolution and accuracy	Time series and correlations
Altitude	Pitch Roll Water height	1° accuracy, 0.1° resolution .2 cm resolution, 1 cm accuracy	None used to correct Ku scatterometer, spot video, and 19 GHz passive microwave signals, and determine if Castor in range

*Water samples stored in glass; measured equation-of-state stored on 5-1/4" floppy disk

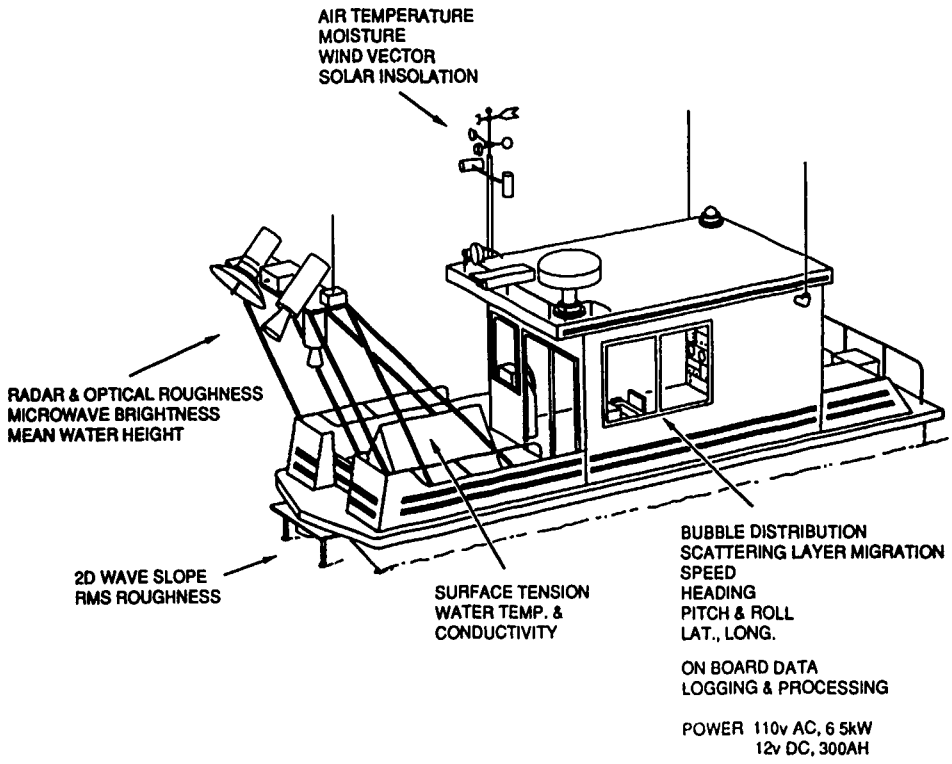

Fig. 9 — Schematic of MARV showing location of all sensors

ocean surface at a 1 Hz rate. The radiation intensity is controlled mainly by surface roughness and foam and is very weakly sensitive to water temperature changes; and environmental package, which measures air temperature, humidity, wind speed and direction, solar insolation, water temperature and conductivity, platform pitch and roll, and water height.

All the data is input to an IBM 7532 computer and stored on a 5-1/4" floppy disk; the disk can store up to 120 min of data.

Initial Deployment and Results: MARV was deployed on a day in June 1990 when the winds were 5 to 7 m/s and the seas averaged 1 m. Limited digital data and video records of the ocean surface were collected. Surface tension time series were obtained by the traditional method [2]. During the deployment, MARV maintained a 15-knot speed into the 1-m seas and the 10 to 15 knot wind and proved to be maneuverable and stable with its payload of 2500 lbs distributed over the forward two-thirds of the craft.

Conclusions: MARV proved its usefulness but also defined its limitations. The concept is sound for use in protected water and light-sea ($\sim$1 m) conditions, exactly when surfactants become an important factor in modulating ocean roughness. The combination of instruments used on MARV in 1990 to examine the ocean surface on a small scale could not be deployed in any other manner—hence the unique capability of MARV. Such a combination of instruments could provide breakthroughs in understanding ocean roughness modulations and their effects on remote sensors.

[Sponsored by CNO]

References

1. J.A.C. Kaiser and R.D. Peltzer, *1989-1990 NRL Review*, pp. 200-204 (June 1990).

2. J.A.C. Kaiser, W.D. Garrett, S.E. Ramberg, and R.D. Peltzer, *1986 NRL Review*, pp. 64-67 (Oct. 1987). ■

Materials Science and Technology

MATERIALS SCIENCE AND TECHNOLOGY

The operating Navy is constructed from a vast array of materials such as metals and metal alloys, ceramics, composites, wood and cellulose products, and solid-state devices. These materials must be able to withstand considerable stresses imposed by the marine environment and by space. Much research at NRL relates to the development of new materials for use in these environments and to the determination of their properties, service performance, and reliability. Reported in this chapter is work on superconductors, elastic constants of anisotropic materials, laser-beam welding, elastic properties of bilayer materials, growth of gallium arsenide, and IR spectroscopy of adsorbates on semiconductors.

These divisions contributed to the work presented in this chapter: Condensed Matter and Radiation Sciences, Materials Science and Technology, Electronics Science and Technology, and Chemistry.

Other current research on materials includes:

- Hydrocarbon radicals on the diamond surface
- Piezoelectric coefficients of composites
- Cuprate superconductors and related materials
- Ultrathin-film crystalline structure
- Crack growth behavior for ductile metals

Pulsed Laser Deposition of High T_c Superconductors

D. B. Chrisey and J. S. Horwitz
Condensed Matter and Radiation Sciences Division

Motivation: Many new and exciting electronic materials of current Navy interest are multicomponent, i.e., they contain specific proportions of three or more elements. For example, the recently discovered high transition temperature (T_c) superconductor $YBa_2Cu_3O_{7-\delta}$ contains four elements. To exploit the novel properties of these materials in thin-film electronic devices, only an extremely low level of defects in the film composition, phase, and structure can be tolerated. Unfortunately, conventional thin-film growth and processing procedures (e-beam evaporation, sputtering, and postdeposit annealing) cannot readily control these defects to the degree dictated by the device design. However, a new physical vapor deposition technique is used at NRL to solve many of the thin film growth problems encountered with high T_c superconductors. The application of this technique is expanding to include a broad spectrum of complex multicomponent materials.

Background: Pulsed laser deposition (PLD) typically uses the focused output from a short pulse, KrF excimer (Δt = 30 ns, λ = 248 nm) to rapidly vaporize a bulk, stoichiometric target. The power densities are approximately 100 MW/cm^2. The laser pulse is focused through a UV transparent window onto a rotating target at a 45° angle of incidence. A substrate is positioned along the target's surface normal to collect the ablated material. Figure 1 shows a schematic diagram of a PLD thin-film deposition chamber.

Novel features of this process include: the presence of both neutral and charged atoms, molecular fragments, and clusters; a highly forward-directed distribution of ejected material (i.e., no significant specular component); a rapid rate of material deposition (~0.1 nm in 10^{-3} s or 100 nm/s); and emission from the electronically excited species created by the laser/surface interaction. Figure 2 shows the laser-produced plume from a $YBa_2Cu_3O_{7-\delta}$ target. In addition, PLD accommodates high background pressures of reactive gases such as oxygen, which is integral to obtaining high critical temperatures (T_c) and critical currents (J_c) in the superconductors.

It is the highly forward-directed nature of the PLD process, though, that ensures the transfer of stoichiometry from the pellet to the thin film. This

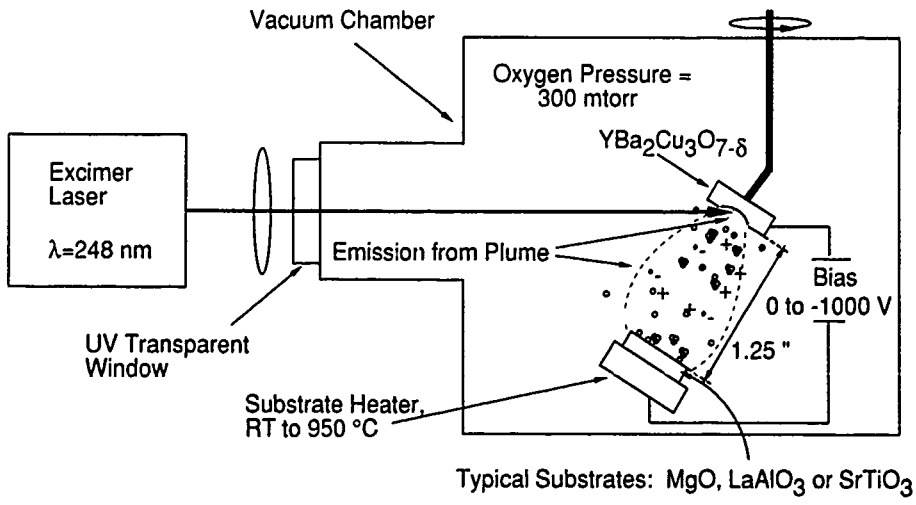

Fig. 1 — The NRL pulsed laser deposition (PLD) apparatus

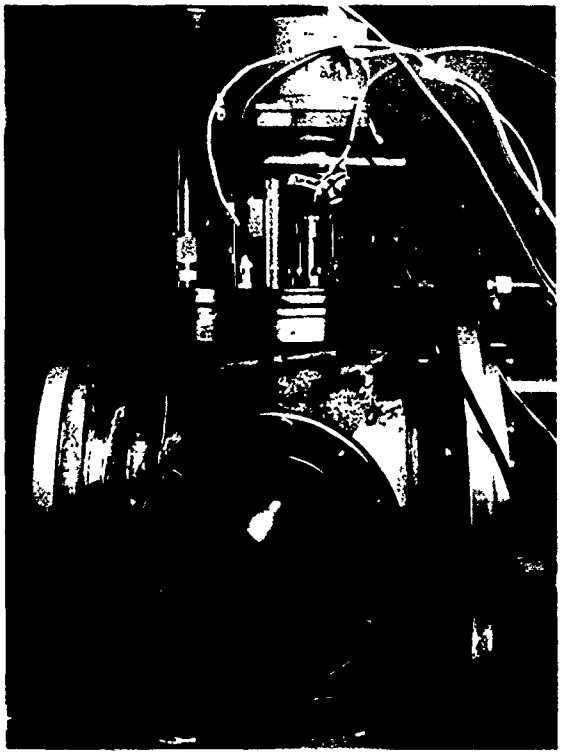

Fig. 2 — Laser-produced plume in the deposition of a $YBa_2Cu_3O_{7-\delta}$ film

feature alone makes PLD an important physical vapor deposition technique and superior to conventional multisource or single-source techniques that suffer from problems of individual constituent deposition control and preferential ejection, respectively. The PLD vapor flux contains species with both high translational and internal energies. The high energy content and stoichiometry of the plume, in addition to the simplicity of the experimental arrangement, yields high quality and reproducible thin-film properties.

Superconducting Thin Films: PLD films are superconducting as deposited and require no postprocessing. The films are characterized in terms of their crystalline phase, orientation, and electrical transport properties. NRL-produced $YBa_2Cu_3O_{7-\delta}$ films on lattice-matched substrates such as $SrTiO_3$ <100> and $LaAlO_3$ <100> are exclusively c-axis oriented, i.e., the conducting planes lie parallel to the substrate's surface. This is very important because the electrical transport properties of this layered perovskite are highly anisotropic. Typical DC transport measurements on these films indicate that the films have T_c of ~90 K and J_c (77 K) of between 2×10^6 A/cm^2 and 4×10^6 A/cm^2. Most relevant for microwave device applications is the high-frequency response as measured by the microwave surface resistance R_s. Figure 3 shows this quantity measured from 20 to 120 K at 36 GHz and then scaled to a typical device operating frequency in the X band (9 GHz). Microwave devices made from $YBa_2Cu_3O_{7-\delta}$ thin films formed by PLD exhibit a factor of 30 improvement in R_s (and thus, device performance) over copper at 77 K.

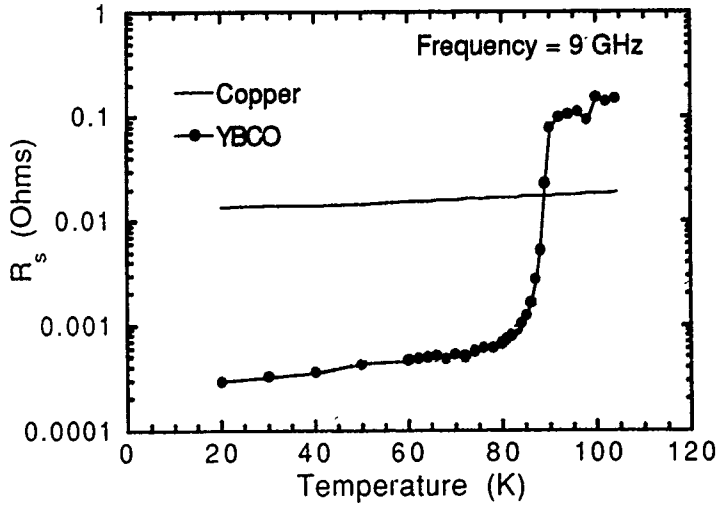

Fig. 3 — Microwave surface resistance for a $YBa_2Cu_3O_{7-\delta}$ film produced by PLD

Summary: A new technique—pulsed laser deposition—is being used to reproducibly deposit high quality thin films of high T_c superconductors for device applications. Researchers in the Microwave Technology Branch routinely pattern these films into passive microwave devices (e.g., filters, resonators, and delay lines) that demonstrate superior performance in comparison with similar devices made from conventional materials. These high T_c devices are fully operational at 77 K. Additional research is being performed on the deposition of multilayers (dielectric/superconductor) for the fabrication of more complex passive and active microwave devices and the investigation of new materials such as the ferroelectric perovskite $PbZr_{1-x}Ti_xO_3$. This material has immediate application as a radiation-hard nonvolatile random access memory (NV-RAMS) unit.

Acknowledgments: Drs. K. S. Grabowski, M. S. Osofsky, H. S. Newman, V. C. Cestone, and M. E. Reeves have made significant contributions to this research.

Sponsored by SPAWARS ■

Determination of Elastic Constants of Anisotropic Materials from Oblique-Angle Ultrasonic Measurements

R. B. Mignogna, N. K. Batra, and K. E. Simmonds
Materials Science and Technology Division

Nondestructive evaluation of composites is highly desirable, both for defect characterization and determining mechanical properties. Ultrasonic methods are especially well suited for finding the elastic properties of materials. The most common technique used to determine the elastic constants of anisotropic materials from ultrasonic wave-speed measurements requires that the material be cut into a number of samples. These samples are cut such that particular material symmetry directions can be accessed for normal incidence wave-speed measurements. This is, in reality, a destructive technique and is not feasible for thin or inhomogeneous anisotropic materials. A truly nondestructive technique is needed for damage assessment and quality control.

The use of oblique-angle ultrasonic measurements for determining anisotropic material elastic constants has been considered for a number of years. Renewed interest in this technique is occurring because of the use of advanced anisotropic composite materials by the Navy, industry, and DoD in general. Some of the early works do not indicate a way to take into account the fact that the energy and phase vector do not, in general, coincide for anisotropic materials. The energy and phase vector do coincide for certain symmetry planes, greatly simplifying the problem. However all of the elastic constants cannot be obtained from this technique alone if ultrasonic measurements are restricted to these planes.

Phase Vector vs Energy Vector: Recently we have shown that, in general, the time of flight along the energy and phase paths are equivalent for fluid immersed, through-transmission ultrasonic measurements [1]. These results have been verified and extended for certain cases in pulse echo by Kline [2].

The importance of showing the equivalence of the time of flight along the energy and phase paths is that it permits a much less complicated mathematical analysis to be used for the inverse problem of determining the elastic constants of a material. The entire analysis can be done in terms of the phase vector; otherwise, it would be necessary to use the energy vector, making this an almost intractable problem.

We have used these developments to obtain an inversion procedure for determining all nine elastic constants from ultrasonic wave measurements for materials having orthorhombic symmetry. The inversion procedure, based on an over-determined Newton-Rhapson method, has been validated in a "closed-loop" manner. By using computer-

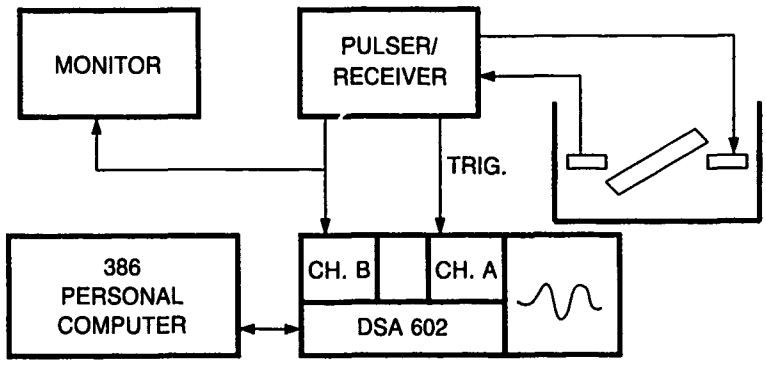

Fig. 4 — Experimental arranagement for determining time of flight

generated data with superimposed random error on the order of magnitude expected in the experimental measurements, it is possible to determine all nine elastic constants used in the forward calculation of the data.

Experimental System and Results: Figure 4 is a schematic diagram of the experimental system. This system may look similar to those found in some commercial ultrasonic immersion C-scan systems, however the requirements are much more stringent. The experimental measurements require precise alignment of the transmitting and receiving transducers with the sample scanning motion of the transducers (the planes formed by their motion) and the rotation axes of the sample. In addition, we must also have detailed knowledge of the transmitting transducer's beam pattern, both in terms of amplitude and phase.

The experimental method for determining the phase vector is valid for any symmetry class material. However, without a priori knowledge of the orientation of the specimen, the reference coordinate system attached to the specimen may be arbitrarily oriented with respect to the symmetry of the material. To use data obtained without some a priori knowledge of the specimen orientation would require a complete, general inversion analysis.

We have demonstrated the ability to determine the phase vectors for a [110] spinel specimen. A slight amount of misorientation (2.7°) of the specimen was detected from the data. The phase-velocity results obtained from the immersion measurements agree well with predicted calculations of the phase velocity based on the elastic constants determined from contact measurements. Figure 5 shows the experimental, predicted, and the rotated prediction times of flight measurements for the spinel crystal.

Although it was not possible to determine the elastic constants from these measurements because of a current lack of generality in the inversion routine, the sensitivity of the measurements to orientation can be seen. We are presently working on a general inversion analysis that will allow us to deal with any symmetry class.

[Sponsored by ONR]

References

1. R. B. Mignogna, in *Rev. Prog. Quantitative NDE*, Vol. 9B, D. O. Thompson and D. E. Chimenti, eds. (Plenum Publishing Corporation, New York, 1990) pp. 1565-72.

2. R. A. Kline, "17th Annual Rev. of Quantitative NDE," La Jolla, CA, July 15-20, 1990. ■

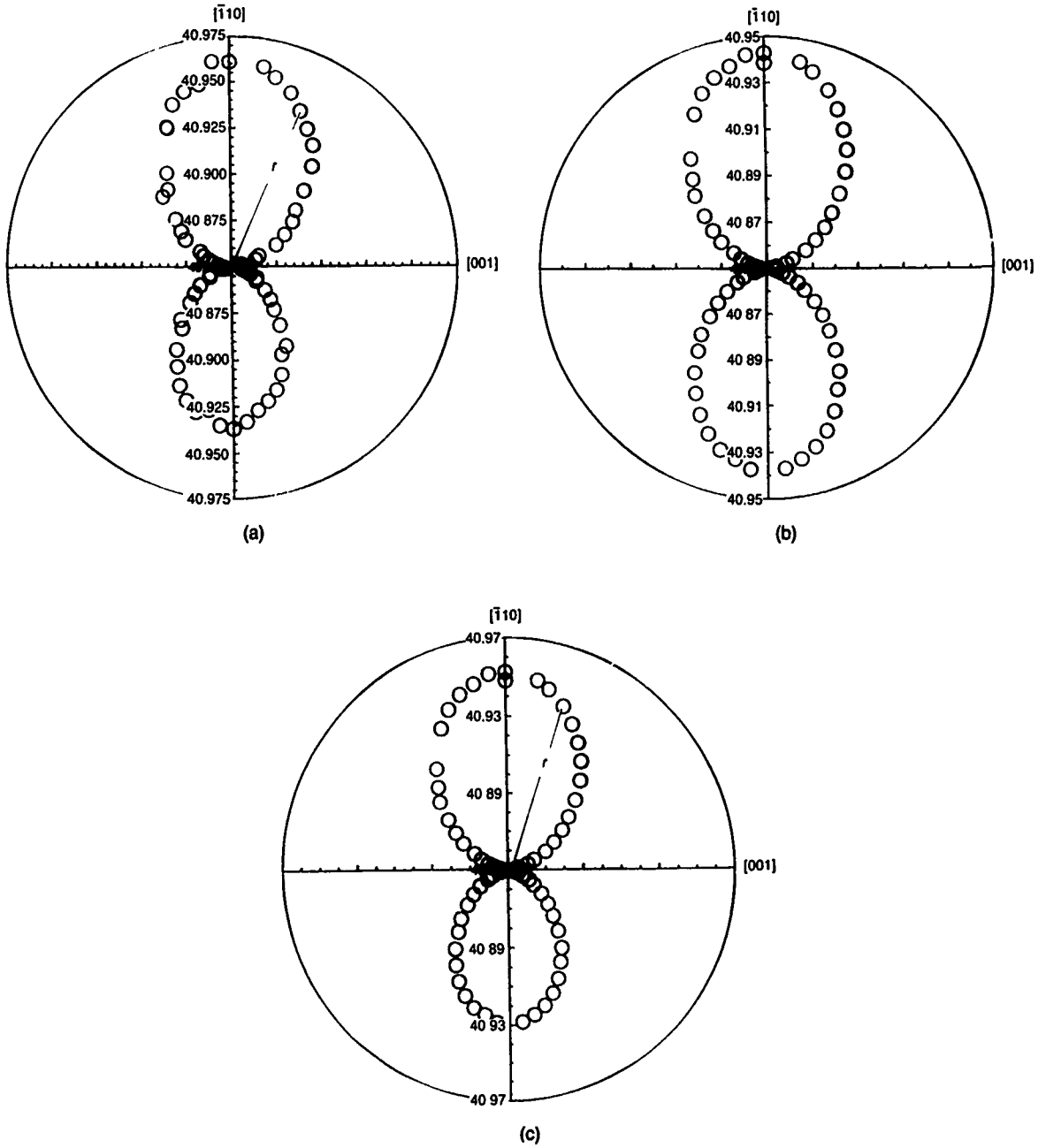

Fig. 5 — Time of flight in μs vs polar angle ϕ_i in spinel at an azimuthal angle $\theta_i = 3°$ (assumed [110] direction is parallel to the specimen normal): (a) experimental results; (b) expected (calculated) results; (c) recalculated values assuming that the [110] direction was misoriented by 2.7° about the [001] direction

Thermal Profiles and Heat-affected Zone Hardness in Laser Beam Welding

E. A. Metzbower
Materials Science and Technology Division

A critical volume in a weldment is the region next to the fusion zone known as the heat-affected zone (HAZ) in which solid-state transformations occurred as the result of the heat flowing out of the fusion zone. In many steels, depending on the composition of the steel and the cooling rate in the HAZ, a martensitic transformation can occur that can make this region brittle or susceptible to hydrogen-induced cracking. Knowledge of the hardness (which is a measure of the strength) of the HAZ is important for Naval structures and platforms.

Laser-beam welding with a continuous-wave CO_2 laser is a high energy density, low heat input process. The result is a narrow HAZ that cools rapidly with very little distortion and a high depth-to-width ratio for the fusion zone. Depending on the laser power, welding speed, plasma-suppression device, and gas used, the shape of the fusion zone can vary from a slight taper to a large taper, nail head, or wine glass configuration. This variation in shape makes modeling of the process difficult.

The thermal profiles in two sets of laser-beam welding experiments on 10 mm-thick BS4360 50D steel plates were measured. These plates were instrumented with thermocouples in the midthickness of the three-piece "sandwich" test pieces. The welds were full penetration and were made at two different laser powers (4.5 and 9.0 kW) and welding speeds (5 and 20 mm/s). From the experimental data, the amount of heat required to flow out of the fusion zone to yield these thermal profiles was calculated. The result was that 50% of the incoming laser energy was required for these thermal profiles. The cross section of the fusion zone (the melt temperature isotherm) for each of these weldments was measured.

Temperature Calculations: A generalized line-source model for laser-beam welding was then used to calculate the temperature profile in a variable grid for the two laser powers and welding speeds by using the calculated efficiency. The two adjustable parameters in the model were adjusted to give a good correlation between the experimental and calculated melt temperature isotherm. The result is that, by knowing the cross section of the laser beam weld, the temperature profiles that result in that cross section can now be calculated. The adjustable parameters permit a good fit to be made to the experimental melt temperature isotherm, regardless of the shape of the fusion zone (Fig. 6.)

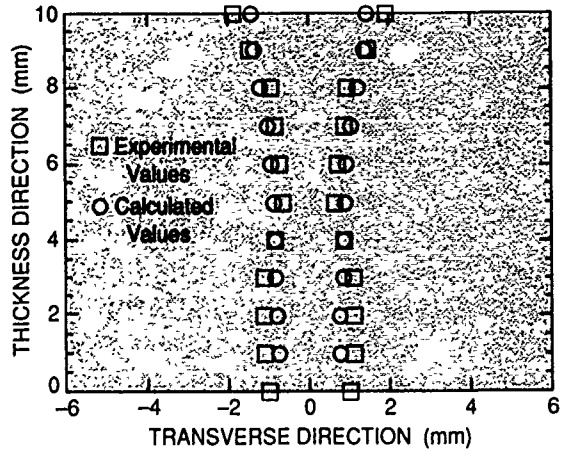

Fig. 6 — Comparison of calculated and experimental melt temperature isotherms for laser-beam weldment made at 9 kW and 20 mm/s

Hardness: The calculation of the hardness across the HAZ has been carried out in only a very few cases. The hardness in the HAZ results from the microstructural transformations and grain growth that occurs. Empirical relationships have been developed among the hardness number of each phase, the chemical composition, and the cooling rate. These relationships were used to calculate the hardness number for each phase. The cooling rate from 800° to 500° C and the chemical composition of the steel were used to calculate the hardness number for each phase (ferrite, pearlite,

bainite, and martensite) that is the daughter product of austenite.

The rule of mixture, which requires that the hardness number of each phase as well as the volume fraction of that phase be known, was used to calculate the hardness. Two completely different methods were used to calculate the volume fraction of ferrite, pearlite, martensite, and bainite that are the result of the decomposition of austenite. The results of these calculations agreed very well with each other. The rule of mixture was then applied to calculate the hardness at any point on the computational grid in the HAZ and fusion zone. These hardness values agreed well with the experimental hardness measurements (Fig. 7).

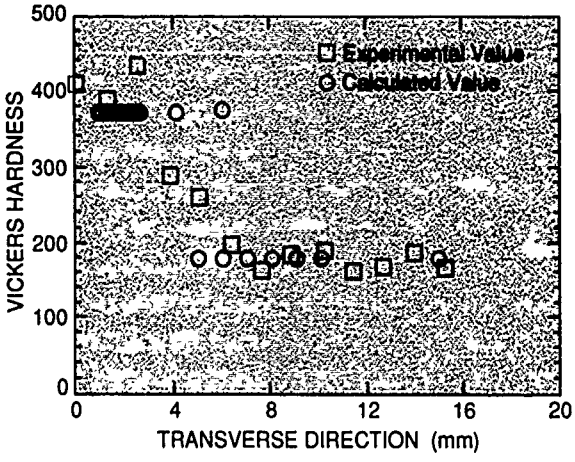

Fig. 7 — Comparison of experimental and calculated Vickers hardness across the fusion, HAZ, and base plate

The hardness values in the HAZ are related to the weldability of the steel. This methodology is applicable to other welding processes. These calculations increase our knowledge of the high-energy-density welding process, a process that will increasingly be used in future Naval applications. This technique could also be used to indicate improvements in the chemical composition of future Naval steels and welding wire.

[Sponsored by ONR]

References

1. E. A. Metzbower, "Laser Beam Welding: Thermal Profiles and HAZ Hardness," *Weld. J.* **69**(7), 272-s - 278-s, July 1990.

2. E. A. Metzbower, "Experimental Laser Welding Thermal Cycles Part I: Welding Efficiency," *J. Laser Appl.* 1(3), 9-15, July 1989. ■

Elastic Properties of Bilayer Materials Determined by the Indentation Test—Axisymmetric Boussinesq Problem

S. C. Sanday, H. Y. Yu,* and B. B. Rath†
Materials Science and Technology Division
**Geo-Centers, Inc.*
†*Materials Science and Component Technology Director*

Intense interest in thin-film technology has been spurred by the growing importance of microelectronics, metal matrix composites, ceramic matrix composites, high transition temperature superconducting films, and compositionally modulated materials. Correspondingly, the determination of film properties has become more important. The need for techniques to study the mechanical properties of thin films, which are usually defined as coatings of thickness of up to a few microns, has recently rekindled an interest in microhardness and submicroindentation devices [1]. One of these techniques consists of pressing an indenter onto the film that is overlaying a substrate and measuring the slope of the unloading curves in the load vs the depth plot obtained from the test that is then used to calculate the elastic modulus $\zeta = 4\mu/(1 - \nu)$ of the thin-film material. It is found that, as the indentation depth d increases, so does the influence of the substrate on the measured elastic constant ζ_c. For small indentation depths relative to the film thickness h, the composite modulus approaches that expected for bulk film material, since the indenter interrogates the film near its surface only. For deep indentations, the

modulus approaches that expected for bulk substrate material. Therefore, the elastic solution of the indented bilayer problem is required for proper interpretation of the experimental results, i.e., to determine the effect of the substrate on the elastic modulus of the film.

Contact Problem: The indentation problem is a mixed boundary value problem more commonly known as Boussinesq's problem. The elastic field caused by the indentation of the film by a rigid indenter has been obtained for spherical, conical, and flat-ended cylindrical indenters [2]. The film is either perfectly bonded to an elastic substrate or is resting frictionlessly on an elastic substrate. The results are obtained by solving a Fredholm integral equation of the second kind with a continuous symmetrical kernel that depends on the bonding conditions. Numerical results are given for several combinations of film and substrate elastic moduli and film thicknesses.

Figure 8 shows that a rigid axisymmetric indenter with a flat, conical, or hemispherical end and axis normal to the film surface presses frictionlessly on the film thickness h, with elastic constants μ and ν, which overlay a substrate with elastic constants μ' and ν'. Figure 9 gives the upper bound of h/a_H vs μ/μ' as a function of selected values (2%, 5%, and 10%) of $(\zeta_c - \zeta)/\zeta$ (a_H is the Hertz radius of the contact area for bulk film material by itself). According to this result, the guidelines may be set for the indentation test; i.e., to chose a priori what the proper substrate is and the required film thickness so that the film's elastic constants may be determined within a predetermined degree of accuracy.

Conclusions: The following conclusions are obtained from the present study: (1) For a given minimum film thickness and a given substrate stiffness, the elastic constants of the film may be determined within a certain accuracy for those cases where the film is perfectly bonded to or in frictionless contact with the substrate. Conversely, if a given accuracy is desired, the required substrate stiffness for a given film thickness or the

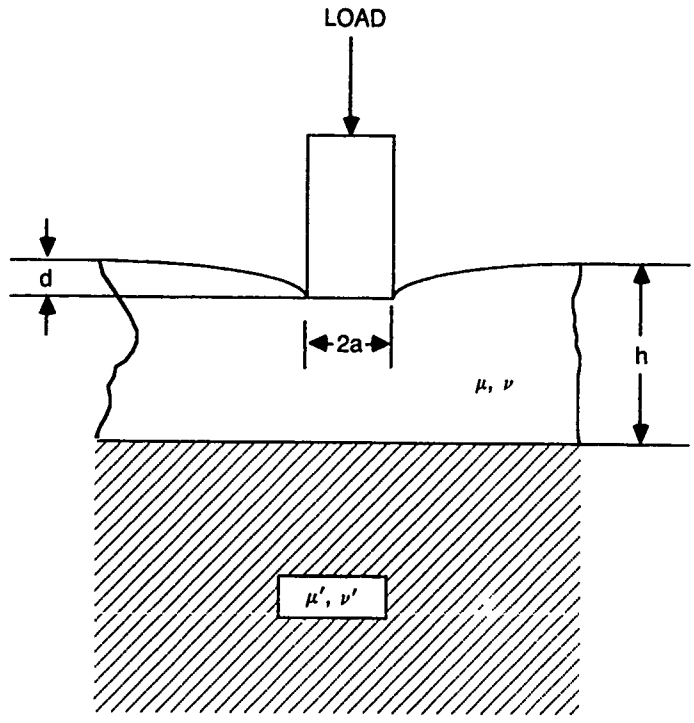

Fig. 8 — A composite medium consisting of a thin film either perfectly bonded to or in frictionless contact with a semiinfinite substrate being indented by a rigid indenter

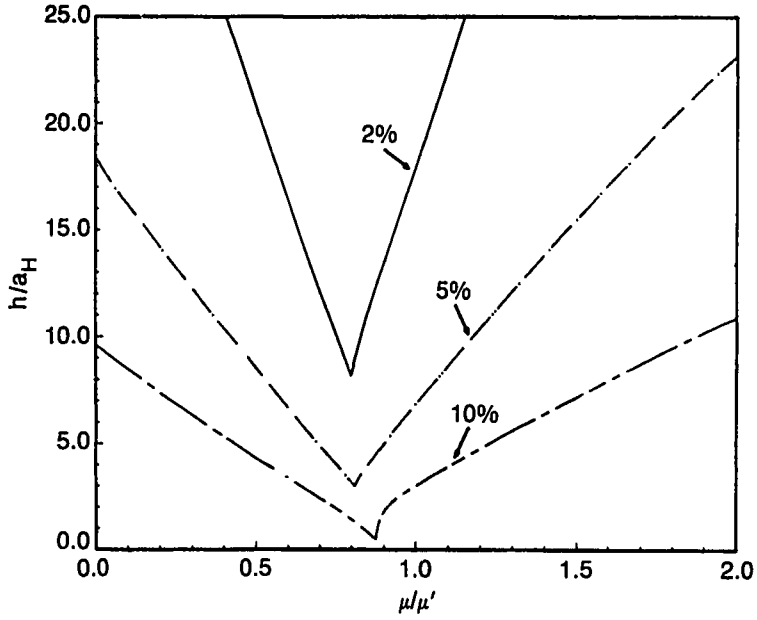

Fig. 9 — Relationship between the normalized film thickness h/a_H and film/substrate stiffness ratio μ/μ' as function of $|\zeta_c - \zeta|/\zeta|$ for accuracies of 2%, 5% and 10%

required minimum film thickness for a given substrate stiffness may be calculated. (2) The results suggest that a good substrate candidate material is about 25% stiffer than the film material regardless of bonding conditions. (3) The ζ_c/ζ ratio vs h/a_H relationships for three different shapes of indenters—conical, spherical, and flat-ended cylindrical—are quite similar despite the large differences in values of the load required for the same penetration depth for the different indenters. Note that this analytical approach is directly applicable to problems in a broad range of engineering disciplines. These include, in addition to the proper determination of film elastic properties as described above, the elastic analysis of ball bearings with surface-coated or surface-modified races, the calculation of elastic forces and displacements in the punching of bilayered materials, and the design of large columns on elastic foundations.

[Sponsored by ONR]

References

1. M. F. Doerner and W. D. Nix, "Plastic Properties of Thin Films on Substrates as Measured by Submicron Indentation Hardness and Substrate Curvature Techniques," *J. Mater. Res.*, **1**, 601 (1986).

2. H. Y. Yu, S. C. Sanday, and B. B. Rath, "The Effect of Substrate on Elastic Properties of Film Determined by the Indentation Test-Axisymmetric Boussinesq Problem," *J. Mech. Phy. Solid*, 38(6), 745-764 (1990). ■

Growth of (100) GaAs by Vertical Zone Melting

R. L. Henry, P. E. R. Nordquist,
R. J. Gorman, and W. J. Moore
Electronics Science and Technology Division

Micrometer- and millimeter-wave integrated circuit (MIMIC) applications of GaAs require crystals that are reproducible and homogeneous with respect to electrical properties. The uniformity requirements for such electrical properties as resistivity, carrier concentrations, and electron mobility demand both crystallographic and chemical perfection of the

GaAs crystals. GaAs is grown commercially by either liquid encapsulation Czochralski (LEC), vertical gradient freeze, vertical Bridgman, or horizontal Bridgman techniques. LEC GaAs is grown in relatively high-temperature gradients that result in high dislocation densities (5×10^4 cm^{-2}) that are not uniform in distribution or in concentration. The nonuniform dislocation density causes a nonuniform concentration of the EL2 defect (an As atom on a Ga site) and, hence, nonuniform electrical properties. All of these growth techniques follow the "normal freeze" model, which is known to result in nonuniform concentrations of impurities (from wafer to wafer along the crystal axis) for impurities with segregation coefficients much different from 1. Nonuniform impurity concentrations cause parallel variations in carrier concentrations and mobilities. The object of our research is to investigate and develop an alternative crystal growth technique that is capable of producing GaAs with improved uniformity and reproducibility.

Zone Melt Model: The vertical zone melt technique (VZM) differs from all of the above-mentioned crystal growth techniques in the fraction of the charge material that is molten at any time. In the "normal freeze" model, the entire charge is melted, and a crystal grows by directional solidification from a seed. The volume of the molten zone decreases as the crystal is grown. In VZM growth, only a portion of the charge material is melted at any given time, and the crystal grows by causing the molten zone to move from a single crystal seed along the length of the charge. The volume of the molten zone remains constant during VZM growth, thus making it possible to either zone level dopants for uniform carrier concentrations or to zone refine to improve the purity of the GaAs.

Growth Procedure: Figure 10 is a schematic of the ampoule used for VZM growth. The GaAs is contained in a pyrolytic boron nitride (PBN) crucible and is encapsulated with boric oxide. PBN is inert and of high purity; boric oxide reduces the loss of volatile arsenic and facilitates removal of the crystal after growth. The ampoule is placed in a multizone furnace consisting of a high-temperature "spike" region bordered by two guard regions of uniform temperature. The spike region melts a portion of the charge, and the guard furnaces maintain the grown crystal at a uniform temperature that is only slightly lower than the solidification temperature. Crystal growth usually entails two passages of the ampoule through the spike region. The first passage forms the charge to the crucible; the second pass melts a portion of the seed and grows a single crystal as the molten zone traverses the charge. Low thermal gradients and the ensuing low thermal stress result in low dislocation densities in the grown crustal. VZM GaAs routinely has uniform dislocation densities of approximately 5×10^3 cm^{-2} (at least an order of magnitude lower than for LEC GaAs) and room-temperature mobilities greater than 6000 cm^2 (V-sec)$^{-1}$. Carbon and neutral EL2 concentrations are regularly 2×10^{15} cm^{-3} and 7×10^{15} cm^{-3}, respectively. Both the defect density and the impurity distribution are more

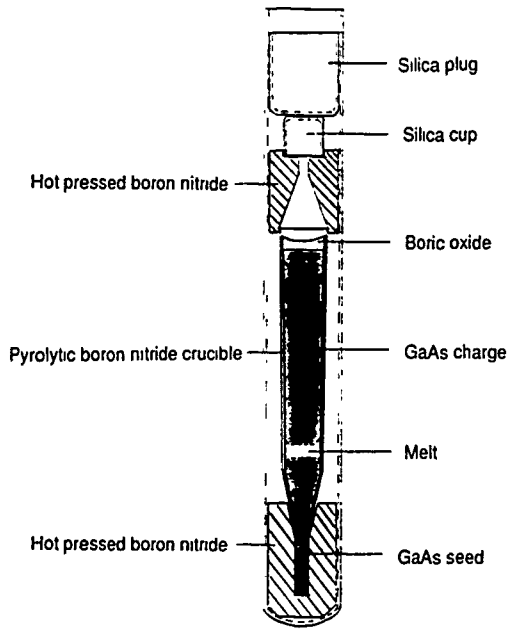

Fig. 10 — The VZM growth ampoule

uniform in VZM GaAs compared to LEC GaAs. Figure 11 shows a 34-mm diameter, (100)-oriented single crystal of GaAs grown by the VZM technique; crystals up to 200 mm in length have been grown.

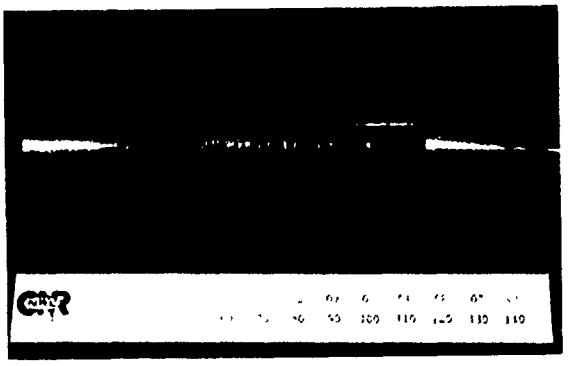

Fig. 11 — (100) GaAs single crystal grown by VZM

Figure 12 shows a plot of the *n*-type carrier concentration along the length of a zone leveled, tin-doped GaAs crystal. The carrier concentration varies from 5.5×10^{16} to 4.5×10^{16} cm^{-3} in going from the first grown portion toward the last grown portion of the crystal. This change in carrier concentration of approximately 20% compares favorably to a change of more than 400% that would be expected for a crystal grown by a "normal freeze" technique.

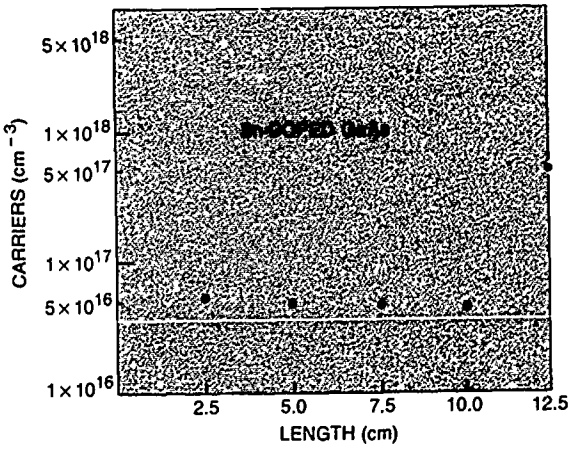

Fig. 12 — $N_d - N_a$ along the crystal axis for a zone leveled, tin-doped GaAs crystal

A MIMIC Phase III program is under way for commercial scaleup to produce 75-mm diameter crystals by the VZM method.

Acknowledgments: We acknowlege Professor John Blakemore and coworkers at the Western Washington University for the EL2 determinations.

[Sponsored by ONT]

Infrared Reflection Absorption Spectroscopy of Adsorbates on Semiconductors

V. M. Bermudez, M. McGonigal,*† S. M. Prokes, and J. E. Butler*
Electronics Science and Technology Division
**Chemistry Division*
†*NRL/NRC Post Doctoral Research Associate*

Nondestructive in situ studies of surface chemical processes under realistic conditions of temperature and pressure are hindered by the lack of applicable diagnostic techniques. There is a particular need for such a capability in the characterization and monitoring of semiconductor processing chemistry (etching, passivation, chemical vapor deposition, etc.). Infrared (IR) vibrational spectroscopy is a potentially powerful technique, but to date, these technologically important applications of surface IR spectroscopy have been limited by a lack of sensitivity relative to that afforded by a bulk metal substrate. This problem is overcome through the use of thin, semiconductor overlayers grown on opaque, metallic underlayers. The resulting samples have the surface chemical properties of the semiconductor with the IR optical properties of the metal. By using this approach, *submonolayer* sensitivity is shown for the adsorption of H_2, H_2O, O_2 and hydrocarbons on Si and for the initial reaction of both ground-state and electronically excited O_2 with GaAs.

The Sensitivity Problem: Optical detection of an adsorbate requires that the electromagnetic field at the surface be maximized. For metals, this is achieved by reflecting light at a high angle of

incidence ($\geq 80°$ with respect to the surface normal) with the polarization set normal to the surface. Nonmetallic substrates exhibit a much lower IR reflectance and, generally, a reduced sensitivity for the detection of adsorbates at low coverages. The solution to this problem takes advantage of the fact that the surface standing-wave field extends a finite distance from the surface (roughly a quarter wavelength or about 1 μm in the mid-IR). Hence, a very thin semiconductor layer (≈ 0.1 μm thick) formed on a metal will appear metallic in IR reflectance. The metal itself need only be sufficiently thick (≈ 0.1 to 0.5 μm) to be opaque in the IR. Such samples can be prepared in a number of ways. Elemental materials (Si or Ge) can be deposited by evaporation onto bulk metals. Metals such as Co can be ion-implanted into Si and annealed, giving a layer of Co silicide (essentially metallic in the IR) buried under a layer of crystalline Si. Compounds (e.g., GaAs) can be grown on metals by molecular beam epitaxy (MBE). A wide range of materials can be studied in this way, limited only by the availability of fabrication technology.

Initial Results: Figure 13 shows data for the chemisorption of isopropyl alcohol (IPA, a common wafer-cleaning agent) on Si in the form of a 40-Å thick layer deposited in vacuum on Ni. The bands near 2100 and 800 cm^{-1} arise from Si-H and Si-O bond-stretching modes, respectively. The others correspond to the C-O stretch (980 cm^{-1}) and to various C-H bending modes. The data show that Si reacts with IPA by breaking the O-H bond, with the H- and $(CH_3)_2CHO$- fragments then bonding to Si atoms. Analysis for C and O by using Auger electron spectroscopy reveals a very low adsorbate coverage, only about 1 IPA molecule for every 50 surface Si atoms. Figure 14 shows data for the initial oxidation of GaAs grown by MBE on a thin layer of Ni silicide. In the absence of electronic excitation of either the GaAs or the O_2, the reaction is relatively slow. However, a hot tungsten filament ($\approx 1500°C$) close to the GaAs during exposure greatly enhances adsorption of the first monolayer. The spectrum for unexcited O_2 shows only a broad band at 850 cm^{-1}, characteristic of Ga-O-As bridges, whereas excited O_2 gives an additional peak at 1000 cm^{-1}. This band is assigned to As = O bonds, which occur in As_2O_5 but not in As_2O_3. The IR data thus indicate a higher As oxidation state for excited vs ground-state O_2. This has important processing implications because of the different reactivity and volatility ofAs_2O_3 and As_2O_5 .

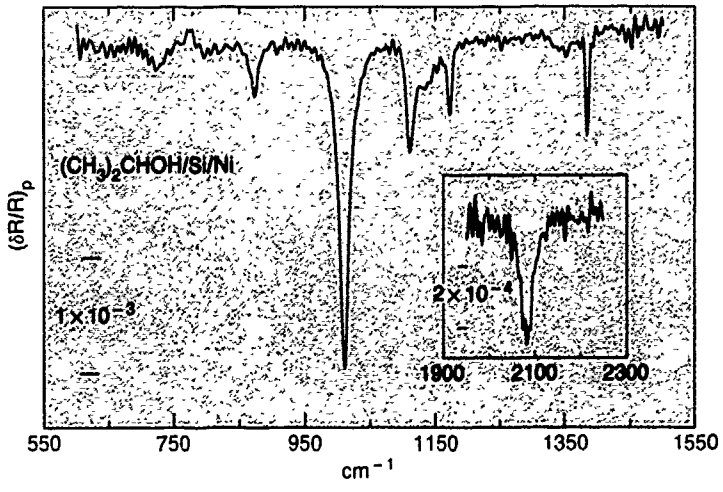

Fig. 13 — Infrared spectrum of isopropyl alcohol (IPA) chemisorbed on the surface of a thin layer of Si deposited on Ni. $(\delta R/R)_p$ is the fractional change in the reflectance of the sample caused by adsorption of IPA. The "*p*" refers to the polarization state of the incident light (normal to the surface plane). The IR photon energy is in wavenumbers (cm^{-1}). Markers are given to show the $(\delta R/R)_p$ scales.

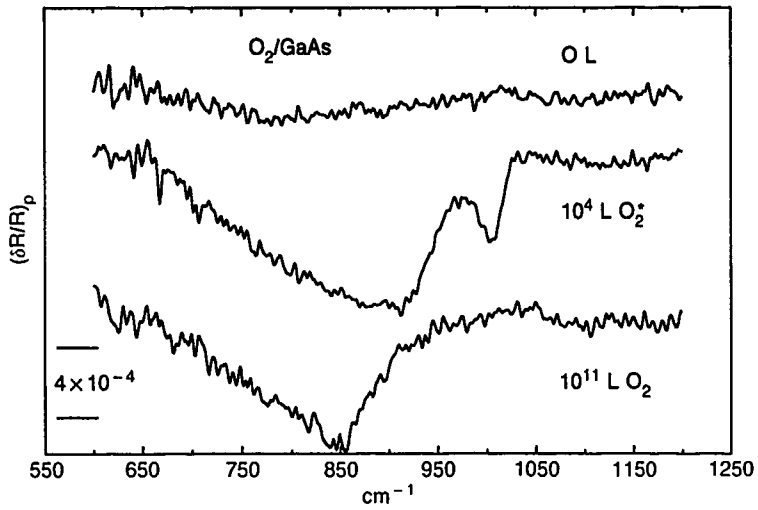

Fig. 14 — Infrared spectra for the chemisorption of ground-state (O_2) and electronically excited (O_2^*) oxygen on GaAs. Excitation of the O_2 is induced by a hot tungsten filament. Exposures are given in Langmuirs *L*, where 1 *L* = 1 s in a gas pressure of 1×10^{-6} torr The 10^{11} *L* spectrum was recorded with the sample in 100 torr of O_2^* Note the much lower exposure required for O_2^* vs O_2 for comparable IR band intensity. The trace labeled "0 *L*" is a baseline spectrum

Future Directions: The methodology outlined above permits studies of chemical processes on nonmetallic surfaces under steady-state conditions (i.e., without interrupting the reaction for surface analysis). Previously, such studies were limited to observation only of species desorbing from the surface. Work in progress includes investigation of the etching of Si and other materials by fluorine and fluorocarbon reagents and the growth of compound semiconductors by organometallic chemical vapor deposition. It is anticipated that reflectance IR spectroscopy can and will be developed into a technique for on-line process monitoring and diagnostics in a manufacturing environment.

[Sponsored by ONR] ■

Numerical Simulation, Computing, and Modeling

NUMERICAL SIMULATING, COMPUTING, AND MODELING

Fundamental and applied research is performed at NRL by using the Cray X/MP supercomputer and other lesser computing devices to simulate and model real-world situations with which the Navy has to deal. Reported in this chapter is work on multidimensional flame instabilities, real-time tracking systems, simulation assessment tools, simulation of shearing force fields, and electrical/thermal component modeling.

The Laboratory for Computational Physics and Fluid Dynamics, the Tactical Electronic Warfare Division, the Research Computation Division, and the Space Systems Development Department contributed to the work presented here.

Other current research in numerical simulating, computing, and modeling includes:

- Simulation of 3-D spacially evolving plane wakes
- Electromagnetic wave scattering
- Simulation of energetic deposition of Ag thin films
- Modeling of fluid exchange processes
- Parallel thought
- Radar scan-pattern models
- Transient signal modeling
- Simulation of corrosion prevention
- Molecular-dynamics simulation

Multidimensional Flame Instabilities

K. Kailasanath and G. Patnaik*
Laboratory for Computational Physics and Fluid Dynamics
**Berkeley Research Associates*
Springfield, Virginia

Instabilities play a dominant role in determining the structure and dynamics of flames in many premixed gases that are near flammability limits. Therefore, it is important to understand flame instabilities to determine the mixture in which the flame does not burn (i.e. flammability limit). Three major instabilities that might occur in laminar flames in premixed gases are: (1) hydrodynamic instability (because of fluid expansion), (2) thermo-diffusive instability (because of unequal heat and mass diffusion), and (3) Rayleigh-Taylor instability (because of buoyancy). Theoretical stability analyses can provide information on the roles of various processes at the onset of instability. However, the prediction of the growth of this instability to the final form is beyond the scope of these analyses. Detailed numerical simulations can be used to understand both the onset of the instability and the evolutionary process that produces the multi-dimensional flame. The term detailed numerical simulation is used to signify that the calculations include all the relevant physical and chemical processes that could lead to the various types of instabilities. NRL has taken the lead to develop the multidimensional, reactive-flow capabilities for performing such complex simulations. Here we present highlights of our research effort.

Cellular Flames in Zero Gravity: Recent experiments in a reduced gravity environment show that even among flames that exhibit a cellular structure, there are significant differences in the dynamics. In some mixtures, the flame cells grow and split into smaller cells while in others, they maintain a cell shape and size that does not change in time. We have used a detailed numerical model to simulate this phenomena. Figure 1 shows a flame in which the cells split into smaller cells. Temperature and OH radical concentrations are used to depict the flame in the picture. We see that the flame, which has only two cells at 80 ms, splits into multiple cells by 100 ms. Further systematic numerical simulations have been used to show that a thermo-diffusive instability mechanism is the dominant mechanism responsible for the formation of these cellular flames [1].

Effects of Gravity: On Earth, upward- and downward-propagating flames have been observed to have very different shapes (or structures). We have used our detailed flame model to simulate these flames and to understand the fundamental reasons for their different structures. We found that mixtures with more than 15% hydrogen in air are affected only slightly by gravity. For mixtures with lesser amounts of hydrogen, significant differences can be noticed between the structure and dynamics of flames propagating upward, downward, or in zero gravity. Figure 2 shows one such case, where OH radical concentrations are used to depict the flame at a sequence of times under upward, zero gravity, and downward propagation. The upward-propagating flame is highly curved and evolves into a bubble rising upwards in the tube; the zero-gravity flame shows a cellular structure; the structure of the downward-propagating flame oscillates between structures with convex and concave curvatures toward the unburned mixture. These observations have been explained on the basis of an interaction between processes leading to buoyancy-induced Rayleigh-Taylor instability and the thermo-diffusive instability [2].

Detailed Flame Model: The simulations discussed have been performed by using FLIC2D, a detailed two-dimensional flame model developed at the Laboratory for Computational Physics and Fluid Dynamics. The model includes the fluid dynamic conservation equations in two dimensions, coupled ω a detailed chemistry

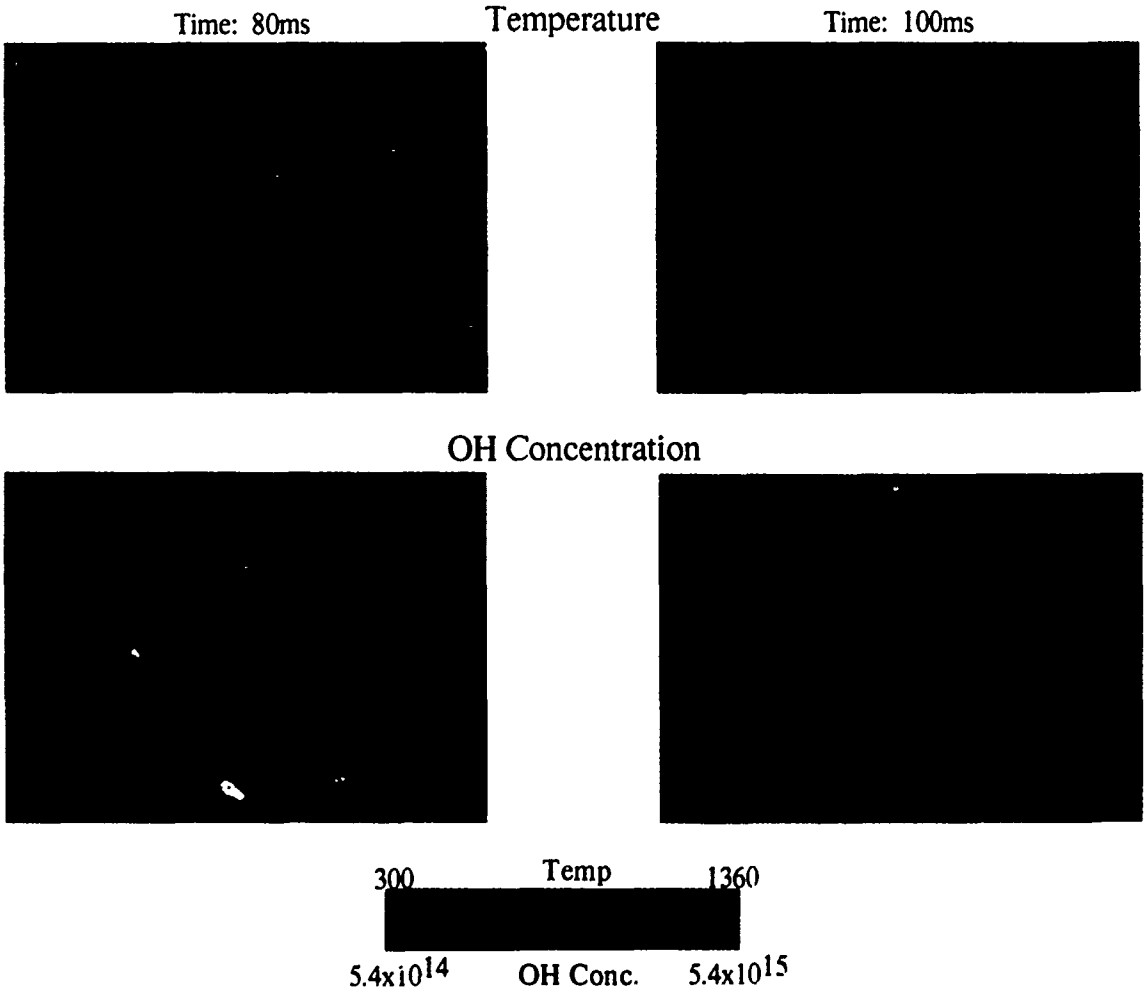

Fig. 1 — Cellular flames in zero gravity, H_2:0_2:N_2/1.5:1:10, 5.1–cm channel

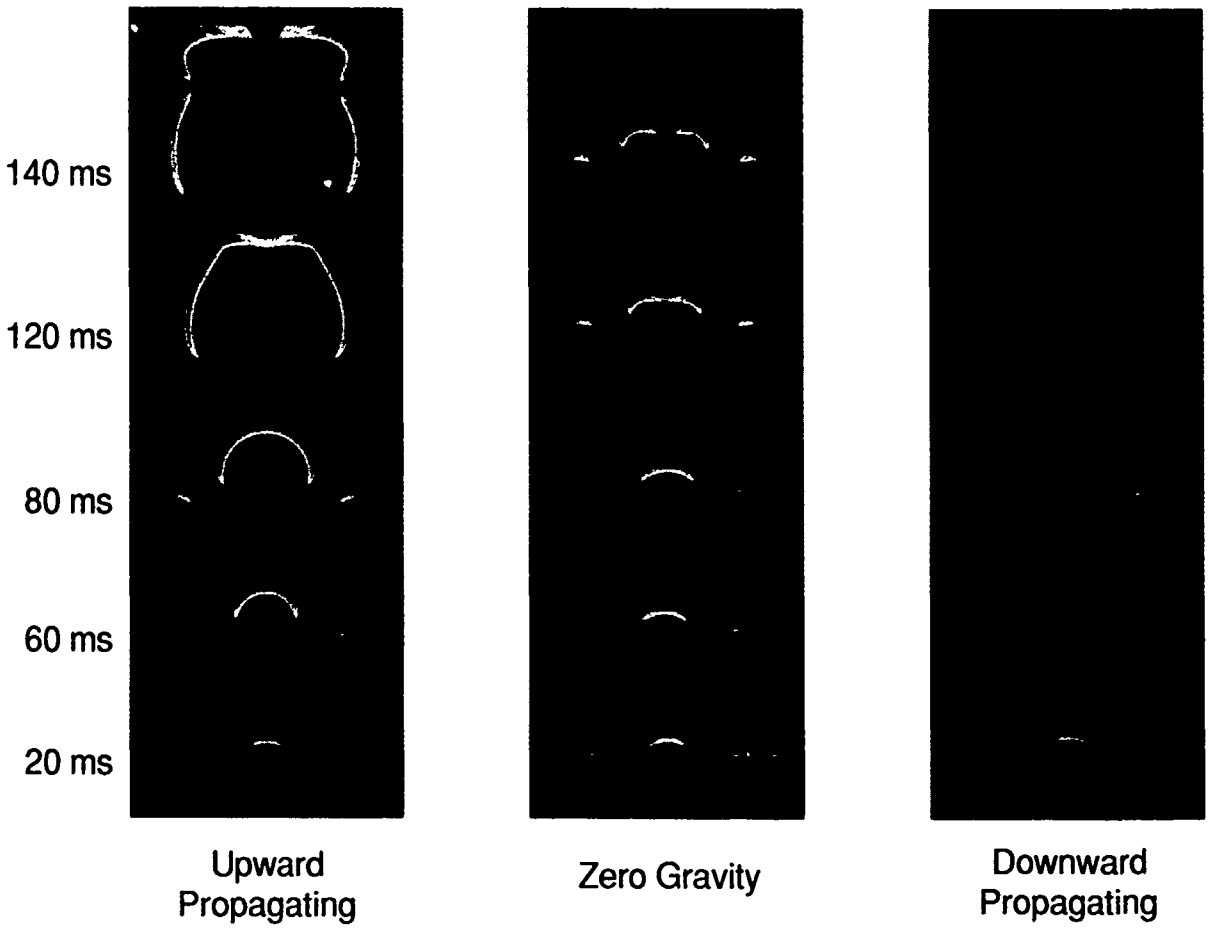

Fig. 2 — OH radial concentrations are used to depict the flame at a sequence of times under upward zero gravity and downward propagation (10% hydrogen–air mixture)

model with fifty reactions and complete thermal conduction and species diffusion models. The large number of computational zones required to achieve the high numerical resolution in two dimensions requires long computational times, especially when we are dealing with detailed chemistry.

Summary: Numerical simulations using a detailed flame model have led to a better understanding of the various instabilities that lead to the complex structure and dynamics of flames. The simulations show that the hydrodynamic instability is important only for flames in very large systems. Gravity plays an important role in determining the behavior of flames with low burning velocity. Typically such flames occur in nearly nonflammable mixtures. Therefore, the study of these multidimensional flame instabilities is important both for the better understanding of flames as well as for safety.

[Sponsored by NASA and ONR]

References

1. G. Patnaik, K. Kailasanath, K.J. Laskey, and E.S. Oran, "Detailed Numerical Simulations of Cellular Flames," Proceedings of the 22nd International Symposium on Combustion, The Combustion Institute, Pittsburgh, pp. 1517–1526, 1989.
2. G. Patnaik, K. Kailasanath, and E.S. Oran, "Effect of Gravity on Flame Instabilities in Premixed Gases," accepted for publication in *AIAA Journal*, American Institute of Aeronautics and Astronautics, Washington, D.C., 1990. ■

New Approaches to Multiple Measurement Correlation for Real-time Tracking Systems

J.K. Uhlmann and M.R. Zuniga
Information Technology Division

Introduction: Gating is an important component of most multiple-target tracking systems. Its function is to identify sensor reports such as radar or IR returns from missiles, planes, etc., which correlate highly with current state estimates or tracks. For small numbers of objects, it is feasible to calculate a probability of correlation for every track/report pair and reject those whose measures of correlation fall below some threshold. For large numbers of objects, however, quadratic growth in the number of pairs for which correlation probabilities are computed by this "brute force" approach represents an enormous bottleneck. This combined problem is of particular concern in high-density tracking environments requiring numbers of objects on the order of 10^5 to 10^6 to be processed in real time. We discuss new theoretic as well as practical results developed at NRL (Patent application case number 73167) that have enabled simulations of the correlation process to be performed on a Sun-4 workstation with scenarios consisting of millions of objects. We also discuss parallelization approaches that suggest the feasibility of processing such scenarios in real time on presently available parallel and multiprocessing architectures such as NRL's Connection Machine and TC-2000.

The Gating Problem: The gating problem can be stated technically as follows. Given a motion model and a set of tracks consisting of current state estimates with associated error covariances and a set of sensor reports consisting of measurement time stamps and position measurements with associated error covariances, determine in real time which pairs (i, j) satisfy the gating criterion

$$S_{ij}(dX_{ij}, \Gamma_j) = \frac{\exp(-dX_{ij}^t \Gamma_j^{-1} dX_{ij}/2}{(2\pi)^{\frac{d}{2}} \sqrt{|\Gamma_j|}}, \quad (1)$$

and

$$S_{ij} \leq S_j, \quad (2)$$

where d is the measurement dimension, dX_{ij} is the residual vector difference of report i and track j (projected to the time of the report), Γ_j is the residual covariance of the track, and S_j is the gating threshold selected for the track. The efficient identification of pairs that satisfy the gate can be accomplished by deriving from the gating threshold a search volume for each report, thus limiting the number of correlation candidates that must be examined. This transforms the problem from probability space into Euclidean space where efficient computational geometric methods can be applied The calculation of the volume depends on the report and track covariances, the gating threshold, and the maximal time differentials between the current states of the tracks and the observation times of the reports. Methods for calculating appropriate search volumes are developed in Refs. 1 and 2.

Efficient Searching: To efficiently identify the tracks within the gating radius of each report, the tracks may be placed into a search structure from which the desired set can be retrieved without having to examine every track. (Techniques for exploiting additional information about the sets of tracks and reports are discussed in Ref. 3.) Multidimensional tree data structures having storage requirements proportional to the number of tracks N_T are known that provide this capability [4]. They require only $O(N_T \log N_T)$ setup time and between $O(d \log N_T + k)$ and $O(N_T^{1-1/d} + K)$ average retrieval time, where k is the average number of tracks found per report and d is the number of dimensions of the search space. The correlation algorithm described in Ref. 1 uses multiple search structures consisting of tracks projected to various times with the scan period. These data structures are relatively

straightforward to map onto a Multiple Instructions or Multiple Data (MIMD) parallel processing machine having P processors to achieve an $O(P)$ speedup. The mapping onto Single Instruction or Multiple Data (SIMD) architectures is somewhat more complicated, but generally efficient techniques have been developed [5].

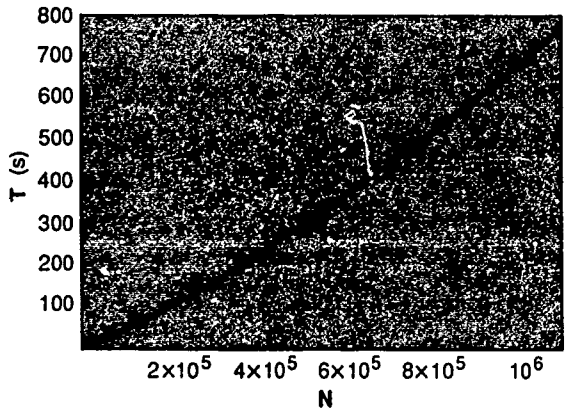

Fig. 3 — CPU times of the search algorithm fitted with an $N \log N$ function (solid line). N = number of tracks = the number of reports. T = the search time in s. Simulation performed on a Sun4 workstation.

Test Results: Rigorous analysis demonstrates that subquadratic scaling can be expected for the over-all gating process even when measurement time stamps are widely distributed [1]. A discussion of the conditions required for the use of efficient search structures is provided in Ref. 3. An optimality criterion for the calculation of search volumes is developed in Ref. 2. To verify run-time behavior predicted by these theoretic results, the authors tested the critical search component of the algorithm on single time steps (or scan periods) from scenarios ranging in size from $N_R = N_T =$ 1024 (1 K) to over one million (1 M) objects. Uniform target density was maintained so that for each scenario, approximately five reports gated with each track. Results in Fig. (3) suggest that for the number of objects tested, the scaling of the search algorithm is dominated by $O(N \log N)$, though careful analysis suggests the possibility of small contributions from higher order (e.g., $N \log^2 N$) terms. We emphasize that the results do not include the time spent evaluating Eq. (1), since the interest here is in scaling behavior; however, note that for a 10-s scan period, as many as 16 K gates are identified in real time. It is also surprising to observe that only a factor of 75 speedup over the Sun-4 used in our tests is required to process 1M objects in real time. NRL has both MIMD and SIMD architectures (BBN TC-2000 and Connection Machine, respectively) as well as Cray and Convex supercomputers on which such a speedup may be attainable.

[Sponsored by SDIO]

References

1. M.R. Zuniga, J.M. Picone, and J.K. Uhlmann, "Efficient Algorithm for Improved Gating Combinatorics in Multiple-Target Tracking," submitted to *IEEE Trans. Aerospace and Electronic Sys.*, Apr. 1990.

2. J.B. Collins and J.K. Uhlmann, "Efficient Gating in Data Association for Multivariate Gaussian Distributions," submitted to *IEEE Trans. Aerospace and Electronic Sys.*, Feb. 1990.

3. J.K. Uhlmann, M.R. Zuniga, and J. M. Picone, "Efficient Approaches for Report/ Cluster Correlation in Multiple-Target Tracking Systems," NRL Report 9281 (1990).

4. J.K. Uhlmann, "Enhancing Multidimensional Tree Structures Using a Bi-Linear Decomposition," NRL Report 9282 (1990).

5. G.E. Blelloch, "Scan Primitives and Parallel Vector Models," Ph.D. dissertation, Department of Electrical Engineering and Computer Science, Massachussetts Institute of Technology, 1988. ■

Coherent Information Management for Coordinated Simulation Assessment

C.E. Dunham
Tactical Electronic Warfare Division

The Naval Research Laboratory's Tactical Electronic Warfare (TEW) Division performs research and develops effective concepts, technologies, and systems to enhance EW in order to provide protection against a diversity of threats. Computational and laboratory facilities are used by both high-level and expert users for battle force EW assessment, concepts testing, requirements validation, and tactics development in scenarios appropriate to the Fleet environment. Coordination of critical information and access to data resources are required for performing an assessment or for structuring a model to address a specific response. At present, information from the variety of analyses and tests performed is available in different formats ranging from paper charts to digitized data. Also, data on related projects have not been fused and verified. The poor accessibility of these types of data to the qualified user has resulted in higher costs and greater manpower expenditures for information gathering.

Our research efforts' goal is to develop software tools that facilitate coordination and assessment in the EW R&D environment. Coordinated Simulation Assessment Tools (CSAT) is a prototype system that supports standards for high-level control and access to data, simulation(s), and model development. We have demonstrated the ability to coordinate and effectively use relevent information and resources with a unique architecture by using the MIT X-Window protocols that integrate the IBM/PC, Macintosh, and VAX-based workstations on the division's LAN (TEWnet).

CSAT Architecture: Our system architecture stresses a hierarchial model for simulation, gateways to nonconforming data environments, modularity with consistent and standard interfaces for operating in an integrated network environment. A synergism of these results is referred to as the Digital Resource Facility (DRF) and is shown in Fig. (4). DRF is a distributed user operating environment that provides high-level, user-friendly access to data resources, consistent interfaces to simulation modeling components, and flexibility to accommodate the casual and expert user.

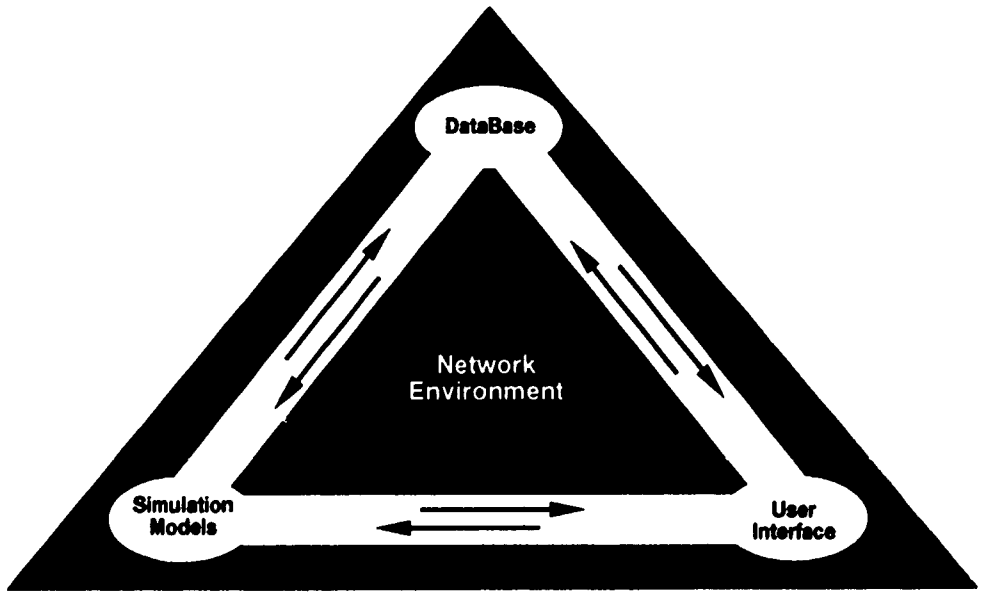

Fig. 4— The Digital Resource Facility provides a distributed network comprised of database resources, simulation environments, and coherent access to multiple users

Simulation Architecture: Our research with current technology and software has lead us to a hierarchical approach in which simulation components can be integrated, synchronized, and controlled. This architecture, when fully developed, will support and be capable of importing model elements from other simulations with minimal conversion effort.

The hierarchial model achieves flexibility by considering the simulation elements as entities, called platforms. Platforms are associated and linked with other platforms either through a local interface or by a global environment. The operation of a specific platform is related only to its interface with other related elements at the same level. At the lowest level are those platforms that collectively contribute to the definition and dynamic attributes at the next higher level. Each level or layer is a collection of modular functions whose definition and structure is achieved by integrating elements at lower layers in a standard way. Each modular unit communicates with other modules that share that layer. Collectively these units provide the data and information that are passed by way of the parent component to similarily related components at the next higher level. By this method, the development (and subsequently, the operation) of a specified platform module is concerned only with its interfaces to other related systems.

Modular Interface: The modular interface allows coherent integration of all aspects of models and data. New capabilities are efficiently integrated into a simulation or a database environment and upgrades (fidelity improvements, improved intelligence data, etc.) are implemented with minimal impact. An added benefit is the ability to rapidly prototype and test alternatives and to select from a collection of models and thereby allocate a model to any selected unit during pre-execution without code changes. Implicit in this approach is the ability to coordinate multi-disciplinary and often nonconforming data environments for query and for direct access to both static and dynamic simulation data. Of particular significance is the availability, as part of a database, of resident interface descriptions and model specification data to verify possible scenarios and to provide efficient configuration management. Figure 5 shows this network coordination.

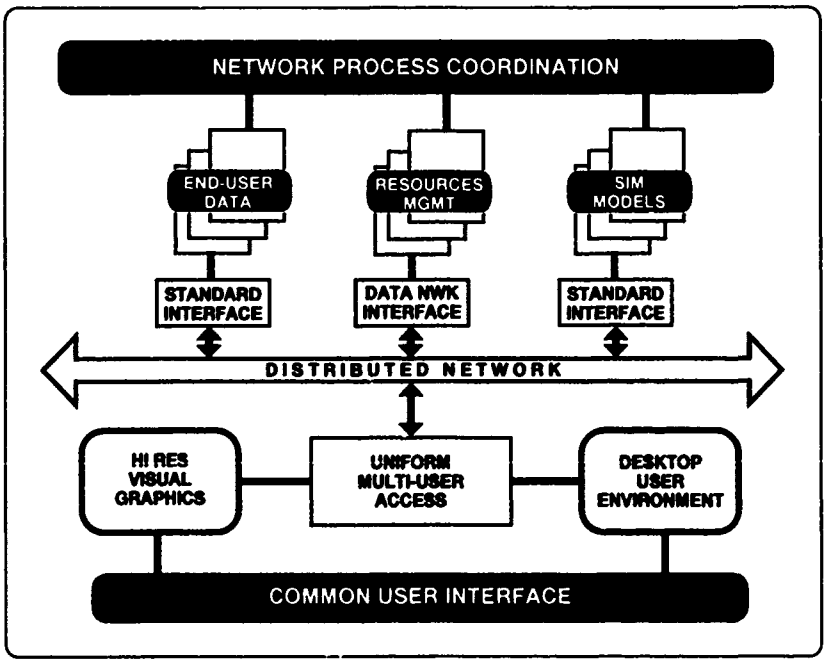

Fig. 5 — The CSAT prototype, as configured on the TEW C-LAN X-Window protocols, is used to implement access to technical data, the simulation environment, and user workstation interfaces

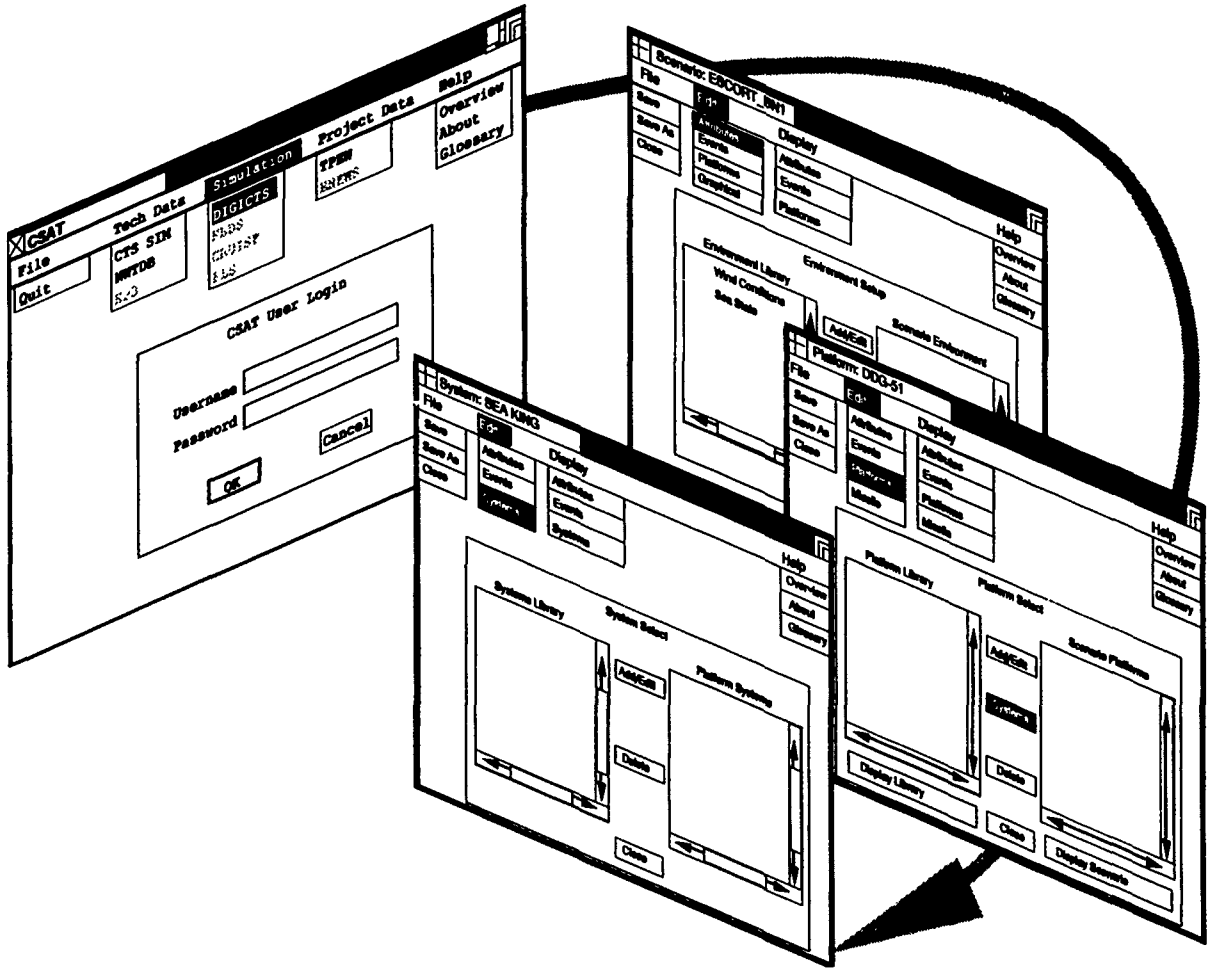

Fig. 6 — Hierarchical view of a typical sequence of windows and pull-down menus as viewed by the analyst when configuring a simulation scenario under CSAT

User Interface: The user interface is comprised of a window hierarchy of pull-down menus. The highest level provides access to technical data, the simulation environment, and administrative functions. Technical data is comprised of gateways to heterogeneous data environments. At the present time, access is provided to the simulation database and to the Navy Warfare Tactical Database (NWTDB). The simulation environment consists of multiple simulation applications. Presently, the CTS simulation is operational and uses the hierarchical model in addition to the development prototype that we are using to establish interconnectivity to other models within the TEW Division. The administrative functions provide access to higher level project information for users at all levels; for example, preparing status reports, executive level queries, programmatic information, etc. This includes word processing functions that allow researchers and project managers to augment information and prepare reports. This is all accomplished at the desktop, and all communications and information is processed by the distributed network. Presently, access is available to the EW Block 6.2 research program. Information processed in this system is used to augment a Tri-Service EW database (JDL/TPEW).

User windows in the CSAT application, as Fig. 6 shows, are designed to provide a consistent "look and feel." This consistency provides access to applications that benefit both the casual and expert user. We have demonstrated that this consistency allows the user to transfer skills from application to application. Access is easy to learn and easy to use and shows substantial improvement in productivity. Within our own research environment, we have noted significant user satisfaction and reduced aggravation. The CSAT family is designed for consistency in both the platforms and the program interface development. This consistency is maintained through the use of the X-Windows protocol that allows the same graphical user interface to appear at all the platforms on which CSAT operates.

Summary: Our results from the (CSAT) development program allow multilevel sharing of EW information from a diversity of resources such as databases, simulation and measurement facilities, and test results. These elements are essential to improving the EW R&D process; activities include determining programmatic requirements, collecting data to perform assessments, and structuring models to address a specific EW response. This requires integrating users with differing levels of technical knowledge to a strong and coherent technical information system. In many cases alternative solutions must be tested, evaluated, and validated in a realistic, technically practical and cost-effective simulation environment. In others, it permits bringing together key information to formulate strategy or simply to formulate a response to questions and queries. The CSAT program is designed to achieve these objectives.

Acknowledgement: Significant contributions to this research continue to be made by the CTS Software Systems Group at NRL in collaboration with Engineering Research Associates, Inc.

[Sponsored by ONT]

Molecular Dynamics Simulations of Shearing Force Fields in a Liquid

J.H. Dunn
Research Computational Division
and
S.G. Lambrakos and P.G. Moore
Materials Science and Technology Division

Introduction: Determining the effect of additives, especially polymers, on the shear viscosity of water is of current interest to the Navy. The shear viscosity of a fluid determines the drag on an object moving through the fluid. Thus, by reducing the shear viscosity, the drag is reduced. One naval application uses water additives near the hulls of submarines. Reducing the shear viscosity of water near the hull of a submarine reduces drag and increases its top speed. The task, then, is to design an additive that will achieve the greatest drag reduction for a given concentration and will, depending on the application, retain its drag-reducing qualities for a sufficient period of time.

Here we describe a method for determining the shear viscosity of a liquid based on nonequilibrium molecular dynamics simulations. This method is based on the work of Gosling et al., [1]. Further, we present the results of computational experiments performed with the method. Finally, we state conclusions concerning the method and its applicability to the analysis of the drag-reducing materials.

Determination of Shear Viscosity: Currently, two basic methods are used for determining shear viscosity by molecular dynamics simulation. One is based on the calculation of shear viscosity from -relation functions computed during the simulation. This method requires fairly long simulations to be statistically significant. The other is non-equilibrium molecular dynamics. This is based on modeling the shear viscosity with a macroscopic equation of motion and fitting the response of the sample to this equation. It is still an open question as to which method is better, since each method has

its relative merits. The correlation function formulation is based on standard equilibrium molecular dynamics methods and is easily implemented. The nonequilibrium formulation is generally more accurate but requires more complex analysis and programming structures and, thus, is less widely used.

We have chosen the nonequilibrium approach to hopefully gain a better understanding of the method. Further, it is more computationally tractable because the object of the simulation is a quantitative determination of drag-reducing influences rather than a shear viscosity measurement. Each nonequilibrium run is short in duration when compared to the equilibrium approach. Thus, one or two nonequilibrium runs at each state point can give an overall qualitative estimate of how the resistance-to-shear varies with parameters such as temperature and pressure for relatively small cost.

The procedure begins by performing molecular dynamics simulations at a specified temperature and pressure, i.e., the state point. Once the sample has reached equilibrium, configurations are saved to use as starting points for the nonequilibrium simulations. These configurations are taken from an ensemble at the state point and represent data points that make up the statistical sample used to characterize shear viscosity. The calculation of shear viscosity requires maintaining steady state conditions on the system. A shearing force that depends only on z is applied in the x direction, and the fluid dynamic equations of motion, the Navier-Stokes equations, become

$$\eta \frac{d^2 u_x}{dz^2} + \left[\frac{\rho}{m}\right] F(z) = 0, \qquad (1)$$

where η is the shear viscosity, ρ is the density, and u_x is the velocity in the x direction. Integrating twice with respect to z gives

$$u_z(z) = \left[\frac{\rho L^2 F_0}{4\pi^2 m\eta}\right] \sin\left[\frac{2\pi z}{L}\right], \qquad (2)$$

where L is the length of the molecular dynamics sample in the z direction. Each equilibrium configuration is subjected to several shearing force magnitudes F_0. During each shearing run, $u_x(z)$ is binned at several time points in the simulation. Figure 7 shows how these velocity histograms are then fit to a sine function

$$u_x(z) = C\left[\frac{F_0}{m}\right] \sin\left[\frac{2\pi z}{\tau}\right], \qquad (3)$$

The Cs are then regressed against (F_0/m) to factor out the force dependence, and an estimate of the shear viscosity for each configuration is calculated by using Eq. (2). These estimates are then averaged, and a standard error is calculated. Thus, the more samples are used, statistically the better the estimate of η.

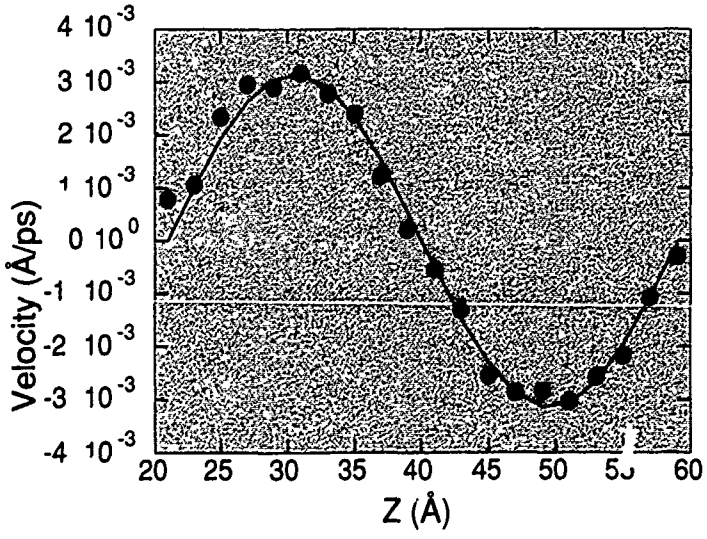

Fig. 7 — Observed and fitted velocity, points and solid line, respectively vs z coordinate in sheared liquid Ar

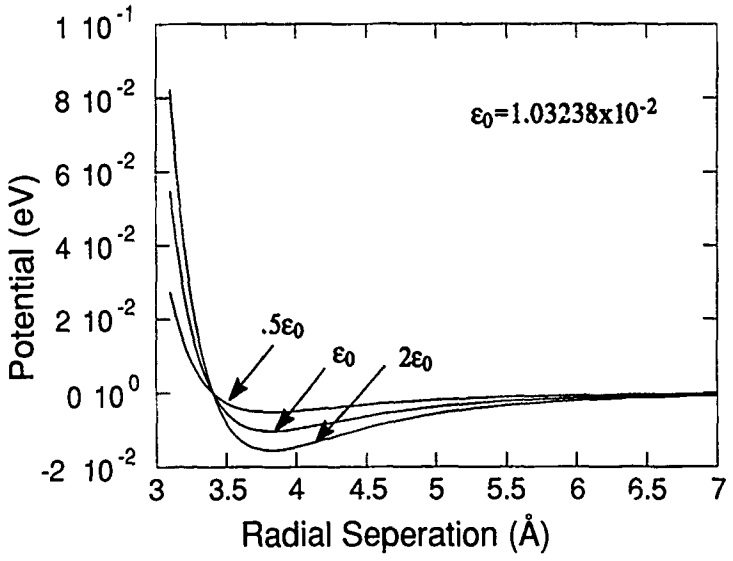

Fig. 8 — Lennard-Jones potential as a function of well-depth

Conclusion: Two distinct computational experiments were performed to investigate the utility of the nonequilibrium approach as a tool for analyzing the influence of additives. First, liquid argon (Ar) was simulated at two temperatures. These results were compared to experimental data, and the experimental results are well within the error bars on the computed values, which are less than 4%. This comparison shows good correlation between computation and experiment over a fairly wide range of temperatures of an inert liquid.

Second, the sensitivity of the method was tested to determine whether changes in the intermolecular potential (in particular, the well depth) would produce changes in shear viscosity. The intermolecular potential is the standard Lennard-Jones 6 to 12 potential. Figure 8 shows that the values of the well depth ϵ varied from the standard Ar values by 50%. As expected, increasing the well depth increases the shear viscosity, as seen in Fig. 9.

These experiments show that the method is both sensitive to changes in the potential function and that it is reasonably accurate. The first result is important if the utility of various polymers as drag reducers is to be differentiated. The second is important so that the relative gain in drag reduction measured by this method is close to the actual gains that will be achieved. This method then offers a faster way of determining the relative utility of different polymers as drag reducing agents than conventional equilibrium methods.

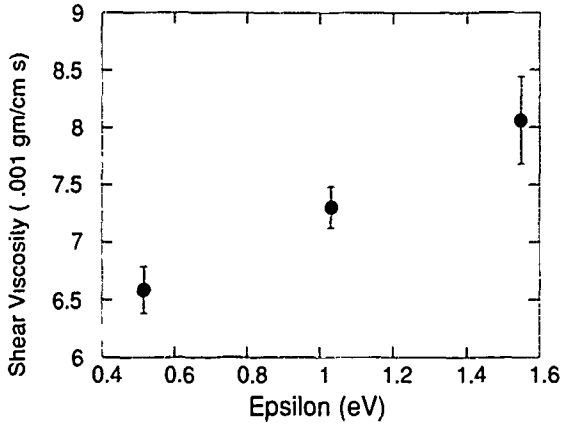

Fig. 9 — Sensitivity of the estimate of shear viscosity to changes in well-depth

[Sponsored by DARPA]

Reference

1. E.M. Gosling, *Molecular Physics* **26**(6), 1475-1484 (1973). ■

Integrated Electrical/Thermal Component Modeling

D.J. Shortt and W.E. Baker, Jr.
Space Systems Development Department

The Space Systems Development Department is concerned with accurately determining the performance of power electronic circuits under various types of thermal conditions for many Navy spacecraft applications.

The electrical performance of practically all components is directly related to the component's temperature. For some low-power and/or low-precision components and circuitry, these effects are noncritical and often ignored. For high-power and/or high-precision components and circuitry, the effects of component temperature are critical and must be accounted for to accurately predict circuit performance.

The commonly used circuit analysis program, Simulation Program Integrated Circuit Emphasis (SPICE), does not have the ability to dynamically modify the temperature of specific circuit elements. But by modeling device thermal characteristics with electrical analogs, the integrated thermal/electrical performance of the modeled devices can be predicted. The models will dynamically simulate individual device temperatures and electrical performance at temperature. The integrated model can be used to analyze the electrical and thermal effects of device power dissipation for many Navy spacecraft electronics applications.

Integrated Component Models: To integrate component temperature effects (self-heating or induced heating) into the simulation, an electrical analog of the thermal "circuit" is coupled to the electrical circuit. Figure 10 shows the electrical analogs of the thermal parameters.

Thermal resistances are calculated from data given in manufacturers data books or determined by tests. These resistances can be the junction-to-case and/or the case-to-sink thermal resistance of a semiconductor or perhaps the case-to-air thermal resistance of a resistor.

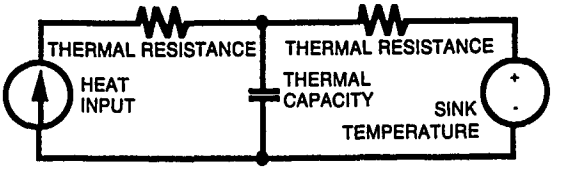

Fig. 10— Thermal circuit

The thermal capacity is determined by multiplying the mass of a device by the specific heat of its predominant material (convert calories to W/s by multiplying by 1.163E - 3). To accurately model a thermal circuit, several series RC circuits may be required. The number of thermal elements to include is determined by the accuracy desired. The current source is the equivalent of heat input, i.e., the power dissipated in a component. The voltage source on the right of the circuit is the temperature of the heat sink or ambient air. Voltages everywhere in the circuit can be interpreted as temperature.

The process of coupling the electrical and thermal performance is to (1) calculate component power dissipation, (2) couple this power as heat input to the thermal circuit, and (3) couple the resulting temperature back to modify the components' electrical parameters.

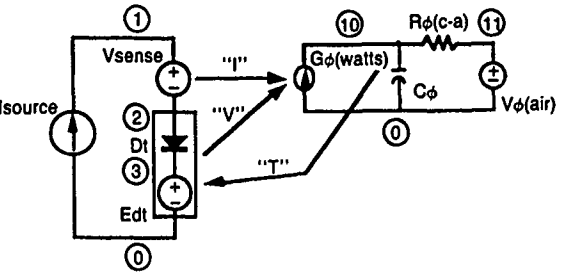

Fig. 11 — Diode electrical/thermal model

Figure 11 shows the circuit components and linkages used in a Personal Computer Simulation Program Integrated Circuit Emphasis (PSPICE) [1] diode simulation [2]. The dependent current source *Go* is used to multiply the component current and voltage to get power dissipation. The thermal capacitance *Co* is calculated from the

specific heat of the material multiplied by its mass. The thermal resistance from the diode junction to the sink ($Ro(c - s)$) is determined from the manufacturer's data sheet. The sink temperature is simulated by the voltage source Vo (air).

A PSPICE listing is included in Ref. 2. Although this process may appear cumbersome, a library of temperature-dependent components can be created for use whenever desired. Once the initial library parts are created, they can be recalled and modified as appropriate.

Implementation and Experimental Results: A solar cell was simulated by using the circuit described in Ref. 3. The electrical/thermal model is based on the description of the performance of the open circuit voltage V_{oc} and the short circuit current I_{sc} as a function of the device temperature. Figure 12 is a schematic of the model.

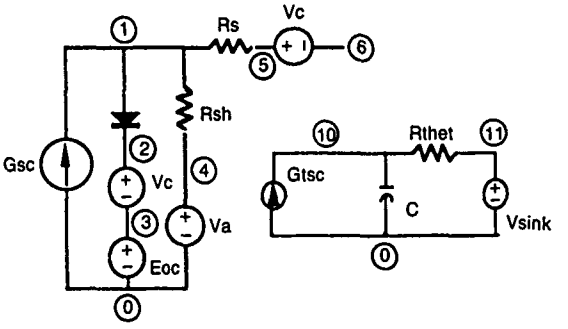

Fig. 12 — Solar cell model

Reference 2 gives the PSPICE netlist for this example. Figure 13 shows the model simulation result with data obtained from laboratory testing. Note that the result accurately predicts the solar-cell power output as the temperature is varied.

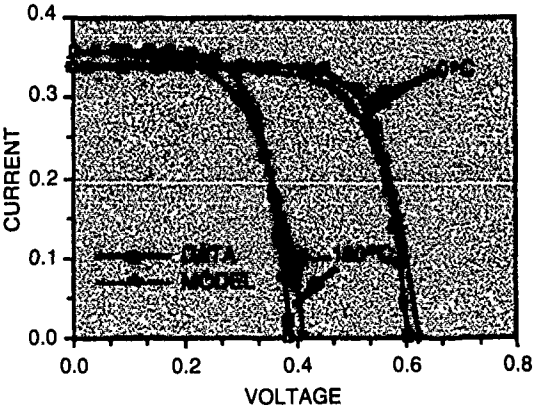

Fig. 13 — Solar cell I/V data

Conclusions: An accurate way of electrically and thermally modeling components in PSPICE is presented and verified. This method uses electrically equivalent thermal models to interactively determine the model performance. This model can be applied to describe many different examples. This paper presents one power example, a solar cell. Reference 2 gives other examples. The simulation results show the model's accurate prediction over a wide range of temperatures.

[Sponsored by ONR]

Reference

1. PSPICE, Microsim Corp., Irvine, CA., 1989.

2. W.E. Baker and D.J. Shortt, "Integrated Electrical/Thermal Component Modeling," Proceedings of the 1990 IECEC.

3. H. Rauschenbach, *Solar Cell Array Design Handbook* (Van Nostrand Reinhold, New York, 1980). ■

Optical Science

OPTICAL SCIENCE

Holography, optical data processing, optical warfare, space and fiber optics, laser development and laser–matter interactions, IR surveillance, and waveguide technology constitute much of NRL's research in optical science. Reporte i in this chapter is work on fiber-optic electromagnetic pulse testing and nonlinear optics.

The Optical Sciences Division performed the work described here.

Other current research in optical science includes:

- Nonlinear optical spectroscopy
- Diamond films
- Laser windows for heavy metal fluoride glass
- High-power semiconductor amplifiers
- Nonlinear mirrors
- Magnetorestrictive oscillators
- Open-loop fiber gyroscopes

Electromagnetic Pulse Testing with a Fiber-Optic Sensor

W.K. Burns, R.P. Moeller, and C.H. Bulmer
Optical Sciences Division

Electromagnetic pulse (EMP) testing of Navy airplanes is an important factor in ascertaining nuclear survivability. Testing is done at large simulators that are capable of generating very high electromagnetic fields (~ 50 kV/m) in a very short (~ 10 ns) pulse. Currently, electromagnetic detection devices used to measure electric field strength measure the rate of change of the electric flux density D. This parameter is directly related to the electric field vector E. These detectors, referred to as D-dot probes, have distinct disadvantages because of their nondielectric nature (which perturbs the field) and their requirements for an integrator to obtain the E field. D-dot sensors generally require electrical power at the sensor head, and signal output is usually over coaxial cable. We have applied fiber-optic technology to this measurement problem, which avoids some of the drawbacks of the D-dot sensors.

Fiber Optical Sensor: The sensor used was an integrated optical light modulator made on an electro-optic substrate (lithium niobate) by a titanium indiffusion process. This modulator converts an electrical signal into amplitude modulation of the transmitted light by converting an applied voltage to an optical index change via the electro-optic effect. An antenna is used to convert the E field into an applied voltage. The modulator was packaged in a metal box about 1 in. $\times$ 3 in. $\times$ 6 in. and connected to optical fibers for signal input and output. The optical signal can be detected remotely and provides a temporal replica of the electrical pulse at the antenna. Future sensors would be placed in a dielectric package.

EMP Test: Testing was carried out at the horizontally polarized dipole EMP simulator at the Naval Air Test Center (NATC), Patuxent River, Maryland. The sensor head was mounted on a movable boom, which could be located various distances from the pulser. The optical sensor output was compared to an EGG D-dot probe. Figure 1 shows the response of both sensors after integration of the D-dot probe signal. The signal fidelity between the two sensors was good, showing that the optical sensor had an adequate response time to measure the short pulse. Figure 2 shows that the optical sensor was approximately linear over the range of test fields, where the optical-sensor output is plotted against D-dot sensor output. The optical sensor does have a sinusoidal output, but it is nearly linear within a limited range, determined by the antenna size. Signal-to-noise ratio (SNR) was always better

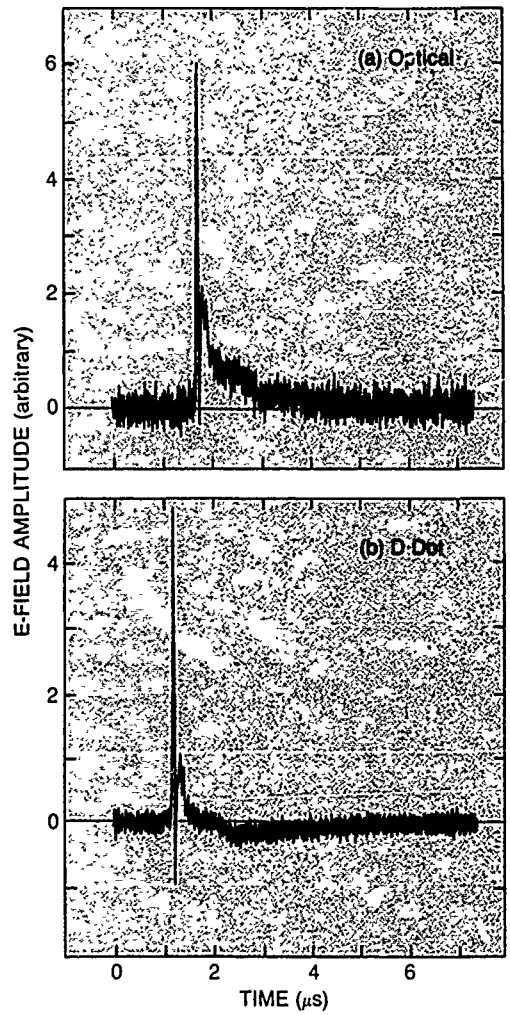

Fig. 1 — Optical and D-dot sensor outputs for an EMP signal: (a) optical; (b) D dot.

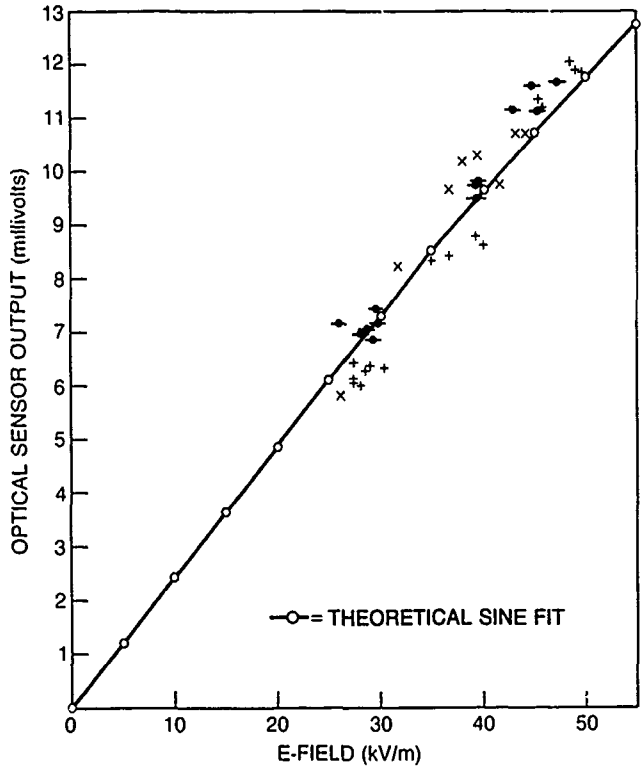

Fig. 2 — Optical sensor signal vs *E* field as measured by the *D*-dot sensor. Solid line is a theoretical sine fit.

then 10 dB and appeared to be limited by laser phase noise.

This initial test is promising because it demonstrates that the optical sensor withstood the high *E* fields and provides outputs with good fidelity, linearity, and SNR. The sensor is small, lightweight, and requires no electrical power at the sensor head. Future improvements in packaging and attention to laser phase noise should yield improved optical sensors for EMP testing.

[Sponsored by NAVAIR] ■

Physics of Semiconductor Quantum Dots in Glass

A. J. Campillo, B. L. Justus, J. A. Ruller,* and E. J. Friebele
Optical Sciences Division
**SFA, Landover, MD 20785*

Nanometer-sized microcrystallites display physical and optical properties significantly different from the bulk behavior of the same material. In particular, the nonlinear optical properties are superior to those of most bulk materials. This unusual behavior results from quantum confinement in three dimensions of the free carriers or excitons. These microcrystallites are often called quantum dots and may have uses in optoelectronic devices and logic and switching applications for communications and optical processing. We have prepared and characterized borosilicate glasses containing quantum dots of Cu(I)Cl and have subsequently studied their unique optical and nonlinear optical properties.

Glass Fabrication and Characterization: Two glasses [1], based on a sodium aluminoborosilicate composition, are used in this study. Because of slight changes in alkali concentration, one is more reduced than the other and is yellow in color; the more oxidized glass is green. The difference in color is due to the presence of copper in different valence states as determined by electron spin resonance. The

glasses are melted in 10 to 40 gram batches at 1400°C in platinum crucibles. The green glass is melted between one and two hours depending on the size of the batch, whereas the yellow glass is melted longer to eliminate the large number of bubbles that are characteristic of the melts. Samples are annealed at 520°C (T_g is 500°C) for three hours, heat treated at 585°C between 1 and 5.5 hours, and then cut and polished as thin as 100 μm for optical measurements. The microstructure is characterized by using a JEOL 200CX transmission electron microscope (TEM). Figure 3 shows the TEM micrograph of the yellow glass, and it is evident that it is phase separated into an interconnected structure. We believe that the light background is the boron-rich phase and the darker, interconnected structure is the silica-rich phase. The small, black CuCl quantum dots exist in the silica-rich phase only. Figure 4 is a TEM micrograph of the green glass and, although it is also phase separated, in this case the silica-rich phase consists of droplets dispersed in the boron-rich phase. The CuCl quantum dots are present on what is believed to be the silica-rich droplets.

Linear and Nonlinear Optical Properties: In CuCl, the optical properties near the bandgap are dominated by excitonic effects. In the CuCl quantum dots, the excitons are photoexcited electron-hole pairs whose center of mass motion is quantized due to the confinement. The energy associated with the confinement is size dependent, resulting in an increase in energy, or blueshift, of the absorption peak of the exciton resonance with decreasing dot size. Figure 5 shows the absorption spectra of three CuCl quantum dot glass samples with radii of 34 Å, 27 Å, and 22 Å. The absorption peaks for each quantum dot sample are blueshifted from the bulk CuCl resonance, and the blueshift, as expected, increases with decreasing dot size. The optical nonlinearity of the quantum dots is associated with the intensity-dependent absorption at the exciton resonance and is also size dependent. We have measured the magnitude of the optical nonlinearity [2] resulting from absorption saturation for each of the CuCl quantum dot samples. The nonlinearities are several orders of magnitude greater than the nonlinearity of the bulk material and increase with increasing dot size. The standard figure of merit used to assess optical

Fig. 3 — TEM micrograph of the yellow CuCl-doped glass, heat treated for 5.5 h at 585°C. The magnification is 200,000.

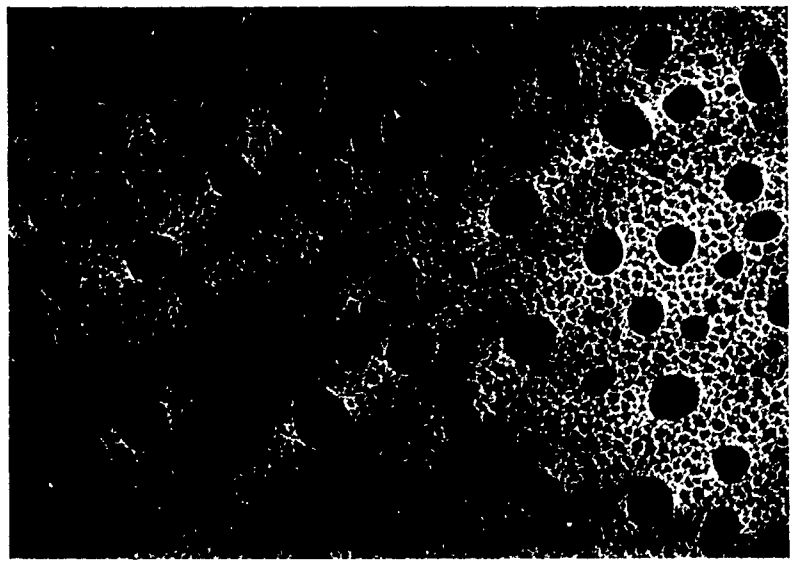

Fig. 4 — TEM micrograph of the green CuCl-doped glass, heat treated for 4 h at 585°C The magnification is 74,000.

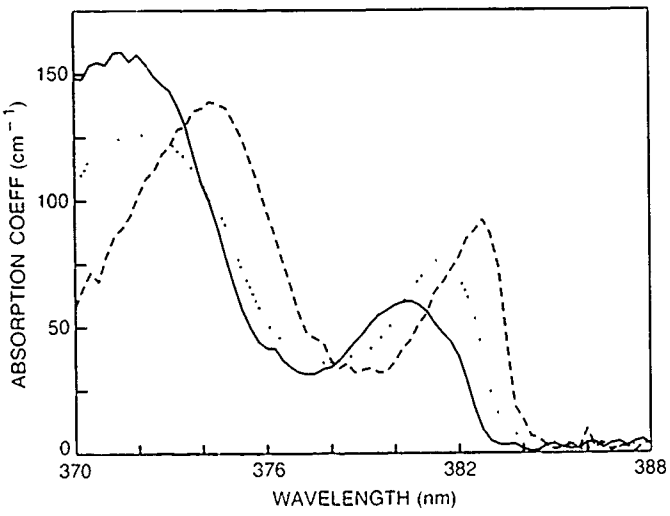

Fig. 5 — Absorption spectra of CuCl quantum dot glass samples, measured at 77 K: 22 Å—solid line, 27 Å—dotted line, 34 Å—dashed line.

nonlinearities of materials increases from 1 cm^3/J for the 22 Å sample to 10 cm^3/J for the 34 Å sample. Such large nonlinearities indicate that CuCl quantum dots in glass can quickly and effectively respond to relatively weak incident light and may be a suitable candidate for optoelectronic applications.

[Sponsored by ONR]

References

1. J.A. Ruller, D.A. Dutt, G.M. Williams, E.J. Friebele, B.L. Justus, and A.J. Campillo, "Characterization of Quantum-Confined CuCl Microcrystals in a Glassy Matrix," *SPIE Proc.* **1327** (1990).
2. B.L. Justus, M.E. Seaver, J.A. Ruller, and A.J. Campillo, "Excitonic Optical Nonlinearity in Quantum-Confined CuCl-doped Borosilicate Glass," *Appl. Phys. Lett.* **57**, 1381 (1990). ■

Space Research and Satellite Technology

SPACE RESEARCH AND SATELLITE TECHNOLOGY

For many years NRL has studied various aspects of space research in the fields of astrophysics and astronomy, atmospheric science, solar-terrestrial interactions, and spacecraft engineering and systems development. Reported in this chapter is work on the measurement of solar wind speed, aspects of cosmic radiation, near-earth beryllium accretion, satellites with low eccentricity, and a high-temperature, superconductivity space experiment.

The Space Science Division, the Condensed Matter and Radiation Sciences Division, the Space Systems Development Department, and the Spacecraft Engineering Department contributed to the work presented here.

Other current work in space and satellite research includes:

- Solar atmosphere phenomenon
- Ultraviolet imaging of space weather
- Solar-flare probes
- Solar prominences
- Passive stabilization of space structures
- Low-power atmospheric compensation experiment (LACE) satellite

Cosmic-Ray Source Composition

R. Silberberg and C.H. Tsao
Space Science Division

The topics of origin, acceleration, and nuclear composition of cosmic rays—the most energetic nuclear particles in nature—are both of basic and applied interest. They are of considerable applied interest because of their deleterious effects that require shielding or other protective measures. The annual cosmic-ray dose outside the shielding atmosphere is several hundred times higher than the dose rate at sea level. Microelectronic computer components on orbiting satellites are affected by cosmic rays that cause single event upsets.

Acceleration of Stellar Wind Particles of a Presupernova Star to Cosmic-Ray Engergies: Recently the cosmic-ray composition at the high energies of 10^{12} to 10^{13} eV per nucleon was measured. Relative to lower energies, the ratio He/H is enhanced by a factor of two and carbon-nitrogen-oxygen (CNO)/H by a factor of about 5. Also, the energy spectrum at energies 10^{13} to 5×10^{15} eV is slightly flatter than at lower energies, as Fig. 1 shows. The shape of this spectrum implies that it is composed of two components, as does the change of nuclear composition. Silberberg et al. [1] found that the component that dominates at energies 10^{13} to 5×10^{15} eV fits the model developed by scientists at Max Planck Institut according to which the shock waves of a young supernova remnant initially accelerate the stellar wind particles of the presupernova star. These stars are the red and blue supergiants and the Wolf-Rayet stars. The surface composition of the supergiants is enriched in helium derived from hydrogen burning via the CNO cycle. In Wolf-Rayet stars, the stellar surface is enriched in products of the helium burning, ^{12}C and ^{16}O.

We found the weighted average nuclear composition of the winds of presupernova stars to agree well with the measured nuclear abundances, supporting our newly proposed model [1].

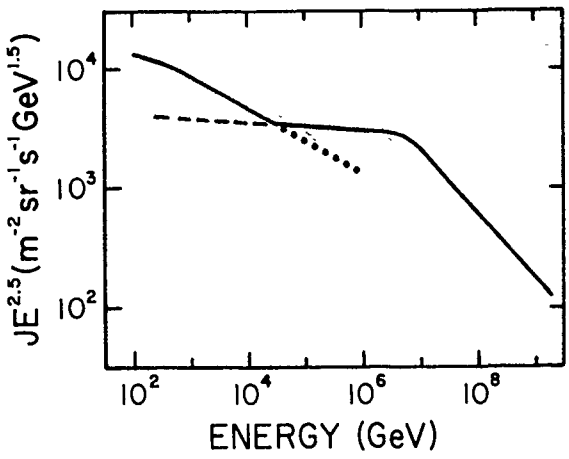

Fig 1 — The cosmic-ray energy spectrum multiplied by $E^{2.5}$ at energies 100 to 10^9 GeV (i.e., at 10^{11} to 10^{18} eV). The significance of the change of slope near 10^4 GeV (i.e., 10^{13} eV) is discussed in the text.

Acceleration of Stellar Flare Particles by the Shock Waves of an Older, Extended Supernova Remnant: Several scientists have contributed to the understanding of the source composition of cosmic rays and how they differ from the general elemental abundance in normal stars, like the sun. (The term "source composition" is the original composition of cosmic rays corrected for the nuclear breakup reactions in the interstellar gas.)

The first major breakthrough was made by scientists in Norway and France who found that that the ratios of cosmic-ray source abundance to general abundance is correlated with the first ionization potential, as shown in Fig. 2. A similar correlation exists between the solar-flare particle abundances to those of the photosphere. Elements with a high first-ionization potential (FIP) have reduced abundances in cosmic rays and in solar flare particles. Scientists in Saclay, France, and the University of Maryland have proposed a model in which flare particles from flare stars leak out into interstellar space and are there accelerated by shock waves of expanding supernova remnants that attain dimensions of 100 light years and more.

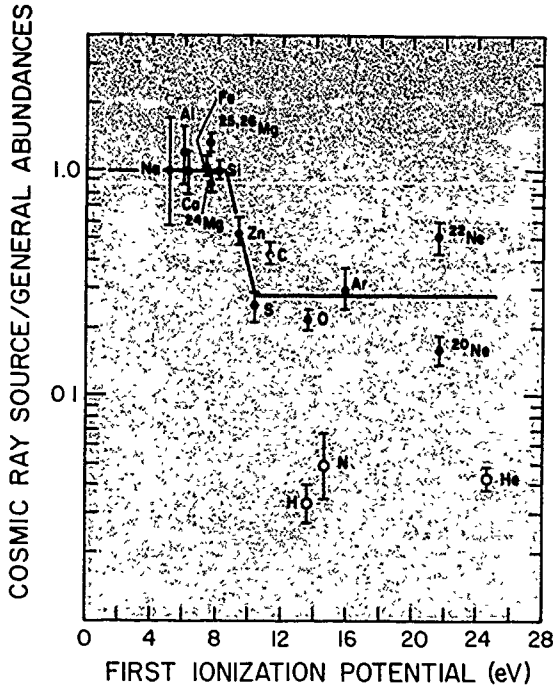

Fig. 2 — The ratio of cosmic-ray source abundance to the general abundances normalized at Si. The curve shows the suppression of elements with FIP > 10 eV. The additional hypotheses for fitting H, He, C, N, O, ^{20}Ne, ^{22}Ne ^{25}Mg, and ^{26}Mg are discussed in the text.

We note some additional anomalies in Fig. 2. The cosmic-ray source abundance of ^{22}Ne exceeds that of ^{20}Ne by a factor of about three, and the C/O ratio has an imperfect fit. The French scientists have shown that these discrepancies are removed by assuming that 3% of the particles accelerated are from Wolf-Rayet stellar winds. These are enriched in ^{22}Ne, ^{25}Mg, ^{26}Mg and ^{12}C.

Figure 2 shows H, He, and N to be underabundant in cosmic rays by a factor of about seven even after correction for the FIP effect (shown by the solid line). We have proposed a model for removing these remaining discrepancies [2]. The explanation is in terms of two effects: we postulate a magnetic rigidity dependent threshold for particle escape from the flare star vicinity into interstellar space. Particles whose orbits are tightly wound around the magnetic field lines are considered to be trapped and prevented from escape; and heavier atoms like Mg at energies near 1 MeV per nucleon are only partly ionized with an effective charge Z_{eff} of about 8 rather than 12. Hence, they have a higher magnetic rigidity than fully stripped nuclei at the same value of energy per nucleon and can escape more readily from the vicinity of the flare star than a fully stripped, lighter nucleus like ^{4}He. Considering the energy spectra of flare particles to be steep (like solar flare spectra), the calculated enhancement factors for heavier nuclei (or suppression factors for the lighter nuclei) explain the apparent anomalies of H, He, N, and ^{20}Ne of Fig. 2. Our calculated cosmic-ray source abundances agree with the observationally deduced ones within 20%.

[Sponsored by ONR]

References

1. R. Silberberg and C.H. Tsao, "An Explanation for Cosmic-Ray Force Abundancies Including Nitrogen," *Astrophys. J. Lett.* **352**, (L99) (1990).

2. R. Silberberg, C.H. Tsao, M.M. Shapiro, and P.L. Biermann, "First Composition of Cosmic-Rays Images 1-1000 TeV per Nucleon," *Astrophys. J.* **363** 265-269 (1990).

■

Discovery of Be-7 Accretion in Low Earth Orbit

G.W. Phillips and S.E. King
Condensed Matter and Radiation Sciences Division

The retrieval of the Long-Duration Exposure Facility (LDEF) spacecraft in January 1990 after nearly six years in orbit offered a unique opportunity to study the long-term buildup of induced radioactivity in the variety of materials on board. We conducted the first complete gamma-ray survey of a large spacecraft shortly after its return to Earth. A surprising observation was the large ^{7}Be activity that was seen primarily on the leading edge of the satellite, implying that it was picked up by LDEF in orbit. This is the first known evidence for accretion of a radioactive isotope onto an orbiting spacecraft.

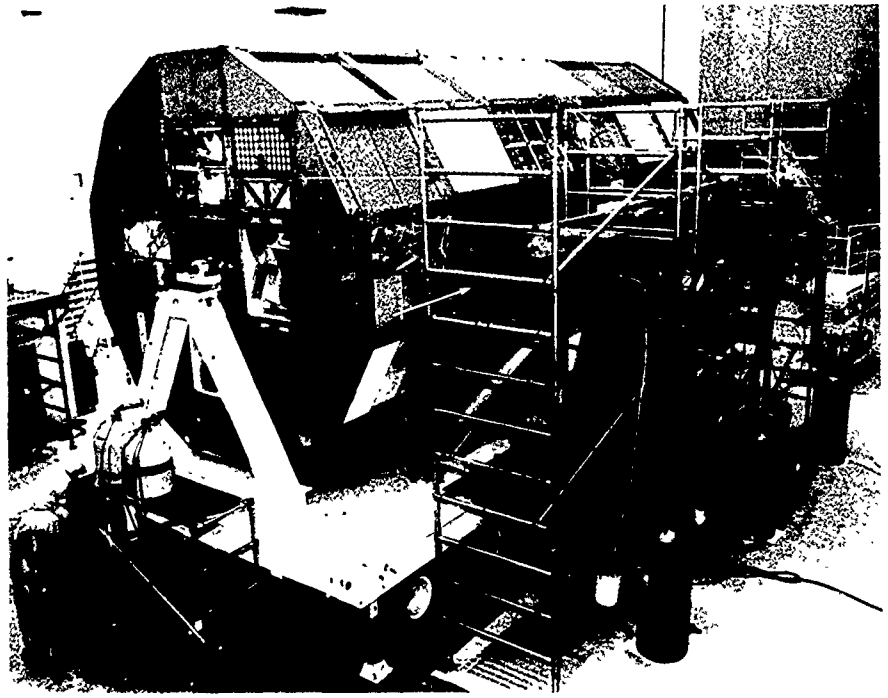

Fig 3 — NRL array (arrow) set up for the radiation survey LDEF The gamma-ray detectors were inside the six rectangular boxes on the rolling scaffolds These were rolled back out of the way during the day and rolled up for taking data during the overnight shifts Single detectors from the Institute of Space Science and Technology are set up at the end of the spacecraft

The LDEF Spacecraft: The LDEF is a large, 12-sided, cylindrical aluminum structure. Along the sides and on both ends were mounted 86 experimental trays designed to study the environment in low Earth orbit and to determine the effects on various materials, coatings, and electronic devices for potential use on future spacecraft, such as the Space Station Freedom. To determine the effects of orientation on exposure, the LDEF was stabilized so that one end was always pointed toward Earth, and one side was always the leading edge with respect to its direction of motion in orbit. It was launched into a low-inclination orbit of 28.5° at an altitude of 480 km, exposing it both to cosmic rays and to high-energy particles trapped in Earth's radiation belts. The orbit had decayed to 310 km when LDEF was retrieved shortly before it would have tumbled to Earth

Radiation Survey: Figure 3 shows the NRL array of high-resolution germanium gamma ray detectors aligned for the survey along one side of LDEF inside a high-bay clean room at the Kennedy Space Center. We accumulated gamma-ray spectra simultaneously for each of the six trays along a side for a minimum of 12 h for each side, allowing us to map the distribution of radioactivity about the spacecraft.

Principal Gamma-Ray Activities: Strong gamma-ray lines were observed in the LDEF spectra at energies of 1274 keV from the decay of ^{22}Na and at 478 keV from the decay of ^{7}Be ^{22}Na, with a 2.6-yr half-life, is produced by spallation reactions of high-energy protons on the aluminum of the spacecraft body and experimental trays. ^{7}Be, with a 53-day half-life, is also an aluminum spallation product, but its intensity was much larger than expected since it has a cross-section two orders of magnitude lower than ^{22}Na Its distribution, as shown in Fig 4, was also much different than ^{22}Na. The ^{22}Na activity was distributed about the spacecraft, but it was slightly

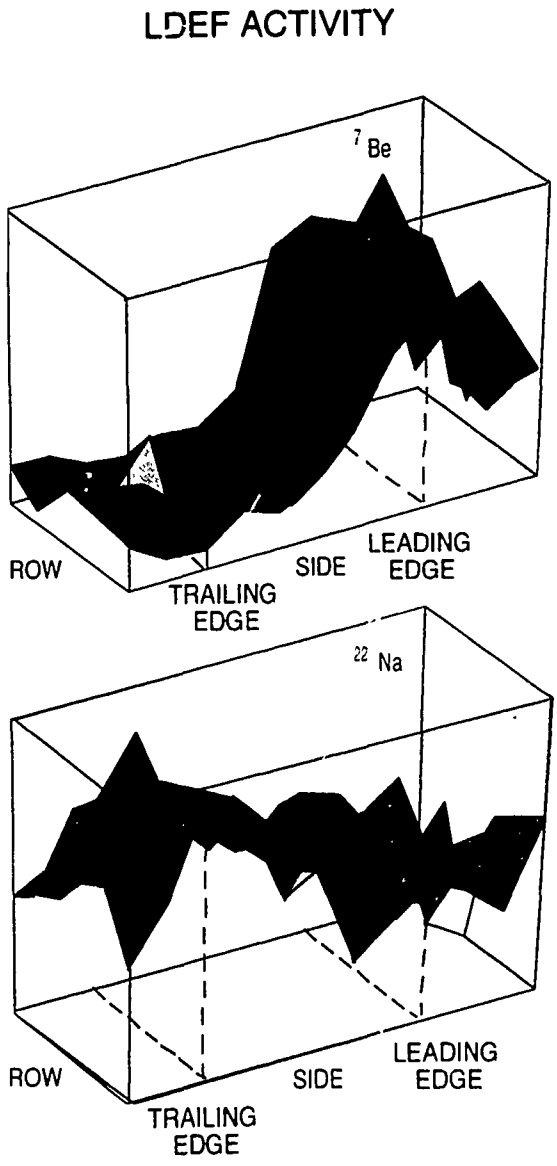

Fig. 4 — The distribution of ^{7}Be and ^{22}Na activities around the LDEF spacecraft. There are 12 sides along the right axis and six rows along the left axis, with data from one experimental tray plotted for each row and side. The dashed lines indicate the positions of the leading and trailing edges. (Figure prepared by Mississippi State University.)

higher on the trailing edge in orbit. This was consistent with the predominant direction of the high-energy trapped protons. However, the ^{7}Be activity was concentrated almost entirely on the leading edge of the spacecraft, which was consistent with it having been picked up by accretion as the spacecraft moved through the rarified atmosphere in low Earth orbit. Spectra taken of individual trays after removal from LDEF, Fig. 5, show that there was essentially no ^{7}Be activity on the trailing edge.

Conclusions and Implications: The primary sources of ^{7}Be in the upper atmosphere are reactions of cosmic rays with nitrogen and oxygen nuclei in the thin residual atmosphere. This mechanism is well known from balloon studies at lower altitudes, and the ^{7}Be yield depends both on the cosmic-ray flux and the atmospheric density. From this we can calculate a maximum ^{7}Be density because of local cosmic-ray production of 3.6×10^{-5} atoms per cubic meter at the lowest LDEF altitude. For comparison, our measure-

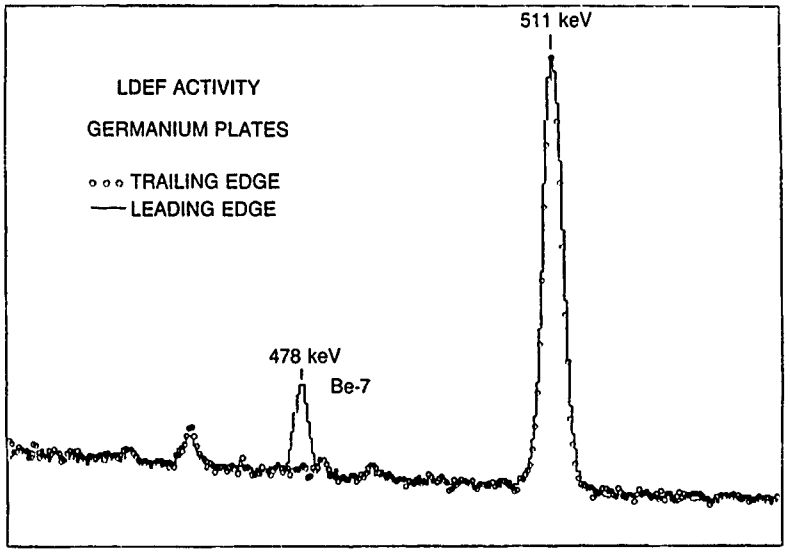

Fig. 5 — Comparison of the ^{7}Be peak in gamma-ray spectra taken by ISST germanium plates from both the leading and trailing edges after they were removed from LDEF. The 478 keV gamma ray from ^{7}Be appears only on the leading edge. The other peaks are background gamma rays.

ments give an average surface density for ^{7}Be on the leading edge of $5.4 \times 10^{9} \pm 25\%$ atoms per square meter. This implies a ^{7}Be density in orbit of at least 0.10 atoms per cubic meter, which exceeds the local production density by about a factor of 3000. To find a production density equal to the observed density, one would have to go far down in altitude, to about 110 to 120 km. Our observations thus imply the large-scale transport of ^{7}Be to low Earth orbit from altitudes of 120 km or below. The mechanisms for mixing of lower to higher altitude atmospheric gases are complex. ^{7}Be, with its relatively short half-life, may prove to be a valuable tracer for future use in refining transport models of the upper atmosphere.

Acknowledgments: Significant contributions to this research were made by R.A. August and J.C. Ritter, of NRL; J.C. Cutchin, of Sachs/Freeman Associates; P.S. Haskins, of the University of Florida; J.E. McKisson, D.W. Ely, and A.G. Weisenberger, of the Institute of Space Science and Technology (ISST); and R.B. Piercey and T. Dybler, of Mississippi State University.

[Sponsored by SDIO] ■

Along Track Formationkeeping for Satellites with Low Eccentricity

J.W. Middour
Space Systems Development Department

An estimation and control algorithm is described for maintaining the orbits of satellites flying in formation. The algorithm may be used on the ground as an aid to satellite controllers but is simple enough to be implemented on board. The satellite to be controlled (the chase vehicle) must possess a general purpose computer along with attitude and maneuvering systems so that changes in orbital velocity can be affected. In addition, there must be some means of measuring the instantaneous range between the chase and target vehicles (e.g., radar, optical, Global Positioning System (GPS) in either of the vehicles.

The Need for Active Control: In several types of space missions, two or more orbiting vehicles must remain in proximity to one another for extended periods. Important examples are: (1) satellite pairs for gravitational research missions; (2) shuttle observation/retrieval operations; and (3) free-flying vehicles that will fly in formation

with Space Station Freedom. In general, the separate vehicles need not be co-orbiting (i.e., flying in a tail chase where one vehicle travels the same trajectory as another but with some temporal offset). When the objective is to measure the space environment in the vicinity of a satellite, the sensor-carrying vehicle should at various times throughout each revolution be displaced radially, along track, and cross track from that satellite. Small differences in the orbital parameters create periodic and long-term variations in the relative positions.

Nonconservative forces acting mainly in the along-track direction cause trajectories to separate from each other. In particular, when the members of the formation have dissimilar ballistic coefficients, a relative drift results from the different orbital decay rates. Left unchecked, even small relative drift rates (on the order of cm/s) can cause the satellites to exceed allowable separation bounds within days. Figure 6 illustrates the case where a chase vehicle has nonzero secular drift with respect to the target vehicle.

The unequal decay rates must be corrected to maintain the formation. The task of a formationkeeping algorithm is two-fold. It must first process measurements from the ranging subsystem to estimate the long-term drift. Second, it must compute the velocity changes necessary to return to the desired separation with zero drift.

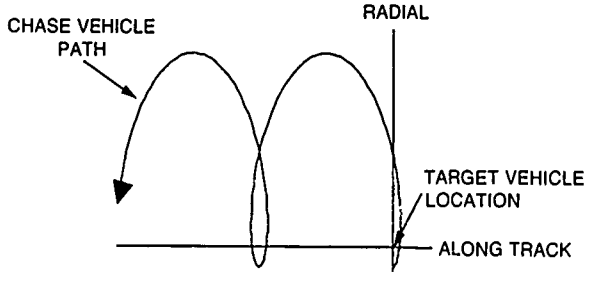

Fig. 6 — Nonzero secular drift

Estimating Relative Drift: If the equations of motion are written for each satellite and then differenced, the resultant equations may be expanded in terms of relative separation and orbital eccentricity. When the separation is small compared to the orbital radius and the eccentricity is near circular, the equations may be put in a form known as Hill's equations. These equations can be solved exactly. A Kalman filter is used to produce an estimate of the initial conditions of Hill's equations based on range measurements. The long-term drift is found by averaging the along-track component of the solution to Hill's equations. Computer simulations show that this technique yields drift estimates to within 5 mm/s.

Controlling the Drift: The task of the control law is to compute the velocity changes (delta-Vs) necessary to return the chase vehicle to its nominal separation with zero drift. This maneuver requires two delta-Vs. The first changes the semimajor axis of the chase orbit relative to the target orbit such that a relative drift is established that will return the chase vehicle to its nominal separation. The second delta-V changes the semimajor axis of the chase vehicle to match that of the target vehicle, thereby eliminating any long-term drift.

Figure 7 illustrates a simulated phase space history for the control law operating together with the estimation algorithm. The impulsive maneuvers appear as discontinuities in the state.

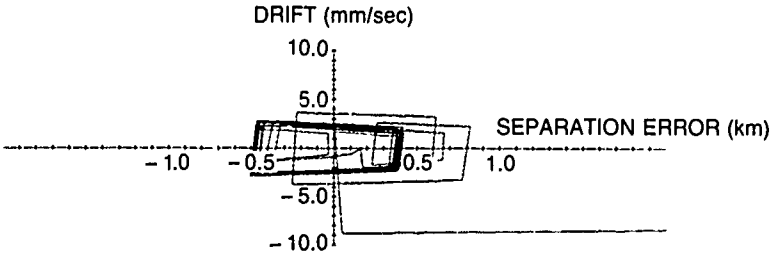

Fig. 7 — Control law phase space diagram

Conclusions: Computer simulations demonstrate that a Kalman-filter-derived estimate of along-track drift that uses instantaneous range measurement affords a high degree of accuracy. This accurate knowledge of the relative orbit dynamics enables control actions to be executed with a minimum of error and wasted propellant. ■

HERCULES: Gyro-based, Real-time Geolocation for an Astronaut Camera

M.T. Soyka and P.J. Melvin
Space Systems Development Department

HERCULES is an autonomous, astronaut-held imaging system that determines the latitude and longitude of points on the Earth, a process termed *geolocation*. A joint Navy-NASA-Army project, the goal of HERCULES is to provide shuttle and space station astronauts with a real-time, on-orbit capability to geolocate to one nautical mile.

Hardware Components: Figure 8 shows three of the devices in the HERCULES system: the camera (top), its storage device (bottom), and a ring-laser gyro (middle). The camera is a modified Nikon F4 that uses a charge-coupled device (CCD) to capture an image. The storage device contains the CCD processor and a removable hard disk that has the capacity to store 40 images, each with a total of one million eight-bit pixels. NASA is developing the CCD and storage device. The Honeywell-supplied gyro weighs five pounds and is expected to introduce errors no larger than 0.01°/h if operated within the limits of its 200°/s maximum slew rate.

The remaining devices in the HERCULES system include a GRiDCASE 1530 portable computer, an attitude processor, and a night-vision image intensifier. The FORTRAN geolocation program for the GRiD and the HERCULES attitude processor (HAP) are being developed at NRL. The HAP includes a CPU (Intel 80960) and a precise clock (accurate to 1 part in 10 million). The image intensifier is provided by the Army's Night Vision Laboratory at Ft. Belvoir, Virginia.

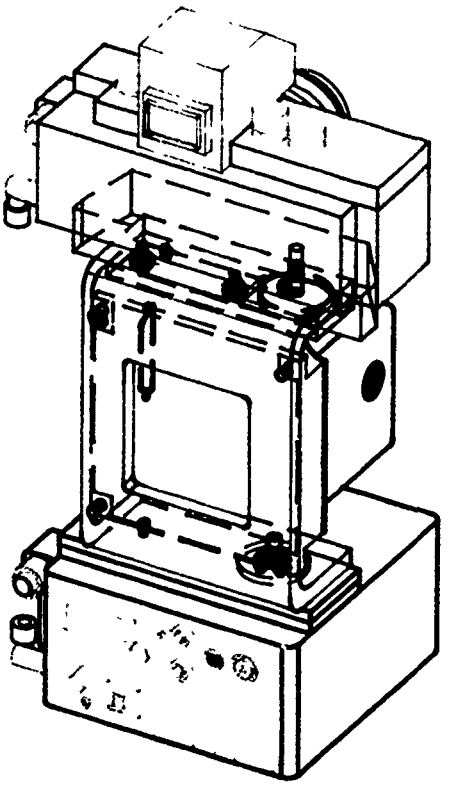

Fig. 8 — HERCULES CCD camera and ring-laser gyro

HERCULES Algorithm: The geolocation concept is based on a simple vector triangle (Fig. 9). The shuttle position vector is propagated on the GRiD in inertial coordinates. The instrument line-of-sight vector is obtained in inertial coordinates by integrating the gyro rates. These two vectors define the nadir angle that is used to compute the slant range to the Earth ellipsoid. The triangle is first computed in inertial coordinates, and the orientation of the Earth relative to the "fixed stars" is computed from time kept by the precise clock. The triangle is then transformed to Earth-fixed coordinates. The components of the geolocation vector then yield the latitude and longitude of the center of the image.

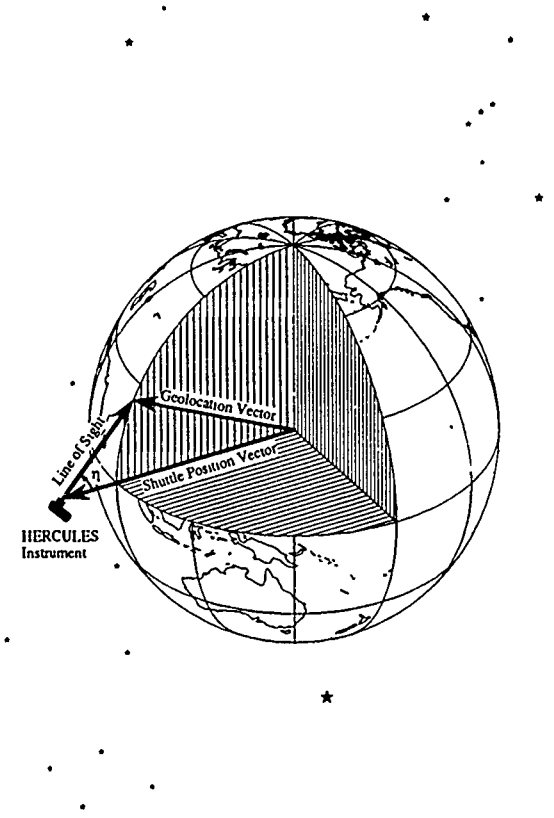

Fig. 9 — HERCULES geolocation triangle

System Initialization: Two steps are necessary before on-orbit geolocation is possible. First, the attitude is initialized by sighting a known star with the cross hairs of the camera. Once initialized, the HAP propagates the attitude by numerical integration of the gyro rates and sends the attitude and time to the GRiD. Attitude initialization is needed approximately once per day to remove the gyro drift errors.

The second step is to enter the initial position and velocity of the shuttle into the GRiD. The orbit is propagated with a force model composed of gravitation plus drag. Gravitation is computed from a seventh-order, spherical harmonic expansion of the geopotential. The drag model is based on the Jacchia 1970 [1] atmospheric density and an empirically derived drag coefficient that is dependent on the shuttle attitude. The greatest error in geolocation comes from shuttle position errors that are due to uncertainity in drag. Ephemeris initialization need be performed only once per viewing session or when maneuvers make the current state vector obsolete.

Real-Time Operation: The latitude and longitude of the line of sight are displayed as the shuttle position is updated in real time. If no geolocation is possible, the inertial line-of-sight direction is displayed. When the camera shutter is released, the CCD image is downloaded to the hard disk, and the geolocation information is appended.

Acknowledgments: Other project members at NRL are Paul DeLaHunt, Robert Higgins, Sam Hollander, Charles Jones, Bernard Kaufman, Marv Levinson, and Henry Pickard. HERCULES is expected to be on the shuttle manifest in 1992.

[Sponsored by Naval Space Command]

Reference

1. L.G. Jacchia, "New Static Models of the Thermosphere and Exosphere with Empirical Temperature Profiles," Smithsonian Astrophysical Observatory Special Report 313, Cambridge, MA (1970). ■

Excellence in Research for Tomorrow's Navy

AWARDS AND RECOGNITION

"We should ask ourselves, 'Are we, as an in-house laboratory, performing our job as Mr. Edison thought we should?' I believe the answer is that we are doing considerably better than he ever imagined we would. We have been responsive to Navy problems, we have maintained sustained technical competence over the many fields of Navy interest, and we have managed to maintain our intellectual independence."

"In the final analysis, these awards recognize exceptional commitment to continued productivity, intellectual integrity, and foiefront work in science and technology."

Dr. Alan Berman, former Director of Research
10th Annual Research Publication Awards Presentation

SPECIAL AWARDS AND RECOGNITION

NRL is proud of its many distinguished scientists and engineers. A few of these have received exceptional honors for their achievements.

Dr. Thomas G. Giallorenzi
Optical Sciences Division

DISTINGUISHED PRESIDENTIAL RANK AWARD

Dr. Giallorenzi was cited for his profound impact on the development of new technology for DoD in his position as Superintendent, Optical Sciences Division. He has developed and managed forefront scientific research in fundamental and applied electro optics. His creativity, breadth of technical knowledge and effectiveness quickly and uniquely contributed to the solution of several important military problems. Among the many technical achievements realized under his leadership are scientific advances made in fiber optics; infrared surveillance from ships, aircraft, and satellites; threat missile detection, undersea surveillance; laser weaponry and countermeasures; and low observables. He enjoys a world-class reputation resulting from his pioneering technical contributions in fiber optics and electro optics.

1990 IEEE/OSA JOHN TYDALL AWARD

"...for his significant technical management and professional contributions to the development and applications of fiber optics and optical fiber sensor technology."

Dr. Gerald M. Borsuk
Electronics Science and
Technology Division

MERITORIOUS EXECUTIVE AWARD, SENIOR EXECUTIVE SERVICE

For "his outstanding leadership and achievements in electronics science and technology that are acknowledged throughout the Navy and the international electronics community."

Dr. Charles H. Heider
Tactical Electronic Warfare Division

MERITORIOUS EXECUTIVE AWARD, SENIOR EXECUTIVE SERVICE

For "his outstanding career achievements and his exceptional degree of success in creating and fostering innovative technological solutions to Naval electronic warfare problems and needs and for developing a soundly based sense of future direction for EW throughout the U.S. Navy as well as in the larger Department of Defense (DoD) and international EW communities."

Dr. Jay P. Boris
Laboratory for Computational Physics and Fluid Dynamics

CAPTAIN ROBERT DEXTER CONRAD AWARD FOR SCIENTIFIC ACHIEVEMENT

"...for inventing and using new computational methods to solve precisely intractible problems in fluid dynamics, chemically reactive flows, energetic materials, pulsed power plasma dynamics, and the environmental and blast effects of nuclear weapons....His leadership has also shown the way nationally and internationally toward practical use of the latest generation of supercomputers for commercial applications in aerospace, weapons system and engine development. He has provided and continues to provide the seminal creative contributions on which these research efforts are based."

Dr.Raymond A. Patten
Optical Sciences Division

NAVY MERITORIOUS CIVILIAN SERVICE AWARD

"For major contributions toward improving the survivability of Navy aircraft; for technical contributions and program leadership that have contributed to the operational employment of electro-optical and infrared countermeasure systems; for the formulation and management of programs to develop advanced countermeasure systems; for development at the Naval Research Laboratory of a center of excellence and leadership in airborne electro-optical and infrared countermeasures."

Jathan N. Stone
Command Support Division

NAVY MERITORIOUS CIVILIAN SERVICE AWARD

"...he was responsible for the development of an improved Thermoluminescent Dosimeter which represented an important advancement in the science of radiation exposure and therefore the relative safety of personnel working with or around radiation hazards. He managed the development of several improvements in personal dosimetry measurement and analysis techniques. These efforts improved reliability of dosimetry technology and has the potential for DoD wide use resulting in the savings of several millions of dollars in dosimetry devices and analysis, and in protective shielding costs. He also combined the resources of the Health Physics Office and the Occupational Safety and Health Office and assumed the additional responsibility for biomolecular safety....and as a result of his tireless efforts created a most effective occupational safety and health physics operation at the Naval Research Laboratory."

Dr. Dimitrios A. Papaconstantopoulos
Condensed Matter and Radiation
Sciences Division

1990 SIGMA XI PURE SCIENCE AWARD

"...for fundamental research in developing and implementing methods in the field of electronic structure theory, and for the application of these advanced methods in such areas as amorphous semiconductors, magnetism, interfaces and alloys, where they have had major impact on DoD materials research."

Dr. Anthony Dandridge
Optical Sciences Division

1990 SIGMA XI APPLIED SCIENCE AWARD

"...for his pioneering work in fiber-optic sensor interferometry, including demodulation schemes and sophisticated hydrophone designs and noise-reduction techniques, which had led to successful sea tests of the All Optical Towing Array (AOTA)."

Carol M. Veronda
Radar Division

1989 COMMANDING OFFICER'S AWARD FOR ACHIEVEMENTS IN THE FIELD OF EQUAL EMPLOYMENT OPPORTUNITY (Supervisory Category)

"In recognition of the many contributions he has made to the promotion of Equal Employment Opportunity at the Naval Research Laboratory and to the Laboratory's Community Outreach Programs."

Dominic Panciarelli
Technical Information Division

1989 COMMANDING OFFICER'S AWARD FOR ACHIEVEMENTS IN THE FIELD OF EQUAL EMPLOYMENT OPPORTUNITY (Non-Supervisory Category)

"In recognition of the many contributions he has made to promote Equal Employment Opportunity at the Naval Research Laboratory and in community programs."

Dr. Richard Tousey
Space Science Division

1990 HALE PRIZE
(presented every two years by the Solar Physics Division of the American Astronomical Society)

For outstanding contributions to the field of solar astronomy.

Dr. Isabella L. Karle
Laboratory for the Structure
of Matter

BIJVOET MEDAL
(from the Bijvoet Center for Biomolecular Research,
Utrecht University, The Netherlands)

"in recognition of her outstanding contributions to X-ray Crystallography."

Dr. Herbert Friedman
E.O. Hulburt Center for
Space Research

Co-recipient of the
NATIONAL SPACE CLUB'S 1990 SCIENCE AWARD

"...for his many contributions to seminal research in space science, particularly in the fields of X-ray astronomy and solar-terrestrial physics."

Dr. Kenneth J. Johnston
Center for Advanced
Space Sensing

THE FIRST MAX-PLANCK RESEARCH PRIZE

Administered jointly by the A.v. Humbolt Foundation and the Max-Planck-Gesellschaft, the prize was awarded for astronomical research for 1990. The prize was funded by the German Federal Minister of Science and Technology to promote a cooperative effort with German scientists and their partners in foreign countries.

***WASHINGTON TECHNOLOGY'S* TOP TEN TECHNOLOGY TALENT OF 1990**

One of the world's leading experts in the arcane world of applying interferometric techniques to astronomical research, (he) has successfully transferred the technology to applied activities. In the area of navigation, (he) has worked to apply radio astronomical techniques to establish a network of "invisible" stars and radio sources to complement the visible stars that for centuries have served as guiding lights to ocean adventurers.

Dr. Warren E. Pickett
Condensed Matter and Radiation Sciences Division

WASHINGTON TECHNOLOGY'S TOP TEN TECHNOLOGY TALENT OF 1990

A leading expert in superconductive theory, he has been a leader in identifying the electronic structure of the high-temperature oxide superconductors.

Dr. Phillip Sprangle
Plasma Physics Division

WASHINGTON TECHNOLOGY'S TOP TEN TECHNOLOGY TALENT OF 1990

Recognized throughout the world as an authority in the field of free electron lasers and particle physics, (he) has made contributions that will benefit the scientific community for years to come.

Dr. Joel M. Schnur
Center for Bio/Molecular Science and Engineering

WASHINGTON TECHNOLOGY'S TOP TEN TECHNOLOGY TALENT OF 1990

Was instrumental in the signing of the Cooperative Research and Development Agreement (CRDA) between NRL and the Shipley Company and in developing and marketing the microlithology technique Shipley sought to several advanced, high-tech products.

Theodore C. Moss
Tactical Electronic Warfare
Division

ACHIEVEMENT AWARD FOR THE TECHNICAL COOPERATIVE PROGRAM (TTCP)

For contributions to TTCP collaboration in countermeasures to monopulse radar.

Dr. Carl E. Landwehr
Information Technology
Division

INSTITUTE OF ELECTRONICS AND ELECTRICAL ENGINEERS (IEEE) COMPUTER SOCIETY'S MERITORIOUS SERVICE AWARD

For contributions to technical and administrative leadership while serving as Chair of the Society's Committee on Security and Privacy.

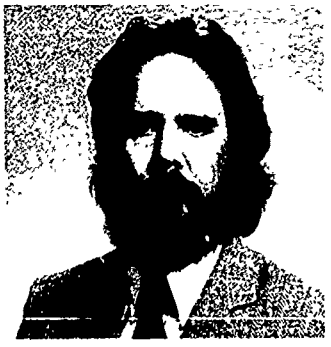

Dr. John D. McLean
Information Technology
Division

OUTSTANDING PAPER AWARD FROM THE 1990 INSTITUTE OF ELECTRONICS AND ELECTRICAL ENGINEERS (IEEE) SYMPOSIUM ON RESEARCH IN SECURITY AND PRIVACY

For his paper entitled "Security Models and Information Flow," describing techniques for evaluating and improving computer security models that prohibit information flow from a computer system's high-level users to its low-level users.

DEPARTMENT OF THE NAVY AWARD OF MERIT FOR GROUP ACHIEVEMENT

Eight NRL researchers from the Optical Sciences Division have been honored for their work on the Fly's Eye Measurement Program. Fly's Eye is a threat-warning sensor program that has provided both proof-of-principle for new infrared (IR) focal plane array processing algorithms and state-of-the-art staring technology to protect tactical aircraft from missiles. Pictured (back row, l-r) are Mr. Merritt Cordray, Mr. Kenneth Sarkady, Dr. Garry Katz, Mr. Joe Havlicek, (front row, l-r) Dr. Melvin Kruer, Dr. Raymond Patten, Dr. Myron Pauli, and Dr. Michael Satyshur

OUTSTANDING CONFERENCE PAPER AWARD FOR THE 1989 IEEE NUCLEAR AND SPACE RADIATION EFFECTS CONFERENCE

Shown are Nelson S. Saks (l), Electronics Science and Technology Division, and Dr. Dennis B. Brown (r), Condensed Matter and Radiation Sciences Division. Their paper is entitled "Interface Trap Formation via the Two-Stage H^+ Process."

1989 IBM 3090 SUPERCOMPUTING COMPETITION

L-r: Drs. Ronald E. Cohen and Warren E. Pickett of NRL's Condensed Matter and Radiation Sciences Division and Professor Henry Krakauer of the College of William and Mary in Williamsburg, Virginia. For their joint research on high-temperature superconductivity by using the IBM 3090 supercomputer at the National Supercomputer Facility, Cornell University. A paper on their research is entitled "First-Principles Phonon Calculations for La_2CuO_4."

INDIVIDUAL HONORS

Laboratory employees received numerous scientific medals, military service awards, academic honors, and other forms of recognition, including election and appointment to offices in technical societies. The following is an alphabetical list of persons who received such recognition in 1990.

President George Bush is shown with Dr. Thomas Giallorenzi, Superintendent of the Optical Sciences Division, after presenting him the Distinguished Presidential Rank and Award.

Aggarwal, I.D., Committee member, 7th International Symposium on Halide Glasses to be held in Lorne Victoria, Australia on March 17-19, 1991.

Anderson, G.W., Member, Advanced Special Receiver Technical Committee, NAVAIR; Member, Professional Advisory Board, Epilepsy Foundation for the National Capital Area.

Andreadis, T.D., Organized and co-chaired 3rd Annual Laser Effects on Night Vision Goggles Conference.

Apruzese, J.P., Member, Program Committee, International Conference on Lasers, 1989.

Armstrong, C.M., Chairman, Vacuum Electronics Subcommittee for the 1989 International Electron Devices Meeting, December 3-6, 1989, Washington, DC.

Barone, F.R., Chairman, Infrared Information Society Specialty Group on Infrared Countermeasures (IRCM) Society, Member Specialty Group on Infrared Countermeasures; Member IRCM Society.

Bartoli, F.J., Co-editor of book entitled *Properties of II-VI Semiconductors: Bulk Crystals, Epitaxial Films, Quantum Well Structures, and Dilute Magnetic Systems*, Materials Research Society (MRS), Pittsburgh, PA, 1990; also co-chaired MRS Symposium on this subject.

Batra, N.K., Associate Technical Editor, *Materials Evaluation*; Member, IEEE Ultrasonics, Ferroelectricity, and Frequency Control Society's Technical Committee; and Session Chairman, IEEE UFFCS Symposium, Montreal (October 1989).

Bernhardt, P.A., Elected Vice-Chairman, URSI Commission H for the U.S. National Committee; appointed Editor, AGU Books Board.

Boos, J.B., Appointed Chairman, Electron Devices Area, 1991 InP and Related Materials Conference.

Boris, J.P., Recipient of U.S. Navy's Captain Robert Dexter Conrad Award for Scientific Achievement; Member, AIAA Fluid Dynamics Technical Committee; Member, Executive Committee, APS Topical Group on Computational Physics (Chair 1978-1989); and Editorial board, Siam Hallmark Book Series, *Engineering Technology Acceleration Through Mathematics and Modeling*.

Borsuk, G.M., Recipient of Presidential Meritorious Rank Award.

Bottka, N., Member, Organizing Committee of the Sixth International Conference on Metalorganic Vapor Phase Epitaxy, 1992; Member, Program Committee of the 1991 International Symposium on GaAs and Related Compounds.

Brown, M.A., Member (second year), AIAA Space Systems Technical Committee.

Dr. Jay P. Boris is the recipient of the Captain Robert Dexter Conrad Award for Scientific Achievement. Shown here with him are RADM William C. Miller, Chief of Naval Research, and his wife, Elizabeth.

Brueckner, G.E., Science Advisor, "Inter-Agency Consultative Group for Space Science," and Co-organizer of an international meeting, "Active Phenomena in Solar System Plasmas," Hong Kong, February 1991.

Bucaro, J.A., Continuing Fellow, Acoustical Society of America.

Bultman, J.D., Member, Committee on Creosote and Creosote Solutions of the American Wood-Preservers' Association; Member, Committee for the Evaluation of Wood Preservatives of the American Wood-Preservers' Association; Member, Editorial Board, *El Guayulero* (published by The Association for the Advancement of Industrial Crops); Associate Editor, *Biotropica* (published by the Association for Tropical Biology); and Scientific Editor (*NRL*), *ONR Naval Research Reviews*.

Buot, F.A., Member, Subcommittee on Modeling and Simulation, International Electron Device Meeting (IEDM) 1990, 1991, sponsored by IEEE; Member, Science and Technology Advisory Council of Washington, DC, (STAC-WDC), voluntary consultant to the Philippine Government Science Policy; Chairperson and discussant, Second Philippine Dialogue on Advanced Science and

Dr. Larry Boyer receives an *NRL Review* Award from Dr. T. Coffey, Director of Research

Technology, Washington, DC, April 2, 1990; Session Chairman, Session IV, "Quantum Transport Modeling and Simulation," Workshop on Computational Electronics, Beckman Institute, May 21–22, 1990; Member, Advisory Committee, Workshop on Computational Electronics, National Center for Computational Electronics, Beckman Institute, University of Illinois at Urbana-Champaign, May 21–22, 1990; and Invited Lecturer, "The Fundamental Equations in Quantum Transport Modeling," in Short Course on Computational Electronics, following the NCCE Workshop on Computational Electronics, Beckman Institute

Burn, J.M., Jr., Received an achievement award from The Technical Cooperation Program for contributions to collaboration in counter-measures to monopulse radar.

Butler, J.W., Member and Session Chair, Organization Committee of Eleventh International Conference for Applications of Accelerators in Research and Industry, Denton, TX, November 5–9, 1990.

Campbell, F.J., Fellow, Institute of Electrical and Electronics Engineers; Fellow, American Institute of Chemists; Member, Subcommittee on Electrical Tests, D-09 Electrical Insulating Materials, ASTM; Member, Naval Aerospace Vehicle Wiring Action Group; Member, Sigma Xi; and listed in *Who's Who in America*, 46th Ed. (1990).

Campillo, T., Appointed to LEOS '90 and '91 Program Committee on "Optical Measurements."

Carruthers, G.R., Editor, *National Technical Association Journal.*

Cherkis, N.Z., Appointed Scientific Advisor (May 1990), Guiding Committee of the General Bathymetric Chart of the Oceans (GEBCO). GEBCO is an IHO/IOC function of the International Hydrographic Bureau (Monaco).

Chubb, S.R., Selected by NSF and the Electric Power Research Institute (EPRI) to serve on special NSF/EPRI advisory committee to assess the direction of research in cold fusion.

Clement, A.E., Patent No. 4.953.951 granted September 4, 1990, "Method for Making Holograms with Coherent Radiation from a Stabilized Laser Diode that has been Actively Cooled," G.C. Gilbreath and A.E. Clement.

Colton, R.J., Co-editor, Proceedings of the 1989 Topical Conference on Nanometer Scale Properties of Surfaces and Interfaces; Program Chairman, Fifth International Conference on Scanning Tunneling Microscopy/Spectroscopy (STM '90) and First International Conference on Nanometer Scale Science and Technology (NANOI), July 1990; and appointed Program Chairman, 38th National Symposium, American Vacuum Society, November 1991.

Commisso, R.J., Executive Secretary, Defense Nuclear Agency-fostered, Advanced Pulsed Power Technical Review Workshop; Chairman, Awards Sub-committee for the Plasma Science and Applications Committee of the IEEE Nuclear and Plasma Sciences Society.

Cooperstein, G., Fellow, American Physical Society; Technical program committee member, IEEE Pulsed Power Conference; Co-chairman, 9th International Conference on High Power Particle Beams.

Corsaro, R.D., Chairperson, ACS Symposium on Sound and Vibration Damping; Editor, *Sound*

and Vibration Damping with Polymers, published by the American Chemical Society (ACS Books).

Cruddace, R.G., Member, ROSAT Cluster Working Group, Institut fur Extra-terrestrische Physik, Max Planck Institut, Garching, Federal Republic of Germany.

Dandridge, A., Appointed to the International Steering Committee of the Sixth International Conference on Optical Fiber Sensors (OFS); appointed to the Technical Program Committee of the Sixth International Conference on Optical Fiber Sensors (OFS); appointed to the Technical Program Committee of the Conference on Lasers and Electro-Optics (CLEO); appointed as Associate Editor of the *Journal of Light Wave Technology*; and 2nd year as Associate Editor of *Applied Optics*.

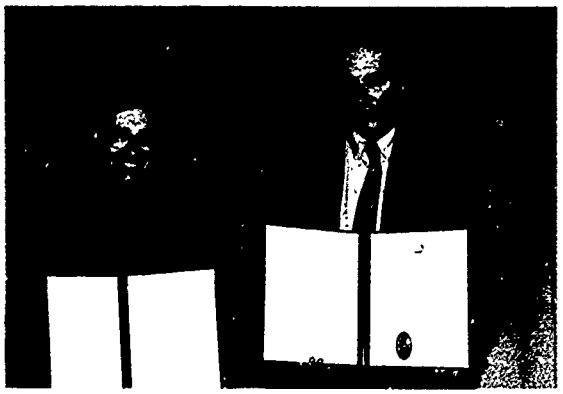

The 1990 Sigma Xi awards were presented to Dr. Anthony Dandridge (left) (Applied Science Award) and to Dr. Dimitrios Papaconstantopoulos (right) (Pure Science Award)

Dasenbrock, R.R., Chosen to be Technical Chairman (AIAA) of 1991 Astrodynamics Conference sponsored by AAS/AIAA; Member, AIAA Astrodynamics Technical Committee.

Davis, J., Editor, Special Issue, *JQSRT* "Radiation from Pulsed Power Driven Plasmas;" Member, Organization Committee of LASERS '90; Member, Organization Committee of SPIE '90; SDIO agent, Ultra Short Wavelength Lasers; Associate Editor, *JQSRT*; and Plenary Speaker at LASERS '90.

Davis, J.L., Elected President of the Washington Area Transputer Users Group (WATUG).

DeGiorgi, V.G., Member, ASTM Committee E-24 Fracture Toughness and Testing; Member, TTCP Panel P-1 Operating Assignment on Fracture Control Technology; and Member, TTCP Panel P-1 Operating Assignment on High Strength - Low Alloy Steels.

Dere, K.P., Member, Scientific Organizing Committee for the Solar Wind 7 meeting and convenor of the session on "Coronal Heating and Solar Wind Acceleration"; Member, Scientific Organizing Committee for the International Conference on Active Phenomena in Solar System Plasmas; and Group Leader, Microflares Group at the Flares 22 Workshop.

Diachok, O.I., Chaired special session on Acoustic Instrumentation at Oceans '90 Meeting; named Chairman of Instrumentation Committee of IEEE Ocean Engineering Society; invited talk on Ocean Tomography at Oceans '90; named Chairman of Special Session on Global Optimization Algorithms for Oceans '91; and Technical Chairman of ASA Spring 1991 Meeting.

Dragonette, L.R., Continuing Fellow, Acoustical Society of America; invited to author chapter in new *Handbook of Acoustics* (Wiley); and Contining Member, Sigma Xi.

Duncan, M.D., Conference committee member and Session Chairman, Scientific Computing and Automation Conference; Publicity liaison, International Quantum Electronics Conference (IQEC '90); and Member, Editorial Board for Scientific Computing and Automation Magazine.

Elam, W.T., Continuing member, External Advisory Committee, Biostructure PRT (X9), National Synchrotron Light Source; Fellow, American Institute of Physics Congressional

Scientist; Member, International Committee on Standards and Criteria on XAFS.

Esterowitz, L., Associate Editor, *Journal of Quantum Electronics*; Program Chairman, Emerging Laser Technology/LEOS; and Co-chairman, Solid State Lasers/Lasers '91, SPIE.

Feldman, B.J., Appointed Guest Editor, *IEEE Journal of Quantum Electronics Special Issue* on "Electronic Transition Gas Lasers;" Appointed Chair, LEOS '91 Subcommittee on "Gas and Short-Wavelength Lasers"; and appointed to "Lasers and Electro-Optics Advisory Board," Office of Naval Technology.

Fisher, S., Appointed to NASA/DOD Committee to look at spacecraft flight experiments.

Flippen-Anderson, J.L., Vice President, American Crystallographic Association; Re-elected to U.S. National Committee for Crystallography.

Friebele, E.J., Chairman, NATO Panel IV, Research Study Group 12, Nuclear Effects Task Group; Fellow, American Ceramic Society.

Fritz, G., Appointed to NASA X-Ray Astronomy Program Working Group.

Gaber, B.P., Executive Committee, Molecular Graphics Society of the Americas.

Gardner, J.H., Member, National Aerospace Plane CFD Technical Support Team.

Garroway, A.N., Served on Executive Board of Experimental NMR Conference; Testified before Presidential Commission on Aviation Security and Terrorism (February 1990).

Gaumond, C.F., Elected Treasurer, Washington, DC Chapter Acoustical Society of America; New Life Member, Naval Institute; and Continuing Member, ASA and APS.

Giallorenzi, T.G., Chairman, Steering Committee IEEE/OSA Optical Fiber Conference (OFC); Member, Optical Society of America R.W. Wood Awards Committee; Member, IEEE Quantum Electronics Award Committee; Member, International Optical Communications Conference Committee; Member, IEEE Semiconductor Laser Devices Conference Committee; Member, IEEE Integrated Opto-electronics Conference Committee; Member, National IRIS Executive Committee; General Chairman, 1990 IEEE/OSA Conference on Lasers and Electro-Optics (CLEO); Associate Editor, *IEEE Proceedings*; Associate editor, *IEEE Lightwave Communications System Journal*; Editorial Board, *Laser Focus* Magazine; recipient of 1990 Distinguished Presidential SES Rank and Award; and recipient of 1990 IEEE/OSA John Tyndall Award.

Gilbreath, G.C., Patent granted February 1990, Navy case number 69674, "Methods for Holographic Correction of Beams of Coherent Light," G.C. Gilbreath and J.W. Wagner; patent granted September 1990, Navy case number 70564, "Method for Making Holograms with Coherent Radiation from a Stabilized Laser Diode that has been Actively Cooled," G.C. Gilbreath and A.E. Clement.

Gold, S.H., Second year as elected member of the Executive Committee of IEEE Nuclear and Plasma Sciences Society; third year as Associate Editor of the *IEEE Transactions on Plasma Science*.

Griscom, D.L., Chairman-elect, Glass and Optical Sciences Division of American Ceramic Society; Fellow, American Ceramic Society.

Groshans, R.G., Member, Committee on Standards (Operations), The American Institute of Aeronautics and Astronautics (AIAA), Space-Based Observation Systems (SBOS).

Gubser, D.U., Organized spring meeting of the Naval Consortium for Superconductivity; Co-editor, *Journal for Superconductivity*; Session Chairman, 1990 Applied Superconductivity Conference; Scientific Session Chairman, Spring Meeting of the American Physical Society; appointed to the Scientific Advisory Board of the New York State

Institute for Superconductivity, 1990; appointed to the Scientific Advisory Board of the University of Illinois Center for Superconductivity, 1990; and Guest Lecturer for the American Institute of Physics Program to enhance science at small colleges.

Haber, I., Co-chairman, 14th International Conference on Computer Simulations of Plasmas.

Heckathorn, H.M., Member, SDIO Environmental Working Group; Member, SDIO User Products Information Group (subpanel of the PSAG-Phenomenology Steering and Analysis Group).

Hubler, G.K., Member, International Committee, Conference on Surface Modification of Metals by Ion Beams; Member; Joint Services Committee on Laser Eye Protection Program; Coordinator, Materials Research Society, Washington Office; and Co-chairman, 7th International Conference on Surface Modification of Metals by Ion Beam.

Jacobs, V., Editor, Proceeding for First International Conference on "Coherent Radiation Processes in Strong Fields," Catholic University, June 18-22, 1990 (to be published by Gordon and Breach).

Joyce, G.R., Fellow, American Physical Society, continuing membership; Member of Program Committee for November 1990 American Physical Society Meeting, Plasma Physics Division.

Kailasanath, K., Senior member, AIAA, 1987-present; Chairman, Continuing Education Subcommittee, AIAA Propellants and Combustion Technical Committee, 1990-present; Member, AIAA Propellants and Combustion Technical Committee, 1988-present; Member, Program Subcommittee, 23rd International Symposium on Combustion, 1990; Organizer, session on "Numerical Modeling," AIAA 28th Aerospace Sciences Meeting, Reno, NV, January 1990; and Organizer, session on "Combustion Modeling and Numerical Simulation," AIAA/ASME/SAE/ASEE 26th Joint Propulsion Conference, Orlando, FL, July 1990.

Karle, I.L., Plenary Lecturer, International Union of Crystallography, Bordeaux, France; Lecturer, International School on Supramolecular Chemistry, Strasbourg, France; and first American to receive the Bijvoet Medal from the Bijvoet Center for Biomedical Research, Utrecht University, The Netherlands.

Karle, J., Elected to membership in American Philosophical Society.

Kaufman, B., Deputy Director of Aerospace Science Group of American Institute of Aeronautics and Astronautics (AIAA); selected as chairman of 1991 Astrodynamics Conference co-sponsored by American Astronautical Society (AAS) and AIAA.

Kelner, G., Elected Member of the Commission D (Electronics and Optical Devices and Applications) of the U.S. Radio and Science National Committee.

Keskinen, M.J., Member, NASA Space Physics Division Strategy Implementation Study Panel for the years 1995-2015.

Killiany, J.M., Selected as Chairman of the Infrared Information Specialty (IRIS) Detector Specialty Group for the period 1990 to 1993.

Klein, B.M., Chairman, Peer Review Board, Pittsburgh Superconductor Center and National Center for Supercomputer Applications; Member, Pennsylvania State Materials Research Laboratory Advisory Committee; and Member, Organizing Committee, The University of Miami Workshop on Electronic Structure and Mechanisms for High Temperature Superconductivity.

Klunder, J., Continuing Member, Acoustical Society of America; Member, ASME.

Kuperman, W.A., Consulting Editor for *Acoustics, Encyclopedia of Applied Physics*, American Institute of Physics.

Kurfess, J.D., Elected Vice-Chairperson, Division of Astrophysics of the American Physical Society.

Lambert, J.M., Member, Executive Council, College of Arts and Sciences, Georgetown University; Reviewer, *Physical Review Letters*, National Science Foundation, American Association for the Advancement of Science, and American Institute of Physics.

Lau, Y.Y., Fellow, American Physical Society, continuing membership.

Lean, J.L., Chairperson, National Academy of Sciences, Committee on Global Change Working Group on Solar Influences on Global Change; Convenor, Special Session on Solar EUV Variability and its Effects on the Earth and Planets, Fall Meeting, American Geophysical Union, San Francisco, CA, December 1990.

Lee, J.N., Navy Member of the Optical Signal Processing Tri-Service Advisory Committee for the Office of Secretary of Defense; Member, Technical Committee, IEEE Ultrasonics Symposium; Member/Treasurer, IEEE/Optical Society of America Journal of Lightwave Technology Steering and Coordinating Committees; Organizer of Symposium on Design Issues in Optical Processing at Optical Society of America Annual Meeting; and Navy Member of Action Group for Image Information Processing of the Subgroup for Computing Technology of the Technical Cooperation Program.

Lehmberg, R.H., Appointed Chairman of CLEO (Conference on Laser's and Electro-Optics) Program Subcommittee on "Lasers for Fusion and Strong Field Physics."

Marks, C.J., Elected National Vice President for Compliance, Federally Employed Women (FEW), term of office July 1990-June 1991.

Marquardt, C.L., Technical Program Committee, Advanced Solid State Lasers, Topical Meeting, Optical Society of America.

McCafferty, E., Member, Corrosion Monograph Committee of the Electrochemical Society; Member, Honorary Member Committee of the Electrochemical Society; and Professorial Lecturer, The George Washington University, Washington, DC.

Mrs. Carolyn Marks (left) is shown being installed as National Vice President for Compliance of the Federally Employed Women's (FEW) organization. Also shown is Ms. Dorothy Nelson, past president of FEW.

McLean, E.A., Vice President of NRL Sigma Xi.

Mehl, M.J., Member, American Geophysical Union (1985-present); Member, American Physical Society (1977-present); and Member, Sigma Xi (1978-present).

Meier, R.R., Member, American Institute of Astronautics and Aeronautics Environmental Interactions Panel to review the Air Force Technology Center Program, Spring 1989.

Metzbower, E.A., Elected Senior Member, Laser Institute of America; served on Board of Directors, Laser Institute of America; served as Chairman of the Electron and Laser Beam Committee of the Joining Division Council, ASM International; and served as General Chairman of International Congress on Applications of Lasers and Electro Optics '89.

Michel, D.J., Fellow, American Society for Materials (ASM) International; Member, Technical Program Committee, Fourth International Symposium on Environmental Degradation in Nuclear Power Systems—Water Reactors; Member, Nuclear Materials Committee, ASM International and The Metallurgical Society; and Professorial Lecturer, The George Washington University.

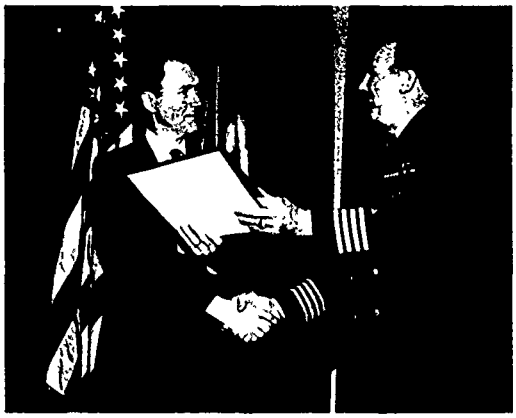

Dr. Raymond Patten is presented the Navy Meritorious Civilian Services Award by CAPT John Donegan, Commanding Officer

Moniz, W.B., U.S. National Leader, TTCP-PTP3 (organic materials).

Moss, T.C., Scientific award, (TTCP) Achievement Award for contributions to TTCP collaboration in Countermeasures to Monopulse Radar. Presented by the Subcommittee for Non-Atomic Military Research and Development (NAMRAD).

Mowery, R.L., Elected Chairman, DoD Instrument Bearing WorkingGroup.

Nagel, D.J., Chairman, Technology Panel, High Power Microwave Program Balanced Technology Initiative; and Member, Proposal Review Committee, X-Ray Lithography Program, Defense Advanced Research Projects Agency (DARPA).

Natishan, P.M., Chairman, Baltimore-Washington Section of the National Association of Corrosion Engineers (1990-1991); First Vice Chairman, National Capital Section of the Electrochemical Society, (1990-1991); Vice Chairman, Baltimore-Washington Section of the National Association of Corrosion Engineers (1989-1990); Second Vice Chairman, National Capital Section of the Electrochemical Society (1989-1990); Representative to the Individual Membership Committee, The Electrochemical Society (1986-present); and Session Chairman, 177th Meeting of the Electrochemical Society, Montreal, Canada (5/8/90).

Neihof, R.A., Convener and Session Chairman, Eighth International Biodeterioration and Biodegradation Symposium; Member Steering Committee, International Association for Stability and Handling of Liquid Fuels.

Ngai, K.L., Organizer and Chairman of the International Discussion Meeting on Relaxations in Complex Systems, Heraklion, Crete, Greece, June 18-29, 1990; Guest Editor of a special issue of the *Journal of Non-Crystalline Solids*, North Holland, Amsterdam; and Member of the International Advisory Committee on the 7th International Conference on Non-Crystalline Solids, August 4-9, 1991, Cambridge, England.

O'Grady, W.E., Served on the nominating committee of the Physical Electrochemistry Division of the Electrochemical Society; Editor for the Physical Electrochemistry Division of the Journal of the Electrochemical Society.

Oran, E.S., Fellow, American Institute of Aeronautics and Astronautics, May 1990; Elected to the Board of Directors, The Combustion Institute, July 1990; Second year as Secretary of Board of Directors, International Colloquium on the Dynamics of Energetic Systems; Elected Vice-Chair, American Physical Society Topical Group on Computational Physics, April 1990; Member of Publications Committee, American Institute of Aeronautics and Astronautics; Second year on American Physical Society, Committee on the Status of Women in Physics; Chair, Program Committee, Physics Computing '91, a joint meeting of the APS and AIP in June 1991; selected as member of the National Science Foundation, Advisory Committee, Division of Chemical and Thermal Sciences, January, 1990; and Continuing Member of the Editorial Board, Progress in Energy and Combustion Science.

Ossakow, S.L., Official U.S. Representative of the National Academy of Sciences' National Research Council to XXIIIrd URSI General

Assembly, Prague, Czeckoslovakia, and co-convenor of special sessions on Theory and Computer Experiments of Plasma Processes; Member of ONR/ AFGL Steering Committee on HF Active Auroral Research Program (HAARP) and Member of Program Committee for the Fourth International School for Space Simulation (ISSS-4), Kyoto/Nara, Japan, March-April 1991.

Ottinger, P.F., Session organizer for IEEE International Conference on Plasma Science.

Pande, C.S., Elected Chairman of Superconducting Materials Committee of the Metallurgical Society.

Papaconstantopoulos, D.A., Member, Organizing Committee of the 20th International Conference on the Physics of Semiconductors; Co-chairman, Conference Committee, Fifth International Conference on the Physics of Electro-Optic Microstructures and Microdevices; and appointed to the Editorial Board of *Journal of Superconductivity* (published by Plenum Publishing Co.).

Parvulescu, A., Continuing Fellow, Acoustical Society of America; Continuing Senior Member, IEEE (since 1950); and Continuing Member, AES, New York Academy of Sciences, MTS, AGU.

Patel, V., Fellow, American Physical Society, continuing membership; Member, National Academy of Sciences Task Group for Geomagnetic Studies; Session Chairman, Nonlinear Plasma Physics Conference, La Jolla, CA, February 1990; Member, NSF Interagency Committee on Solar-Terrestrial Research; and Board Member, Institute for Advanced Physics Studies, La Jolla, CA.

Pederson, M.R., Chairman, March APS Meeting, Materials Research Topical Group, Sessions G8, 09; Organizer of the ACS Symposium, Chemical Vapor Deposition of Diamond (and C-BN, SiC); and Chairman, Fall Materials Research Society Meeting, Clusters and Cluster-Assembled Materials.

Peterson, E.L., Selected as Guest Editor for Proceedings of HEART Conference to be published in *Journal of Radiation Effects Research & Engineering*; Elected Member at Large on IEEE Nuclear and Space Radiation Effects Conference Steering Committee.

Pickett, W.E., Editorial Board, *Journal of Superconductivity* (published by Plenum Publishing Co.); Treasurer, Greater Washington Solid State Physics Colloquium Committee; Elected Fellow of the American Physical Society; and co-authored 2nd prize paper in the IBM Supercomputing Competition.

CAPT John Donegan, Commanding Officer, presents Dr. Warren Pickett with a 1990 Alan Berman Research Publication Award

Prokes, S.M., Appointed to the Materials Research Society Publications Committee; Elected full member of Sigma Xi; and appointed Session Chair for "SIGE EPITAXY" at the Fall Materials Research Society Meeting.

Provenzano, V., Vice Chairman, Electrical, Optical and Magnetic Phenomenon Committee of TMS; Member, AIME Physical Metallurgy Committee Structural Materials Committee and Composite Committee; Member, ASM Flow and Fracture Committee; and Program Chairperson, Symposium, "Microcomposites and Nanophase Materials," AIME Annual Meeting, New Orleans, LA.

Quarles, G.J., Member Postdeadline Review Program Committee, IEEE LEOS Annual Meeting; Materials and Components Session Chairman, SPIE OE/LASER '90 Conference: Solid State Lasers.

Rath, B.B., Member, Editorial Board, International Materials Review; Chairman, Surface and Interface Committee of ASM-International; Member, Guidance and Evaluation Board, Department of Energy; Conference Organizer and Proceedings Co-editor of Interface Science and Engineering,; Editorial Board, International Materials Review; Steering Committee Member, Light Metal Center, University of Virginia; Review Board, Colorado School of Mines; Congressional Feasibility Study Group on DoD Center for Materials Research; National Research Council Panel Member of "Materials Science and Engineering for the '90s;" ASEE Review Panel for NIST Post Doctoral Fellow Selection; Elected Honorary Member of the Materials Research Society of India; Public Affairs Council of the American Association of Engineering Societies; Conference Keynote Speaker, University of Connecticut; Navy Representative to the Technical Cooperation Panel-P; and Physical and Materials Science Working Group of the Indo-U.S. Subcommission on Science and Technology.

Reinecke, T.L., Member, American Rhodes Scholarship Selection Committee; Fellow, American Physical Society; and Member, Steering Committee, Greater Washington Solid State Physics Colloquium.

Rendell, R.W., Appointed to Committee on "Glass Transition, Viscous Liquids and Small Molecule Glasses," for the 1990 International Discussion Meeting on Relaxations in Complex Systems, 18-29 June 1990, Heraklion, Crete, Greece.

Ripin, B.H., Elected Councillor-at-Large of the American Physical Society; Member, Fusion Policy Advisory Committee of the Department of Energy; Chairman, Publication Committee of APS Division of Plasma Physics, Advisory Panel on Physics of Fluids, Task Force on APS Journal Financing; Member, Review Committee on *Physical Review Letters*; Member, Editorial Boards of: *Physical Review A* and *Laser and Particle Beams* Journals; and Fellow, American Physical Society.

Ritter, J.C., Elected to the Nominating Committee for the IEEE Nuclear and Space Radiation Effects Conference, July 1990; invited to review SHAPE Technical Center NATO Satellite Survivability Efforts and provide new directions for future work, Shape Technical Center, The Hague, Netherlands, March 1990; Member, Combined Release and Radiation Effects Satellite Science Team; invited by DNA to serve on US/UK Joint Working Group 36 and to present "Space Systems and Survivability," London, England, September 1990; and invited by SDIO to present "High Temperature Superconductivity Space Experiment" and "Detection of BE-7 on Long Duration Exposure Facility Satellite" to US/UK Score Meeting, London, England, June 1990.

Rodriguez, P., Group Achievement Award: NASA Shuttle Imaging Radar-B Science Team, September 21, 1990.

Rolison, D.R., Member, Advisory Board of Analytical Chemistry, *Journal of the American Chemical Society*, January 1990-December 1992; Discussion Leader, 1st Gordon Research Conference on Zeolitic and Layered Materials, June 10-15, 1990.

Rooney, D.L., Appointed Financial Chairperson of the IEEE Computer Society Design Automation Standards Subcommittee (DASS).

Rosen, M., Member, SDIO SDS Threat Working Group.

Russell, J.N., Jr., Trustee, Alpha Sigma Educational Trust Fund.

Saks, N.S., Selected Technical Chairman, 1992 Nuclear and Space Radiation Effects Conference; received Outstanding Conference

Paper Award for the 1989 IEEE Nuclear and Space Radiation Effects Conference for the paper by Nelson S. Saks, and Dennis B. Brown, "Interface Trap Formation via the Two-Stage H^+ Process."

Sandberg, W.C., Selected Chairman, Research Priority Subgroup, Society of Naval Architects and Marine Engineers; Selected Chairman, Hydrodynamics Committee, Society of Naval Architects and Marine Engineers; Member, Technical and Research Steering Committee of the Society of Naval Architects and Marine Engineers.

Sartwell, B.D., General Chairman, International Conference on Metallurgical Coatings, April 22–26, 1991, San Diego, CA; Editor, *Surface and Coatings Technology Journal*, published by Elsevier Sequoia, Lausanne, Switzerland; Member, Interagency Working Group on Ion Implantation, organized by U.S. Army Material Command; Member, Executive Committee of the Vacuum Metallurgy Division of the American Vacuum Society; and Senior Editor, Proceedings of the Joint Eighth International Conference on Thin Films and 17th International Conference on Metallurgical Coatings, published by Elsevier Sequoia, December 1990.

Sass, A.H., Listed in Marquis', *Who's Who in America*.

Schmitt, A.J., Organizing committee member, 1991 Topical Conference on the Physics of Radiatively Driven ICF Targets.

Schnur, J., Chairman, 1990 Gordon Conference—Organic Thin Films; 1989-Top 10 Technologist: *Washington Technology* Magazine.

Sheinson, R.S., Elected Secretary, Eastern Section of the Combustion Institute.

Silberberg, R., Co-editor, *Currents in Astrophysics and Cosmology*, Cambridge University Press, England, 1991; Co-editor, *Cosmic Rays, Supernovae, and the Interstellas Medium*, Kluwes Academic Publishers, Dorecrecht, Holland, 1991.

Skelton, E.F., Spokesperson for High Pressure Insertion Device Team at National Synchrotron Light Source, Brookhaven National Laboratory; Elected Representative for Energy Dispersive Group (1990–91) on Users Executive Committee, National Synchrotron Light Source, Brookhaven National Laboratory; and invited to serve on NSF Review Panel for Cornell High Energy Synchrotron Source, (CHESS) October 24–25, 1990.

Sleger, K.J., Chairman, 1990 IEEE GaAs IC Symposium; Organizer, 1990 Tri-Service MIMIC CAD Workshop; Deputy Member, Advisory Group on Electron Devices, Group A.

Smidt, F.A., Co-chairman, Organizing Committee, International Conference on Surface Modification of Metals by Ion Beams; U.S. Government-TTG-A, Sub-Group C (Technology Export Control Advisory Group on Coatings); American Society for Materials (National Committee), Advisory Technical Awareness Council; and Fellow, Acoustical Society of America International.

Smith, W.R., Member, ASW Signal Processing Committee.

Sprangle, P.A., Fellow, American Physical Society, continuing membership; Member, Sigma Xi, continuing membership; Chairman, committee to select winner of 1991 APS, Division of Plasma Physics Award for Excellence in Plasma Physics Research; Member, DOE Advanced Accelerator R&D Review Panel, May 1990; named one of *Washington Technology* Magazine's Top Ten Talents of 1989; and Chairman, Invited Symposium at APS Spring Meeting, April 1990.

Stackpole, L.S., Elected Chair of the Military Librarians Division, Special Library Association; Elected Delegate to the Maryland Governor's Conference on Libraries and Information Services; and third year as member of the FEDLINK Advisory

Committee, Federal Library and Information Center Committee, Library of Congress.

Stapor, W.J., Member, Brookhaven National Laboratory Heavy Ion Booster Steering Committee, 1990; Chairman, Single Event Upset Session, 11th International Conference on the Application of Accelerators in Research and Industry, November 4-7, 1990; and Member, Combined Release and Radiation Effects Satellite (CRRES) Microelectronics Package Working Group, 1990.

Mr. Jathan Stone receives the Navy Meritorious Civilian Service Award from CAPT R. W. Michaux, Chief Staff Officer

Stoneman, R.S., Member, Technical Program Committee, Emerging Laser Technology/ Lasers and Electro-Optics Society (LEOS).

Strom, U., Program Advisor, 15th International Conference on Infrared and Millimeter Waves, December 10-14, 1990, Orlando, FL.

Swean, T.F., Jr., Appointed to Advisory Panel to review University of Southern California University Research Initiative Program on "Dynamics and Control of Turbulent Shear Flows."

Tait, G., Elected Officer, IEEE Microwave Theory and Techniques Society, Washington, DC/Northern Virginia Chapter.

Tatem, P.A., Chairperson (second term), Arrangements Committee, Eastern Section of the Combustion Institute.

Thoenes, K.L., Elected to Users Council of Defense Technical Information Center's Users Group.

Thompson, R.B., Appointed to National Research Council Panel on "New Measurement Technologies for the Oceans," September 1990; Editorial Board, *Journal of Molecular Graphics*.

Tolstoy, A., Invited paper on Ocean Tomography at Oceans '90 Meeting; Member (second year), Technical Specialty Group, ASA; invited paper at the Propagation and Noise in Underwater Acoustics Symposium in Auckland, New Zealand; invited seminar at Catholic University; and invited seminar at Woods Hole.

Trunk, G.V., Third year as chairman of KTP-2 (this is a technical exchange on radar data processing under the auspices of subgroup K (radar) within The Technical Cooperation Program (TTCP)).

Trzaskoma, P.P., Officer (Councillor), National Capital Section of The Electrochemical Society; Past President, Council of Local Sections of The Electrochemical Society; Member, Board of Directors of The Electrochemical Society; and Member, H.H. Uhlig Award Committee of The Electrochemical Society.

Valenzuela, G.R., Selected to Electromagnetics Academy, MIT, Cambridge, MA; Member, Organizing and Technical Program Committees for International Geoscience and Remote Sensing Symposium (IGARSS) '90, College Park, MD; and Co-organizer of Plenary Session on Global Change for IGARSS '90.

Venezky, D.L., Appointed Member of the American Chemical Society's Council Committee on International Activities; elected Member on the Chemical Society of Washington Board of Managers.

Vogt, P.R., Appointed to National Academy of Sciences Committee to Develop a National Research Initiative/Coordination on Geomagnetics; Associate Editor, *Bulletin of Geological Society of America*; and invited to

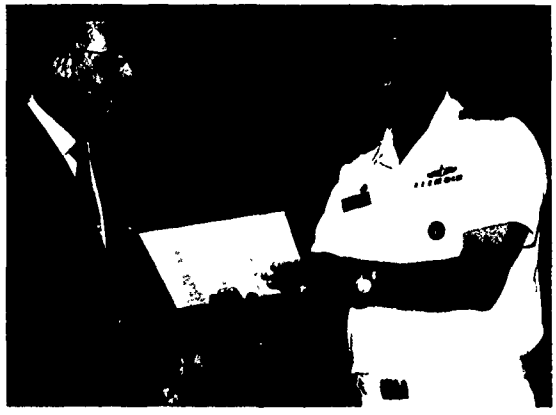

CAPT John Donegan presents Mr. Carol Veronda the 1989 Commanding Officer's Award for Achievement in the Field of Equal Employment Opportunity (Supervisory Category)

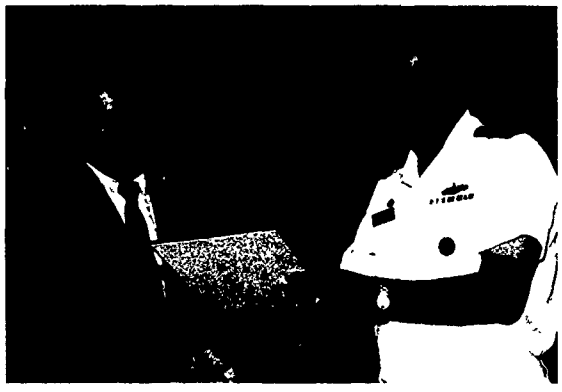

Mr. Dominic Panciarelli receives the 1989 Commmanding Officer's Award for Achievement in the Field of Equal Employment Opportunity (Non-Supervisory Category) from CAPT John Donegan

organize and chair a special session of American Geophysical Union Winter Meeting on Rapid Detection of Underwater Volcanic/Tectonic Events.

Wagner, R.J., Member, Program Committee of the IRIS Specialty Group on Infrared Materials.

Waterman, J.M., Member, Mercury-Cadmium-Telluride (MCT) Workshop Program Committee.

Webb, D.C., Member, Technical Program Committee, 1990 Ultrasonics Symposium, IEEE; Member, Technical Program Committee, 1990 International IEEE Microwave Theory and Techniques Symposium; Member, OUSD Working Group of U.S. Japan Cooperative R&D in Dual Mode Seeker Technology.

Whitlock, R.R., Member, Technical Program Committee, 1991 American Physical Society (APS) Topical Conference on Shock Compression of Condensed Matter.

Wieting, T.J., Editor, Proceedings on the Fourth National Conference on High-Power Microwave Technology; Member, Program Committee and Session Chairman, Fifth National Conference on High-Power Microwave Technology, 1990; Chairman, OUSD Microwave Effects Panel; Member, OUSD HPM Systems Effects Assessment Team (SEAT); Member, OUSD Team on Project Tiger Grip; Member, Review Group on AF Project Seek Needle; Member, OUSD HPM Foreign Asset Assessment Team (FAAT); and Member, U.S. Member and Subgroup Chairman on Hardening, NATO-AGARD Workshop on High-Power Microwave.

Wilhelm, P.G., Appointed to the Space Transportation Technical Committee of the American Institute of Aeronautics and Astronautics.

Wilsey, N.D., Elected to Editorial Board, *Journal of Materials Science: Materials in Electronics*.

Wood, K., Member, Spaces Science and Astrophysics Technical Committee of American Institute of Aeronautics and Astronautics (AIAA); Member, Grid Science Team (NASA); and Member, Cases Science Working Group (NASA).

Yen, N., Fellow, Acoustical Society of America, continuing membership; Continuing Member, IEEE, AAAS, ACM, NRL Chapter Sigma Xi.

Young, F.C., Elected Member, Executive Committee of the IEEE Plasma Science and Applications Committee (3-year term).

Zedd, M.F., Member, American Institute of Aeronautics and Astronautics' Atmospheric Flight Mechanics Working Group to develop a recommended practice for flight vehicle coordinate systems.

ALAN BERMAN RESEARCH PUBLICATION AND EDISON PATENT AWARDS

The Annual Research Publications Awards Program was established in 1968 to recognize the authors of the best NRL publications each year. These awards not only honor individuals for superior scientific accomplishments in the field of naval research, but also seek to promote continued excellence in research and in its documentation. In 1982, the name of this award was changed to the Alan Berman Research Publications Award in honor of its founder.

There were 239 separate publications published in 1990 that were considered for recognition. Of those considered, 35 were selected. These selected publications represent 125 authors, each of whom received a publication awards certificate, a bronze paperweight, and a booklet listing the publications that received special recognition. In addition, NRL authors share in their respective division's monetary award.

The winning papers and their respective authors are listed below by their research units. Non-Laboratory coauthors are indicated by an asterisk.

Also listed are the two recipients of the NRL Edison (Patent) Awards established in January 1991 to recognize NRL employees and their patent attorneys for outstanding patents issued to NRL by the U.S. Patent and Trademark Office during the preceding calender year. The award recognizes significant NRL contributions to science and engineering as demonstrated by the patent process that are perceived to have the greatest potential benefit to the country.

Space Science Division

The Seasonal Variation of Water Vapor and Ozone in the Upper Mesosphere: Implications for Vertical Transport and Ozone Photochemistry
Richard M. Bevilacqua, Darrell F. Strobel,*
Michael E. Summers, John J. Olivero,* and Mark Allen,*

The Gamma-Ray Light Curves of SN 1987A
Mark D. Leising and Gerald H. Share

Laboratory for Computational Physics and Fluid Dynamics

Reinitiation and Feedback in Global Instabilities of Subsonic Spatially Developing Mixing Layers
Fernando F. Grinstein, Elaine S. Oran, and Jay P. Boris

Ablative Rayleigh-Taylor Instability in Three-Dimensions
Jill P. Dahlburg and John H. Gardner

Center for Advanced Space Sensing

Aerosol Size Distribution and Optical Properties Found in the Marine Boundary Layer Over the Atlantic Ocean
William A. Hoppel, James W. Fitzgerald, Glendon M. Frick, Reginald E. Larson, and Eugene M. Mack*

Hydrodynamics of Ship Wake Surfactant Films
Rodney D. Peltzer, Jermone H. Milgram,* Richard A. Skop,* Jack A. Kaiser, Owen M. Griffin, and William R. Barger, Jr.

Condensed Matter and Radiation Sciences Division

Fundamentals of Ion-Beam Assisted Deposition. I. Model of Process and Reproducibility of Film Composition
Deborah Van Vechten, Graham K. Hubler, Edward P. Donovan, and Franics D. Correll

Fundamentals of Ion-Beam-Assisted Deposition. II. Absolute Calibration of Ion and Evaporant Fluxes
Graham K. Hubler, Deborah Van Vechten, Edward P. Donovan, and Carmine A. Carosella

Surface Space-Charge Dynamics and Surface Recombination on Silicon (III) Surfaces Measured with Combined Laser and Synchrotron Radiation
James P. Long, Hassan R. Sadeghi,* Jack C. Rife, and Milton N. Kabler

Plasma Physics Division

Improved Beam Confinement in the Modified Betatron with Strong Focusing
C.A. Kapetanakos, L.K. Len,* Tab Smith, Joseph Golden,* Kevin Smith,* Spencer J. Marsh,* Demos Dialetis,* Joseph Mathew, Peter Loschialpo, and Jeng-Hsien Chang

Transition from I^4 to I^2 Scaling of K-Shell Emission in Aluminum Array Implosions
Ward Thornhill, Kenneth Whitney, and Jack Davis

Acoustics Division

Experimental Investigation of the Wave Propagation on a Point-Driven, Submerged Capped Cylinder Using K-Space Analysis
Earl G. Williams, Brian H. Houston, and Joseph A. Bucaro

Optimal Time-Domain Beamforming with Simulated Annealing Including Application of a priori Information
William A. Kuperman, Michael D. Collins, John S. Perkins, and Nolan R. Davis

Radar Division

Convergence Properties of Gram-Schmidt and SMI Adaptive Algorithms
Karl Gerlach and Frank Kretschmer, Jr.

Looking Over the Horizon
James M. Headrick

Information Technology Division

Learning Sequential Decision Rules Using Simulation Models and Competition
John J. Grefenstette, Connie Loggia Ramsey, and Alan C. Schultz

Security Models and Information Flow
John D. McLean

Tactical Electronic Warfare Division

High-Resolution, Six-Channel Interferometer Development and Performance
Roger D. Oxley

Low Observable (LOB) Antenna Systems
David G. Enders, Armondo D. Elia, and Gerald E. Friedman

Underwater Sound Reference Detachment

A Planar Array for the Generation of Evanescent Waves
David H. Trivett,* L. Dwight Luker, Sheridan Petrie,
Arnie Lee Van Buren, and Joseph E. Blue

Laboratories, Offices, and Scientific Staff Reporting Directly to Associate Directors of Research

Parallel Zippers Formed by α-helical Peptide Columns in Crystals of Boc-Aib-Glu(OBzℓ)-Leu-Aib-Ala-Leu-Aib-Ala-Lys(Z)-Aib-OMe
Isabella Karle, Judith L. Flippen-Anderson, Kuchibhotla Uma,* and Padmanabhan Balaram*

Dry Storage of Liposome-Encapsulated Hemoglobin: A Blood Substitute
Alan S. Rudolph and Richard O. Cliff*

Chemistry Division

Measurement of Translational Displacement Probabilities by NMR: An Indicator of Compartmentation
Allen N. Garroway and David G. Cory*

Theoretical and Experimental Investigation of the Reaction
$BH+D_2 \rightarrow BHD_2$
Norris J. Caldwell,* Jane K. Rice, Herbert H. Nelson, George F. Adams,* and Michael J. Page

Materials Science and Technology Division

A Competitive Adsorption Model for the Inhibition of Crevice Corrosion and Pitting
Edward McCafferty

Synchronization in Chaotic Systems
Louis M. Pecora and Thomas L. Carroll

Optical Sciences Division

Design Parameters for an Infrared Surveillance System
Joseph Michalowicz, John Kershenstein, Thomas Giallorenzi, Robert Lucke, Martin McHugh, Jr., Edward Stone, John Hornstein, and Alan Schaum

Control of Transverse Spatial Modes in Transient Stimulated Raman Amplification
Michael Duncan, Rita Mahon,* Lawrenece Tankersley,* and John Reintjes

Electronics Science and Technology Division

A $Si_{0.7}$ $Ge_{0.3}$ Strained-Layer Etch Stop for the Generation of Thin Layer Undoped Silicon
David Godbey, Harold Hughes, Francis Kub, Mark Twigg,* Leslie J. Palkuti,* Peter Leonov,* and Jih-Jong Wang*

Lattice Weyl-Wigner Formulation of Exact Many-Body Quantum-Transport Theory and Applications to Novel Solid-State Quantum-Based Devices
Felixberto Buot and Kevin L. Jensen

Space Systems Development Department

Effects of Multi-Pump Beam Coupling on Intensity Enhancement of a Probe Beam in Photorefractive Two-Wave Mixing
G. Charmaine Gilbreath and Frederick M. Davidson*

Experimental Measurements of Modal Transients and Theoretical Thermal Modeling of Laser Diodes, Laser-Diode Technology and Applications II
Wendy L. Lippincott, Anne E. Clement, and William C. Collins

Spacecraft Engineering Department

Painting the Phase Space Portrait of an Integrable Dynamical System
Shannon Coffey, Andre Deprit,* Etienne Deprit, and Liam Healy*

Deriving Component Pyroshock Test Specifications from System Level Test Data
Aaron A. Salzberg

Space Systems Technology Department

Cascaded Detector for Multiple High-PRF Pulse Doppler Radars
Karl Gerlach and Grealie A. Andrews, Jr.

A Superconducting Hydrogen Maser Resonator Made From Electrophoretic $YBa_2Cu_3O_{7-\delta}$
D. Opie,* Harlan Schone,* Matthias Hein,* Gunther Muller,*
Helmut Piel,* Dorothea Wehler,* Vincent J. Folen, and Stuart Wolf

NRL Edison (Patent) Awards

Metal Clad Lipid Microstructures
Joel M. Schnur, Paul J. Schoen, Jr., Jeffrey M. Calvert, and Ronald R. Price

Tunable, Continuous Wave Thulium-Doped, Solid State Laser
Leon Esterowitz, Robert C. Stoneman, and George Jameson

AWARDS FOR *NRL REVIEW* ARTICLES

Awards for *NRL Review* articles were established during 1990 to recognize authors who submit outstanding research articles for this scientific publication. The articles are judged on the relevance of the work to the Navy and the DoD, readability to the college-graduate level, and the use of graphics that are interesting and informative. The first awards were presented for the following articles that appeared in the *1989–1990 NRL Review.*

FEATURED RESEARCH ARTICLE

Solid-State Supercomputing
Larry L. Boyer, Barry M. Klein, Dimitrios A. Papaconstantapoulos, and Warren E. Pickett
Condensed Matter and Radiation Sciences Division

DIRECTORATE AWARDS FOR SCIENTIFIC ARTICLES

General Science and Technology Directorate

High-Performance Infrared Filters and Mirrors
Edward P. Donovan
Condensed Matter and Radiation Sciences Division

Warfare Systems and Sensors Directorate

High-Resolution Waveforms in Radar Surveillance
George J. Linde
Radar Division

Materials Science and Component Technology Directorate

Glass Fibers with Metallic Cores
Jack D. Ayers
Materials Science and Technology Division

Navy Center for Space Technology

Visualizing Phase Flows in Dynamical Systems
Shannon L. Coffey, Etienne M. Deprit, and Liam M. Healey
Spacecraft Engineering Department

Programs for Professional Development

PROFESSIONAL DEVELOPMENT

NRL has established many programs for the professional and personal development of its employees so that they may better serve the needs of the Navy. These programs develop and retain talented people and keep them abreast of advanced technology management skills. Graduate assistantships, fellowships, sabbatical study programs, cooperative education programs, individual college courses, and short courses for personal improvement contribute to professional development.

Programs are also available for non-NRL employees. These enhance the Laboratory's research program by providing a means for non-NRL professionals to work at the Laboratory and thus improve the exchange of ideas, meet critical short-term technical requirements, and provide a source of new, dynamic scientists and engineers. The programs range from two-year graduate fellowships, faculty and professional interchanges, and undergraduate work to an introduction of gifted and talented high school students to the world of technology.

PROGRAMS FOR NRL EMPLOYEES

During 1990, under the auspices of the Employee Development Branch, NRL employees participated in about 5000 individual training events. Many of these were presented as either videotaped or on-site instructed courses on diverse technical subjects, management techniques, and enhancement of such personal skills as efficient use of time, speed reading, memory improvement, and interpersonal communications. Courses are also available by means of computer-based training (CBT) and live television courses for monitoring nationwide.

One common study procedure is for employees to work full time at the Laboratory while taking job-related scientific courses at universities and schools in the Washington area. The training ranges from a single course to full graduate and postgraduate programs. Tuition for training is paid by NRL. The formal programs offered by NRL are described here.

GRADUATE PROGRAMS

• The **Advanced Graduate Research Program** (formerly the Sabbatical Study Program, which began in 1964) enables selected professional employees to devote full time to research or pursue work in their own or a related field for one academic year at an institution of their choice without the loss of regular salary, leave, or fringe benefits. NRL pays all educational costs, travel, and moving expenses for the employee and dependents. Criteria for eligibility include professional stature consistent with the applicant's opportunities and experience, a satisfactory program of study, and acceptance by the institution selected by the applicant. The program is open to paraprofessional (and above) employees who have completed 6 years of Federal Service, 4 of which are required at NRL.

Dr. Arthur Jordan, of the Space Science Division, participated in the Advanced Graduate Research Program, spending a year at the Massachusetts Institute of Technology

• The **Edison Memorial Graduate Training Program** enables employees to pursue advanced studies in their fields at local universities. Participants in this program work 24 hours each workweek and pursue their studies during the other 16 hours. The criteria for eligibility include a minimum of 1 year of service at NRL, a bachelor's or master's degree in an appropriate field, and professional standing in keeping with the candidate's opportunities and experience.

• To be eligible for the **Select Graduate Student Program**, employees must have a college degree in an appropriate field and must have maintained at least a B average in undergraduate study. Students accepted in this program devote a full academic year to graduate study. While attending school, they receive one half of their salary, and NRL pays for tuition, books, and laboratory expenses. During the summer, they work at the Laboratory and receive normal pay and fringe benefits.

John J. Harper, of the Information Technology Division, participated in the Select Graduate Program at the University of Virginia

• The **Naval Postgraduate School** (NPS), located in Monterey, California, provides graduate programs to enhance the technical preparation of Naval officers and civilian employees who serve the Navy in the fields of science, engineering, operations analysis, and management. It awards a Master of Arts Degree in National Security Affairs and a Master of Science Degree in many technical disciplines. In addition, a Doctor of Philosophy Degree may be earned in select fields of science and engineering.

NRL employees desiring to pursue graduate studies at NPS may apply for a maximum of six quarters away from NRL, with thesis work accomplished at NRL. Specific programs are described in the NPS Catalog. Participants will continue to receive full pay and benefits during the period of study.

• Under the **Foreign Liasion Scientist Program**, assistance is provided to the Chief of Naval Research (CNR), the Chief of Naval Operations (CNO), and the Commandant of the Marine Corps (CMC) in discharging their responsibilities on matters of general scientific and technical interest to the United States in the United Kingdom, Europe, and Far East in foreign liaison offices that are maintained in several areas of the world. Foreign liaison scientists serve in these offices to establish relationships with overseas scientists and scientific activities, to monitor contract and treaty agreements, and to promote the exchange of information and research results between foreign sources and the U.S. Navy R&D establishment. Each year NRL will make assignments to the Office of Naval Research European Office (ONEUR), London, England, and the Office of Naval Research Liaison Office, Far East (ONRFE), Tokyo, Japan. The purpose of such assignments is to acquaint a limited number of NRL's technical professionals with the functions of international operations, including such activities as developing productive liaison with foreign scientists and research activities, representing the interests of the U.S. Navy in multinational conferences and scientific meetings, and preparing technical reports and papers with editorial interpretation for appropriate audiences in the United States.

• In addition to NRL and university offerings, application may be made to a number of noteworthy programs and fellowships. Examples of such opportunities are the **Alfred P. Sloan Fellows Programs, Brookings Institute Advanced Study Program, The Fellowship in Congressional Operations** and the **Women's Executive Leadership Program**. These and other programs are announced from time to time as schedules are published.

• Research conducted at NRL may be used as **thesis material for an advanced degree.** This original research is supervised by a qualified employee of NRL who is approved by the graduate school. The candidate should have completed the required course work and should have satisfied the language, residence, and other requirements of the graduate school from which the degree is sought. NRL provides space, research facilities, and supervision but leaves decisions on academic policy to the cooperating schools.

CONTINUING EDUCATION

• Local colleges and universities offer **undergraduate and graduate courses** at NRL for

employees interested in improving their skills and keeping abreast of current developments in their fields. These courses are also available at many other DoD installations in the Washington, DC area.

• The Employee Development Branch at NRL offers to all employees **short courses** in a number of fields of interest including technical subjects, computer operation, supervisory and management techniques, and clerical/secretarial skills. Laboratory employees may attend these courses at nongovernment facilities as well. Interagency courses in management, personnel, finance, supervisory development, and clerical skills are also available.

For further information on any of the above programs, contact the Employee Development Branch (Code 3840) (202) 767-2956.

TECHNOLOGY TRANSFER

• The **Office of Research and Technology Applications Program** ensures the full use of the results of the Nation's federal investment in research and development by transferring federally owned or originated technology to state and local governments and the private sector.

• The **Navy Science Assistance Program** establishes an information loop between the Fleet and the R&D shore establishments to expedite technology transfer to the user. The program addresses operational problems, focuses resources to solve specific technical problems, and develops a nucleus of senior scientific personnel familiar with the impact of current research and system performance on military operations.

The Navy's Scientists-to-Sea Program offers Navy researchers and R&D managers the opportunity to learn firsthand about factors that affect shipboard system design and operations. The program includes personnel from NRL. The trips generally last from three to ten days. The Scientists-to-Sea Program is scheduled to continue indefinitely with new embarkations offered on a quarterly basis.

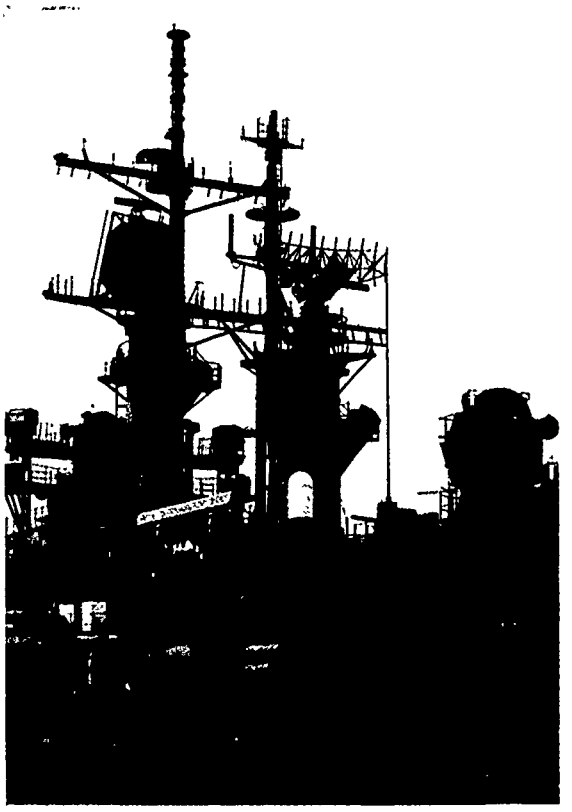

Dr. Fred Stonesifer, of the Materials Science and Technology Division, participated in the Scientist-to-Sea Program on board the USS *Richmond K. Turner* (CG-20). His four-day cruise was out of Puerto Rico.

Inquiries concerning NRL's technology transfer programs should be made to Dr. Richard Rein or to Dr. George Abraham (Code 1003.1), at (202) 767-3521.

PROFESSIONAL DEVELOPMENT

NRL has several programs, professional society chapters, and informal clubs that enhance the professional growth of employees. Some of these are listed below.

• The **Counseling Referral Service** (C/RS) helps employees to achieve optimal job performance through counseling and resolution of problems such as family, stress and anxiety, behavioral, emotional, and alcohol- or drug-related problems that may adversely impact job performance.

C/RS provides confidential assessments and short-term counseling, as well as training workshops and referrals to additional resources in the community. Contact Ms. Barbara Fornoff or Dr. Ralph Surette, Code 9012, (202) 767-6857.

• A chartered chapter of **Women in Science and Engineering** (WISE) was established at NRL in 1983. Informal monthly luncheons and seminars are scheduled to inform scientists and engineers of women's research at NRL and to provide an informal environment for members to practice their presentations. WISE also sponsors a colloquium series to feature outstanding women scientists. (Contact Dr. Wendy Fuller at (202) 767-2793, Dr. Debra Rolison at (202) 767- 3617, or Dr. Cha-Mei Tang at (202) 767-4148.)

• **Sigma Xi**, the Scientific Research Society, encourages original investigation in pure and applied science. As an honor society for research scientists, individuals who have demonstrated the ability to perform original research are elected to membership in local chapters. The NRL chapter, comprised of approximately 400 members, encourages original research by presenting awards annually in pure and applied science to outstanding NRL staff members. The chapter also sponsors lectures at NRL on a wide range of scientific topics for the entire NRL community. The lectures are delivered by scientists from all over the nation and the world. The highlight of the lecture series is the Edison Memorial Lecture, usually featuring a Nobel laureate. (Contact Dr. Susan K. Numrich at (202) 404-7345.)

• Employees interested in developing effective self expression, listening, thinking, and leadership potential are invited to join either of two NRL chapters of **Toastmasters International**. Members of these clubs, who possess diverse career backgrounds and talents, meet three times a month in an effort to learn to communicate not by rules but by practice in an atmosphere of understanding and helpful fellowship. NRL's commanding officer endorses Toastmasters (see NRLINST 12410.11), and the Employee Development Branch pays for membership and educational materials for those employees whose supervisors see a need for their active training in public speaking or organizational communication skills. (Contact Mrs. Kathleen Parrish at (202) 767-2782.)

The Forum Toastmasters sponsored a Youth Leadership Program at the neighboring Leckie Elementary School

EQUAL EMPLOYMENT OPPORTUNITY (EEO) PROGRAMS

Equal employment opportunity is a fundamental NRL policy for all persons, regardless of race, color, sex, religion, national origin, age, or physical/mental handicap. The EEO Office's major functions include affirmative action in employment; discrimination complaint process; EEO training of supervisors, managers, and EEO collateral duty personnel; advice and guidance to management on EEO policy; and the following special emphasis programs.

• The **Federal Women's Program (FWP)** supports and enhances employment and advancement opportunities for women and addresses issues that affect women in the workplace. It provides counseling and referral services and sponsors a chapter of Women in Science and Engineering to recognize outstanding female scientists and engineers. Distinguished women scientists are guest lecturers at quarterly presentations.

• The **Hispanic Employment Program (HEP)** focuses on working with supervisors, managers, and subcommittees to recruit and place qualified Hispanics. The program is involved with Hispanic community organizations and local schools and provides activities specifically designed to offer employment opportunities to Hispanics. "El Ingeniero" (The Engineer), which encourages Hispanic youth to pursue a career in engineering, is one such program.

• The **Black Employment Program (BEP)** concentrates on recruiting, placing, developing and advancing Black employees throughout NRL. It also encourages Black employees to achieve their maximum potential.

NRL's Commanding Officer, CAPT John Donegan, presents the first-place essay award for grades 1-3 to Monica Dewitt as NRL celebrates Black History Month

• The **Individuals with Handicaps Program (IHP)** assists management to improve employment and advancement opportunities for qualified handicapped and disabled-veteran employees. It also advises on accommodations necessary for handicapped persons. It recruits handicapped summer students from colleges and universities for technical positions in engineering and science and paraprofessional positions in accounting and administration; it also seeks Cooperative Education Program (Co-op) candidates who are pursuing degrees in engineering, computer sciences, or the physical sciences.

• The **Asian-American/Pacific Islander Program (API)** identifies areas of concern regarding the recruitment, selection, advancement, retention, and utilization of Asian-American/Pacific Islander employees throughout NRL. The program interacts with API professional/community organizations to address employment concerns.

NRL celebrated its first Asian-Pacific Heritage observance with a performance by the PACAS Dance Troupe

• The **American Indian/Alaskan Native Employment Program (AI/ANEP)** focuses on the employment concerns of AI/ANEP employees. The program provides counseling and referral services for NRL's AI/ANEP on recruitment, hiring, placement, promotion, retention, and other areas of employee interest.

• The **Federal Employment Opportunity Recruitment Program (FEORP)** is designed to establish, maintain, and update targeted recruitment programs to reduce the conspicuous absence or manifest imbalance categories of NRL employment through innovative internal and

external recruitment. In addition, it fosters relationships with minority and women's institutions and organizations.

Special programs are held during the year to promote an awareness of the contributions and capabilities of women and minorities. (Contact the EEO Office at (202) 767-2486 for all EEO programs.)

The Commanding Officer, CAPT John Donegan, answers questions posed by NRL's Partners in Education students from the nearby Leckie Elementary School about the Payload Checkout Facility's anechoic chamber

OTHER ACTIVITIES

• The **Community Outreach Program** traditionally has used its extensive resources to foster programs that provide benefits to students and other community citizens. Volunteer employees assist with and judge science fairs, give lectures, tutor, mentor, coach, and serve as classroom resource teachers. The Program also sponsors Black History Month art and essay contests for local schools, student tours of NRL, a student Toastmasters Youth Leadership Program, an annual Christmas party for neighborhood children, and an annual collection for Children's Hospital. (Contact the Public Affairs Office at 767-2541.)

Contestants in a dance contest held during NRL's annual Children's Christmas Party for neighboring schools

• Other programs that enhance the development of NRL employees include computer clubs (Edison, Atari, Commodore, and NRL-IBM PC) and the Amateur Radio Club. The Recreation Club accommodates the varied interests of NRL's employees with its numerous facilities, such as a 25-yard, 6-lane indoor swimming pool; a gymnasium with basketball and volleyball; a weight room and exercise area; table tennis; meeting rooms; softball and basketball leagues; jacuzzi whirlpool; sauna; classes in five different martial arts groups, aerobics exercise, swimming, and swimnastics; and specialized sports clubs (running, skiing, biking, golfing). The Showboaters, a nonprofit drama group that presents live theater for the enjoyment of NRL and the community, performs in two major productions each year in addition to occasional performances at Laboratory functions and benefits for local charities. The most recent productions were "Godspell" and "You Can't Take it With You." Though based at NRL, membership in Showboaters is not limited to NRL employees.

PROGRAMS FOR NON-NRL EMPLOYEES

Several programs have been established for non-NRL professionals. These programs encourage and support the participation of visiting scientists and engineers in research of interest to the Laboratory. Some of the programs may serve as stepping-stones to federal careers in science and technology. Their objective is to enhance the quality of the Laboratory's research activities through working associations and interchanges with highly capable scientists and engineers and to provide opportunities for outside scientists and engineers to work in the Navy laboratory environment. Along with enhancing the Laboratory's research, these programs acquaint participants with Navy capabilities and concerns.

RECENT Ph.D., FACULTY MEMBER, AND COLLEGE GRADUATE PROGRAMS

• The **National Research Council (NRC)/ NRL Cooperative Research Associateship Program** selects associates who conduct research at NRL in their chosen fields in collaboration with NRL scientists and engineers. The tenure period is 2 years. The Office of Naval Research offers the associate posttenure research grants tenable at an academic institution.

• The American Society for Engineering Education (ASEE) administers the **Office of Naval Technology (ONT) Postdoctoral Fellowship Program** that aims to increase the involvement of highly trained scientists and engineers in disciplines necessary to meet the evolving needs of naval technology. Appointments are for 1 year (renewable for a second and sometimes a third year). These competitive appointments are made jointly by ONT and ASEE.

• The American Society for Engineering Education also administers the Navy/ASEE **Summer Faculty Research Program** for university faculty members to work for 10 weeks with professional peers in participating Navy laboratories on research of mutual interest.

• The **NRL/United States Naval Academy (USNA) Cooperative Program for Scientific Interchange** allows faculty members of the U.S. Naval Academy to participate in NRL research. This collaboration benefits the Academy by providing the opportunity for USNA faculty members to work on research of a more practical or applied nature. In turn, NRL's research program is strengthened by the available scientific and engineering expertise of the USNA faculty.

• The **Office of Naval Research Graduate Fellowship Program** helps U.S. citizens obtain advanced training in disciplines of science and engineering critical to the U.S. Navy. The 3-year program awards fellowships to recent outstanding graduates to support their study and research leading to doctoral degrees in specified disciplines such as electrical engineering, computer sciences, material sciences, applied physics, and ocean engineering. Award recipients are encouraged to continue their study and research in a Navy laboratory during the summer.

For further information about the above five programs, please contact Mrs. Jessica Hileman at (202) 767-3865.

• The **United States Naval Academy Ensign Program** assigns Naval Academy graduates to NRL to work in areas of their own choosing commensurate with their academic

qualifications. These graduates provide a fruitful summer of research assistance, while gaining valuable experience in the Navy's R&D program. (Contact CDR Tom Nadeau at (202) 767-2103.)

PROFESSIONAL APPOINTMENTS

• **Faculty Member Appointments** use the special skills and abilities of faculty members for short periods to fill positions of a scientific, engineering, professional, or analytical nature.

• **Consultants and experts** are employed because they are outstanding in their fields of specialization, or because they possess ability of a rare nature and could not normally be employed as regular civil servants.

• **Intergovernmental Personnel Act Appointments** temporarily assign personnel from the state or local government or educational institution to the Federal Government (or vice versa) to improve public services rendered by all levels of government.

UNDERGRADUATE COLLEGE STUDENT PROGRAMS

Several programs are tailored to the undergraduate that provide employment and work experience in naval research. These are designed to attract applicants for student and full professional employment in the Laboratory's shortage category positions, such as engineers, physicists, mathematicians, and computer scientists. The student employment programs build an understanding of NRL job opportunities among students and educational personnel so that educators can provide students who will meet NRL's occupational needs. The employment programs for college students include the following:

• The **Cooperative Education Program** alternates periods of work and study for students pursuing bachelor degrees in engineering, computer science, or the physical sciences. Several universities participate in this program.

• The **Federal Junior Fellowship Program** hires students entering college to be assistants to scientific, professional, or technical employees.

• The **Summer Employment Program** employs students for the summer in paraprofessional and technician positions in engineering, physical sciences, and computer sciences.

• The **Student Volunteer Program** helps students gain valuable experience by allowing them to voluntarily perform educationally related work at NRL.

• The **1040-Hour Appointment** employs students on a half-time basis to assist in scientific work related to their academic program.

• The **Gifted and Talented Internship Program** provides a meaningful part-time employment experience for high school students who plan to pursue a bachelor's degree in engineering, computer science, or the physical sciences.

For additional information, contact Mrs. Cathy Downing at (202) 767-3030.

HIGH SCHOOL PROGRAMS

• The **DoD Science & Engineering Apprentice Program** employs high school juniors and seniors to serve for 8 weeks as junior research associates. Under the direction of a mentor, students gain a better understanding of research, its challenges, and its opportunities through participation in scientific programs. Criteria for eligibility are based on science and mathematics courses completed and grades achieved; scientific motivation, curiosity, and capacity for sustained hard work; a desire for a technical career; teacher recommendations; and achievement test scores. The Naval Research Laboratory Program is the lead program and the largest in the Department of Defense.

For additional information on these programs, please contact the Employee Development Branch, Code 3840, at (202) 767-2956.

Dr. Harold Szu, of the Tactical Electronic Warfare Division, discusses neural networks with Westinghouse Science Talent Search second-place winner, David Liu

Ms. Patti Dunsavage views an ion-implanted aluminum specimen on an X-ray photoelectron spectrometer. Ms. Dunsavage was one of six local high-school students hosted by Dr. Noel Turner, of the Chemistry Division. The students participated in the Young Scholars Instrumentation Institute Program supported by the National Science Foundation at the nearby Prince George's Community College and NRL's Community Outreach Program.

Ninety-one students participated in the Science and Engineering Apprenticeship Program in 1990. Here Dr. John-David Bartoe spoke to the group about his experiences as a payload specialist aboard the Space Shuttle

General Information

GENERAL INFORMATION

"...The scientific and technical accomplishments of NRL, along with its scientific and technical staff, are the envy of the research and development community around the world. This Laboratory has a 67-year record of important innovation, of important contributions to science and technology, and of major contributions to the development of defense systems....The scientific and technical staff at NRL are proud of their work, they are proud of their laboratory, they are proud of their colleagues, and they are proud of their accomplishments."

Dr. Timothy Coffey
NRL's Director of Research
at the Alan Berman Research Publication
Awards Ceremony, March 2, 1990

TECHNICAL OUTPUT

The Navy continues to be a pioneer in initiating new developments and a leader in applying these advancements to military requirements. The primary means of informing the scientific and engineering community of the advances made at NRL is through its technical output—reports, articles in scientific journals and books, papers presented to scientific societies, and topical conferences, patents, and inventions.

This section lists a portion of NRL's output for FY 1990. The omitted parts are oral presentations (about 2000), reports that carry a military security classification, and letter reports to sponsors.

Type of Contribution	Unclass.	Class.	Total
Papers in periodicals, books, and proceedings of meetings	1197	3	1200
NRL Reports	30	16	46
NRL Memorandum Reports	117	26	143
Books	5	0	5
Patents granted			44
Statutory Invention Registrations (SIRS)			1

A complete listing of the publications by NRL authors, including reports, articles in scientific journals and books, patents, etc. will appear in the *Bibliography of NRL Publications* as a separate publication.

Key Personnel

Code	Office		Extension*
	EXECUTIVE DIRECTORATE		
1000	Commanding Officer	CAPT P.G. Gaffney II USN	73403
1001	Director of Research	Dr. T. Coffey	73301
1002	Chief of Staff Officer/Insepctor General	CAPT R.W. Michaux, USN	73621
1003	Associate Director of Research for Strategic Planning	Dr. W.M. Tolles	73584
1004	Scientific Consultant to Director of Research	Dr. P. Mange	73724
1005	Head, Office of Management and Administration	Ms. M. Oliver	73086
1006	Head, Exploratory Development Program Office	Dr. S. Sacks	73666
1200	Head, Command Support Division	CAPT R.W. Michaux, USN	73621
1240	Head, Safety Branch	Mr. K. King†	72232
1270	Officer in Charge, Cheasapeake Bay Detachment	LCDR B. Jones, USN	301-257-4002
1280	Officer in Charge, Flight Support Detachment	LCDR G.R. Viggiano, USN	301-863-3751
1500	Head, Program Coordination Office	Dr. R.T. Swim	73314
3008	Legal Counsel	Ms. H. Halper†	72244
3803	Deputy EEO Officer	Mr. W. Williams†	72486
4810	Public Affairs Officer	Mr. J.W. Gately, Jr.†	72541
	BUSINESS OPERATIONS DIRECTORATE		
3000	Associate Director of Research	Mr. R.E. Doak	72371
3200	Head, Contracting Division	Mr. J. Ely	75227
3300	Comptroller	Mr. D.T. Green	73405
3400	Supply Officer	CDR W.E. Ralls, Jr., USN	73446
3500	Public Works Officer	Mr. D.K. Woodington	73371
3800	Head, Civilian Personnel Division	Mrs. B.A. Duffield	73421
	GENERAL SCIENCE AND TECHNOLOGY DIRECTORATE		
4000	Associate Director of Research	Dr R.A. LeFande‡	73324
4100	Supt., Space Science Division	Dr. H. Gursky	76343
4200	Center for Advanced Space Sensing	Dr. K. Johnston	72351
4400	Dir., Lab. for Computational Physics and Fluid Dynamics	Dr. J.P. Boris	73055
4600	Supt., Condensed Matter & Radiation Sciences Division	Dr. D.J. Nagel	72931
4700	Supt., Plasma Physics Division	Dr. S. Ossakow	72723
4800	Head, Technical Information Division	Mr. P.H. Imhof	73388
	WARFARE SYSTEMS AND SENSORS RESEARCH DIRECTORATE		
5000	Associate Director of Research	Mr. R.R. Rojas	73294
5100	Supt., Acoustics Division	Dr. D.L. Bradley	73482
5300	Supt., Radar Division	Dr. M.I. Skolnik	72936
5500	Supt., Inforamtion Technology Division	Dr. R.P. Shumaker	72903
5700	Supt., Tactical Electronic Warfare Division	Dr. J.A. Montgomery	76278
5800	Head, Resarch Computation Division	Mr. R.F. Saenger	72751
5900	Supt. Underwater Sound Research Detachment	Dr. J.E. Blue	407-856-5230
	MATERIALS SCIENCE AND COMPONENT TECHNOLOGY DIRECTORATE		
6000	Associate Director of Research	Dr. B.B. Rath	73506
6030	Head, Laboratory for Structure of Matter	Dr. J. Karle	72665
6090	Center for Biomolecular Science and Engineering	Dr. J. Schnur	73344
6100	Supt., Chemistry Division	Dr. J.S. Murday	73026
6300	Supt., Materials Science & Technology Division	Dr. D.U. Gubser	72926
6500	Supt., Optical Sciences Division	Dr. T.G. Giallorenzi	73171
6800	Supt., Electronics Science and Technology Division	Dr. G.M. Borsuk	73525
	NAVAL CENTER FOR SPACE TECHNOLOGY		
8000	Director	Mr. P.G. Wilhelm	76547
8100	Supt., Space Systems Development Department	Mr. R.E. Eisenhauer	70410
8200	Supt., Spacecraft Engineering Department	Mr. R.T. Beal	76407
8300	Supt., Space Systems Technology Department	Mr. L.M. Hammarstrom	73920

*Direct-in-Dialing (202)76, Autovon 29-
†Additional duty
‡Acting

ORGANIZATIONAL CHART
RESEARCH ADVISORY COMMITTEE

COMMANDING OFFICER
Code 1000
CAPT P.G. Gaffney II,
USN

DIRECTOR OF RESEARCH
Code 1001
Dr. T. Coffey

ASSOCIATE DIRECTORS OF RESEARCH

OFFICE OF STRATEGIC PLANNING
CODE 1003
Dr. W M. Tolles

BUSINESS OPERATIONS DIRECTORATE
Code 3000
R E Doak

GENERAL SCIENCE AND TECHNOLOGY DIRECTORATE
Code 4000
Dr R.A. Lefande*

WARFARE SYSTEMS AND SENSORS RESEARCH DIRECTORATE
Code 5000
R R Rojas

MATERIALS SCIENCE AND COMPONENT TECHNOLOGY DIRECTORATE
Code 6000
Dr B.B Rath

NAVAL CENTER FOR SPACE TECHNOLOGY
Code 8000
P G Wilhelm

ORGANIZATIONAL CHART (Continued)
EXECUTIVE DIRECTORATE

EXECUTIVE COUNCIL (DIVISION DIRECTORS)

COMMANDING OFFICER
Code 1000
CAPT P.G. Gaffney II, USN

RESEARCH ADVISORY COMMITTEE

CHIEF STAFF OFFICER INSPECTOR GENERAL INTERNAL REVIEW
Code 1002
CAPT R W. Michaux, USN

DIRECTOR OF RESEARCH
Code 1001
Dr. T. Coffey

SAFETY OFFICER
Code 1240
K. King

LEGAL COUNSEL
Code 3008
H. Halper

DEPUTY EQUAL EMPLOYMENT OPPORTUNITY OFFICER
Code 3803
W. Williams

PUBLIC AFFAIRS OFFICER
Code 4810
J.W. Gately, Jr.

OFFICE OF STRATEGIC PLANNING
Code 1003
Dr. W.M. Tolles

SCIENTIFIC CONSULTANT TO THE DIRECTOR OF RESEARCH
Code 1004
Dr P Mange

OFFICE OF MANAGEMENT AND ADMINISTRATION
Code 1005
M. Oliver

EXPLORATORY DEVELOPMENT MANAGER
Code 1006
Dr S Sacks

DIVISION DIRECTORS

COMMAND SUPPORT DIVISION
Code 1200
CAPT R W. Michaux, USN

- Security
- Military Operations
- Military Administration and Personnel
- Flight Support
- Flight Support Detachment
- Safety
- Chesapeake Bay Detachment

PROGRAM COORDINATION OFFICE
Code 1500
Dr. R.T. Swim

CHESAPEAKE BAY DETACHMENT
Code 1270
LCDR B. Jones, USN

FLIGHT SUPPORT DETACHMENT
Code 1280
LCDR G.R Viggiano, USN

BUSINESS OPERATIONS DIRECTORATE
Code 3000
R.E. Doak

CONTRACTING DIVISION
Code 3200
J. Ely*
- Contract Negotiations
- Acquisition Strategies/Training
- Advance Acquisition Planning
- Contractual Execution
- Contract Administraion
- Acquisition Policy Interpretations and Implementation

FINANCIAL MANAGEMENT DIVISION
Code 3300
D. Green
- Budget
- Accounting
- Disbursing
- Asset Management
- Systems Operations

SUPPLY DIVISION
Code 3400
CDR W.E. Ralls, Jr., USN
- Small Purchasing
- Technical Screening
- Receipt Control
- Material Distribution
- Shop Stores
- Disposal and Storage

PUBLIC WORKS DIVISION
Code 3500
D.K. Woodington
- Engineering
- Maintenance and Utilities
- Contracts
- Maintenance Control
- Administrative
- Programming
- Project Management
- Facilities Support

CIVILIAN PERSONNEL DIVISION
Code 3800
B. Duffield
- Staffing and Classification
- Employee Development
- Employee Relations
- Special Recruitment Programs

GENERAL SCIENCE AND TECHNOLOGY DIRECTORATE
Code 4000
Dr. R.A. Lefande*

SPACE SCIENCE DIVISION
Code 4100
Dr. H. Gursky
- X-Ray Astronomy
- Upper Atmospheric Physics
- Gamma & Cosmic Ray Astrophysics
- Solar Physics
- Solar Terrestrial Relationships
- Ionospheric Effects
- E O Hulburt Center for Space Research
- Engineering Management
- Ultraviolet Measurement
- Solar Spectroscopy

CENTER FOR ADVANCED SPACE SENSING
Code 4200
Dr. K. Johnston
- Radio/IR/Optical Sensors
- Atmospheric/Ocean Sensing
- Imaging Systems and Research

LABORATORY FOR COMPUTATIONAL PHYSICS AND FLUID DYNAMICS
CODE 4400
Dr. J.P. Boris
- Reactive Flow and Dynamical Systems
- Fluid/Structure Interactions
- Fluid Dynamics Developments
- Computational Physics Developments
- Mathematical Physics

CONDENSED MATTER AND RADIATION SCIENCES DIVISION
Code 4600
Dr. D.J. Nagel
- Radiation Effects
- Directed Energy Effects
- Surface Modification
- Dynamics of Solids
- Complex Systems Theory

PLASMA PHYSICS DIVISION
Code 4700
Dr. S. Ossakow
- Radiation Hydrodynamics
- Laser Plasma
- Charged-Particle Physics
- Pulse-Power Physics
- Space Plasma Physics
- Beam Physics

TECHNICAL INFORMATION DIVISION
Code 4800
P. Imhof
- Information Services
- Technical Library/Software Support
- Publications
- Graphic Design Services
- Systems/Photographic
- Historian

ANIZATIONAL CHART (Continued)

WARFARE SYSTEMS AND SENSORS RESEARCH DIRECTORATE
Code 5000
R.R. Rojas

ACOUSTICS DIVISION
Code 5100
Dr. D. Bradley
- Acoustics Media Characterization
- Applied Ocean Acoustics
- Physical Acoustics
- Signal Processing
- Acoustic Systems

RADAR DIVISION
Code 5300
Dr. M.I. Skolnik
- Radar Analysis
- Radar Techniques
- Search Radar
- Target Characteristics
- Identification Systems
- Airborne Radar

INFORMATION TECHNOLOGY DIVISION
Code 5500
Dr. R P. Shumaker
- Navy Center for Applied Research in Artificial Intelligence
- Communication Systems
- Transmission Technology
- Battle Management Technology
- Human-Computer Interaction
- Secure Information Technology

TACTICAL ELECTRONIC WARFARE DIVISION
Code 5700
Dr. J.A Montgomery
- Offboard Countermeasures
- EW Support Measures
- Airborne EW Systems
- Ships EW Systems
- Advanced Techniques

RESEARCH COMPUTATION DIVISION
Code 5800
R.F. Saenger
- Software
- User Services
- Computer Operations and Communications

UNDERWATER SOUND REFERENCE DETACHMENT
Code 5900
Dr J E. Blue
- Acoustic Materials
- Technical Services
- Electronics
- Transducer Measurements
- Computer

MATERIALS SCIENCE AND COMPONENT TECHNOLOGY DIRECTORATE
Code 6000
Dr. B.B. Rath

LABORATORY FOR STRUCTURE OF MATTER
Code 6030
Dr J Karle
- Energetic Materials
- Analytical Theory
- Physiologically Active Materials
- Macromolecular Structure and Function
- Nanodiffraction and Nanoscopy
- Crystal Growth

CENTER FOR BIOMOLECULAR SCIENCE AND ENGINEERING
Code 6090
Dr J Schnur
- Biosystems
- Biosensors
- Advanced Materials

CHEMISTRY DIVISION
Code 6100
Dr. J S Murday
- Chemical Dynamics and Diagnostics
- Polymeric Materials
- Surface Chemistry
- Navy Technology Center for Safety and Survivability

MATERIALS SCIENCE AND TECHNOLOGY DIVISION
Code 6300
Dr D Gubser
- Physical Metallurgy
- Composites and Ceramics
- Mechanics of Materials
- Material Physics

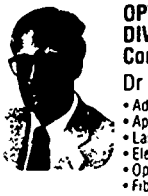

OPTICAL SCIENCES DIVISION
Code 6500
Dr T G Giallorenzi
- Advanced Concepts
- Applied Optics
- Laser Physics
- Electro optical Technology
- Optical Techniques
- Fiber Optics Technology

ELECTRONICS SCIENCE AND TECHNOLOGY DIVISION
Code 6800
Dr G M Borsuk
- Solid State Devices
- Electronic Materials
- Surface and Interface Sciences
- Microwave Technology
- Vacuum Electronics

NAVAL CENTER FOR SPACE TECHNOLOGY
Code 8000
P.G. Wilhelm

SPACE SYSTEMS DEVELOPMENT DEPARTMENT
Code 8100
R.E. Eisenhauer
- Spacecraft Engineering
- Advanced Systems Development
- Communication Systems Technology
- Terrestrial Systems
- SDI Office

SPACECRAFT ENGINEERING DEPARTMENT
Code 8200
R T Beal
- Design Manufacturing and Processing
- Systems Analysis and Test
- Control Systems
- Concept Development

SPACE SYSTEMS TECHNOLOGY DEPARTMENT
Code 8300
L M Hammarstrom
- Space Applications
- Systems Engineering and Analysis
- Advanced Concepts and Processing

*ACTING

- - - - - ADDITIONAL DUTY

CONTRIBUTIONS BY DIVISIONS, LABORATORIES, AND DEPARTMENTS

Space Science Division (4100)

Cosmic-Ray Source Composition
by Rein Silberberg and Chen Hsiang Tsao

Laboratory for Computational Physics and Fluid Dynamics (4400)

Multidimensional Flame Instabilities
by Kazhikathra Kailasanath and Gopal Patnaik (Berkeley Research Associates)

Condensed Matter and Radiation Sciences Division (4600)

Synchrotron X-Radiation Research
by Milton N. Kabler, David J. Nagel, and Earl F. Skelton

Pulsed Laser Deposition of High T_c Superconductors
by Douglas B. Chrisey and James S. Horwitz

Discovery of Be-7 Accretion in Low Earth Orbit
by Gary W. Phillips and Steven E. King

Plasma Physics Division (4700)

Laser-Produced, Strongly Coupled Plasmas
by Andrew N. Mostovych and Kevin J. Kearney

The Dense Z-Pinch: A Possible Shortcut to Fusion Power
by John D. Sethian, Anthony E. Robson, and Kent A. Gerber

Acoustics Division (5100)

A New Approach to Ocean Acoustic Tomography by Alexandra Tolstoy and Orest I. Diachok

Underwater Acoustic Imaging
by Lawrence J. Rosenblum, Behzad Kamgar-Parsi, and Edward Belcher (Applied Physics Laboratory, University of Washington)

Mushroomlike Currents on the Ocean Surface
by Richard P. Mied and Gloria J. Lindemann

Radar Division (5300)

Adaptive Radar
by Frederick W. Lee and Mark E. Burroughs

Calculating the Radar Cross Section from Multiple-bounce Interactions
by Dale A. Zolnick

A Neural Network Classified for Similar Objects
by Abraham Schultz

Information Technology Division (5500)

Active Learning and Bias Adjustment
by Diana ¯. Gordon

Maintenance Expert for Surface Ship Sonar System
by Joseph A. Molnar

New Approaches to Multiple Measurement Correlation for Real-time Tracking Systems
by Jeffrey K. Uhlmann and Miguel R. Zuniga

Tactical Electronic Warfare Division (5700)

Spectral Emission and Infrared Targets with an FT-IR Interferometer Spectrometer
by John W. Dries and Anh-Thu Phan (Mesa, Inc.)

Coherent Information Management for Coordinated Simulation Assessment
by Charles E. Dunham

Research Computation Division (5800)

Molecular Dynamics Simulations of Shearing Force Fields in a Liquid
by Jeffrey H. Dunn, Sam G. Lambrakos, and Peter G. Moore

Underwater Sound Reference Detachment (5900)

Propagation of Thermoacoustic Waves in Elastic Media
by Anthony J. Rudgers

Edge Diffraction Detection Technique
by Jean C. Piquette

Improved Reliability Submarine Sonar Connector
by George D. Hugus

Materials Science and Component Technology Directorate

Elastic Properties of Bilayer Materials Determined by the Indentation Test— Axisymmetric Boussinesq Problem
by Santiago C. Sanday, Hsiang Y. Yu (Geo-Centers, Inc.), and Bhakta B. Rath

Laboratory for Structure of Matter (6030)

Synthesis and Structures of New Energetic Materials
by Richard D. Gilardi and Clifford F. George

Center for Bio/Molecular Science and Engineering (6090)

Drug Detection by Using an Antibody-based Sensor: The Flow Immunosensor
by Gregory A. Wemhoff, Anne W. Kusterbeck, and Frances S. Ligler

Chemistry Division (6100)

Miscibility Studies of Polymeric Blends
by Kenneth J. McGrath, Joel B. Miller, Charles M. Roland, and Allen N. Garroway

Corrosion and Preventing It—the Navy's Water-Cooled VLF Transmitters: A Vital Submarine Link
by Angela M. Ervin, Kate A.S. Hardy, and John C. Cooper

Infrared Reflection Absorption Spectroscopy of Adsorbates on Semiconductors
by Victor M. Bermudez, Marianne McGonigal, Sharka M. Prokes, and James E. Butler

Materials Science and Technology Division (6300)

Synchronization in Chaotic Systems
by Louis M. Pecora and Thomas L. Carroll

Determination of Elastic Constants of Anisotropic Materials from Oblique-Angle Ultrasonic Measurements
by Richard B. Mignogna, Narendra K. Batra, and Kirth E. Simmonds

Thermal Profiles and Heat-affected Zone Hardness in Laser Beam Welding
by Edward A. Metzbower

Elastic Properties of Bilayer Materials Determined by the Indentation Test— Axisymmetric Boussinesq Problem
by Santiago C. Sanday, Hsiang Y. Yu (Geo-Centers, Inc.), and Bhakta B. Rath

Molecular Dynamics Simulations of Shearing Force Fields in a Liquid
by Jeffrey H. Dunn, Sam G. Lambrakos, and Peter G. Moore

Optical Sciences Division (6500)

Infrared Countermeasures for Naval Aircraft
by Myron R. Pauli and Melvin R. Kruer

Electromagnetic Pulse Testing with a Fiber-Optic Sensor
by William K. Burns, Robert P. Moeller, and Catherine H. Bulmer

Physics of Semiconductor Quantum Dots in Glass
by Anthony J. Campillo, Brian L. Justus, Jacqueline A. Ruller, and Edward J. Friebele

Electronics Science and Technology Division (6800)

High-Temperature Superconductor Microwave Devices
by Harvey S. Newman and Jeffrey M. Pond

α-SiC Buried-Gate Junction Field Effect Transistors
by Galina Kelner and Steven C. Binari

Growth of (100) GaAs by Vertical Zone Melting
by Richard L. Henry, Paul E.R. Nordquist, Robert J. Gorman, and William J. Moore

Infrared Reflection Absorption Spectroscopy of Adsorbates on Semiconductors
by Victor M. Bermudez, Marianne McGonigal, Sharka M. Prokes, and James E. Butler

Space Systems Development Department (8100)

Integrated Electrical/Thermal Component Modeling
by Daniel J. Short and William E. Baker

Along Track Formationkeeping for Satellites with Low Eccentricity
by Jay W. Middour

HERCULES: Gyro-based, Real-time Geolocation for an Astronaut Camera
by Mark T. Soyka and Peter J. Melvin

Space Systems Technology Department (8300)

Development of a Mobile Oceanographic Platform
by Jack A.C. Kaiser, Frederick K. Fine, Peter W. Richardson, Norman J. Pollack, and Robert Baldwin (Bendix/Allied Signal Corporation)

EMPLOYMENT OPPORTUNITIES FOR ENTRY-LEVEL AND EXPERIENCED PERSONNEL

This *NRL Review* illustrates some of the exciting science and engineering carried out at NRL as well as the potential for new personnel.

The Naval Research Laboratory offers a wide variety of challenging positions that involve the full range of work from basic and applied research to equipment development. The nature of the research and development conducted at NRL requires professionals with experience. Typically, there is a continuing need for electronics, mechanical aerospace, ceramic, and materials engineers; metallurgists with bachelor's and/or advanced degrees; and physical and computer scientists with Ph.D. degrees. Opportunities exist in the areas described below.

Ceramic and Materials Scientists/Engineers. These employees work on the mechanical properties, coating and materials processing, and materials research.

Electronics Engineers. These engineers work in the following areas: communications satellite design, analog and digital signal processing, information processing, strategic and tactical communication systems design, instrumentation, microcomputer design, satellite attitude-control systems, image processing, IR sensors, focal plane arrays, radar, inverse scattering phenomena, statistical communication theory, electro-optics, hardware/software interfacing, artificial intelligence, electromagnetic (EM) scattering, digital electronics, fiber optics, optical information processing, semiconductor device processing, microwave tubes, threat systems analysis, electroacoustic optics, RF measurement design, EM propagation, EM theory, HF radar propagation analysis, electronic warfare simulation, pulsed power technology, vacuum electronics, microwave technologies, networking techniques, speech processing, Navy C^3I, electronic countermeasure systems design, spacecraft attitude controls, and orbitology.

Mechanical and Aerospace Engineers. These employees may be assigned to satellite thermal design, structural design, propulsion, experimental fluid mechanics, experimental structural mechanics, solid mechanics, elastic/plastic fracture mechanics, materials characterization of composites, finite element methods, nondestructive elevation, characterization of fracture resistance of structural alloys, and combustion.

Computer Science Graduates. Employees in this field are involved with artificial intelligence, software engineering, software systems specifications, computer design/architecture, systems analysis, and command information systems.

Chemists. Chemists are recruited to work in the areas of inorganic and organometallic synthesis, solution kinetics and mechanisms, surface analysis, organic chemistry, combustion, colloid/surface chemistry, fire suppression, and nuclear decay.

Physicists. Physics graduates may concentrate on such fields as electromagnetics, image processing, inverse scattering phenomena, acoustics,

inversion theory, mathematical modeling of scattering processors, radar system development, electro-optics, focal plane arrays, signal processing, plasma physics, astrophysics, semiconductor technology, relativistic electronics, beam/wave interactions, low-temperature physics, superconductivity, physical/chemical vapor disposition of thin and thick coatings, wave propagation, ionospheric physics, computational hydrodynamics, computational atomic physics, and supersonic, gas-dynamic numerical modeling.

FOR FOREIGN NATIONALS

U.S. citizenship is required for employment at NRL.

APPLICATION AND INFORMATION

Interested applicants should submit a resume or an application for Federal Employment Form (SF-171), which can be obtained from local offices of the Office of Personnel Management and Personnel Offices of Federal agencies, to the address below.

Direct inquiries to;

Naval Research Laboratory
Civilian Personnel Division, Code 3830 RV 91
Washington, DC 20375-5000
202-767-3030

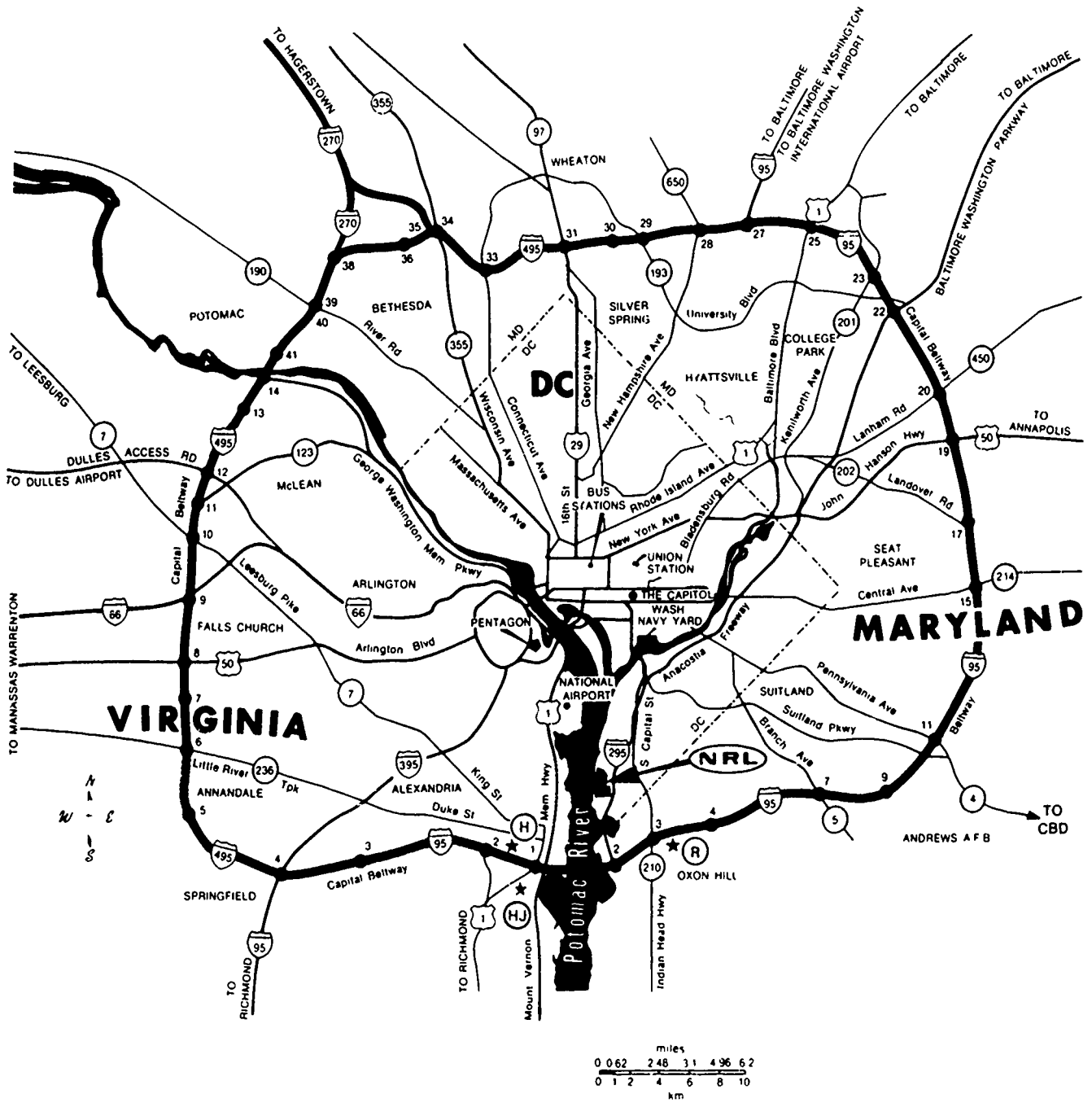

LOCATION OF NRL IN THE CAPITAL AREA

INDEX FOR THE 1991 *NRL REVIEW*

1991 NRL REVIEW STAFF

The *NRL Review* is a result of the collaboration of the scientific, engineering, and support staffs with the Technical Informtion Division (TID). In addition to the scientists and engineers who provided material for the *NRL Review*, the following have also contributed to its publication.

Senior Science Editor: Dr. John D. Bultman
Senior TID Editor: Patricia Staffieri
TID Consultant: Kathleen Parrish

Head, Technical Information Division: Peter H. Imhof

Graphic design: J. Morrow

Graphic support: S. Guilmineau, T. Rufty, and B. Zevgolis

Photographic production: G. Bennett, R. Bussey, G. Fullerton, J. Marshall, C. Morrow, M.C. Petit-Frere, M. Savell, and W. Wiggins

Computerized composition production: D. Gloystein and J. Kogok

Editorial assistance: I. Barron, J. Burke, M. Long, and S. Oresky

Production coordination: T. Calderwood

Production assistance: R. Bankert, D. Montgomery, L. Sprankel, and A. White

Distribution: J. Harris and B. Jolliffe

REVIEWED AND APPROVED
May 1991

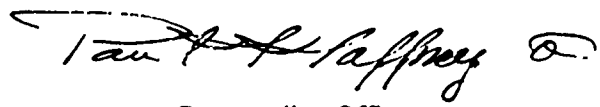

Commanding Officer